

NASA Contractor Report 165951

NASA-CR-165951
19840020736

Development and Flight Evaluation of an Augmented Stability Active Controls Concept

Wiley A. Guinn

LOCKHEED-CALIFORNIA COMPANY
BURBANK, CALIFORNIA

CONTRACT NO. NAS1-15326

SEPTEMBER 1, 1982

LIBRARY COPY

SEP 28 1982

LANGLEY RESEARCH CENTER
LIBRARY, NASA
HAMPTON, VIRGINIA

FOR EARLY DOMESTIC DISSEMINATION

~~Because of its possible commercial value, this data developed under U.S. Government Contract NAS 1-15326 is being disseminated within the U.S. in advance of general publication. This data may be duplicated and used by the recipient with the expressed limitations that the data will not be published nor will it be released to foreign parties without prior permission of Lockheed-California Company. Release of this data to other domestic parties by the recipient shall only be made subject to these limitations. The limitations contained in this legend will be considered void after July 1984. This legend shall be marked on any reproduction of this data in whole or in part.~~



National Aeronautics and
Space Administration

Langley Research Center
Hampton, Virginia 23665



NF01953

NASA Contractor Report 165951

Development and Flight Evaluation of an Augmented Stability Active Controls Concept

Wiley A. Guinn

LOCKHEED-CALIFORNIA COMPANY
BURBANK, CALIFORNIA

CONTRACT NO. NAS1-15326

SEPTEMBER 1, 1982

FOR EARLY DOMESTIC DISSEMINATION

~~Because of its possible commercial value, this data developed under U.S. Government Contract NAS 1-15326 is being disseminated within the U.S. in advance of general publication. This data may be duplicated and used by the recipient with the expressed limitations that the data will not be published nor will it be released to foreign parties without prior permission of Lockheed-California Company. Release of this data to other domestic parties by the recipient shall only be made subject to these limitations. The limitations contained in this legend will be considered void after July 1984. This legend shall be marked on any reproduction of this data in whole or in part.~~



National Aeronautics and
Space Administration

Langley Research Center
Hampton, Virginia 23665

1182-77685#

DEVELOPMENT AND FLIGHT
EVALUATION OF AN AUGMENTED
STABILITY ACTIVE CONTROLS CONCEPT

Coordinated by: Wiley A. Guinn

Lockheed-California Company
Burbank, California

SUMMARY

A limited authority pitch active control system (PACS) was developed for a wide body jet transport (L-1011) with a flying stabilizer to enhance flying qualities for relaxed static stability flight conditions. Development activities included system architecture definition, control law development, component fabrication and testing, piloted flight simulation tests, vehicle simulation tests, ground checkout tests, and flight tests.

The PACS consists of two dual channel digital computers and associated software that provide command signals to a dual channel (active/standby configuration) series servo which controls the stabilizer power actuator. Analog input signals to the computer are pitch rate, column-minus-trim position, and dynamic pressure. A center-of-gravity (c.g.) management system was installed on the flight test aircraft to provide a range of c.g. locations from 25 to 39% mac for handling qualities evaluation tests. The aircraft cruise neutral point is at 40% mac. The stabilizer has a geared elevator that was downrigged .09 rad (5 deg) to provide the required nose down control authority for the aft c.g. flight conditions.

The flight test program was conducted by three different pilots who used Cooper-Harper ratings to quantitatively express their opinion of the aircraft handling qualities. The reference flight condition for handling quality evaluation was at 25% mac c.g. with PACS off. Tests were performed at cruise and high speed flight conditions within the linear stability region at c.g. locations of 25, 35, 37, and 39% mac with PACS on and off. The handling qualities with the c.g. at 39% mac (+ 1% static stability margin) and PACS on were judged to be as good as the handling qualities with the c.g. at 25% mac and PACS off. The flight test evaluation of the PACS demonstrated that the aircraft handling qualities can be maintained as the static stability is relaxed by moving the c.g. to within + 1% of the neutral point.

CONTENTS

| | Page |
|---|------|
| SUMMARY | i |
| LIST OF FIGURES | vii |
| LIST OF TABLES | xi |
| LIST OF SYMBOLS | xiii |
| INTRODUCTION | 1 |
| Background | 1 |
| Program Objectives | 1 |
| Scope of Program | 1 |
| 1 BASELINE AIRCRAFT | 3 |
| 1.1 General Description | 3 |
| 1.2 Downrigged Elevator | 3 |
| 1.3 C.G. Management System | 3 |
| 1.3.1 System Configuration | 8 |
| 1.3.2 System Performance | 10 |
| 2 PITCH ACTIVE CONTROL SYSTEM DESCRIPTION | 11 |
| 2.1 General Description | 11 |
| 2.2 Control System | 11 |
| 2.2.1 Series Servo | 14 |
| 2.2.2 Tie-in-Mechanism | 17 |
| 2.2.3 Power Servo Modification | 19 |
| 2.3 Avionic System | 19 |
| 2.3.1 System Architecture | 19 |
| 2.3.2 Sensor Descriptions | 19 |
| 2.3.3 Computer Functions | 21 |
| 2.3.4 Avionic System Operation | 23 |
| 2.4 PACS Installation | 24 |
| 3 DESIGN AND ANALYSIS | 31 |
| 3.1 Flying Qualities | 31 |
| 3.1.1 Handling Qualities Criteria | 31 |
| 3.1.2 Flight Conditions | 32 |
| 3.1.3 Aerodynamic Data | 32 |
| 3.1.4 PACS Concept | 34 |
| 3.1.5 Augmentation Authority | 39 |
| 3.2 Functional System | 42 |
| 3.2.1 Analysis Methods | 42 |
| 3.2.2 Results of Analysis | 43 |
| 3.3 Avionics | 44 |
| 3.3.1 Control Law Development | 44 |
| 3.3.2 CSMP Simulations | 55 |

CONTENTS (Continued)

| | Page |
|--|--------|
| 3.4 Stress | 61 |
| 3.4.1 Primary Structure Analysis | 61 |
| 3.4.2 System Component Analysis. | 62 |
| 3.4.3 Proof and Operation Test Requirements. | 64 |
| 3.5 Weight and Ballast | 65 |
| 3.5.1 Weight and Ballast Status. | 65 |
| 3.5.2 C.G. Management System | 65 |
| 3.5.3 Inertia Data | 67 |
| 3.6 Structural Loads Analysis. | 71 |
| 3.6.1 Analysis Methods | 71 |
| 3.6.2 Analysis Results | 75 |
| 3.6.3 Structural Operating Restrictions. | 78 |
| 3.7 Flutter. | 79 |
| 3.7.1 Introduction | 79 |
| 3.7.2 Analysis Methods | 79 |
| 3.7.3 Conditions Analyzed. | 81 |
| 3.7.4 Analysis Results | 82 |
| 3.7.5 Conclusions. | 84 |
| 3.8 Safety Analysis. | 86 |
| 3.8.1 Analysis Approach. | 86 |
| 3.8.2 PACS Safety Provisions | 89 |
| 3.8.3 Analysis Results | 89 |
| 4 LABORATORY AND GROUND TESTS. | 93 |
| 4.1 Wind-Tunnel Tests. | 93 |
| 4.1.1 Low Speed. | 93 |
| 4.1.2 High Speed | 94 |
| 4.2 PACS Component Tests | 97 |
| 4.2.1 Components Tested. | 97 |
| 4.2.2 Pallet Tests | 97 |
| 4.2.3 Series Servo Tests | 98 |
| 4.2.4 Rate Gyro Tests. | 98 |
| 4.2.5 Vibration Qualification Tests. | 98 |
| 4.3 Visual Flight Simulation | 99 |
| 4.3.1 PACS Optimization. | 99 |
| 4.3.2 Simulated Failures | 102 |
| 4.4 Vehicle System Simulator Tests | 104 |
| 4.4.1 VSS Description. | 104 |
| 4.4.2 Data Acquisition | 105 |
| 4.4.3 Test Results and Conclusions | 106 |
| 4.5 Aircraft Ground Test | 107 |
| 4.5.1 Water Ballast System | 107 |
| 4.5.2 Controls Proof and Operations. | 107 |
| 4.5.3 PACS Verification. | 107 |
| 4.5.4 Ground Vibration Test. | 110 |

CONTENTS (Continued)

| | Page |
|---|------|
| 5 FLIGHT TEST | 117 |
| 5.1 Flight Flutter Test | 117 |
| 5.1.1 Data Acquisition. | 117 |
| 5.1.2 Test Procedure. | 117 |
| 5.1.3 Flutter Clearance | 123 |
| 5.1.4 PACS Feedback Transfer Functions. | 123 |
| 5.1.5 Conclusion. | 129 |
| 5.2 Handling Qualities. | 129 |
| 5.2.1 Handling Qualities Tests. | 129 |
| 5.2.2 Handling Qualities Test Results | 131 |
| 6 CONCLUSIONS AND RECOMMENDATIONS | 139 |
| APPENDIX A - FUEL SAVINGS | 140 |
| APPENDIX B - DOWNRIGGED ELEVATOR MODIFICATIONS. | 142 |
| APPENDIX C - C. G. MANAGEMENT SYSTEM. | 145 |
| APPENDIX D - AVIONICS SYSTEM DESIGN | 150 |
| REFERENCES. | 163 |

This Page Intentionally Left Blank

LIST OF FIGURES

| Figure | | Page |
|--------|--|------|
| 1 | General arrangement of flight test aircraft | 4 |
| 2 | Flight test airplane (L-1011 S/N 1001) | 6 |
| 3 | Elevator control drive system (ELCON II left side) | 7 |
| 4 | Stabilizer/elevator gearing | 8 |
| 5 | C.G. management system of flight test aircraft | 9 |
| 6 | Longitudinal control system with PACS | 12 |
| 7 | Pitch control system block diagram | 13 |
| 8 | Schematic of the L-1011 control system with the PACS series servo | 14 |
| 9 | Series servo functional elements | 16 |
| 10 | Series servo authority | 17 |
| 11 | Series servo tie-in mechanism | 18 |
| 12 | PACS avionics system architecture | 20 |
| 13 | Near-term PACS avionics system block diagram | 22 |
| 14 | Near-term PACS block diagram | 25 |
| 15 | Location of PACS components | 27 |
| 16 | PACS pitch rate gyros | 23 |
| 17 | Location of several PACS components | 29 |
| 18 | PACS pallet installation in flight test aircraft | 30 |
| 19 | Flight envelope | 33 |
| 20 | Elevator downrig required for nose-down control | 35 |
| 21 | L-1011-1 S/N 1001 High-speed pitching moment characteristics . | 36 |
| 22 | The effect of PACS gain-lag functions on short-period characteristics | 40 |
| 23 | Maneuver stability, cruise | 41 |
| 24 | PACS analytical block diagram | 45 |
| 25 | Pitch damper gain schedules | 47 |

LIST OF FIGURES (Continued)

| Figure | | Page |
|--------|---|------|
| 26 | Short-period characteristics, cruise | 49 |
| 27 | Short-period characteristics, landing. | 50 |
| 28 | Phugoid characteristics, cruise. | 51 |
| 29 | Pilot feed-forward gain schedule | 53 |
| 30 | Maneuver stability, landing. | 54 |
| 31 | Pitching moment variation with angle of attack | 56 |
| 32 | Pitch rate response for $\alpha < .087$ rad (5 deg) with PACS on and off . | 58 |
| 33 | Angle of attack (α) and load factor response for pilot step force commands with PACS on and off | 59 |
| 34 | RMS turbulence response, cruise. | 60 |
| 35 | Horizontal stabilizer load and strength envelope | 63 |
| 36 | Elevator control system limit strength and hinge moment envelopes | 65 |
| 37 | Ballast location requirements | 67 |
| 38 | Ballast configuration that complies with space and floor loading requirements | 68 |
| 39 | C.G. envelope and travel | 69 |
| 40 | Aircraft inertia cases | 70 |
| 41 | Aircraft inertia data. | 70 |
| 42 | Component inertia data | 71 |
| 43 | Wing limit static loads, 75% semispan. | 76 |
| 44 | Horizontal tail limit static loads, 32% semispan | 76 |
| 45 | Horizontal tail limit dynamic gust loads, 32% semispan | 77 |
| 46 | Effect of pilot recovery time on peak load factor during PACS undetected hardover failure | 78 |
| 47 | Horizontal tail PACS oscillatory failure limit loads, 32% semispan | 79 |
| 48 | Composite summary of structural operating restrictions | 80 |
| 49 | Definition of feedback amplitude ratio margin (FARM) | 82 |
| 50 | Typical phase vs FARM plot | 83 |
| 51 | Phase vs FARM comparison of analysis and flight test data | 85 |

LIST OF FIGURES (Continued)

| Figure | | Page |
|--------|---|------|
| 52 | Probability versus consequence of occurrence | 90 |
| 53 | Low-speed longitudinal stability and nose-down controlability for the landing configuration $\delta_F = .785$ rad (45 deg) | 94 |
| 54 | Elevator nose-down control effectiveness $M = 0.86$, $\delta_H = +.017$ rad (1 deg) | 95 |
| 55 | Effect of elevator downrig on stabilizer hinge moment. $M = 0.9$, $\delta_H = +.017$ rad (1 deg). | 96 |
| 56 | Effect of downrig on elevator hinge moment. $M = 0.9$, $\delta_H = +.017$ rad (1 deg). | 96 |
| 57 | Handling qualities rating scale. | 101 |
| 58 | Flight simulation results in cruise - condition 10, configuration 3. | 102 |
| 59 | PACS vehicle system simulator test configuration | 105 |
| 60 | PACS flight flutter clearance envelope | 124 |
| 61 | PACS flight flutter test points for heavy fuel conditions. . . | 125 |
| 62 | Flight flutter test points for minimum fuel condition. | 126 |
| 63a | FARM plot for heavy fuel aircraft at 3658 meter (12,000 ft.) altitude at $M = .74$ (2x nominal gain). | 127 |
| 63b | FARM plot for heavy fuel aircraft at 6706 meter (22,000 ft.) altitude at $M = .83$ (2x nominal gain). | 127 |
| 63c | FARM plot for heavy fuel aircraft at 11278 meter (37,000 ft.) altitude at $M = .85$ (2x nominal gain). | 128 |
| 63d | FARM plot for minimum fuel aircraft at 6706 meter (22,000 ft.) altitude at $M = .87$ (2x nominal gain). | 128 |
| 64 | Maneuvering characteristics, flight condition 15, c.g. = 39% mac, AACS on | 132 |
| 65 | Comparison of damping response characteristics, PACS off and on | 134 |
| 66 | Pilot Cooper-Harper Ratings | 136 |
| 67 | VFS ratings compared to S/N1001, AACS on | 137 |
| 68 | Potential fuel savings for aft c.g. locations | 140 |
| 69 | Isometric view of elevator | 143 |
| 70 | Counter balance arms before and after modification | 144 |

LIST OF FIGURES (Continued)

| Figure | | Page |
|--------|--|------|
| 71 | Water ballast system | 147 |
| 72 | Near-term PACS interface block diagram | 151 |
| 73 | Functional block diagram of modified Collins ACC-201 computer. | 153 |
| 74 | PACS signal equalization | 156 |
| 75 | PACS Computer software monitoring procedure | 157 |
| 76 | PACS servo monitor hardware comparators | 159 |
| 77 | PACS servo monitor software comparators | 160 |
| 78 | Software organization | 162 |

LIST OF TABLES

| TABLE | | Page |
|-------|--|------|
| 1 | Aircraft Geometry and Weight | 5 |
| 2 | Flight Conditions | 34 |
| 3 | Stability and Control Derivatives | 37 |
| 4 | Summary of Linear Column Force Gradients, Cruise, Mach = .83, h = 10,000 m (33,000 ft), AACS On | 54 |
| 5 | Loading Limits | 66 |
| 6 | Comparison of Frequency and Damping for Open and Closed Loop (2 Times Nominal Gain) Analyses | 84 |
| 7 | PACS Configurations Tested | 101 |
| 8 | Simulated Failures | 103 |
| 9 | Pitch Rate Static Gain | 108 |
| 10 | Column Minus Trim Static Gain (System Gain Setting = 1) | 109 |
| 11 | Stabilizer Deflection | 110 |
| 12 | PACS Functional and Modal Ground Vibration Test Series | 111 |
| 13 | PACS Transfer Function Test Series | 112 |
| 14 | Static Gain PACS Closed Loop | 113 |
| 15 | Summary of Aircraft Ground Vibration Test Modal Frequencies ~ Hz | 114 |
| 16 | Modal Results | 116 |
| 17 | Transducers Monitored for Flutter Tests | 118 |
| 18 | Summary of Flight Flutter Tests | 119 |
| 19 | Flight Test Conditions | 130 |
| 20 | Pilot Comments on PACS Operation in Turbulence | 135 |
| 21 | Water Ballast Operating Procedures | 149 |

This Page Intentionally Left Blank

LIST OF SYMBOLS

AACS - Aileron Active Control System

a.c. - Alternating current

A/D - Analog/Digital converter

ASAP - Advanced System Analysis Program

BL - Butt line

C - Structural damping

C_{D_u} - $\frac{U}{2} \frac{\partial C_D}{\partial U}$, change in drag coefficient due to speed

C_{D_α} - $\frac{\partial C_D}{\partial \alpha}$, change in drag coefficient due to angle of attack

$C_{D_{\delta_{AC}}}$ - $\frac{\partial C_D}{\partial \delta_{AC}}$, change in drag coefficient due to AACS deflection

C_{H_e} - Elevator hinge moment coefficient

C_{H_H} - Stabilizer hinge moment coefficient

C_L - Lift coefficient

C_{L_q} - $\frac{2U}{mac} \frac{\partial C_L}{\partial q}$, change in lift coefficient due to pitch rate

C_{L_u} - $\frac{U}{2} \frac{\partial C_L}{\partial U}$, change in lift coefficient due to speed

C_{L_α} - $\frac{\partial C_L}{\partial \alpha}$, change in lift coefficient due to angle of attack

$C_{L_{\dot{\alpha}}}$ - $\frac{2U}{mac} \frac{\partial C_L}{\partial \dot{\alpha}}$, change in lift coefficient due to rate of change at angle of attack

LIST OF SYMBOLS (Continued)

- $C_{L_{\delta_{AC}}}$ - $-\frac{\partial C_L}{\partial \delta_{AC}}$, change in lift coefficient due to AACS deflection
- $C_{L_{\delta_H}}$ - $-\frac{\partial C_L}{\partial \delta_H}$, change in lift coefficient due to stabilizer deflection
- C_m - Pitching moment coefficient
- C_{m_q} - $-\frac{2U}{mac} \frac{\partial C_m}{\partial q}$, change in pitching moment coefficient due to pitch rate
- C_{m_u} - $-\frac{U}{2} \frac{\partial C_m}{\partial U}$, change in pitching moment coefficient due to speed
- C_{m_α} - $-\frac{\partial C_m}{\partial \alpha}$, change in pitching moment coefficient due to angle of attack
- $C_{m_{\dot{\alpha}}}$ - $-\frac{2U}{mac} \frac{\partial C_m}{\partial \dot{\alpha}}$, change in pitching moment coefficient due to rate of change of angle of attack
- $C_{m_{\delta_{AC}}}$ - $-\frac{\partial C_M}{\partial \delta_{AC}}$, change in pitching moment coefficient due to AACS deflection
- $C_{m_{\delta_H}}$ - $-\frac{\partial C_M}{\partial \delta_H}$, change in pitching moment coefficient due to stabilizer deflection
- $C_{m_{.25mac}}$ - Pitching moment coefficient about 1/4 chord of the mean aerodynamic chord
- CADAM - Computer Aided Design and Manufacturing
- c.g. - Center of gravity
- cm - Centimeter
- CSMP - Continuous System Modeling Program
- C-T - Column-minus-trim signals
- D/A - Digital/Analog Converter

LIST OF SYMBOLS (Continued)

| | |
|------------------|--|
| dB | - Decibel |
| d.c. | - Direct current |
| deg | - Degree |
| EHV | - Electro-hydraulic valve |
| F _{COL} | - Pilot column force |
| FARM | - Feedback amplitude ratio margin - $20 \log \frac{\delta_{out}}{\delta_{in}}$ |
| FCES | - Flight Control Electronic System |
| FM | - Frequency modulated |
| Freq | - Frequency |
| FS | - Fuselage station |
| F _S | - Stick force |
| F.S. | - Full scale (Sensor signal value) |
| ft | - Feet |
| g | - Acceleration of gravity |
| gpm | - Gallons per minute |
| h | - Altitude |
| Hg | - Chemical symbol for mercury |
| H.M. | - Hinge moment |
| HP | - Hewlett Packard |
| hr | - Hour |
| HS | - Horizontal Stabilizer |
| ICSSP | - Interactive Continuous System Simulation Program |
| in | - Inches |
| j | - $\sqrt{-1}$, imaginary number |

LIST OF SYMBOLS (Continued)

| | |
|----------|--|
| K_{LV} | - Stabilizer-to-column gearing ratio |
| K_Q | - Pitch rate feedback loop gain |
| K_1 | - Switching step gain of C-T digital computer loop |
| K_2 | - Switching step gain of PR digital computer loop |
| K_3 | - Switching step gain for combined C-T and PR signal |
| KCAS | - Knots calibrated airspeed |
| KEAS | - Knots equivalent airspeed |
| KFFD | - Column Feed Forward Loop gain |
| kg | - Kilograms |
| Kts | - Knots |
| lb | - Pounds |
| LVDT | - Linear variable displacement transducer |
| M | - Mach number |
| m | - Meter |
| M_D | - Maximum dive Mach number |
| M_{MO} | - Maximum operating Mach number |
| mac | - Mean aerodynamic chord |
| MDLC | - Maneuver Direct Lift Control |
| min | - Minutes |
| M.S. | - Margin of Safety |
| N | - Newton |
| n_L | - Load factor |

LIST OF SYMBOLS (Continued)

| | |
|---------------|---|
| N_z | - Normal acceleration |
| $N_{z_{RMS}}$ | - Root-mean-square Normal Acceleration |
| OEW | - Operation empty weight |
| P_a | - Pascal |
| PACS | - Pitch active control system |
| psi | - Pounds per square inch |
| PR | - Pitch rate |
| PWRFAC | - Power factor |
| Q_c | - Dynamic pressure |
| rad | - Radians |
| RMS | - Root-mean-square |
| RPM | - Revolutions per minute |
| RSS | - Relaxed Static Stability |
| s | - Laplace transform parameter |
| sec | - Second |
| S.F. | - Safety factor |
| SOL | - Solenoid |
| SW_4 | - Switch to provide step gain for the digital computer circuits |
| SW_5 | - Switch to engage computer in the PACS or provide test signals |
| T_h | - Change in thrust due to altitude |
| T_m | - Change in thrust due to Mach number |
| TEU | - Trailing edge up |

LIST OF SYMBOLS (Continued)

| | |
|----------------------|---------------------------------------|
| V | - Volts |
| V_D | - Maximum dive speed |
| V_E | - Equivalent airspeed |
| V_{MO} | - Maximum operating limit speed |
| VAC | - Volts, alternating current |
| VDC | - Volts, direct current |
| VFS | - Visual Flight Simulator |
| VSS | - Vehicle System Simulator |
| W | - Weight |
| WBL | - Wing butt line |
| WL | - Water line |
| ZFW | - Zero fuel weight |
| α | - Angle of attack |
| δ_{Col} | - Column deflection |
| δ_e | - Elevator deflection |
| δ_F | - Flap deflection |
| δ_H | - Stabilizer deflection |
| δ_{SS} | - Series servo displacement |
| $\delta_{SS_{RMS}}$ | - Root-mean-square servo displacement |
| ζ | - Damping ratio |
| $\dot{\theta}$ | - Pitch rate |
| $\dot{\theta}_{RMS}$ | - Root-mean-square pitch rate |

LIST OF SYMBOLS (Continued)

- τ_Q - Pitch rate feedback loop lag
- ω_d - Damped natural frequency
- ω_n - Undamped natural frequency

INTRODUCTION

Background

Jet aircraft fuel cost has increased from 12¢ per gallon in 1972 to \$1.00 or more in 1982. As a result, the fuel cost portion of aircraft direct operating cost has increased from 25% to nearly 60%. This trend was recognized early by aircraft manufacturers and government leaders. Therefore, in 1975 the U.S. Congress requested NASA to set up a program to develop fuel saving technology for commercial transports.

The NASA Aircraft Energy Efficiency (ACEE) program was initiated in 1976. In February 1977 Lockheed received an ACEE program contract for "Development and Flight Evaluation of Active Control Concepts for Subsonic Transport Aircraft" (NASA Contract NAS1-14690). The contract resulted in the development of an aileron active control system (AACS) which provided wing load alleviation. The AACS allowed a 5.8% wing span increase for the L-1011-500 (in service date 1980) which decreased fuel consumption by approximately 3% (Reference 1). Also, studies were conducted under the contract to evaluate benefits of a pitch active control system (PACS). Piloted flight simulations were conducted on a moving base simulator with an L-1011 cab. These tests showed that a lagged pitch rate damper provided flying qualities with static longitudinal stability relaxed to near neutral and in heavy turbulence that are equivalent to those of the baseline airplane. The aft c.g. simulation results provided a sufficient basis for proceeding to a flight evaluation of the defined augmentation control laws with relaxed static stability (RSS).

In December 1978 Lockheed was awarded the current contract for "Development and Flight Evaluation of an Augmented Stability Active Control with Small Horizontal Tail." In May 1980 the program was restructured to develop the PACS for improvement of flying qualities at aft c.g. flight conditions utilizing a standard L-1011 tail.

Program Objectives

The purpose of this program is to develop fuel saving technology for commercial transports. The primary goal is to develop technology for a PACS that provides good handling qualities at c.g. locations near the neutral point. This c.g. location minimizes the trim drag and results in significant fuel savings (see Appendix A).

Scope of Program

An L-1011 aircraft was equipped with a PACS and flight demonstration tests were performed. The PACS development included hardware modification of an existing digital computer, programming of software with the appropriate control laws, and fabrication of a previously designed series servo. Basic

aircraft modifications were installation of a water ballast type c.g. management system and downrigging the elevator to provide sufficient nose down control authority for aft c.g. flight conditions. Three Mach .83 cruise conditions, a high speed flight condition, and landing approaches were performed to evaluate the PACS handling quality characteristics with relaxed static stability margins.

1. BASELINE AIRCRAFT

Features of the baseline aircraft are given in this section except for the PACS which is discussed separately in Section 2.

1.1 General Description

The Lockheed L-1011 is a current generation, subsonic, commercial transport aircraft as shown in Figure 1. The aircraft is powered by three Rolls Royce RB.211-22B high-bypass ratio turbofan engines and has a flying stabilizer with geared elevator. Aircraft geometry and weight data are given in Table 1.

A unique version of the L-1011 aircraft was used throughout the PACS program analysis, design, and flight test. Features of this aircraft are shown in Figure 2. This test aircraft (S/N 1001) is a basic L-1011-1 with extended-span wing and aileron active control system (AACS) which were installed during a previous contract (NAS1-14690). A downrigged elevator, c.g. management system, and PACS were added during the current program.

1.2 Downrigged Elevator

The elevator was downrigged .09 rad (5 deg) to provide the additional nose down control authority to permit flight at the aft c.g. locations.

Each elevator on the L-1011 is independently connected by a mechanical system to the horizontal stabilizer as shown in Figure 3. The specific configuration on the flight test aircraft is designated as Elevator Control II (ELCON II). This configuration consists of a drive cable, return cable, quadrant (unsymmetrical cam), and an elevator push rod. The drive and return cables are attached to the fuselage structure at one end and the quadrant at the other end. Consequently, as the flying stabilizer is rotated over the range of +.017 rad (+1 deg) (trailing edge down) to -.244 rad (-14 deg), the unsymmetrical cam action of the quadrant moves the elevator push rod to rotate the elevator as shown in Figure 4 for the standard and downrigged elevator configurations. Modifications required for downrigging the elevator are discussed in Appendix B

1.3 C.G. Management System

The c.g. management system provides a means to locate the flight test aircraft center of gravity at any location between 25% and 39% mac for handling quality tests.

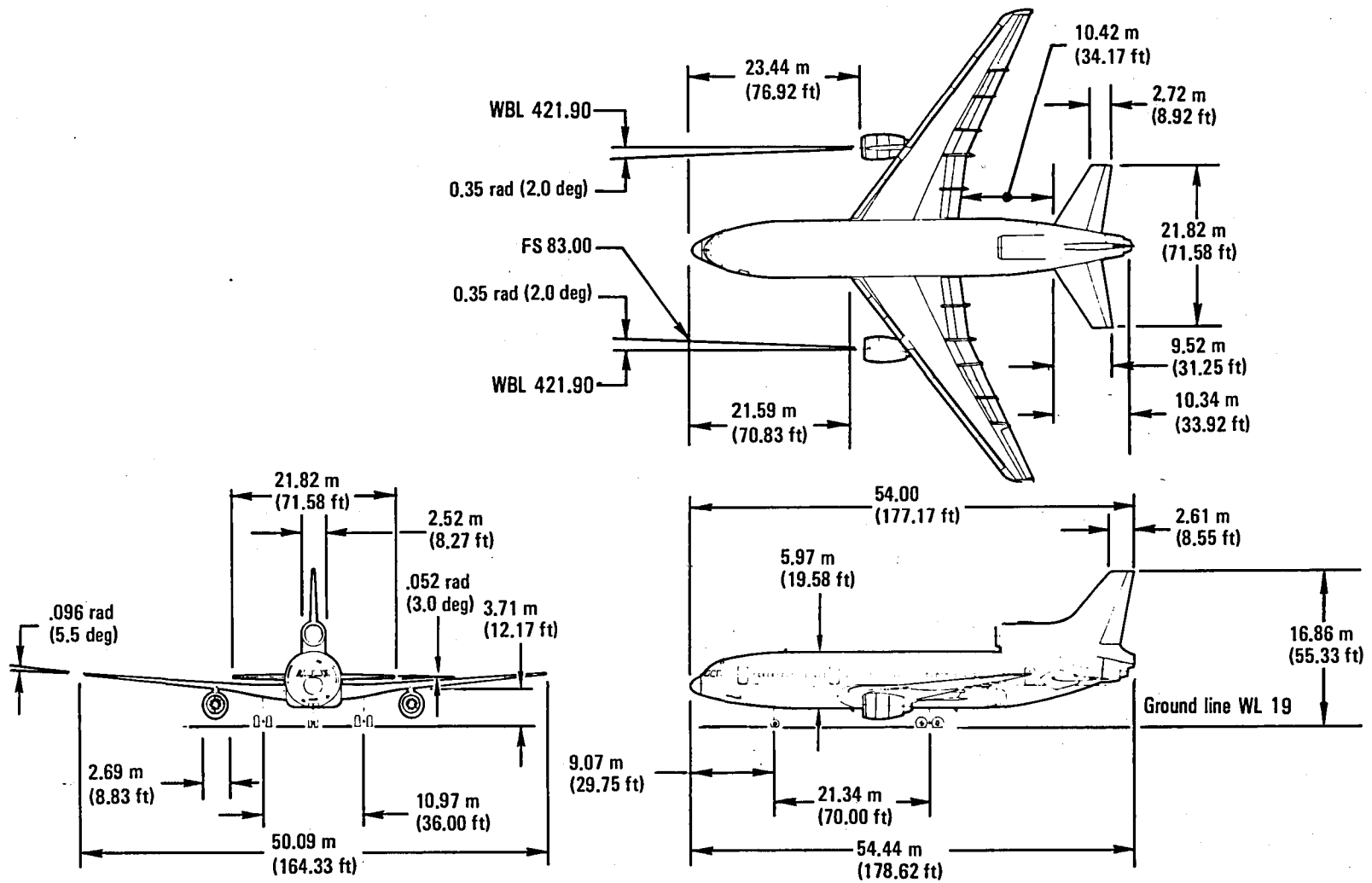


Figure 1. - General arrangement of flight test aircraft.

TABLE 1. AIRCRAFT GEOMETRY AND WEIGHT

| | |
|------------------------|--|
| WING | |
| Reference Area | 321.07m ² (3456 ft ²) |
| Reference mac | 7.46m (24.46 ft) |
| Span | 50.09 m (164.33 ft) |
| Aspect Ratio | 7.817 |
| Sweepback | .611 rad (35 deg) |
| HORIZONTAL TAIL | |
| Area | 119.10m ² (1282 ft ²) |
| Span | 21.82m (71.58 ft) |
| Aspect Ratio | 4.0 |
| Sweepback | .611 rad (35 deg) |
| Tail Volume | .919 |
| VERTICAL TAIL | |
| Area | 51.10m ² (550 ft ²) |
| Span | 9.04m (29.67 ft) |
| Aspect Ratio | 1.6 |
| Sweepback | .611 rad (35 deg) |
| Rail Volume | .066 |
| WEIGHT | |
| Maximum Ramp | 192,323 kg (424,000 lb) |
| Maximum Takeoff | 191,416 kg (422,000 lb) |
| Maximum Landing | 162,386 kg (358,000 lb) |
| Zero Fuel | 141,729 kg (312,460 lb) |
| Operating Empty | 118,388 kg (261,000 lb) |

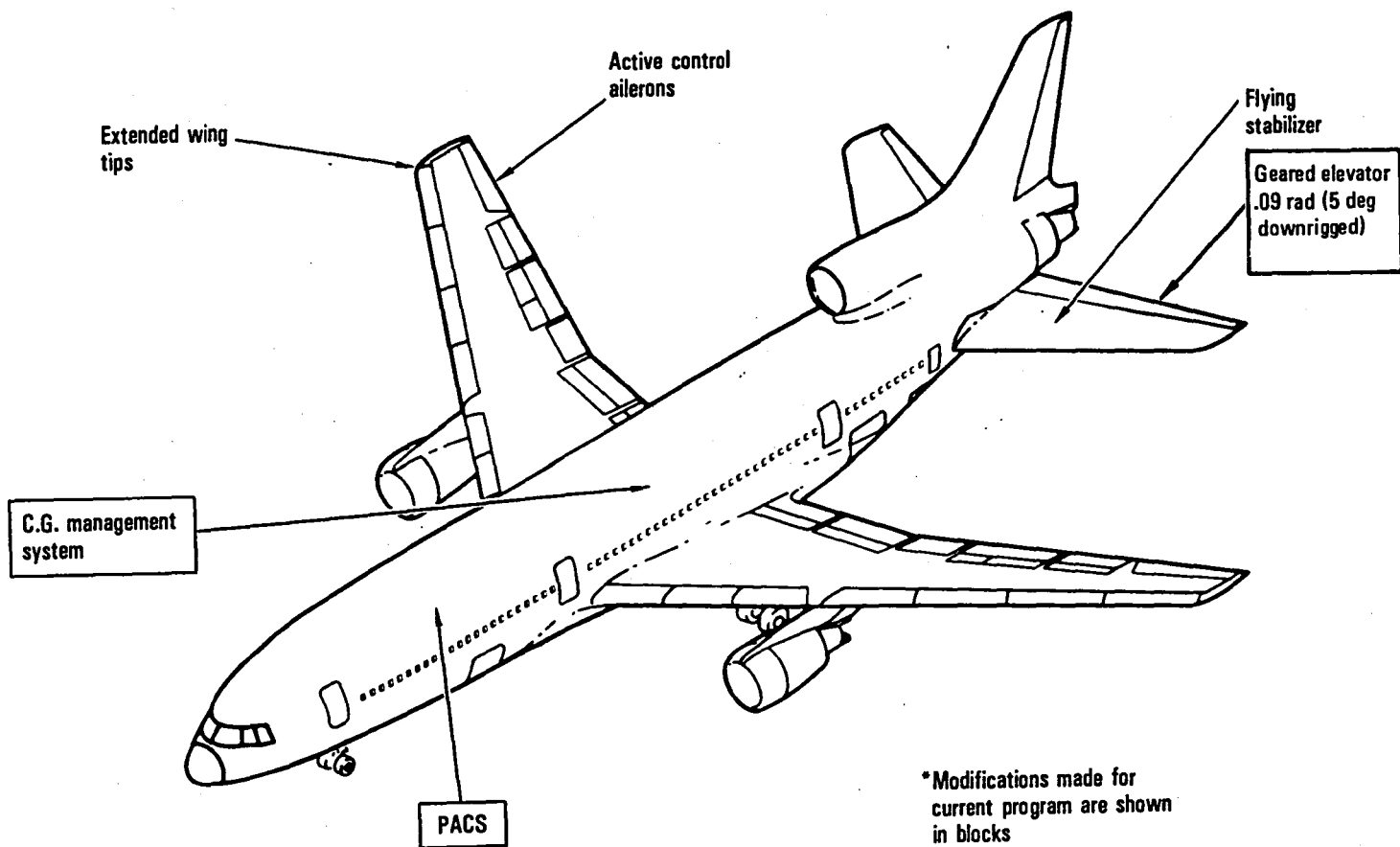


Figure 2. - Flight test airplane (L-1011 S/N 1001).

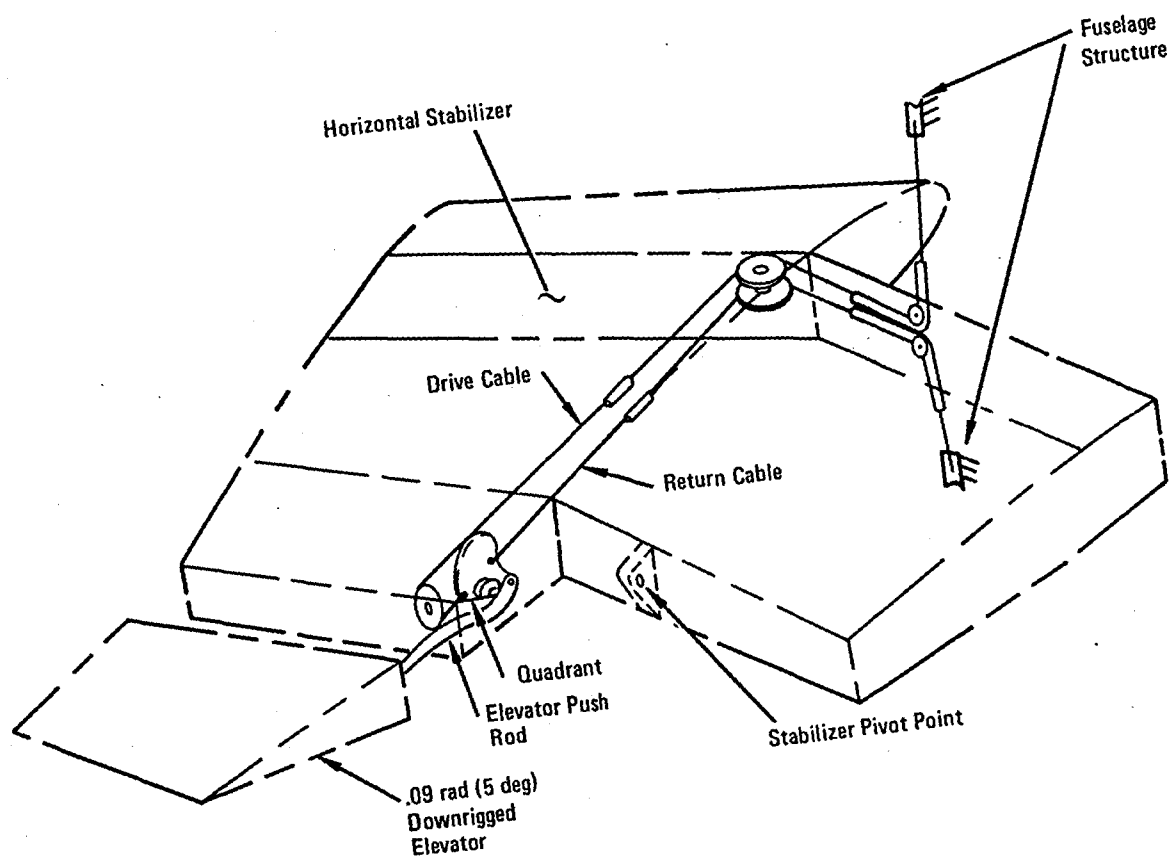


Figure 3. - Elevator control drive system (ELCON II left side).

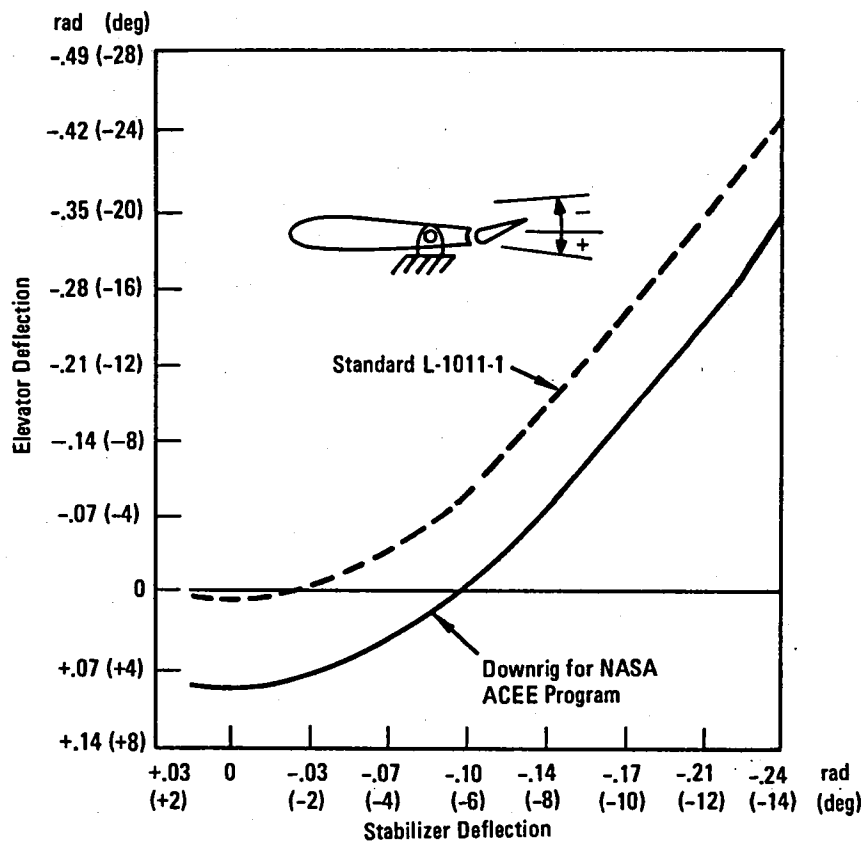






Figure 4. - Stabilizer/elevator gearing.

1.3.1 System Configuration.—Figure 5 shows the water-ballast/fixed-ballast c.g. management system that was developed. The types of ballast shown in the figure are:

- Fixed lead or steel ballast — 
- Non-transferable (fixed) water ballast (Aft Passenger Deck) — 
- Transferable water ballast tanks (empty) — 
- Transferable water ballast tanks (filled with water) — 

The top half of the figure represents the ballast arrangement for the c.g. at 25% mac. This arrangement shows the tanks in the forward part of the aircraft (forward cargo compartment) to be filled with water and tanks in the aft part of the aircraft (center cargo compartment) to be empty.

The bottom half of Figure 5 represents the ballast arrangement for the c.g. at 39% mac. This arrangement shows that all water has been transferred from the forward tanks to the aft tanks. Detail design and operation of the system is discussed in Appendix C.

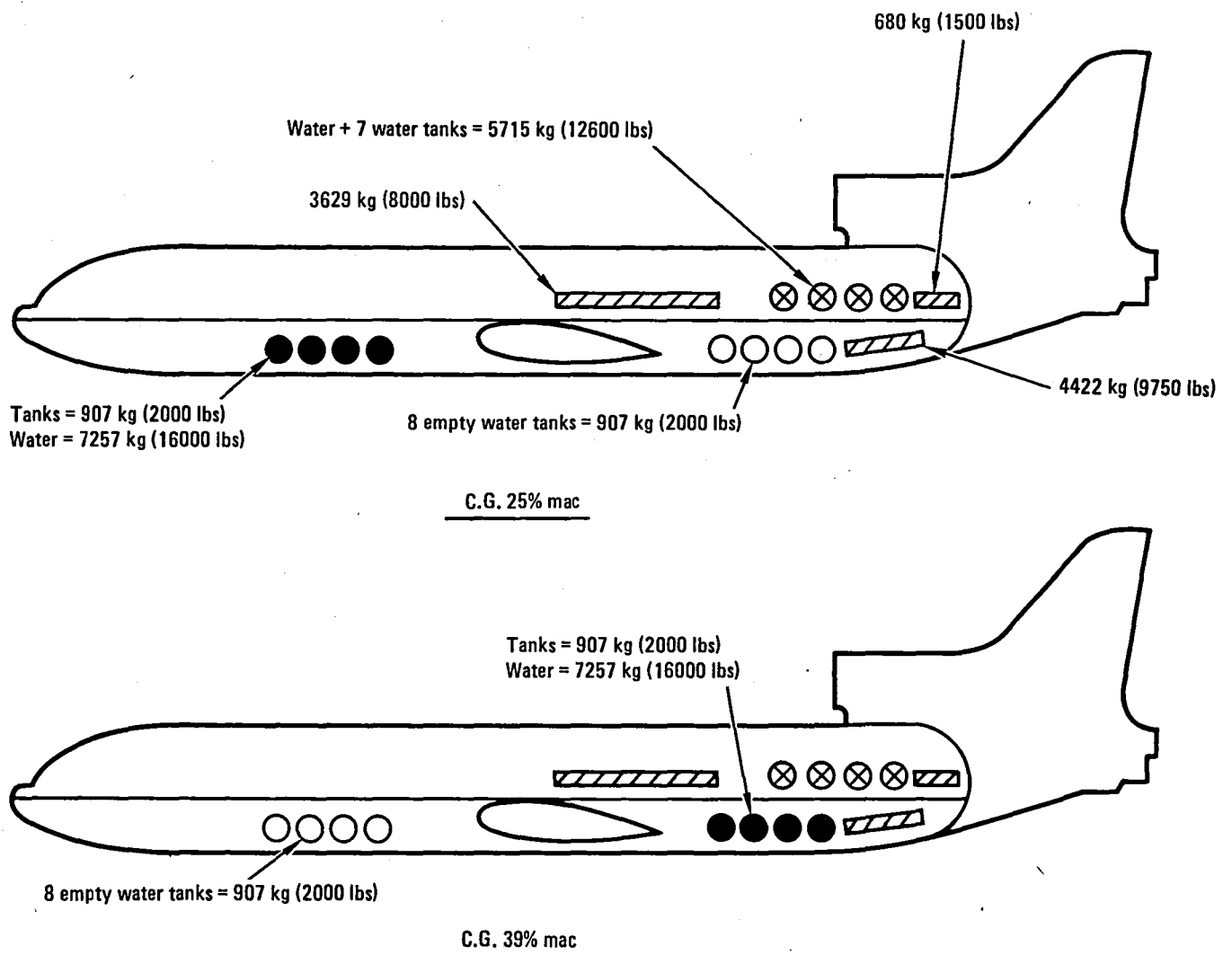


Figure 5. - C.G. management system of flight test aircraft.

1.3.2 System Performance.-The water ballast transfer rate is 453.6 kg/min (1000 lb/min). Thus, 16 minutes are required to transfer all of the water from the forward tanks to the aft tanks and vice versa.

Emergency dumping of water from the transferable water tanks in the cargo compartments and the fixed water ballast on the aft passenger deck occurs at 907.2 kg/min (2000 lb/min) and can be completed in 16 minutes.

2. PITCH ACTIVE CONTROL SYSTEM DESCRIPTION

This section provides a general description of the PACS and then gives details of the control and avionics systems. Also, the position of PACS components in the aircraft are shown.

2.1 General Description

A simplified block diagram of the longitudinal control system of the Lockheed L-1011 aircraft equipped with PACS is depicted in Figure 6. The original control system consisted of control column, control cable, horizontal stabilizer power actuator, and stabilizer which are represented by the dashed lines. PACS components and associated signal flow paths are represented by the solid lines.

Three types of sensors provide analog signals to the PACS digital computer: Column-Trim sensor, pitch rate gyro, and dynamic pressure sensor.

The digital computer initially evaluates quality of the sensor signals. Signals that are determined to be valid are processed and sent to the pitch series servo. Signals that are determined to be invalid and which cannot be compensated for in the computer will cause the PACS to be disengaged.

Electrical signals received by the pitch series servo electro-hydraulic valves control modulating pistons which actuate mechanical controls to the stabilizer power servos. Hydraulic pressure flow from the power servos to the hydraulic actuators control the stabilizer incidence angle to provide the desired pitch attitude of the aircraft.

The symbol \otimes in Figure 6 represents the summing point at which control column and PACS signals are combined. Stabilizer rotation limits are .017 rad (+ 1 deg) to .244 rad (-14 deg) according to the sign convention shown in the figure. The total stabilizer angle within these limits consists of limited rotation ($\pm .0131$ rad, $\pm .75$ deg at $-.0175$ rad (-1 deg) stabilizer angle) provided by the PACS plus rotation caused by pilot control column inputs.

2.2 Control System

The pitch attitude of the L-1011 is controlled by the incidence angle of the horizontal stabilizer/elevator. The stabilizer control system (Figure 7) is an irreversible hydro-mechanical system consisting of the following components:

- Pilot input

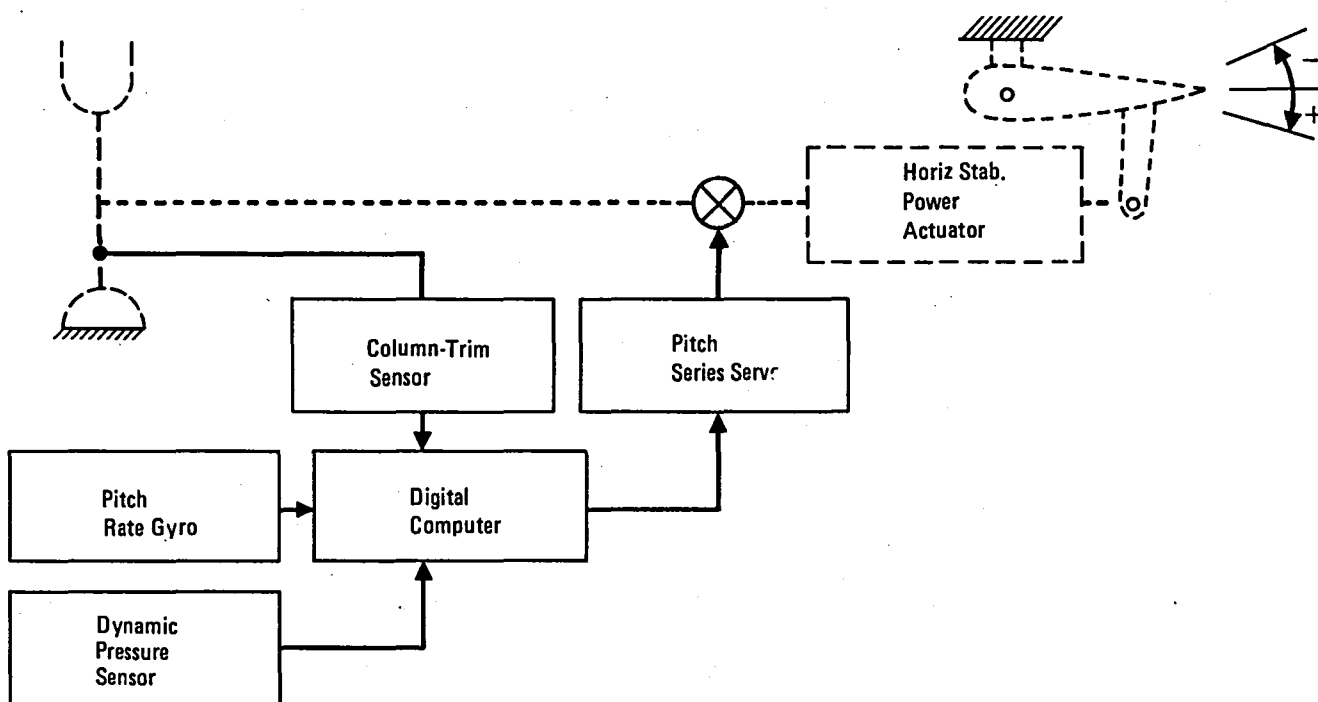


Figure 6. - Longitudinal control system with PACS.

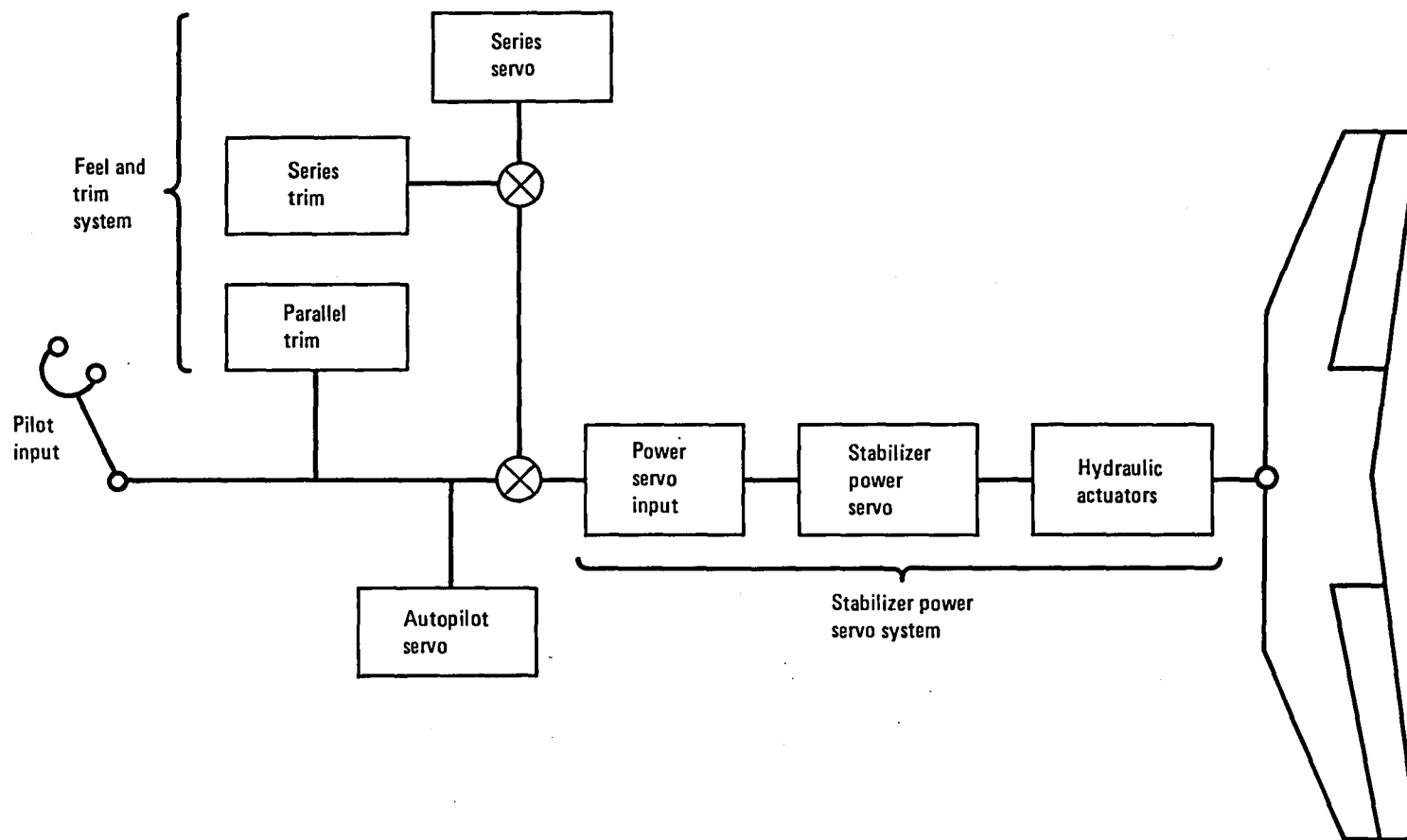


Figure 7. - Pitch control system block diagram.

- Feel and trim system
- Autopilot servo
- Stabilizer power servo system

The PACS function is to augment longitudinal stability by controlling the horizontal stabilizer through a redundant limited-authority servo in series with the pilot input. To minimize interaction with the pilot, the PACS series servo signal was summed with series trim to provide an input into the stabilizer power servo system. A schematic of the control system with the PACS series servo is shown in Figure 8.

2.2.1 Series Servo.— The series servo design and development was started under a Lockheed funded program which was discontinued due to a change in aircraft requirements. Since the National Water Lift (NWL) servo design had been completed and met the requirements of the NASA program, it was used for the near-term program.

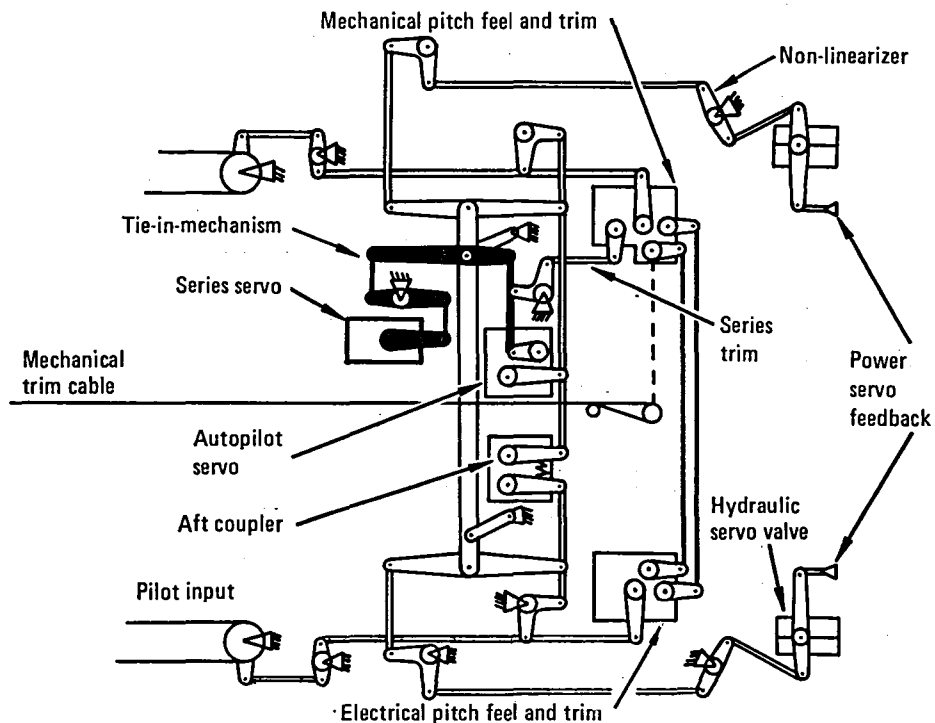


Figure 8. - Schematic of the L-1011 control system with the PACS series servo.

2.2.1.1 Series servo configuration: Figure 9 is a block diagram of the functional elements of the National Water Lift series servo. The electro-hydraulic elements (EHV's, SOL's, and LVDT's), provide a dual-dual interface with the avionics. The series servo is normally operated in an active-standby configuration with both mod pistons fully operative and monitored by the avionics system. In this configuration, the active mod piston is coupled to the output lever, while the standby mod piston is decoupled by the hydraulically-operated mod piston coupler. Shutdown of the active channel causes this channel to be bypassed hydraulically and the standby channel to be coupled to the output lever (mod piston coupler provides a pivot as shown in Figure 9). Shutoff or failure of the standby channel while the active channel is operating requires no configuration change by the coupler, but if both channels are shut off or have failed, a lock mechanism centers the active mod piston to lock the output lever in mid-position. The lock mechanism which is spring loaded to operate in the absence of hydraulic supply pressure is hydraulically retracted by either active or standby channel engagement. The mod piston coupler is a multiple piston element which is operated by standby channel hydraulic pressure and prevented from operation by active channel hydraulic pressure. Engagement of each channel is achieved by two solenoid valves (SOL's) in series controlling a spring-operated bypass/shutoff valve. The dual solenoid valves enhance the shutoff reliability in the event of system malfunction. Dual-coil electro-hydraulic valves (EHV's) and dual-coil linear variable displacement transducers (LVDT's) are used in each channel for compatibility with the dual-dual avionics circuitry.

2.2.1.2 Series servo characteristics: Specifications for the series servo are given below:

- Output stroke - ± 1.91 cm ($\pm .75$ inches)
- Output velocity - $\frac{23.93}{19.20}$ cm/sec $\left(\frac{9.42}{7.56} \text{ in/sec} \right)$
- Servo loop gain - 40 rad/sec (2,300 deg/sec)
- Linkage - all linkages and mod pistons are dual
- EHV - 2.60 liters/min (.688 gpm)
- LVDT's - .38 volt/cm/volt (0.962 volts/inch/volt)
stroke - ± 1.12 cm ($\pm .440$ inches)

The PACS authority in terms of stabilizer angle varies with aircraft trim setting. Figure 10 shows the change in stabilizer angle (Δ stabilizer angle) for a 1.91 cm (0.75 inch) series servo output stroke, as a function of the stabilizer trim angle. Thus, at high flight speeds that correspond to low stabilizer trim settings the series servo stabilizer authority is small;

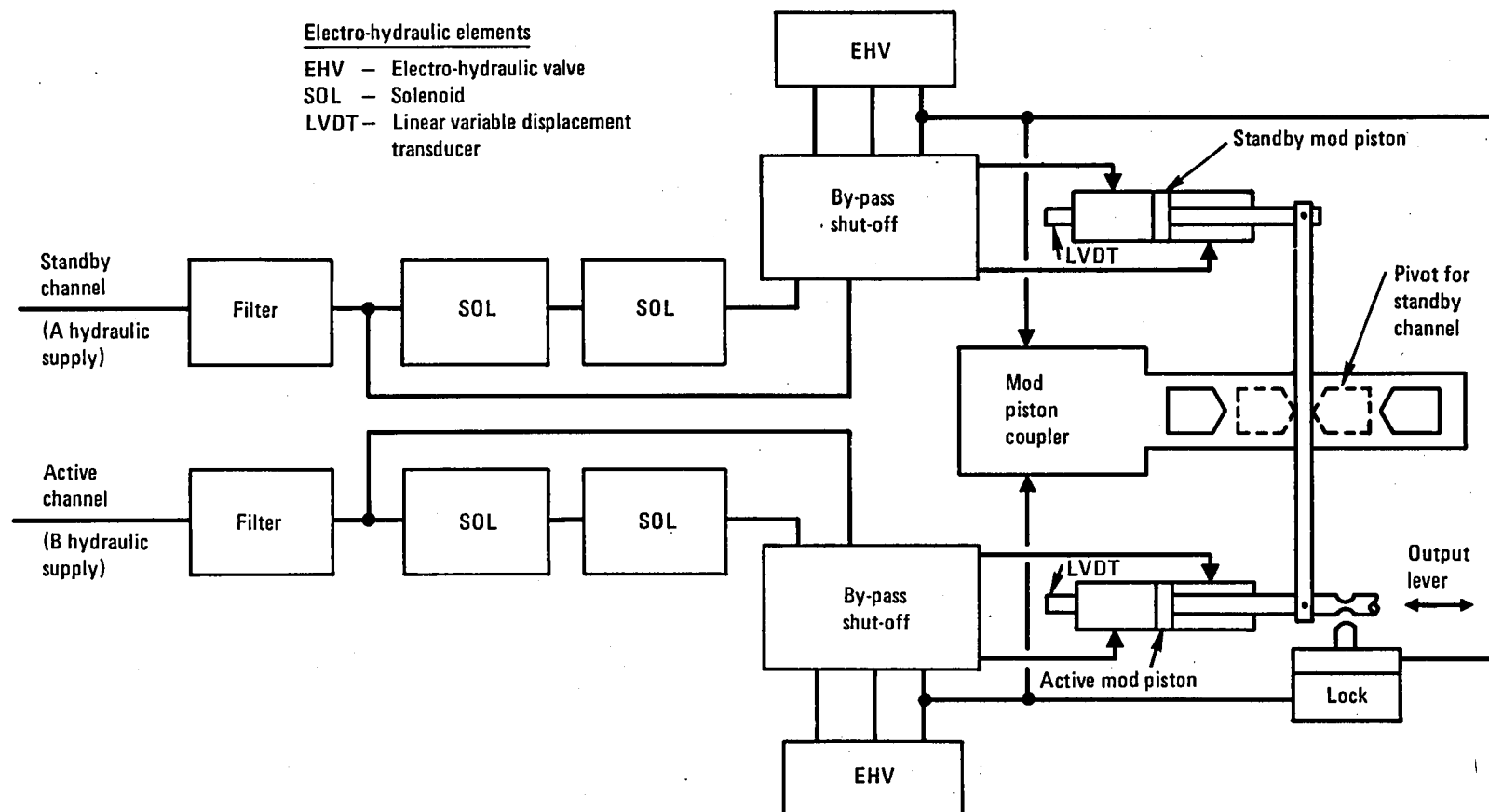


Figure 9. - Series servo functional elements.

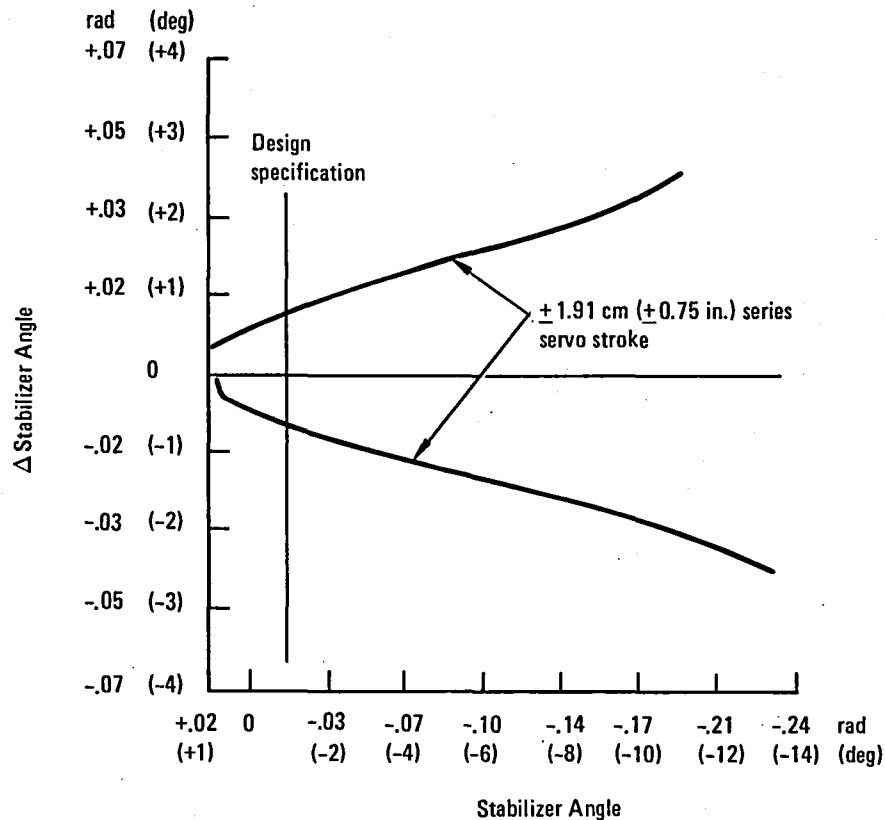


Figure 10. - Series servo authority.

whereas, at takeoff and landing speeds that correspond to large stabilizer trim settings the series servo stabilizer authority is significantly increased. This variable authority is intrinsic to the design of the L-1011 control system and is a result of the variable mechanical advantage contained in the non-linearizer (Figure 8).

The series servo shares the ground point with the trim control to provide a ground for the stabilizer input control. To overcome a system jam in flight, the pilot may impose a heavy load on the trim wheel. The resulting load into the series servo is 444.5 kg (980 lbs) maximum. The servo lock was designed to react static and dynamic loads of this magnitude.

2.2.2 Tie-in-Mechanism.- The tie-in mechanism sums the series servo output with the pitch trim output into the stabilizer control mechanism. In Figure 8, the mechanism is depicted by dark shaded linkage. It is a dual load path mechanism with each load path capable of reacting the maximum system loads. A photograph of the tie-in mechanism is shown in Figure 11.

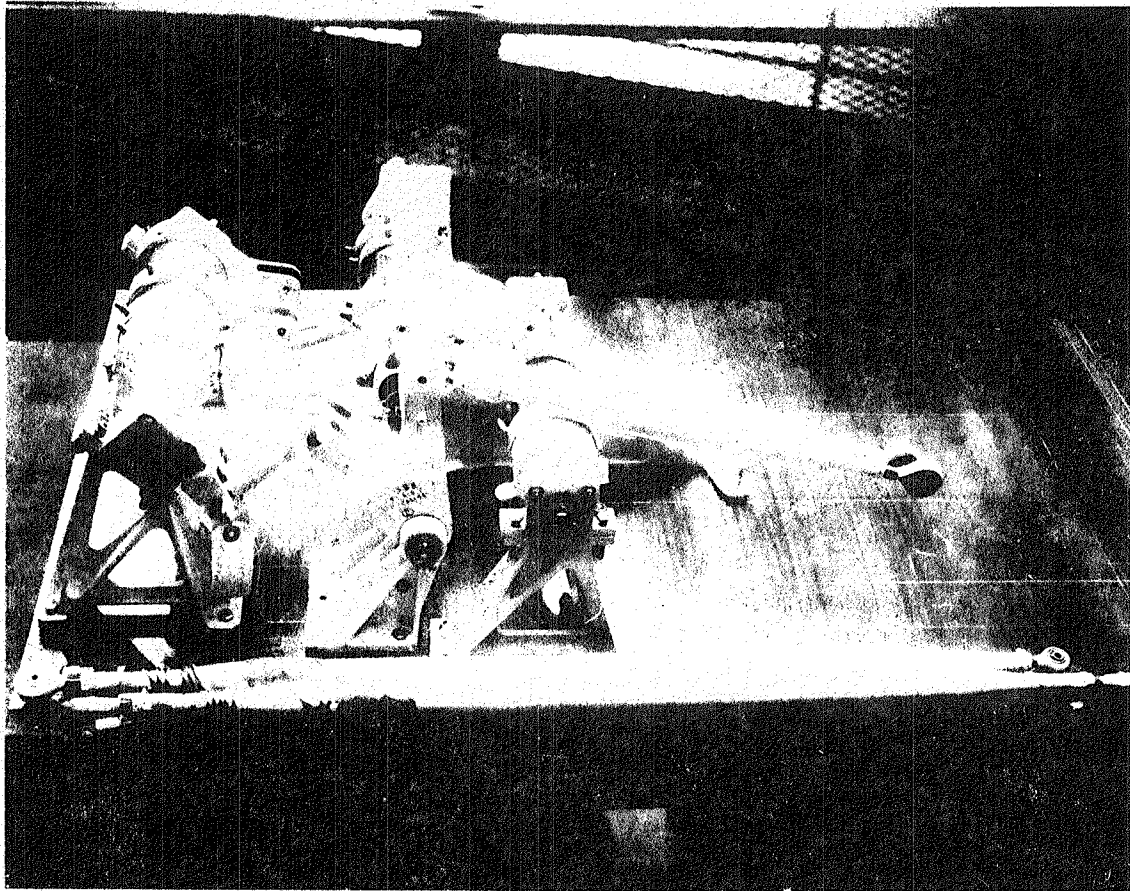


Figure 11. - Series servo tie-in mechanism.

The structural bulkhead and some of the stabilizer controls were modified to accept the increased system loads resulting from the series servo output.

2.2.3 Power Servo Modification.- The power servos were modified to install dual linear variable differential transducers (LVDT) to provide an accurate stabilizer position signal. One dual LVDT was designed into each power servo. The LVDT is actuated by the feedback arms of the servo which accurately track the stabilizer position.

2.3 Avionics System

The near-term PACS avionics system was developed by modification of two Collins ACC-201 digital computers and utilizes analog sensors. This section describes the system architecture, components, and operation. Avionics system design details are given in Appendix D.

2.3.1 System Architecture.- The PACS consists of two identical digital computers, each with dual processing channels as shown in Figure 12.

Sensors that provide inputs to the computers are shown at the top of Figure 12. The column minus trim (C-T) sensors have a quadruplex arrangement. Thus, a separate C-T sensor supplies a signal to each of the computer channels. The pitch rate gyros (PR) and dynamic pressure (Q_c) sensors have a triplex arrangement. As shown in the figure, channel A of each computer receives signals from separate PR and Q_c sensors whereas the B channel of each computer shares the signals of the number 3 sensors.

The interface between the computer and series servo is shown in the lower part of Figure 12. Computer 1 controls the active series servo channel and computer 2 controls the standby channel. The dashed lines represent servo position (SP) feedback from the mod piston LVDT's.

2.3.2 Sensor Descriptions.- Analog signals are provided by each of the sensors shown in Figure 12.

The C-T signals are provided by LVDT's which are located within the L-1011 pitch autopilot servo. The signals are proportional to the control column displacement relative to the pitch trim neutral force position. Before the C-T signals are transmitted to the PACS, they are processed by the trim augmentation computer. This computer validates status of computer d.c. power and by inference verifies a.c. power available within the computer for LVDT excitation. The power validation is required because the C-T LVDT signal is usually near null voltage and signal verification is difficult except for dynamic conditions. Demodulated d.c. C-T signals are provided by the trim augmentation computer to the PACS computer.

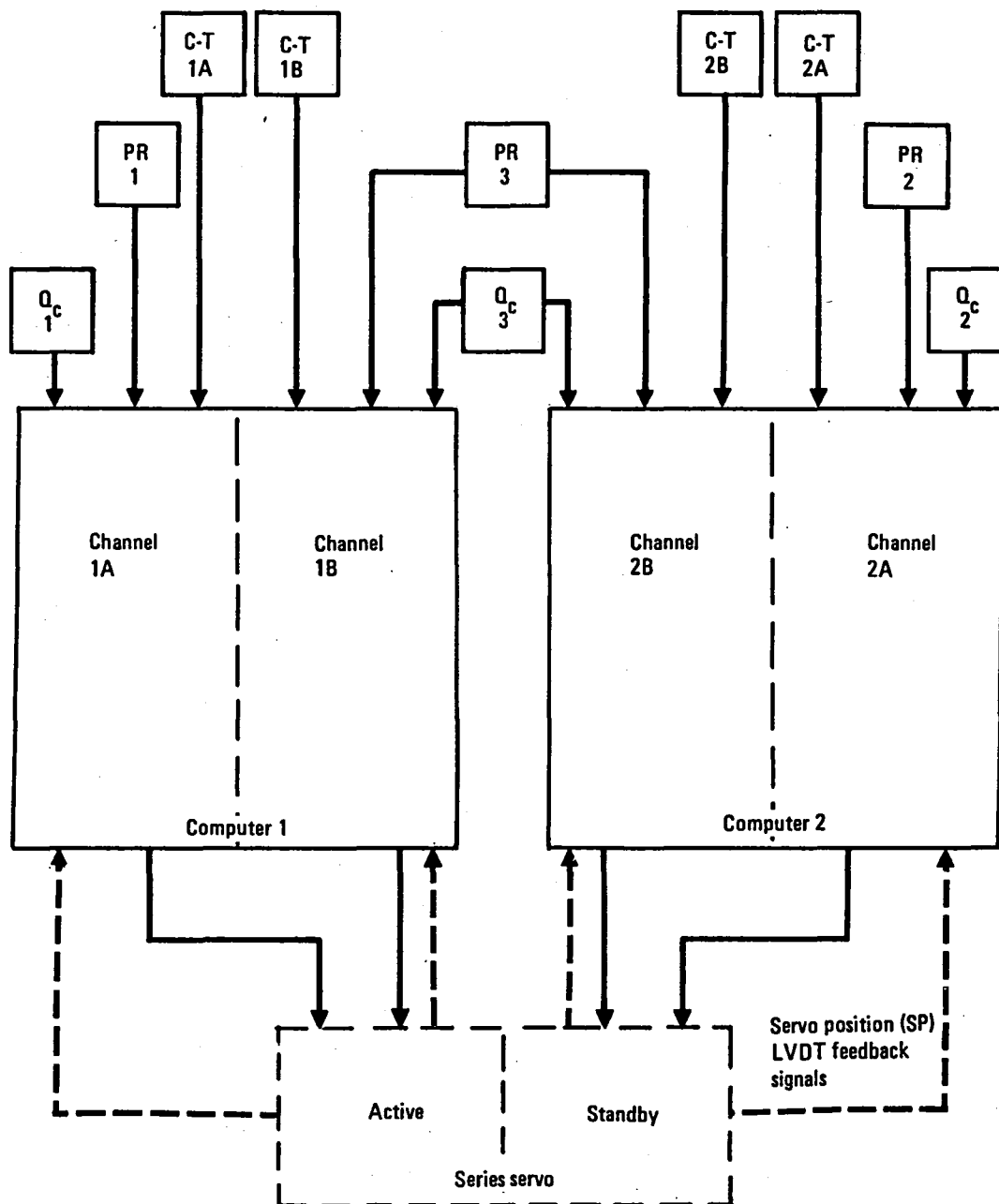


Figure 12. - PACS avionics system architecture.

Smiths Industries pitch rate gyros sense aircraft rotation about the pitch axis. The spin motor is excited by 115 volt a.c. power which also operates the PACS computer. The signal pick-off device is excited by 26 volts a.c. supplied by the PACS computer. These gyros were available from stock at Lockheed because they are used in the L-1011 yaw stability augmentation system.

Dynamic pressure sensors are used to schedule system gains and feedback time constants. These sensors were available on the flight test aircraft as part of the AACS.

2.3.3 Computer Functions.— A block diagram of the PACS avionics system is given in Figure 13. The C-T, PR, and Q_c sensor input signals used by the system are shown on the left side of the figure along with the sensor excitation voltage reference.

The C-T, PR, and Q_c signals are processed through a noise filter which limits the pass band frequency to minimize the possibility of aliasing in the conversion from analog to digital (A/D). The signal is scaled to prevent overflow. Twelve bit resolution is used which produces a least count of 4.88×10^{-4} times the full scale signal value shown above the A/D blocks on the diagram. All of the control law filter calculations are implemented by using a Tustin bilinear transformation and are performed with 32 bit fixed point operation at an iteration rate of 80 per second. After conversion to the digital domain, signals from each channel are subjected to a voting process to select the best statistical signal for processing by the computer. Each signal is normalized in the 1/PWRFAC (power factor) block as needed to minimize the effects of sensor excitation voltage variations on the loop gain.

Since the C-T signal is proportional to the column displacement from the neutral force position of the stabilizer control system and the stabilizer effectiveness varies as a function of Q_c , the signal is scheduled as a function of Q_c in the KFFD (feed-forward gain) block to minimize stick force per g variation over the airspeed range. The signal is lagged to match control system response and then passed through an eight second washout which provides for optimized aircraft response for sustained column displacement from the trim position. For experimentation, the washout may be bypassed so that the C-T signal provides a sustained command to the servo loop rather than a transient command when the washout is used. The software pallet flight test gain switch SW_4 provides a means for varying signal gain. The switch was installed to provide the capability to change the software gain in increments by positioning of the switch. It is a three position switch that provides gain variation for the C-T and PR signal blocks K_1 and K_2 and the summed C-T plus PR signal block K_3 . The switch gain factor was set as shown in Figure 13 for each signal path.

The PR signal is processed in a similar manner to the C-T signal except for the washout and is sent to the summing point. Gain scheduling of the

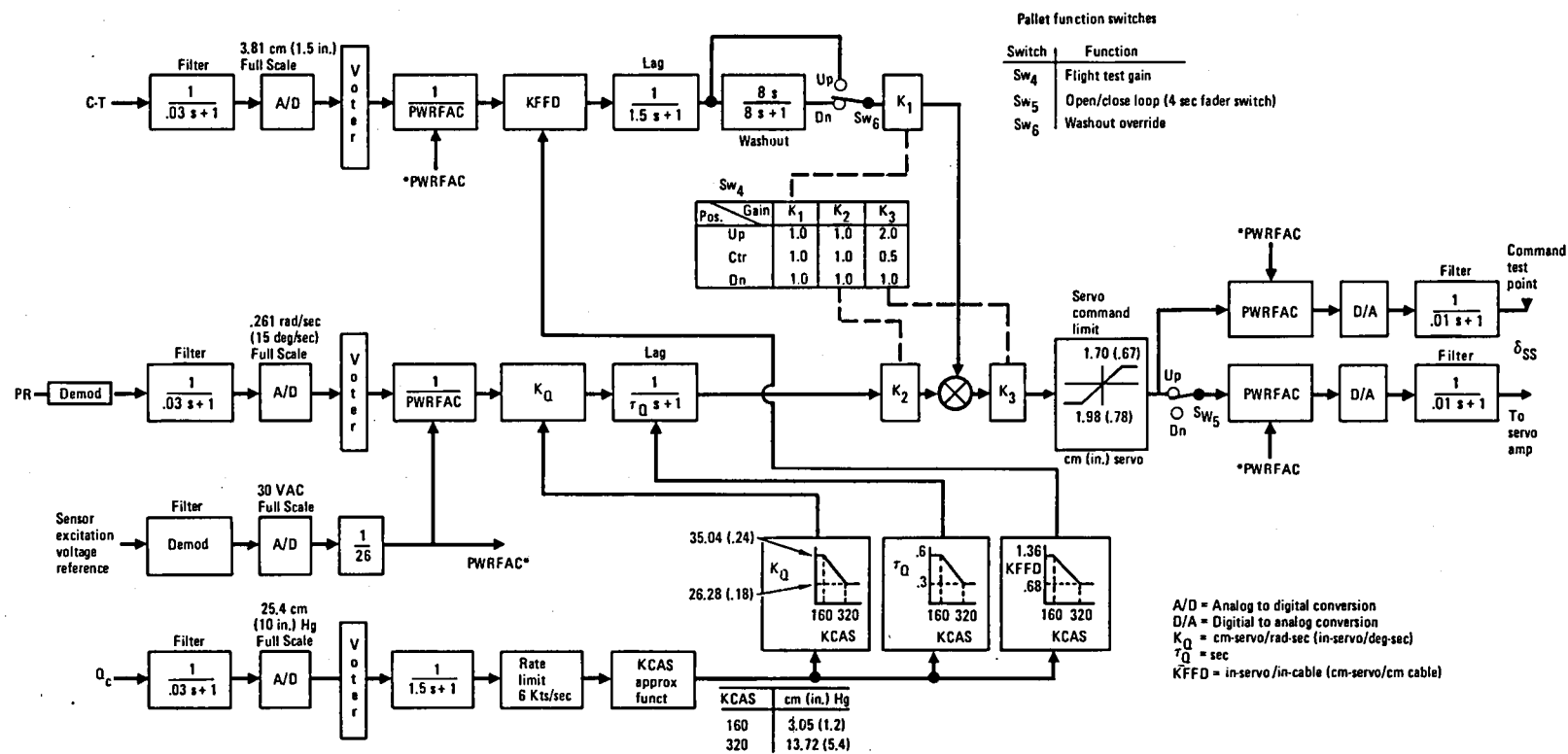


Figure 13. - near-term PACS avionics system block diagram.

signal as a function of Q_c is accomplished in block K_Q and lag scheduling is accomplished in the succeeding block.

The C-T and PR signals are summed in the software to provide command signals for the series servo. The signal is passed through block K_3 and is asymmetrically limited as designated by the block (servo command limit) to match the servo mechanical stroke limits in the nose up and nose down directions. When switch SW₅ is open, the computer is in the test mode. For normal flying switch SW₅ is closed to engage the PACS. For both the test and PACS engaged modes, the command signal is normalized (PWRFAC block) to account for varying voltage of the 26 VAC power to the series servo position transducers. The servo command is converted from a 12 bit digital format to an analog signal. This signal is filtered by a short time constant low pass analog smoothing filter to reduce cross channel time skew differences seen by the servo monitors. The resulting analog signal is summed with the series servo position feedback LVDT, amplified and sent to the series servo electro-hydraulic transfer valve. This computer/series servo interface is shown in the near-term PACS block diagram (Figure 14).

Processing of the Q_c signal includes a 6 Kts/sec rate limit and a KCAS approximating function. The airspeed signal is used to schedule the K_Q , τ_Q , and KFFD functions as indicated in the Figure 13.

The series servo loop is closed by means of servo position feedback from LVDT's (Figure 14) located within the series servo. These LVDT's sense actuator stroke and provide a proportional a.c. signal. The a.c. signal is demodulated in the PACS computer to provide a d.c. analog signal which is summed with the servo command D/A signal in the servo amplifier.

2.3.4 Avionic System Operation. - System engagement and automatic monitoring are discussed below.

2.3.4.1 System engagement: Each channel of the computer can be independently engaged by a switch in the flight station on the flight control electronic system (FCES) panel. However, if faults exist which can result in incorrect operation, the channel will not engage and the switch FAIL legend and PACS FIRST FAIL indicator legend will be illuminated on the flight station control panel.

2.3.4.2 System automatic monitoring: Each power-up cycle includes a software test of the clock frequency and the random access memory (RAM). Thereafter, the program memory is continuously monitored by the processor instruction set (CKSUM).

General software execution is monitored with a hardware device that derives its power from the software control. If the foreground fails to execute at approximately 80 times per second, the hardware monitor will not receive the required signal and will force a disengagement.

The servo D/A command from the two processors is compared by a software procedure.

A hardware monitor associated with each channel compares the left and right electro-hydraulic servo valve currents from the two processors. A second hardware monitor is used to isolate open electro-hydraulic servo valve coils.

A software procedure simulates the series servo and compares the model position with the actual position derived from the servo position transducer. The 26 VAC excitation of the series servo position transducer is monitored by the software.

2.4 PACS Installation

The location of PACS components is shown in Figure 15. This section discusses the installation of each of the major components of the system and photographs of the installed equipment are included where possible for PACS peculiar equipment.

The column-minus-trim position sensors (LVDT'S) are located within the pitch autopilot servo.

The pitch rate gyros are installed in the forward cargo compartment overhead between the transverse beams which support the passenger cabin floor. Figure 16 is a photograph of the three gyros as installed.

The Q_c sensors are installed in the forward electronics service center.

The pitch series servo is partially shown on Figure 17. A clear photograph of this unit is difficult to obtain because of space restrictions in the confined area in which it is located.

The PACS pallet installed in the forward passenger cabin provides space for mounting two PACS computers, four core memories, four test adapters, a Digital Equipment Corporation PDP-11 minicomputer, and a terminal for control and monitoring of the test adapters. Figure 18 shows the pallet with the fault isolation panel on top.

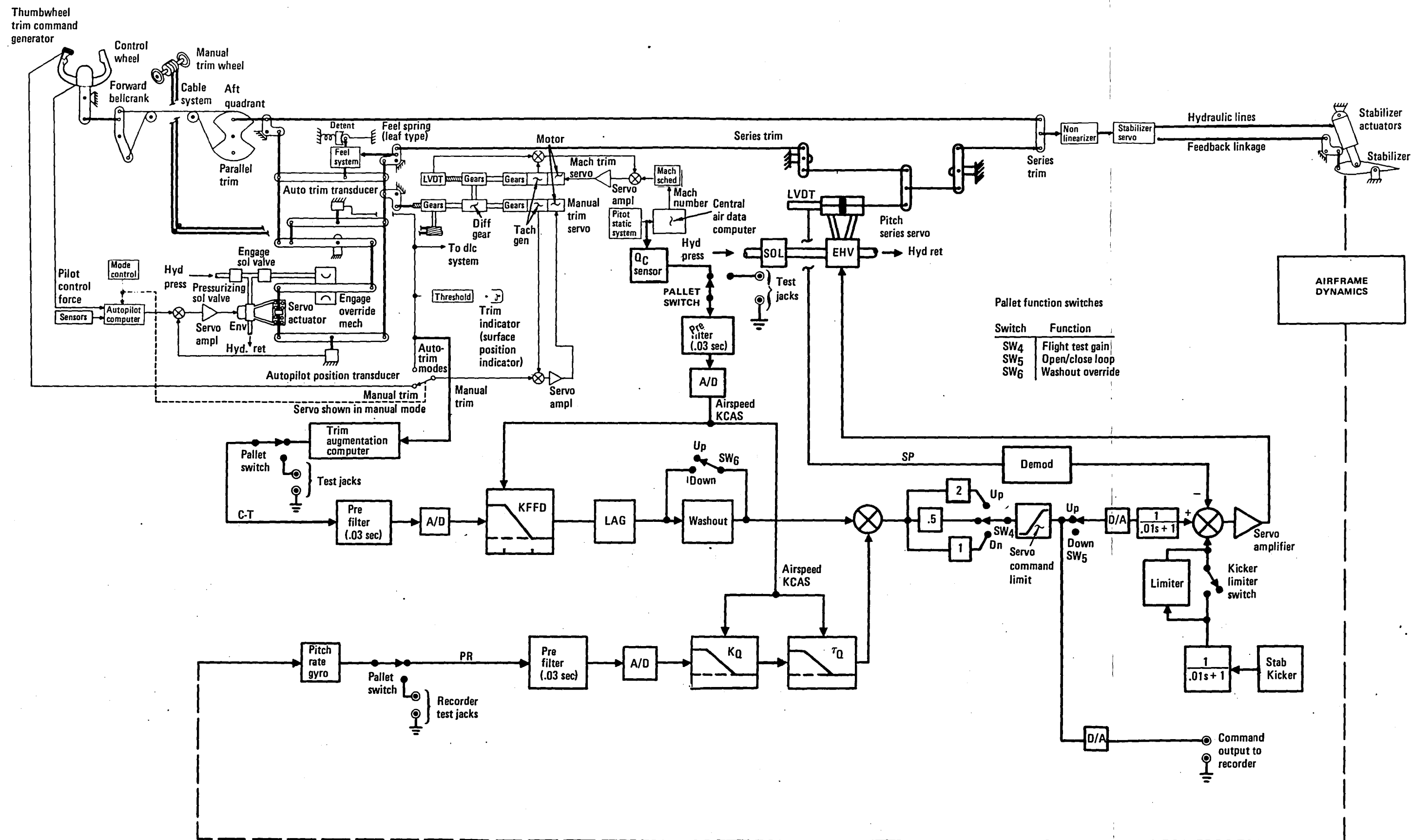


Figure 14. - Near-term PACS block diagram.

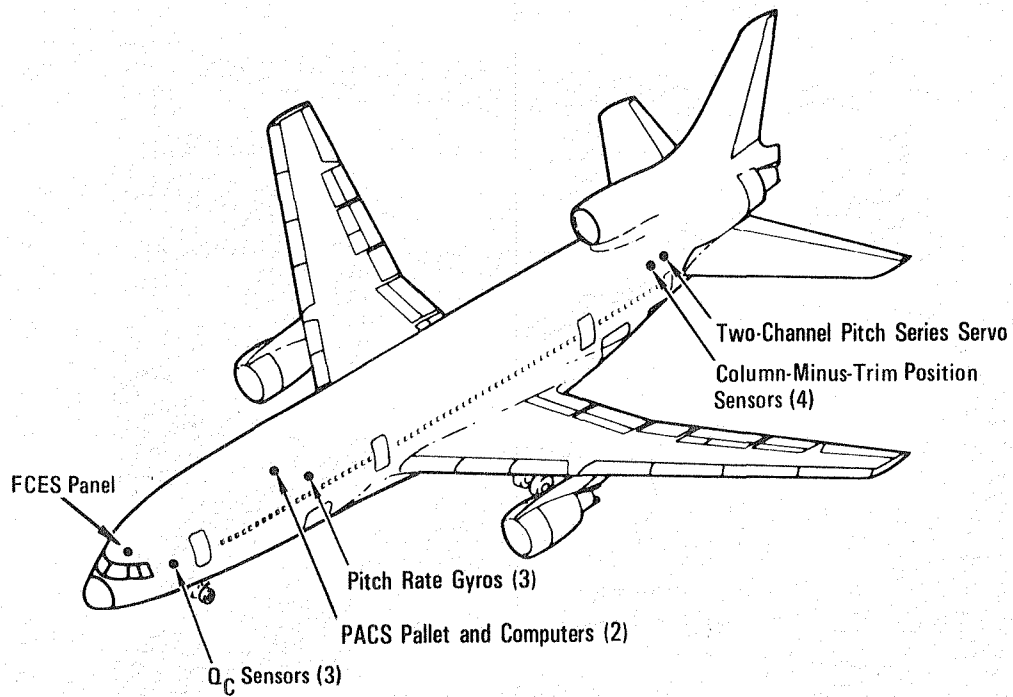
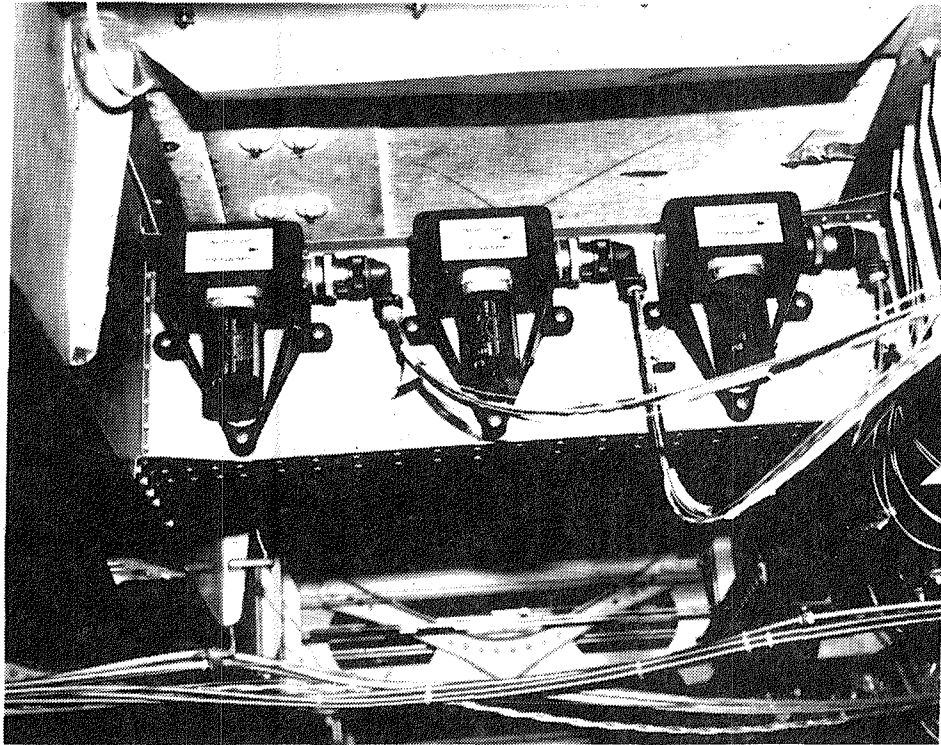
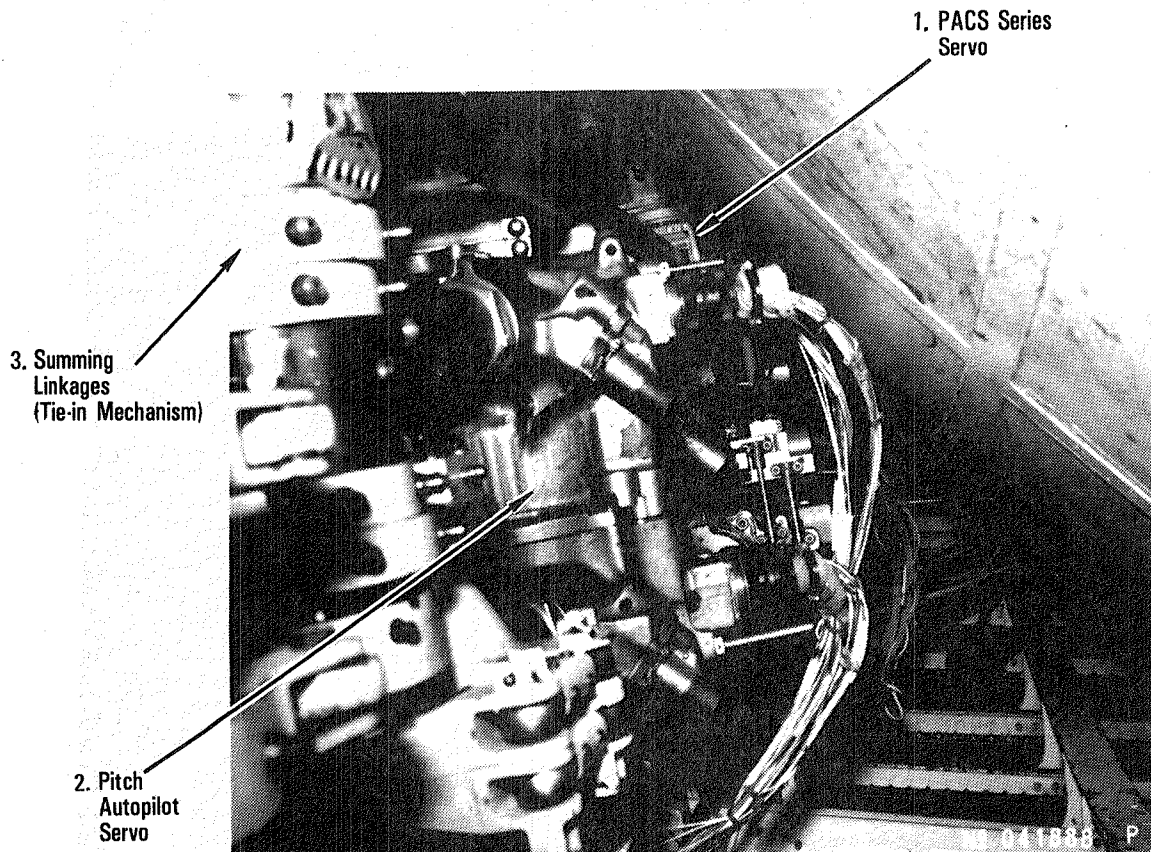


Figure 15. - Location of PACS components.



The plate on which the gyros are mounted is 6.04 cm (2.38 inches) to the right of the aircraft centerline and between the FS 729 and 749 floor beams.

Figure 16. - PACS pitch rate gyros.

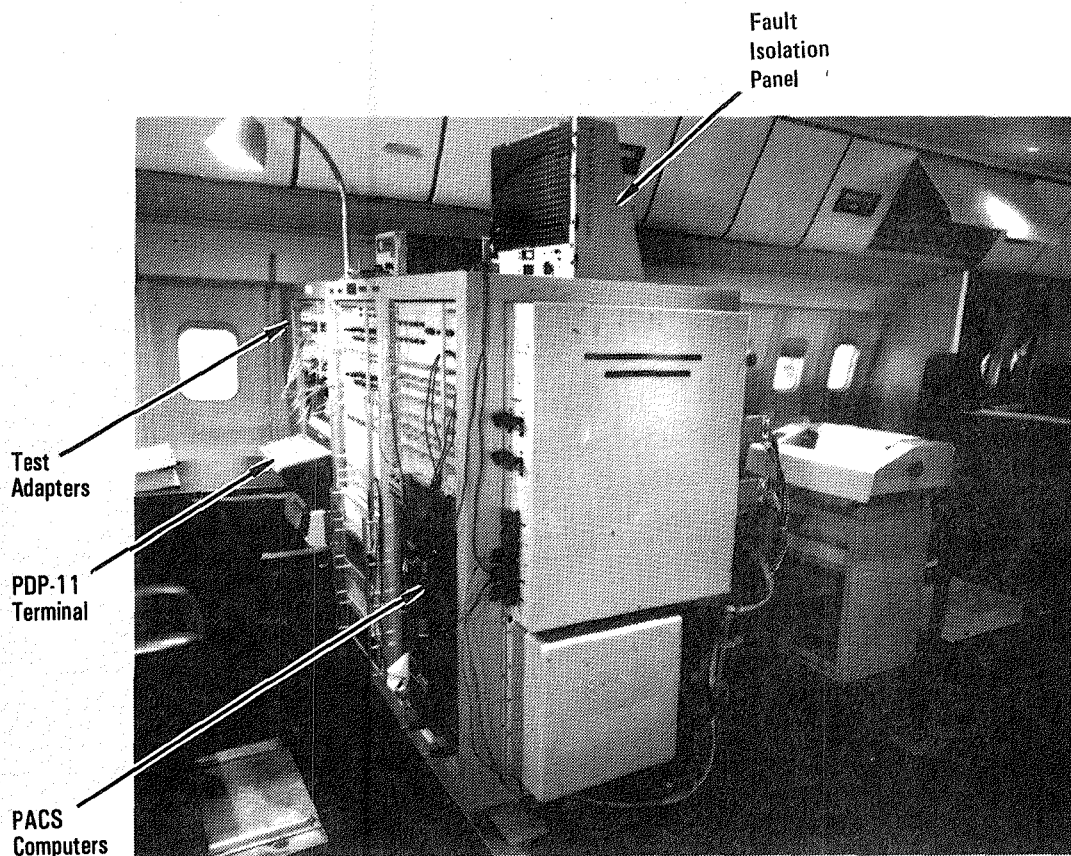


1. Center background - PACS series servo.
2. Left center foreground - Pitch autopilot servo in which the column minus trim LVDT's are located.
3. Left foreground - Summing linkages which connect the series servo to the pitch primary flight controls.

NOTE: The curved surface in the upper right is the aft pressure bulkhead. The skin of the airplane is in the lower right of the photograph.

View is toward the left side of the aircraft.

Figure 17. - Location of several PACS components.



PACS computers are the black boxes installed in the lower part of the pallet. The pallet also contains computer wiring intercept capability, magnetic core memories for PACS program storage, and a PDP-11 terminal for interfacing with the transfer busses of each PACS computer. View is looking towards the left and forward.

Figure 18. - PACS pallet installation in flight test aircraft.

3. DESIGN AND ANALYSIS

This section describes approaches and methods used in development of the near-term PACS.

3.1 Flying Qualities

The process of relaxing the requirement for longitudinal static stability causes a significant degradation in flying qualities of the airplane. This degradation in flying qualities is manifested by a deterioration of airplane handling in terms of: (1) dynamic characteristics, particularly the short-period but to some extent the phugoid also, (2) maneuver stability force-feel characteristics, (3) speed stability, and (4) trimmability. Therefore, it is necessary to incorporate an augmentation system into the airplane to compensate for this degradation in flying qualities.

The objective of this phase of the study is to develop a stability and control augmentation system: (1) which will permit a commercial transport type aircraft to operate at reduced static margins approaching the neutral point, and (2) which can be incorporated into current operational aircraft in the near term.

3.1.1 Handling Qualities Criteria.- The approach to developing the near-term pitch active control system was to use the current L-1011 in the manual control mode as the minimum standard of acceptable performance. The relaxed stability airplane with augmentation was designed such that handling qualities are at least as good as those of the current L-1011.

The L-1011 is designed to meet Part 25 of the Federal Aviation Regulations (Reference 2). This specification tends to be qualitative in nature so a number of other references were used to formulate a more quantitative set of design criteria. Among the more widely recognized criteria are:

- Military Specification, Flying Qualities of Piloted Airplanes, MIL-F-8785C (Reference 3).
- SAE Design Objectives for Flying Qualities of Civil Transport Aircraft, Aerospace Recommended Practice, ARP 842B (Reference 4).

These references are used primarily as a source for defining dynamic response requirements, and in particular the modal characteristics (e.g., short-period and phugoid frequency and damping). The philosophy adopted in this study was to develop an augmentation system which generally satisfies all of the above listed criteria including FAR Part 25 requirements.

3.1.2 Flight Conditions. - Development of the stability augmentation system concentrated on regions of the flight envelope which were defined for the test program. These flight regimes are depicted by the shaded areas shown in Figure 19. The specific conditions defined for augmentation system analysis and development are listed in Table 2.

3.1.3 Aerodynamic Data. - L-1011 S/N 1001 is a unique configuration in that it is the original Dash 1 version which has the long fuselage, but it has the extended wing tips and active aileron control system (AACS) common only to the shorter fuselage Dash 500 derivative. Furthermore, for the relaxed static stability flight test program, the elevator was downrigged to compensate for the loss in nose-down control capability as the c.g. is moved aft. The elevator downrig was designed to provide a nose-down angular acceleration margin of -0.1 rad/sec^2 (5.73 deg/sec^2) at the critical high angle of attack condition shown in Figure 20.

As a result of these unique configuration differences, it was necessary to perform wind-tunnel tests to define the basic airplane longitudinal aerodynamic characteristics and to determine the effect of elevator downrig on horizontal tail loads. The wind-tunnel test program is discussed in Section 4.1.

The high-speed longitudinal aerodynamic data were further refined in the nonlinear, high angle of attack region based on results of flight test data matching performed in connection with the L-1011-500 certification program. The resulting basic controls undeflected lift versus pitching moment characteristics are shown in Figure 21. In this figure, each moment coefficient versus lift coefficient curve is plotted in the standard format. However, to distinguish Mach number effects clearly, the axes of each curve are displaced horizontally as a function of Mach number.

Low-speed longitudinal stability data for the flight test aircraft in the landing configuration are shown in Section 4.1.

The primary difference in drag between the flight test aircraft, and a standard L-1011-1 is the small reduction in induced drag due to the extended wing tips. This has such a small effect on the stability and control analysis that drag polars are not presented in this report.

The longitudinal control effectiveness of the S/N 1001 stabilizer and elevator is basically the same as for a standard L-1011-1 except for the five degrees elevator downrig which is discussed in Section 4.1.

Part of the aerodynamic task was to determine the longitudinal stability and control derivatives required for development of the PACS. These derivatives were determined by means of a standard computer program which determines initial trim conditions for a particular flight condition, and which uses an incrementing procedure to extract linear derivatives from the nonlinear aerodynamic data at these trim conditions. Table 3 presents a listing of the initial trim conditions and corresponding stability and control derivatives for the flight conditions defined in Table 2.

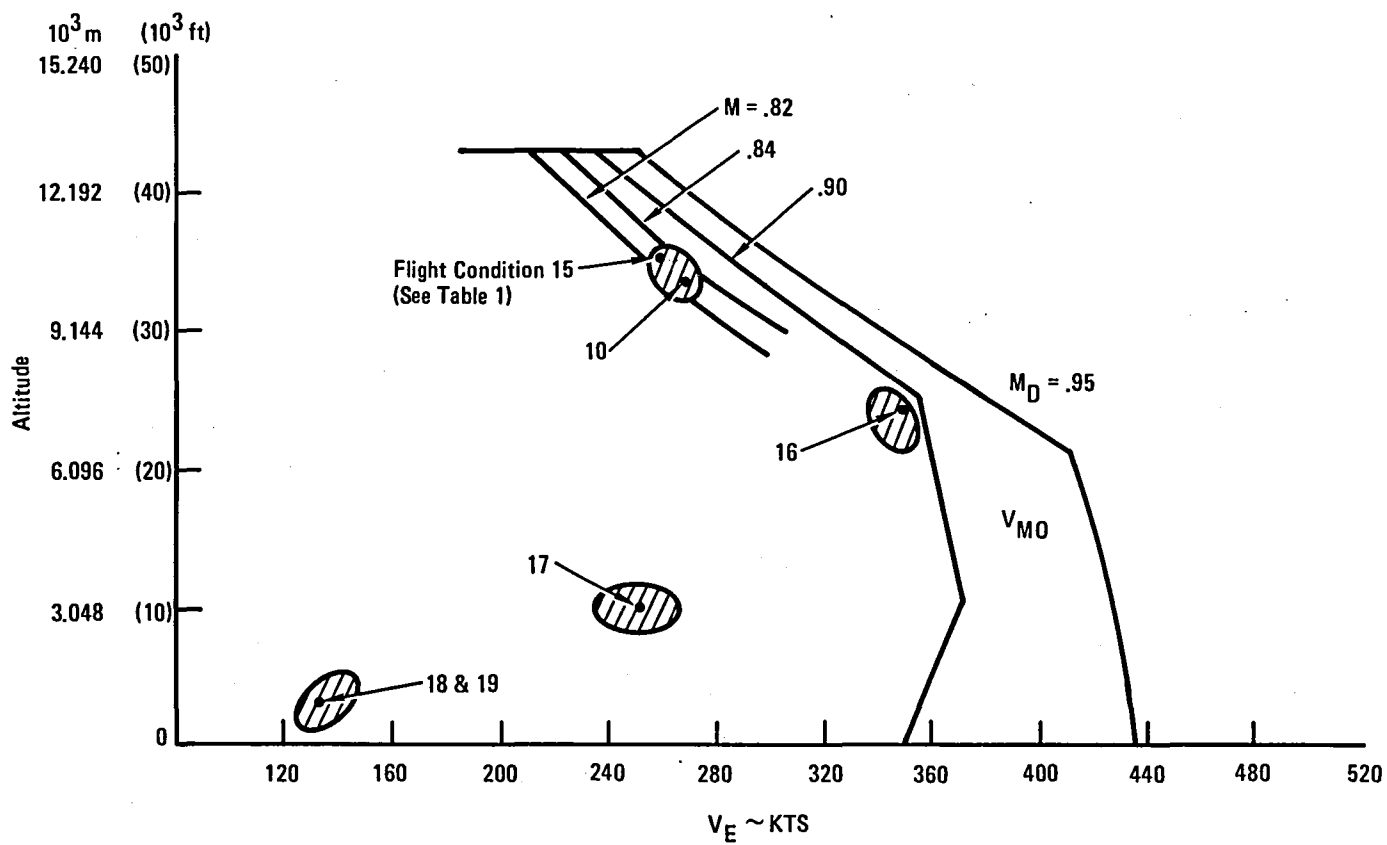


Figure 19. - Flight envelope.

TABLE 2. - FLIGHT CONDITIONS

| FLIGHT CONDITION | WEIGHT 1000 kg (lb) | c.g. % mac | ALTITUDE 1000 m (ft) | V _E (KEAS) |
|---|------------------------|---------------|-------------------------|------------------------------|
| 10. Cruise W/δ = 6.3 x 10 ⁵ kg (1.4 x 10 ⁶ lb) | 163.3 (360) | 25 to 39 | 10.1 (33) | 280 (M = 0.83) |
| 15. Cruise W/δ = 7.3 x 10 ⁵ kg (1.6 x 10 ⁶ lb) | 163.3 (360) | 25 to 39 | 11.0 (36) | 260 (M = 0.83) |
| 16. MMO/VMO | 158.8 (350) | 25 to 39 | 7.6 (25) | 357 |
| 17. Holding | 152.0 (335) | 25 to 39 | 3.0 (10) | 250 |
| 18. Landing (δF = .576 rad (33 deg)) | 149.7 (330) | 25 to 39 | 0.6 (2) | 135 (1.3 V _S) |
| 19. Takeoff (δF = .384 rad (22 deg)) | 172.4 (380) | 25 to 39 | 0.6 (2) | 137 (1.2 V _S) |

3.1.4 PACS Concept.— The near-term augmentation system was formulated from a knowledge of characteristics of the unaugmented airplane at relaxed stability conditions as determined from previous flight simulation results (Reference 1). The simulation revealed that:

- Flying qualities of the unaugmented airplane remained in the acceptable region (Cooper-Harper ratings of 3½ to 6½) for initial trim conditions of reduced but slightly positive stability approaching the neutral point.
- Short-period angular frequency and damping characteristics are marginally satisfactory and continue to degrade as the c.g. is moved aft toward the neutral point.

Based on this knowledge, it was concluded that good handling qualities could be achieved with a relatively simple augmentation system, which would also be highly reliable. This system was conceived as a lagged pitch rate damper with a washed-out column feed-forward loop. The damper serves to provide the necessary short-period frequency and damping characteristics while also suppressing turbulence effects, and the feed-forward was designed to "quicken" the pitch rate response and reduce stick force gradients without affecting system stability. A block diagram of the near-term pitch active control system is shown in Figure 14.

The various elements of the near-term PACS were designed based primarily on a consideration of short-period dynamics and maneuver stability characteristics. Elements of the pitch damper loop were selected to give improved short-period characteristics while minimizing interference to pitch control inputs by means of the lag function. The feed-forward loop was designed to provide column force-feel characteristics in maneuver equivalent to the basic airplane at conventional static stability conditions and to further compensate for whatever pitch control interference the pilot may feel due to the damper.

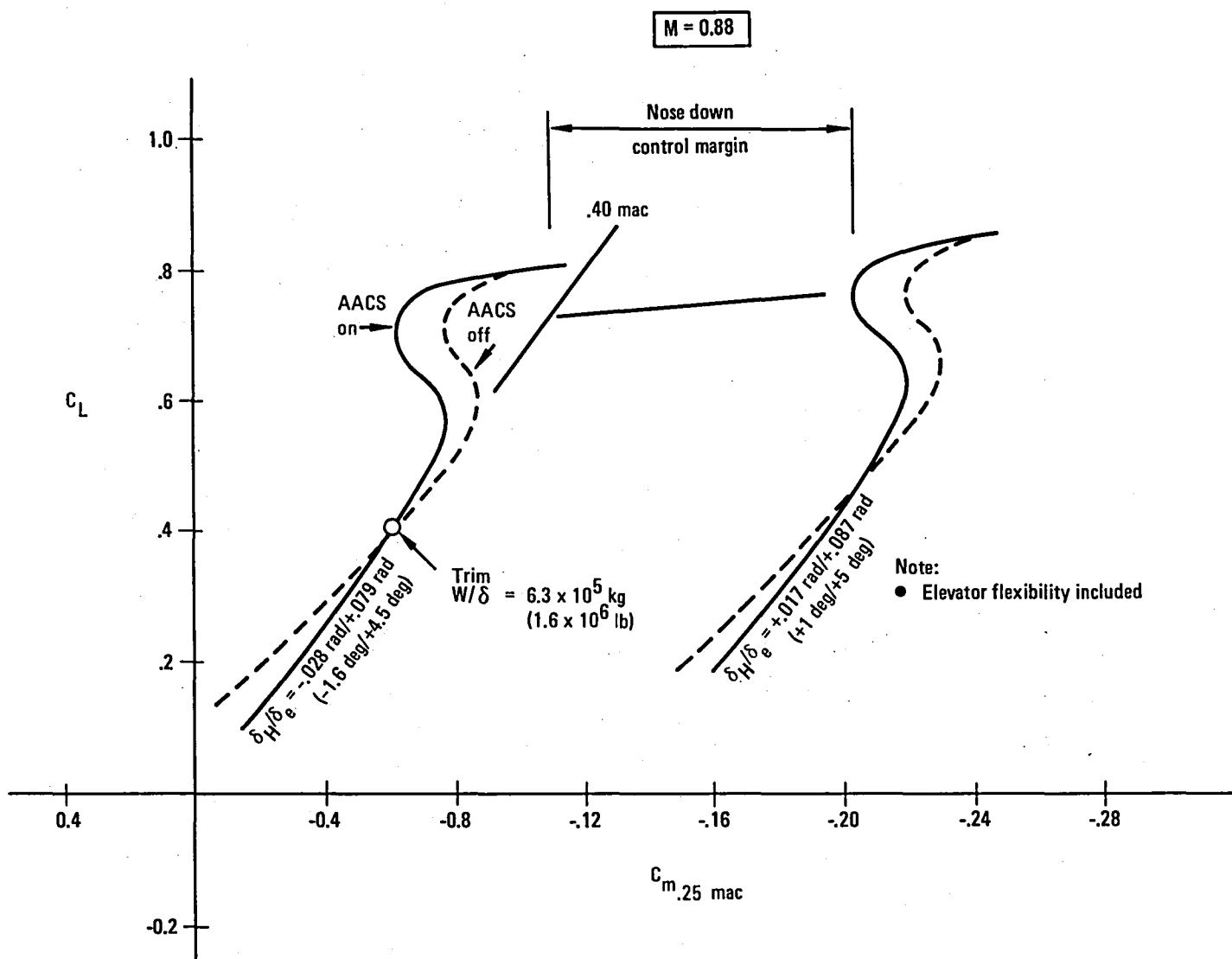


Figure 20. - Elevator downrig required for nose-down control.

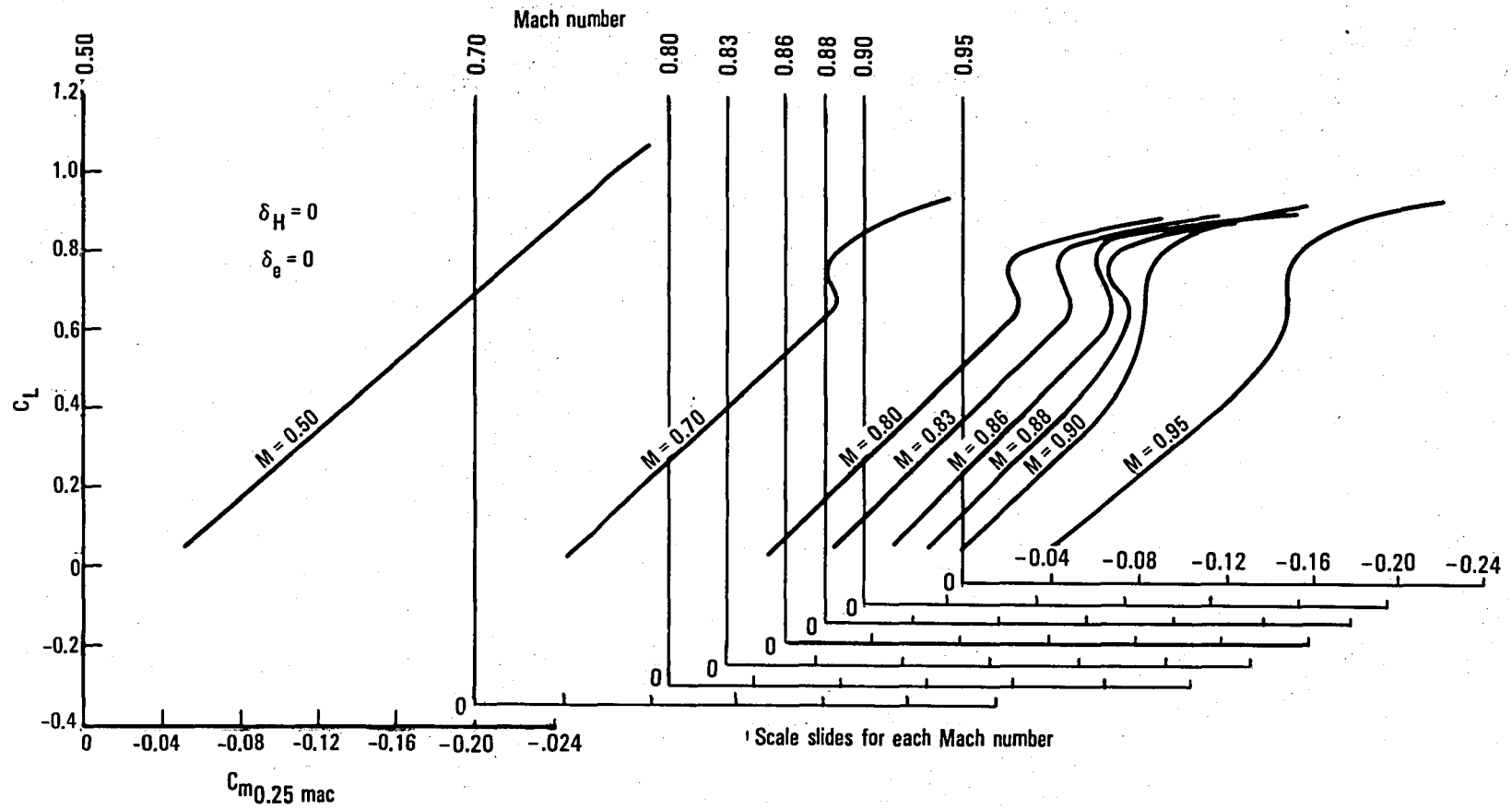


Figure 21. - L-1011-1 S/N 1001 High-speed pitching moment characteristics.

TABLE 3a. - STABILITY AND CONTROL DERIVATIVES (S.I. UNITS)

(SHEET 1 OF 2)

FLIGHT CONDITIONS

| | 10 | | 15 | | 16 | | 17 | | 18 | | 19 | |
|--|---------|--------|---------|--------|---------|--------|---------|--------|---------|--------|---------|--------|
| W ~ kg | 163,300 | | 163,300 | | 158,800 | | 152,000 | | 149,700 | | 172,400 | |
| V _E ~ Kts | 280 | | 260 | | 357 | | 250 | | 135 | | 137 | |
| h ~ m | 10,100 | | 11,000 | | 7,600 | | 3,000 | | 600 | | 600 | |
| δ_F ~ rad | 0 | | 0 | | 0 | | 0 | | .576 | | .384 | |
| c.g. ~ % mac | 25 | 39 | 25 | 39 | 25 | 39 | 25 | 39 | 25 | 39 | 25 | 39 |
| α ~ rad | .0550 | .0517 | .0646 | .0607 | .0321 | .0304 | .0850 | .0799 | .1784 | .1647 | .2284 | .2115 |
| δ_H ~ rad | -.0471 | -.0300 | -.0522 | -.0328 | -.0335 | -.0225 | -.0583 | -.0373 | -.1244 | -.0670 | -.1232 | -.0585 |
| $C_{L\alpha}$ ~ rad ⁻¹ | 7.32 | 7.27 | 7.33 | 7.32 | 7.39 | 7.39 | 5.50 | 5.50 | 6.30 | 6.30 | 5.73 | 5.73 |
| $C_{D\alpha}$ ~ rad ⁻¹ | .456 | .412 | .646 | .535 | .246 | .232 | .253 | .187 | 1.135 | .951 | 1.165 | 1.023 |
| $C_{m\alpha}$ ~ rad ⁻¹ | -1.43 | -.42 | -1.43 | -.41 | -1.22 | -.18 | -1.13 | -.36 | -1.46 | -.64 | -1.46 | -.66 |
| C_{Lq} | 9.89 | 9.89 | 9.87 | 9.87 | 10.14 | 10.14 | 8.31 | 8.31 | 8.00 | 8.00 | 8.00 | 8.00 |
| C_{mq} | -20.21 | -19.04 | -19.47 | -18.38 | -20.64 | -19.22 | -18.09 | -16.93 | -16.95 | -15.83 | -16.96 | -15.84 |
| $C_{L\dot{\alpha}}$ | 4.18 | 4.18 | 4.14 | 4.14 | 4.75 | 4.75 | 2.40 | 2.40 | 2.00 | 2.00 | 2.00 | 2.00 |
| $C_{m\dot{\alpha}}$ | -10.21 | -9.62 | -10.12 | -9.54 | -11.77 | -11.10 | -6.06 | -5.73 | -5.20 | -4.92 | -5.20 | -4.92 |
| $C_{L\delta_H}$ ~ rad ⁻¹ | 1.43 | 1.33 | 1.50 | 1.34 | 1.30 | 1.29 | 1.42 | 1.32 | 1.89 | 1.39 | 1.86 | 1.39 |
| $C_{m\delta_H}$ ~ rad ⁻¹ | -3.54 | -3.09 | -3.68 | -3.12 | -3.20 | -3.01 | -3.51 | -3.07 | -4.66 | -3.25 | -4.60 | -3.24 |
| $C_{L\delta_{AC}}$ ~ rad ⁻¹ | .079 | .079 | .101 | .102 | -.009 | -.009 | .152 | .155 | .237 | .237 | .202 | .213 |
| $C_{D\delta_{AC}}$ ~ rad ⁻¹ | -.010 | -.011 | -.009 | -.010 | -.013 | -.013 | -.007 | -.007 | .005 | .003 | .011 | .009 |
| $C_{m\delta_{AC}}$ ~ rad ⁻¹ | -.131 | -.120 | -.147 | -.134 | -.065 | -.066 | -.183 | -.162 | -.259 | -.232 | -.218 | -.200 |
| C_{L_u} | .4240 | .4089 | .5065 | .4911 | .0656 | .0729 | .0126 | .0122 | 0 | 0 | 0 | 0 |
| C_{D_u} | .0868 | .0790 | .1283 | .1096 | .0299 | .0281 | -.0013 | -.0014 | 0 | 0 | 0 | 0 |
| C_{m_u} | -.0323 | .0254 | -.0576 | .0134 | -.0945 | -.0886 | .0090 | .0103 | 0 | 0 | 0 | 0 |
| T _m ~ N | 3630 | 2350 | 20460 | 17440 | 10090 | 8990 | -37540 | -37420 | -93260 | 89820 | 118950 | 118950 |
| T _h ~ N/m | -2.8 | -2.6 | -4.2 | -3.9 | -3.4 | -3.2 | -2.5 | -2.3 | -6.0 | -5.5 | -11.4 | -11.4 |

TABLE 3b. - STABILITY AND CONTROL DERIVATIVES (ENGLISH UNITS)
(SHEET 2 OF 2)
FLIGHT CONDITIONS

| | 10 | | 15 | | 16 | | 17 | | 18 | | 19 | |
|---|---------|---------|---------|---------|---------|---------|---------|---------|---------|---------|---------|---------|
| W ~ lbs | 360,000 | | 360,000 | | 350,000 | | 335,000 | | 330,000 | | 380,000 | |
| V _e ~ Kts | 280 | | 260 | | 357 | | 250 | | 135 | | 137 | |
| h ~ ft | 33,000 | | 36,000 | | 25,000 | | 10,000 | | 2,000 | | 2,000 | |
| $\delta_F \sim \text{deg}$ | 0 | | 0 | | 0 | | 0 | | 33 | | 26 | |
| c.g. ~ % mac | 25 | 39 | 25 | 39 | 25 | 39 | 25 | 39 | 25 | 39 | 25 | 39 |
| $\alpha \sim \text{deg}$ | 3.15 | 2.96 | 3.70 | 3.48 | 1.84 | 1.74 | 4.87 | 4.58 | 10.22 | 9.44 | 13.09 | 12.12 |
| $\delta_H \sim \text{deg}$ | -2.70 | -1.72 | -2.99 | -1.88 | -1.92 | -1.29 | -3.34 | -2.14 | -7.13 | -3.84 | -7.06 | -3.35 |
| $C_{L\alpha} \sim \text{deg}^{-1}$ | .1278 | .1268 | .1280 | .1277 | .1289 | .1289 | .0960 | .0960 | .1100 | .1100 | .1000 | .1000 |
| $C_{D\alpha} \sim \text{deg}^{-1}$ | .00796 | .00720 | .01128 | .00934 | .00429 | .00405 | .00441 | .00326 | .01980 | .01660 | .02034 | .01785 |
| $C_{m\alpha} \sim \text{deg}^{-1}$ | -.0250 | -.0073 | -.0250 | -.0071 | -.0213 | -.0032 | -.0197 | -.0063 | -.0255 | -.0111 | -.0255 | -.0115 |
| C_{Lq} | 9.89 | 9.89 | 9.87 | 9.87 | 10.14 | 10.14 | 8.31 | 8.31 | 8.00 | 8.00 | 8.00 | 8.00 |
| C_{mq} | -20.21 | -19.04 | -19.47 | -18.38 | -20.64 | -19.22 | -18.09 | -16.93 | -16.95 | -15.83 | -16.96 | -15.84 |
| $C_{L\dot{\alpha}}$ | 4.18 | 4.18 | 4.14 | 4.14 | 4.75 | 4.75 | 2.40 | 2.40 | 2.00 | 2.00 | 2.00 | 2.00 |
| $C_{m\dot{\alpha}}$ | -10.21 | -9.62 | -10.12 | -9.54 | -11.77 | -11.10 | -6.06 | -5.73 | -5.20 | -4.92 | -5.20 | -4.92 |
| $C_{L\delta_H} \sim \text{deg}^{-1}$ | .0250 | .0232 | .0261 | .0234 | .0227 | .0225 | .0248 | .0230 | .0329 | .0243 | .0325 | .0243 |
| $C_{m\delta_H} \sim \text{deg}^{-1}$ | -.0617 | -.0540 | -.0642 | -.0545 | -.0559 | -.0525 | -.0612 | -.0535 | -.0813 | -.0567 | -.0802 | -.0566 |
| $C_{L\delta_{AC}} \sim \text{deg}^{-1}$ | .00137 | .00138 | .00177 | .00178 | -.00015 | -.00015 | .00266 | .00271 | .00414 | .00414 | .00352 | .00372 |
| $C_{D\delta_{AC}} \sim \text{deg}^{-1}$ | -.00018 | -.00019 | -.00016 | -.00017 | -.00023 | -.00023 | -.00012 | -.00013 | .00008 | .00005 | .00019 | .00015 |
| $C_{m\delta_{AC}} \sim \text{deg}^{-1}$ | -.00228 | -.00209 | -.00257 | -.00233 | -.00114 | -.00116 | -.00320 | -.00282 | -.00450 | -.00405 | -.00380 | -.00349 |
| C_{L_u} | .4240 | .4089 | .5065 | .4911 | .0656 | .0729 | .0126 | .0122 | 0 | 0 | 0 | 0 |
| C_{D_u} | .0868 | .0790 | .1283 | .1096 | .0299 | .0281 | -.0013 | -.0014 | 0 | 0 | 0 | 0 |
| C_{m_u} | -.0323 | .0254 | -.0576 | .0134 | -.0945 | -.0886 | .0090 | .0103 | 0 | 0 | 0 | 0 |
| T _m ~ lb | 816 | 529 | 4602 | 3924 | 2270 | 2023 | -8446 | -8419 | -20980 | -20206 | -26759 | -26759 |
| T _h ~ lb/ft | -.19 | -.18 | -.29 | -.27 | -.23 | -.22 | -.17 | -.16 | -.41 | -.38 | -.78 | -.78 |

Preliminary analysis of the pitch damper loop was performed to determine the effect of gain and lag time constant quantities on short-period characteristics. At the time of this preliminary analysis, the augmentation system did not contain all of the hardware elements later defined as part of the avionics system analysis and did not include the effect of active ailerons used for maneuver load control. Therefore, additional analysis of short-period characteristics was performed as part of the avionics system development which is discussed in Section 3.3. Example results of the preliminary parametric study are shown in Figure 22. These data show the effect of loop gain and lag time constant on system angular frequency and damping characteristics. The approach for selecting the proper configuration of loop gain and lag time constant was guided not only by the need to provide acceptable short-period dynamics but also suitable maneuver stability characteristics without requiring excessive augmentation authority, which would have a critical effect on structural loads in the case of a hardover failure. It was necessary to meet this delicate balance of requirements for the range of c.g. and other flight conditions planned for the test program.

Maneuver stability analysis progressed on the basis of a preliminary selection of pitch damper loop gain and lag time constant schedules selected from the short-period analysis. Based on these characteristics, it was found that the pitch damper portion of the augmentation system produces somewhat higher maneuver stability column force gradients at the relaxed static stability aft limit than the basic airplane has at mid c.g. without augmentation. The effect of feed-forward compensation is to reduce the column force gradients to levels comparable to the basic unaugmented airplane at typical c.g. locations. By means of the maneuver stability analysis, the feed-forward loop gain was designed such that the column maneuver force gradients at the relaxed static stability aft limit were about the same as the basic unaugmented airplane at normal operating c.g.'s. Typical maneuver stability analysis results are shown in Figure 23 which shows the column maneuver force characteristics for a cruise condition. Data are shown for the basic airplane at mid c.g. (25% mac) without augmentation and at the relaxed stability aft limit (39% mac) with and without augmentation. These data show that the airplane with augmentation damper and feed forward has about the same characteristics at the relaxed static stability aft c.g. limit (39% mac) as the basic unaugmented airplane at mid c.g. (25% mac).

3.1.5 Augmentation Authority.— In specifying the stability augmentation authority requirements, it was necessary to reach a compromise between that which would provide optimum flying qualities and that which would be structurally allowable from a hardover failure standpoint. During a preliminary meeting with structural loads engineers, it was estimated that the aircraft structure probably would not tolerate a hardover failure of more than $\pm 1^\circ$ of horizontal tail deflection at certain critical high-speed flight conditions. Therefore, subsequent flying qualities analysis was performed by selecting the augmentation system loop gains so as not to saturate this limit for the various maneuvers and turbulence conditions encountered in flight.

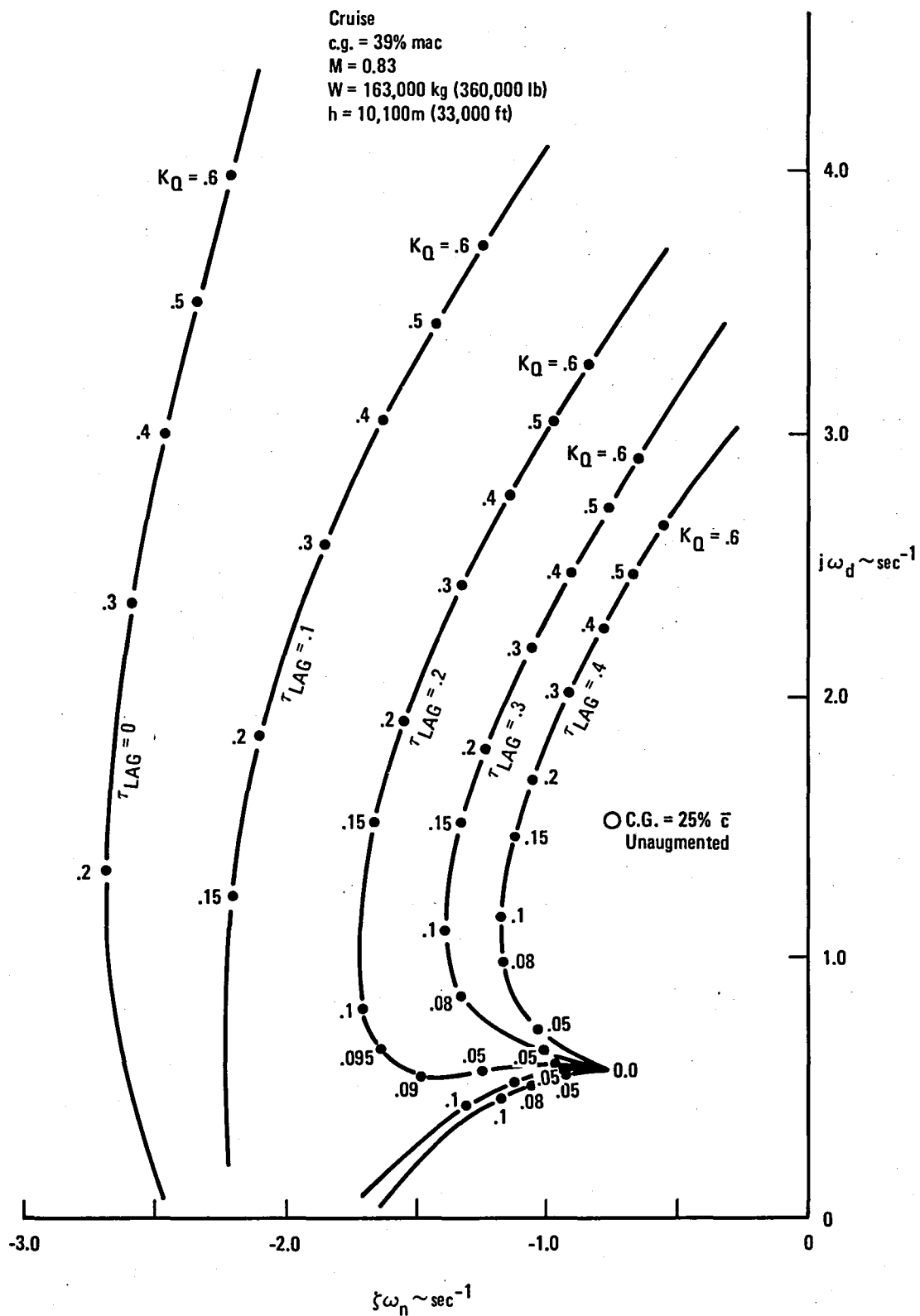


Figure 22. - The effect of PACS gain-lag functions on short-period characteristics.

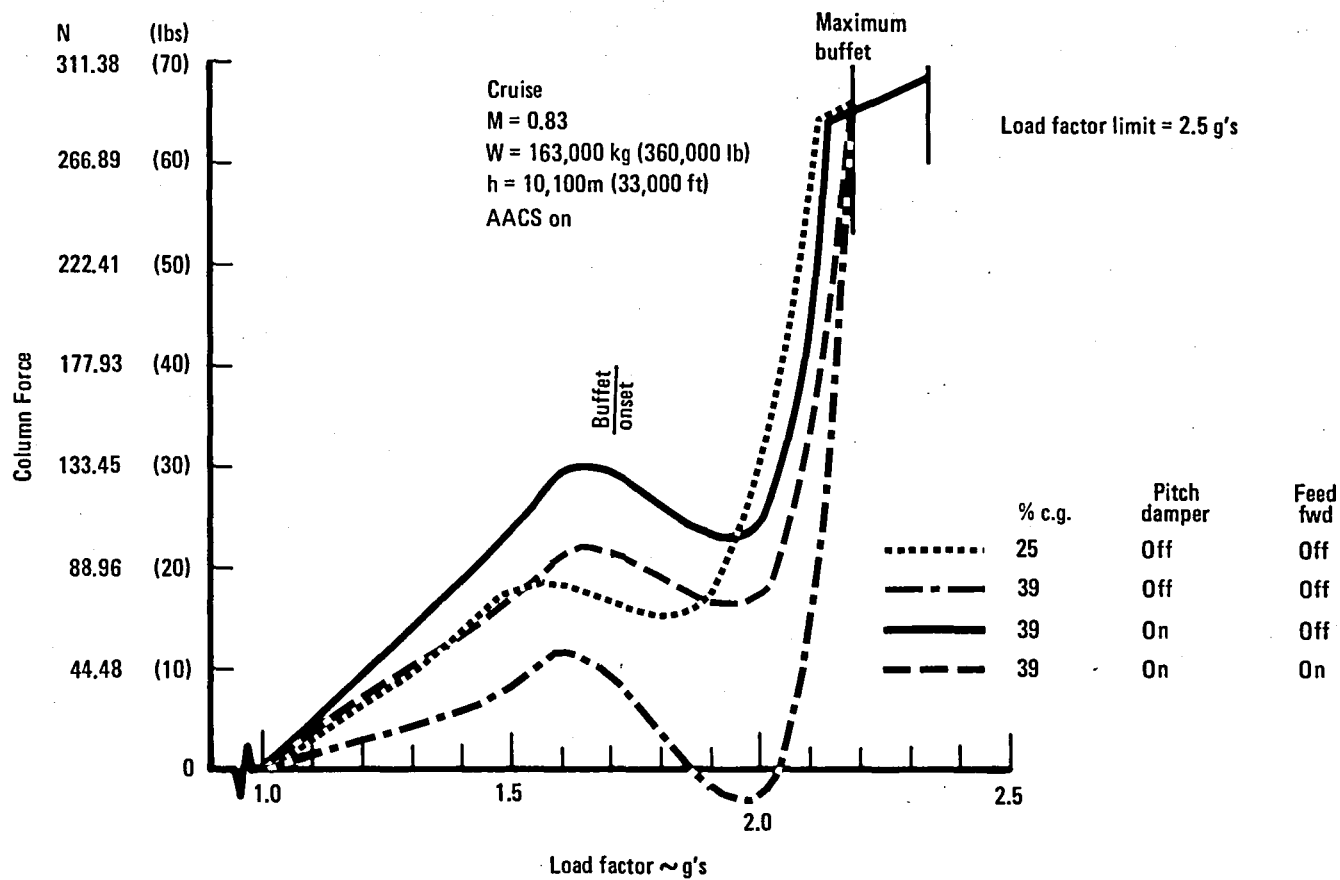


Figure 23. - Maneuver stability, cruise

3.2 Functional System

The PACS augments aircraft longitudinal stability by controlling the horizontal stabilizer through a redundant limited-authority series servo in response to signals from column-trim sensors, pitch rate gyros, and dynamic pressure sensors. To meet the aerodynamic and avionics requirements for the optimum surface control, the analysis of the stabilizer system involved the series servo as well as the control mechanism. The stabilizer is a single surface with quadruple hydraulic input that presents many unique problems for which the servo system had to be analyzed. The system was analyzed for series servo rates, gains, velocities, and output load effects on the control system and the effect of control loads on the series servo and tie-in mechanism. In addition, series servo position in the input control mechanism subjects the servo to input control system jam loads. The jam load may be cyclical or a constant load which must be reacted by an active or an inactive servo. Jam loads, normal control friction, and inertia loads affect the series servo rates, gains and output velocities.

A non-linearizer linkage consisting of two four-bar linkages (Figure 8) changes the gearing ratio in the input to the power servos as the stabilizer angle changes. This mechanism allows the total control column motion to be maintained within reasonable travel limits by programming the control column versus stabilizer. The gearing gain change results in high loads at the series servo and the tie-in mechanism for large stabilizer angles.

The series servo must not only react these system loads but also must provide a fast acting and reliable system ground for pilot and autopilot in the event of a failure in electrical, hydraulic, or mechanical systems. Servo shutdown and change-over times from the active to the stand-by system were analyzed and evaluated against system requirements for both an operational system and a system with high friction or jams. In the event of a jam upstream of the servo (between control column and the series servo) the jam loads become cyclical due to power servo feedback arm bungee action as the control system is actuated at a stabilizer trim position.

The redesigned elevator drive system was analyzed for the effects of the increased loads due to the downrigging of the elevator and structural interference.

3.2.1 Analysis Methods.— Design layouts, computer graphics, and other computer programs were utilized to investigate control system kinematics and to determine system loads.

3.2.1.1 Layouts: The following design studies were made on a drawing board:

- Series servo tie-in mechanism design
- Tie-in mechanism space studies

- Elevator structural interference studies
- Elevator push rod
- Series servo space studies
- Structural modification to accommodate series servo and tie-in mechanism

3.2.1.2 Computer graphics: The Computer Aided Design and Manufacturing (CADAM) program can simulate the motion of eight different types of mechanism building blocks/units: the link, fourbar, fivebar, lazy tongs, cam, track, slot, and actuator. These building blocks can be linked together to depict real mechanisms and their motions. CADAM was used for the following design studies:

- Tie-in mechanism motion studies
- Elevator drive geometry studies
- Detail drawing design
- Series trim kinematics

3.2.1.3 Interactive Continuous System Simulation Program (ICSSP): The ICSSP is an interactive graphic computer program for the digital mathematical differential equations terminating in one independent variable. It is a more versatile tool than CADAM for complete system simulation. It was used for the following studies:

- Series servo kinematics
- Control system kinematics with series servo in the system
- Autopilot and series servo interaction
- Series servo and series trim interaction
- Series servo authority and rate

3.2.2 Results of Analysis. - The analysis results (curve and tabular form) serve the Aerodynamics and Avionics Departments for use in their evaluation and analysis.

The series servo authority is given in Figure 10. The nonlinearizer (Figure 8) causes the incremental stabilizer angle to vary with the trim angle for a constant output stroke of the series servo. The design output authority at the stabilizer is ± 0.013 rad (.75 deg nominal) at -0.017 rad (-1 deg) stabilizer trim angle.

The series servo maximum output load (444.5 kg, 980 lbs) is determined by the forces which are required to react jammed control loads. These loads may be static or dynamic loads depending on the location of the jam in the control system. They may be generated by:

- Series servo output
- Control column input
- Mechanical trim input
- Surface feedback motion (within feedback arm ability)

3.3 Avionics

This section reports the avionics design and analysis methods. PACS control law development and analytic simulation are discussed in detail.

3.3.1 Control Law Development.- In Section 3.1.4, the basic concepts of the near-term PACS were introduced. This section describes in more detail the analytical modeling of the complete PACS and the stepwise design procedure used to arrive at the final control law.

Classical synthesis techniques were applied in the design of the near-term PACS control law due to its inherent simplicity. Lockheed developed analytical computer programs used to support the analysis of the control law are the Advanced System Analysis Program (ASAP) and the Continuous Systems Modeling Program (CSMP). Both these programs are operated by the control systems designer from interactive computer graphics terminals. ASAP contains standard root locus, Bode, Nyquist, and other linear analysis tools used in the synthesis and analysis of feedback control systems. CSMP provides the capability to simulate nonlinear control systems and verify their performance in the time domain.

Figure 24 is the basic PACS analytical block diagram with the significant control system dynamics represented by Laplace domain transfer functions. The airframe was modeled with rigid body longitudinal equations of motion. Structural vibrations were not included in the model since the control system bandwidth is sufficiently limited to minimize excitation of structural modes. The control law filters and gains which are digitally implemented in the PACS computer are enclosed by the dashed line. These digital computations are performed at an 80 per second iteration rate. Since this is a very high rate relative to the filter time constants of the control law, the discrete

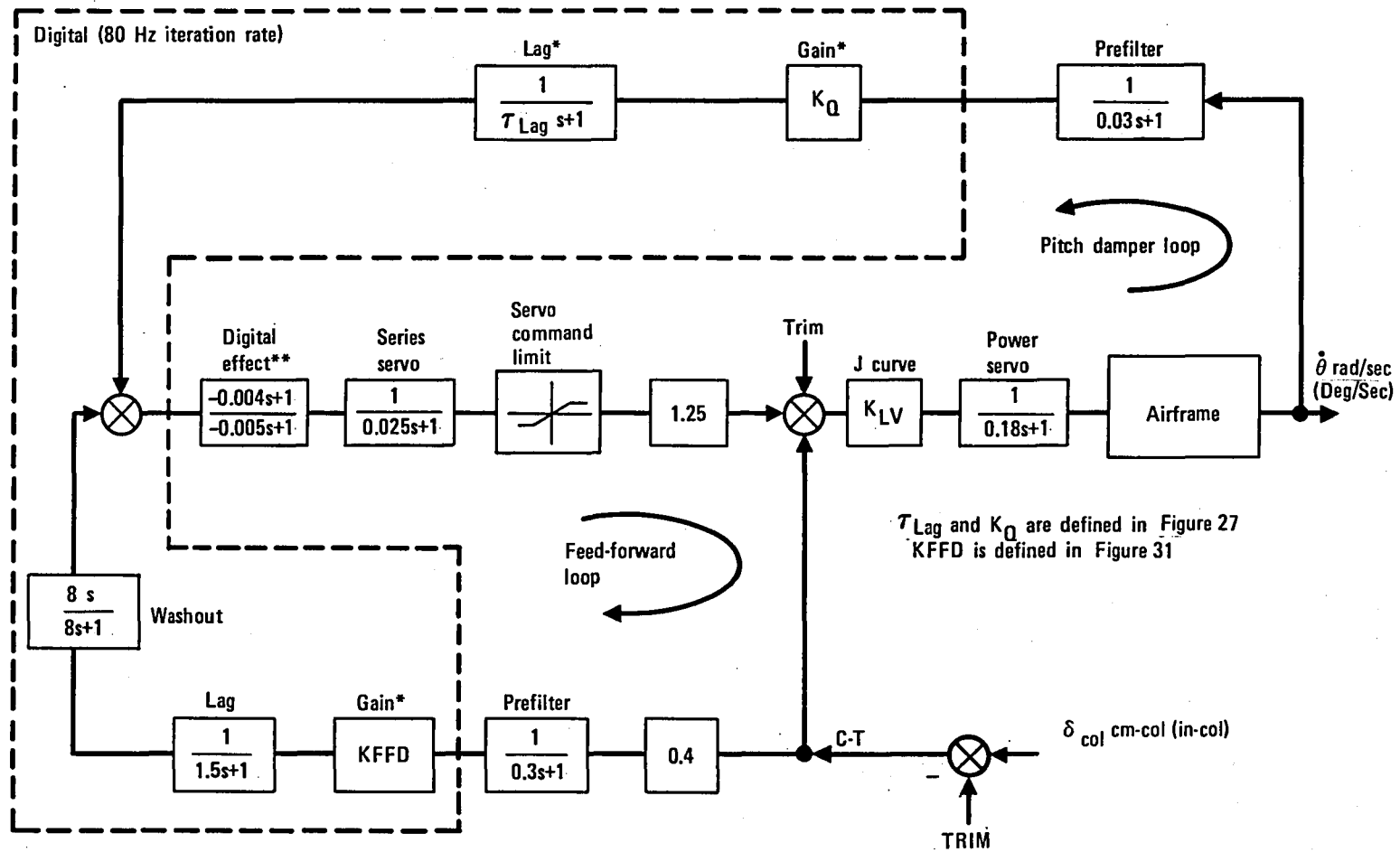


Figure 24. - PACS analytical block diagram.

domain filters are accurately represented by the continuous domain transfer functions. Input signal prefilter, series servo, and stabilizer power servo transfer characteristics are accurately approximated with first order filters since their bandpass frequencies are high relative to the aircraft rigid body response frequencies.

Analysis of the PACS control law concentrated on the six flight conditions defined in Table 2. Considered in the analysis were the effects of other systems which are operational during manual piloting. These systems are the aileron active control system (AACS) used for wing load alleviation, the Mach trim system, and the direct lift control (DLC) which is active only in the landing flap configuration. As brought out in Section 3.1, the design philosophy of the near-term PACS was to make the augmented airplane flying qualities at the 39% mac c.g. configurations consistent with the flying qualities of the basic airplane at 25% mac c.g. Consistent flying qualities were judged analytically by comparing the position of dominant characteristic roots and the maneuver stick force gradients of the augmented airplane with those of the basic airplane. The control law synthesis was restricted to 1 g trim flight stability conditions. At cruise conditions where Mach number exceeds 0.7 the aircraft stability is reduced in high angle-of-attack regions due to nonlinear aerodynamic pitching moment characteristics. Although these reduced stability regions were not considered in the synthesis processes, performance of the augmented flight test airplane proved as good or better in the high angle-of-attack regions when judged relative to the basic airplane performance.

The following sections describe the stepwise design of the pitch damper and feed-forward elements of the PACS control law.

3.3.1.1 Pitch damper: The pitch damper was analyzed by plotting the locus of roots of the longitudinal characteristic equation as the damper gain and lag time constant were varied. Root loci were calculated for c.g. locations at 25, 35 and 39% mac. Although the augmented characteristic equation is of higher order than the unaugmented equation, dominant short period and phugoid second order roots are still identifiable for use in a design criteria. A compromise set of damper gains and lag time constants were chosen to control the short period roots to locations which would produce theoretically good handling qualities based upon previous experience with the baseline L-1011 characteristic roots and proven handling qualities. As a criteria the augmented short period roots were selected to have a damping ratio between .35 and .8 and a natural frequency equal to or greater than that of the unaugmented airplane at 25% mac c.g. To satisfy the criteria at all flight conditions, the gain (K_0) and lag time (τ_{LAG}) constants were scheduled with airspeed as shown in Figure 25.

The damper design was performed with and without the AACS active. To achieve equivalent short period damping ratios for both configurations a higher gain was required with AACS active due to the destabilizing effect of the ailerons. With AACS operating the airplane responds in pitch as if the static margin was reduced by 5%. Since AACS is normally always active

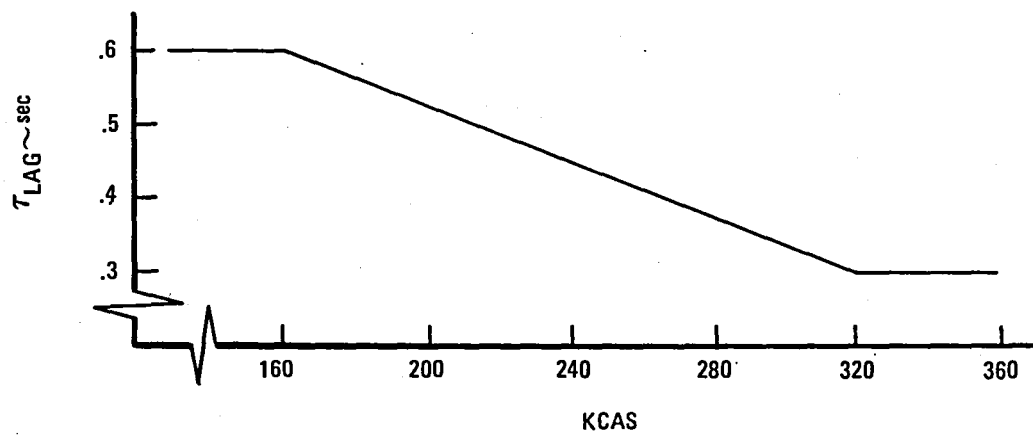
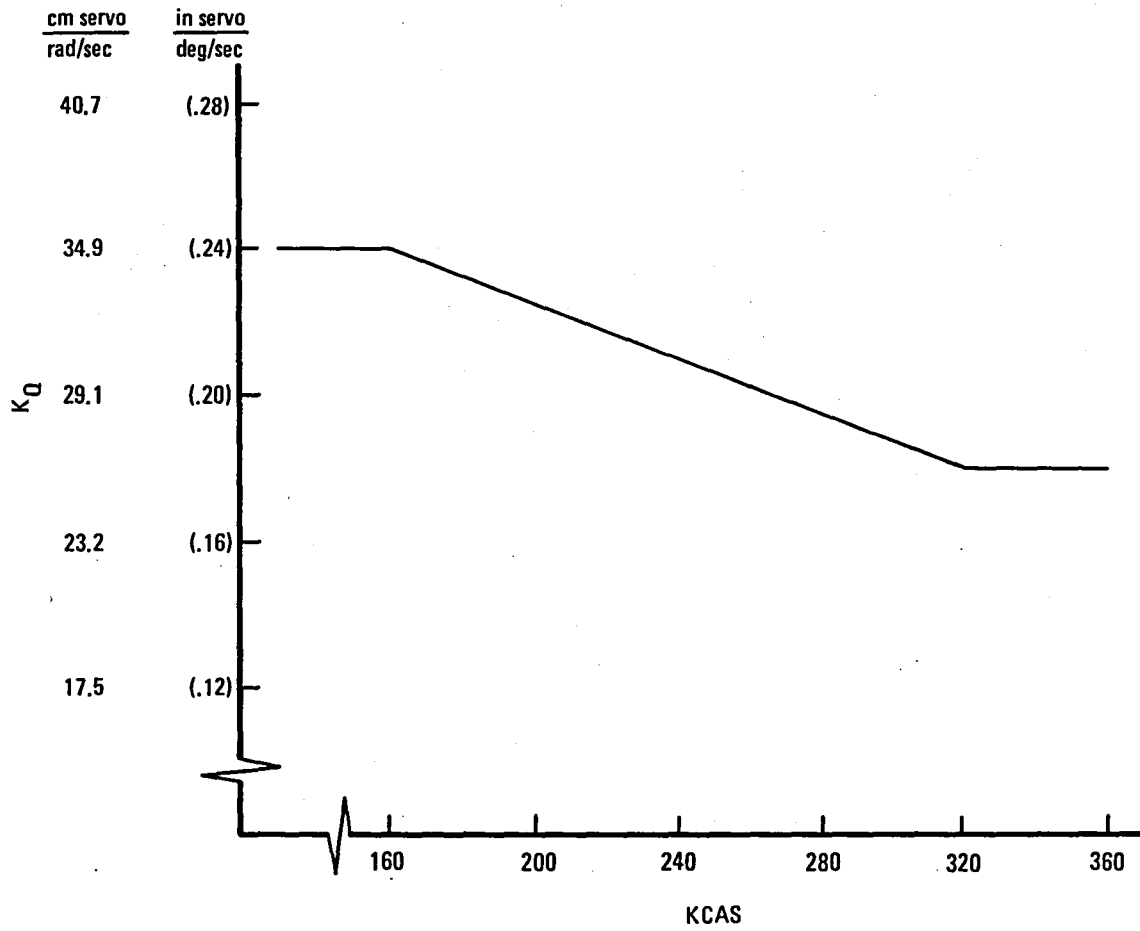


Figure 25. - Pitch damper gain schedules.

and gain scheduling independent of AACS status is a desirable simplification, the higher gain was scheduled with airspeed for the final control law. All results shown for the augmented L-1011 are based on this schedule unless otherwise noted.

Figure 26 shows the short-period characteristics for a typical cruise condition with and without augmentation. Shown for comparison are the frequency and damping requirements for Level 1 handling qualities on military aircraft as specified in MIL-F-8785C, Reference 3. The unaugmented L-1011 with AACS inactive nearly satisfies the Level 1 requirements at the 39% mac c.g. With AACS active at the 39% mac c.g., the unaugmented L-1011 exhibits an overdamped short period response and the need for augmentation is more pronounced. The augmented L-1011 satisfies the MIL-F-8785C requirement with and without the AACS active. Figure 27 shows the short period characteristics for the landing configuration. The effect of AACS on the unaugmented L-1011 characteristics is much smaller in landing than in cruise. The augmented L-1011 shows improved frequency characteristics while retaining good damping.

The pitch rate damper gain and lag time constants required for good short period characteristics also provide adequate compensation to stabilize the phugoid mode at the relaxed static stability (RSS) condition. Figure 28 shows a typical cruise phugoid root locus with the AACS active. The augmented L-1011 phugoid damping is positive at the RSS condition and is approximately equal to the unaugmented L-1011 damping at the conventional aft c.g. limit. (35% mac). At other flight conditions a similar trend was observed which suggests that, in general, increased pilot attention should not be required to hold airspeed at the RSS condition relative to the unaugmented L-1011 at the conventional aft c.g. limit.

The sensitivity of the augmented airplane stability to variations in damper loop gain was determined. Characteristic roots were calculated for the nominal damper gain multiplied by .5, 1.5 and 2. gain factors. At the six flight conditions examined with these gain factors, no high frequency instabilities resulted and the low frequency instabilities had a shortest time to double amplitude no worse than for the unstable roots previously determined for the unaugmented airplane at the normal aft limit. This analysis was valid only for rigid body aircraft modes. Refer to Section 3.7 for flutter stability analysis with the 2.0 gain factor.

A root locus analysis was performed to examine the benefits of incorporating stabilizer position feedback into the gain and lag time constant scheduling functions to minimize short period frequency and damping variations with c.g. The results of this study produced several gain schedules which were bivariate functions of airspeed and stabilizer position. Although some reduction in short period damping variation with c.g. was realizable, it was concluded that the benefits for the near-term relaxed static stability range did not warrant the additional scheduling complexity.

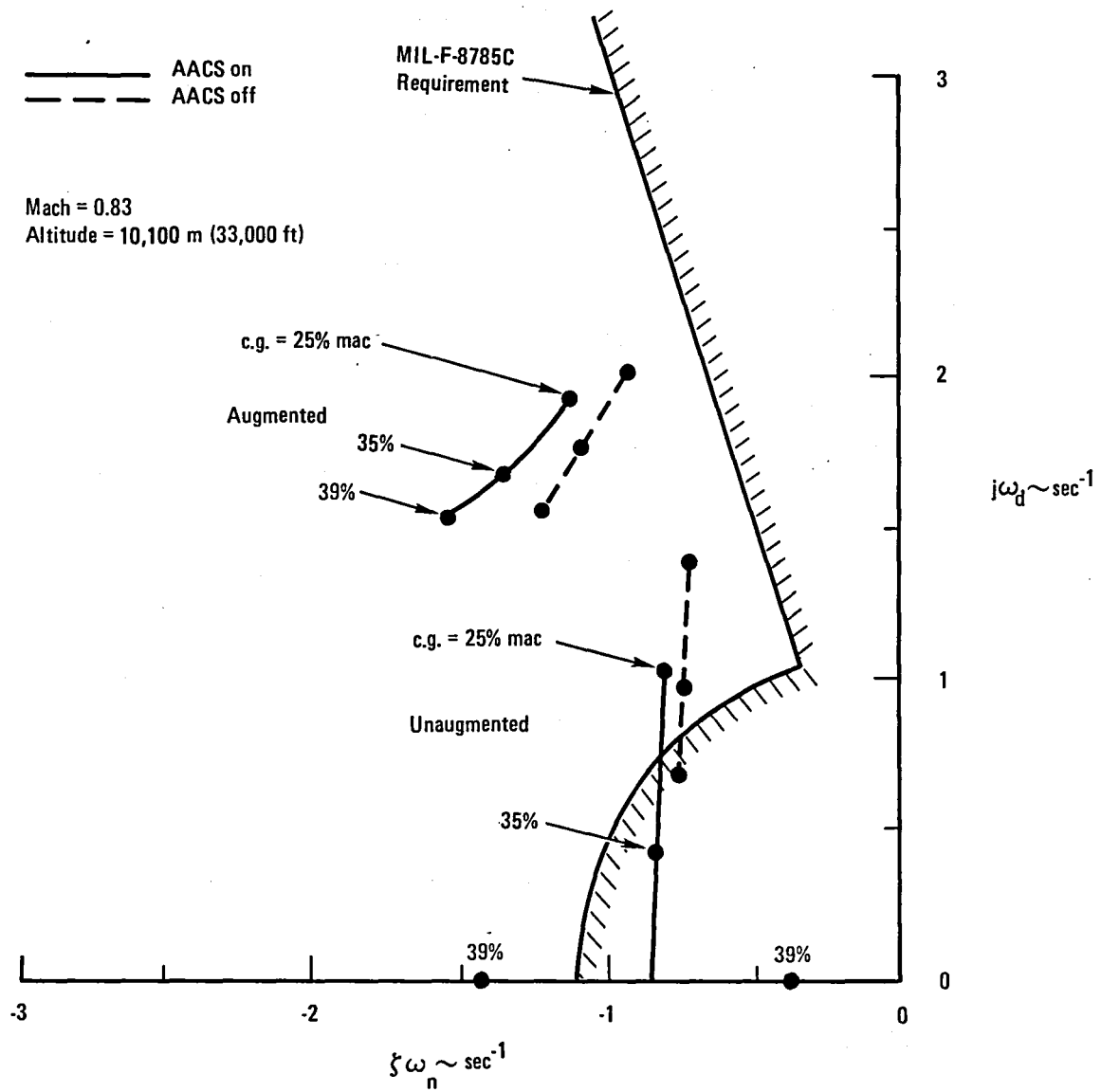


Figure 26. - Short-period characteristics, cruise.

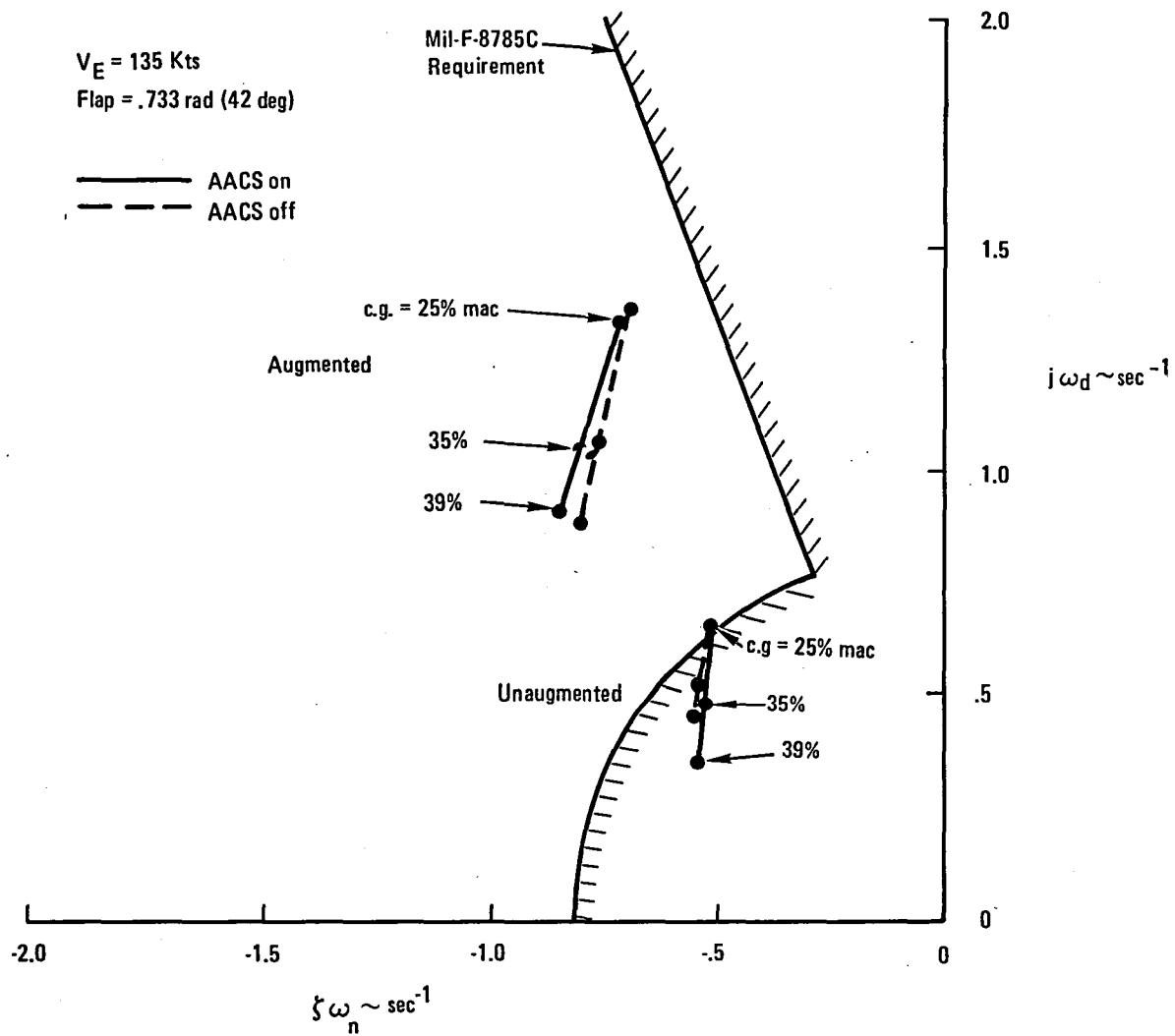


Figure 27. - Short-period characteristics, landing.

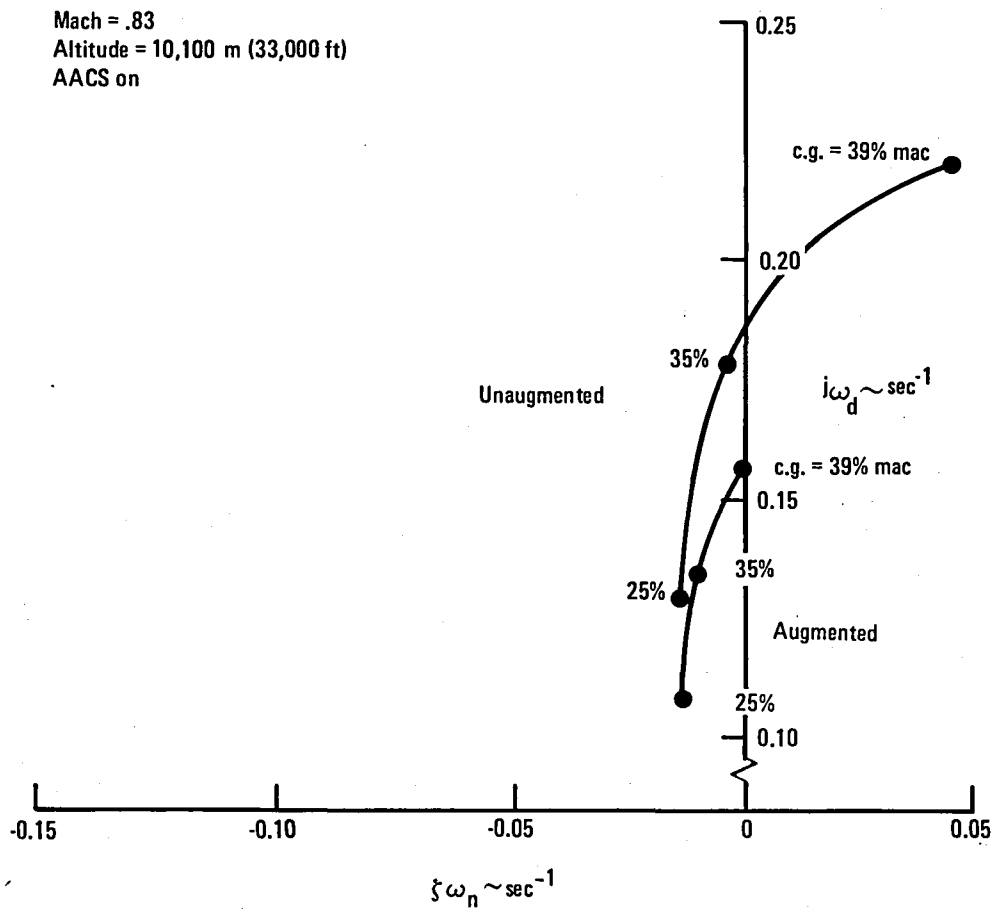


Figure 28. - Phugoid characteristics, cruise.

3.3.1.2 Feed-forward: The airplane maneuvering stick force per g and transient short period response characteristics are changed when the pitch damper loop is closed. To readjust these characteristics, a feed-forward of column displacement with respect to trim is provided in the PACS control law. Referring again to the analytical block diagram in Figure 24, the three primary elements in the feed-forward path are the static gain (KFFD), a 1.5 second lag, and an 8 second washout or high pass filter.

The feed-forward gain was determined with the 8 second washout assumed removed. With $KFFD = 0$, the pitch rate feedback during steady state maneuvers deflects the series servo in a manner that subtracts from the pilot's column input. Thus to achieve the required stabilizer deflection to hold a given maneuver load factor, the pilot must provide additional column input. Hence maneuvering stick forces increase when the damper loop is closed. The amount of stick force increase is more during coordinated steady state turns than for symmetric pull-ups due to the higher body pitch rate sensed in a turn. For example, the pitch rate required to sustain a load factor of 2.0 is 1.5 times higher in a turn than in a symmetric pull up.

With a non-zero KFFD gain, the stick force associated with a steady state pitch rate can be adjusted. As a practical design procedure, symmetric maneuvering force gradients for the augmented airplane were made to match those of the basic airplane at the 25% mac c.g. This was done based upon linear force gradients calculated at the 1 g trim flight condition. Feed-forward gains determined with this procedure necessarily result in a near-zero series servo deflection with stick force inputs since the feed-forward essentially cancels the feedback signal from pitch rate. Figure 29 shows how the feed-forward gains are scheduled with airspeed to optimize mid c.g. maneuvering force gradients at all flight conditions.

The feed-forward gain designed for the mid c.g. condition provides a good compromise for static gradients at other c.g.'s. Table 4 summarizes the linear force gradients for the 25% and 39% mac c.g.'s at the nominal cruise conditions. The highest gradients occur at the 25% c.g. in a steady turn maneuver and the lowest gradients occur at the 39% with a symmetric pull-up maneuver.

With the feed-forward active the highest and lowest gradients are roughly centered about the 169 N/g (38 lbs/g) reference gradient. With the feed-forward off (damper only PACS) the aft c.g. gradients are only slightly lower than the reference gradient but the mid c.g. gradients are considerably higher. If more information about c.g. position were available for scheduling control law gains, e.g. from stabilizer trim position, nearly constant gradients could be maintained by reducing the feed-forward gain as the c.g. moved aft of 25% c.g. However, in lieu of c.g. information, slightly lower gradients at the aft c.g. condition were preferred over the higher gradients at the mid c.g. condition.

Figure 23 shows the complete nonlinear steady turn maneuver stability chart at the same cruise condition referred to in Table 4. The figure verifies that the linear gradient design provides adequate force characteristics at the 39% c.g. up to maximum buffet when compared to the force characteristics of the basic unaugmented airplane at the 25% c.g. location. Figure 30 shows the maneuver stability for the landing condition. At this condition, the pitch rate gain is high enough to saturate the series servo without the feed-forward compensation. With the feed-forward active, saturation does not occur and the maneuver forces are nearly linear up to the maximum lift coefficient.

Having established the feed-forward gain based upon static maneuver force considerations, the next step in the design process was to choose the column-minus-trim first-order filter time constant. This was done by comparing pitch rate time responses to column force step inputs with different amounts of lag in the feed-forward path. The initial build up in pitch rate of the augmented airplane closely matches that of the baseline airplane at the 25% c.g. if the feed-forward lag is set at a value equal to the sum of the damped period of the short period mode plus the pitch rate lag in the damper feedback path. This sum ranges from about 1 to 2 seconds over the design speed envelope of the airplane. Using the average value of 1.5 seconds, the pitch rate response was evaluated at all flight conditions and found satisfactory for both the mid and aft c.g. locations.

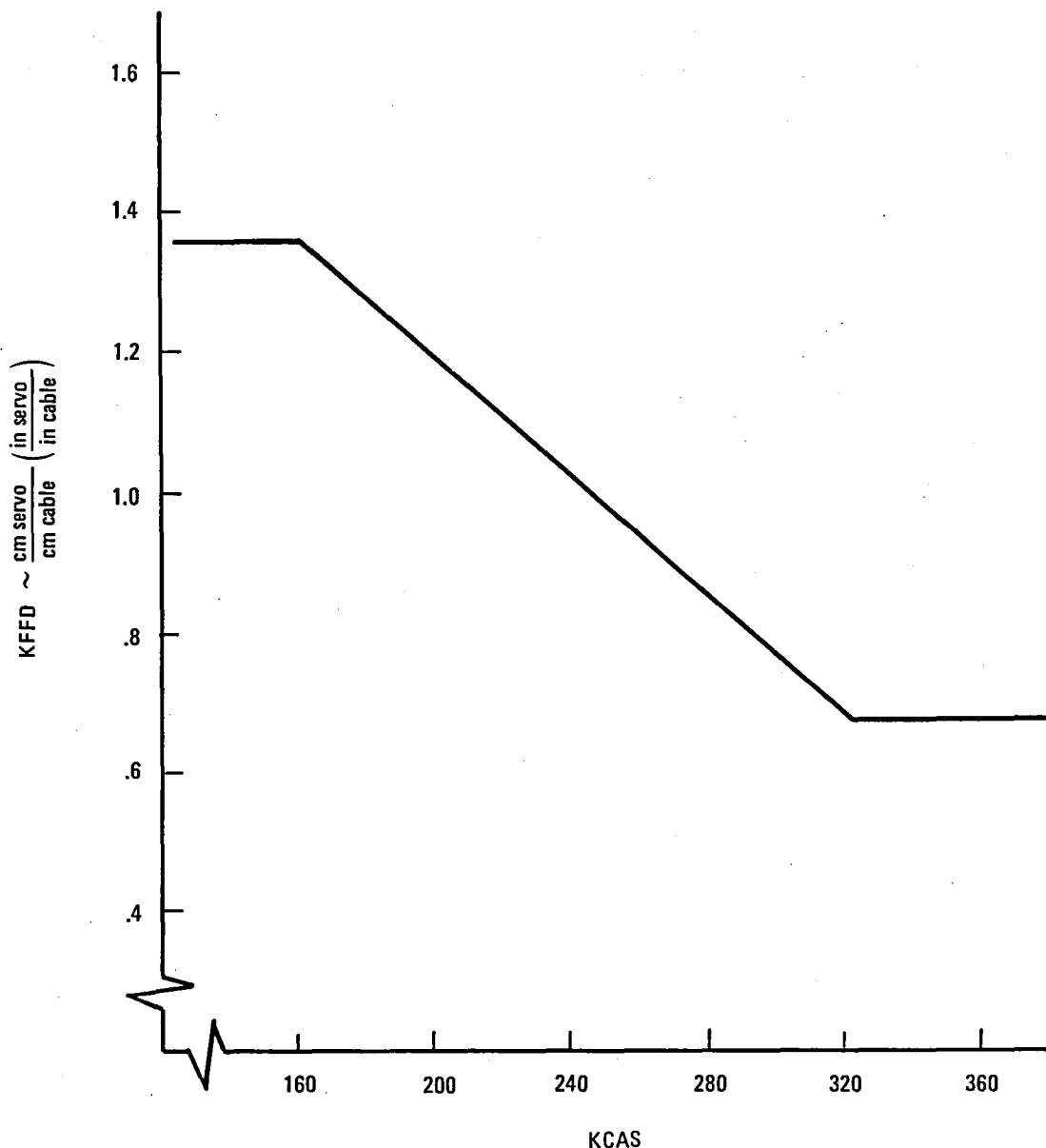


Figure 29. - Pilot feed-forward gain schedule.

TABLE 4. SUMMARY OF LINEAR COLUMN FORCE GRADIENTS, CRUISE,
MACH = .83, h = 10,100 m (33,000 ft), AACS ON

| MANEUVER | c.g. % mac | PACS STATUS | | |
|---------------------|---------------|----------------------|--------------------|-------------------------|
| | | PACS OFF N/g lb/g | NORMAL N/g lb/g | DAMPER ONLY N/g lb/g |
| • Symmetric Pull-Up | 25 | 169 (38) | 169 (38) | 236 (53) |
| | 39 | 62.3 (14) | 102 (23) | 142 (32) |
| • Steady Turn | 25 | 147 (33) | 200 (45) | 280 (63) |
| | 39 | 71.2 (16) | 160 (36) | 160 (36) |

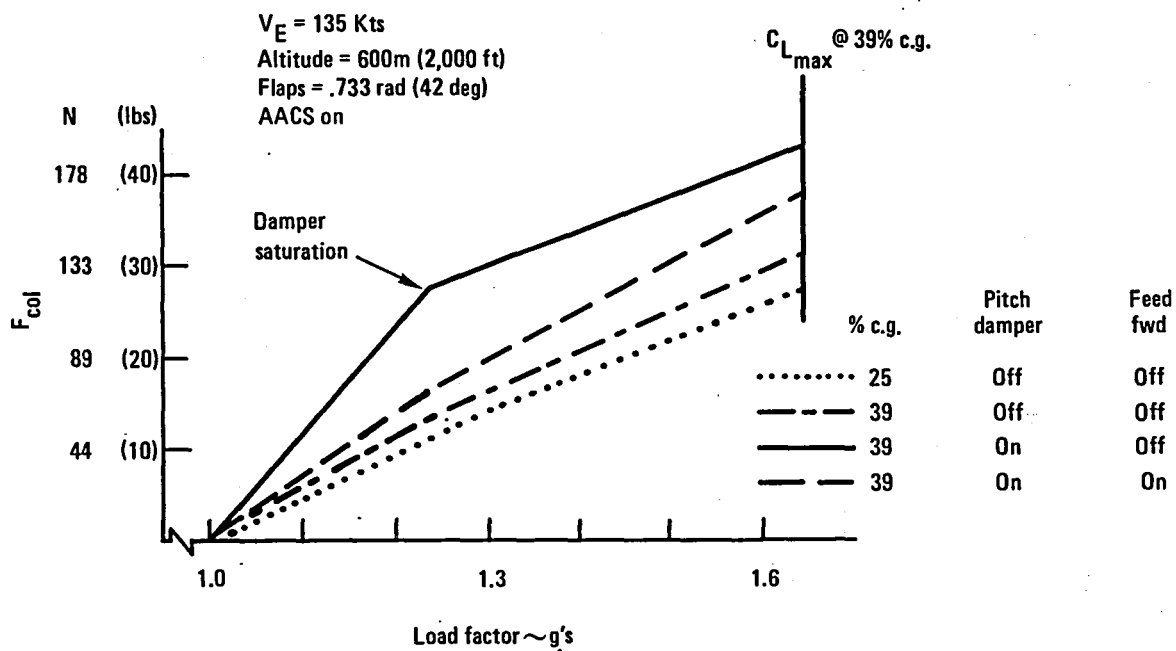


Figure 30. - Maneuver stability, landing.

The final element of the feed-forward computational path is an 8 second high pass filter or washout. This filter allows short term column inputs to pass but nulls the long term inputs. This provides different amounts of feed-forward compensation for different maneuver durations. A short term maneuver was arbitrarily defined as one which takes place without a significant phugoid response. Thus the 8 second washout time constant was selected to mirror the low frequency pitch rate response to column inputs at the nominal mid c.g. cruise condition. The time constant is equal to the inverse of the damped natural frequency of the phugoid mode. The pilot column forces on short term maneuvers will be lighter than those for long term steady state type maneuvers. The maneuver stability charts depicting column forces with and without feed-forward compensation at a given load factor (see Figure 23) are representative of the short term and long term force characteristics respectively. Provisions for evaluating handling qualities with and without the washout were included in the final control law.

3.3.2 CSMP Simulations.- A CSMP program was used to allow closure of PACS control loops around a nonlinear 3 degree-of-freedom model of the aircraft including control surfaces and actuators. Necessary control system nonlinearities such as digital signal processing delays, servo hysteresis, and saturation effects were included to accurately model a practically functioning system. This program was then used to document the L-1011 aircraft time history responses to control column and atmospheric turbulence inputs. The aircraft and control law configurations evaluated included combinations of:

- 1) AACCS on and off
- 2) Pitch rate gain zero and nominal
- 3) PACS feed-forward gain zero and nominal
- 4) PACS feed-forward with and without the $8s/(8s+1)$ washout.

3.3.2.1 Column responses: Responses to column inputs were generated for several flight conditions with emphasis on the 25% and 39% mac c.g. locations. The time history responses correlated well with the predicted behaviors based upon characteristic root placement and static gain analyses. To illustrate the significant results obtained with the PACS control law, small and large angle-of-attack aircraft responses are presented below for the Mach .83 10,100 m (33,000 ft) altitude cruise condition.

As mentioned in earlier sections, the nature of the aircraft response at Mach numbers greater than .7 depends strongly upon the angle-of-attack regions encountered by the aircraft. Figure 31 shows the pitching moment variation with angle of attack at the Mach .83 condition. As long as the angle of attack remains below .087 rad (5 deg) the aircraft aerodynamic

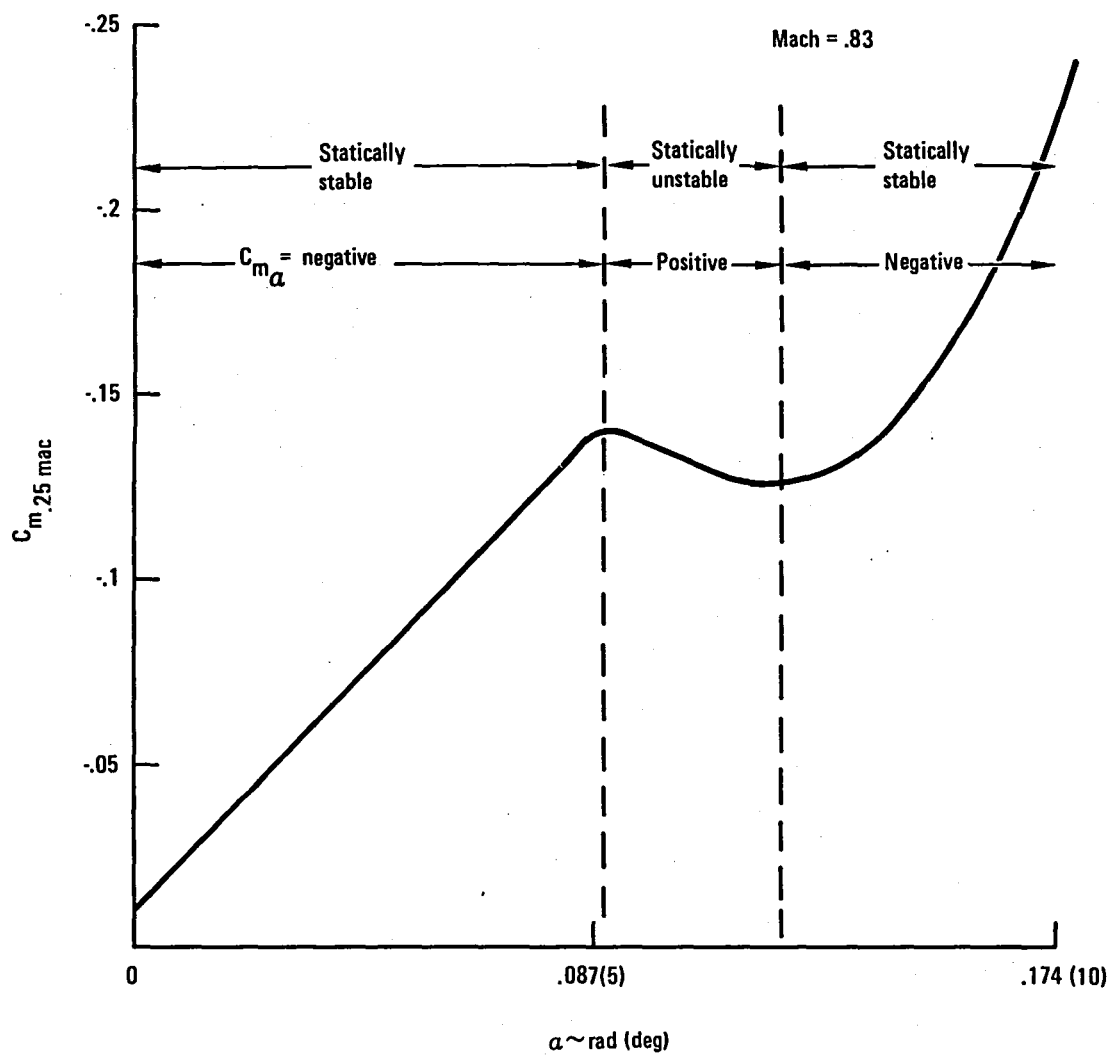


Figure 31. - Pitching moment variation with angle of attack.

characteristics are essentially linear and frequency and damping parameters estimated from time history responses correlate well with the design values calculated for the dominant characteristic roots.

Figures 32a, 32b, and 32c show the small angle of attack short period pitch rate response characteristics for the augmented and unaugmented airplanes with c.g. locations of 12%, 25% and 39% mac respectively. It can be seen from these figures that the PACS provides good short period responses at all c.g.'s. The most significant improvement occurs at the 39% mac c.g. where the unaugmented airplane no longer exhibits a well defined second order response and the pitch rate does not stabilize after the pilot column pulse is completed. At the 25% mac c.g. the pitch rate overshoots and transient decay times with and without PACS compare well with the damping ratios and damped natural frequencies associated with the characteristic roots previously shown in Figure 26.

The curves in Figure 33 show the angle of attack and load factor responses to stick force (F) steps for the augmented (PACS on) and unaugmented (PACS off) aircraft with a 39% c.g. Responses are shown for step force amplitudes of 33.3 N (7.5 lbs) to 89.0 N (20 lbs) in increments of 11.1 N (2.5 lbs). When the step force input causes the aircraft angle of attack to enter the unstable pitching moment region a pitch-up phenomenon occurs. In the unstable region ($\alpha = .087$ to $.122$ rad, 5 to 7 deg) the aircraft cannot generate enough nose-down pitching moment to balance the nose-up stabilizer moment commanded by the pilot force input. As a result, the aircraft pitches up and eventually reaches a stable angle of attack above $.122$ rad (7 deg) at a corresponding higher load factor.

By comparing the load factor responses shown in the lower part of Figure 33, it can be seen that during the first 5 seconds after step insertion, the unaugmented airplane peak load factor is proportional to force for input amplitudes approaching 44.5 N (10 lbs). The augmented airplane peak load factors is proportional to force load input amplitudes approaching 89.0 N (20 lbs). This improved force characteristic achieved with PACS agrees well with the improvement shown in the static maneuvering force characteristics previously referred to in Figure 23.

3.3.2.2 Turbulence response (column fixed): The effect of atmospheric turbulence on aircraft response with and without augmentation was simulated for cruise flight condition 10 (Table 2) at four different c.g.'s.

Air turbulence was simulated by inserting random vertical and horizontal gust velocity inputs into the nonlinear CSMP aerodynamic equations. The magnitude and filtering of the gust velocities were controlled to the Dryden form of the random turbulence equations. Figure 34 shows the stabilized root-mean-square (RMS) values of pitch rate ($\dot{\theta}$), vertical acceleration (N_z), and series servo displacement (δ_{ss}) calculated for 400 second runs with a

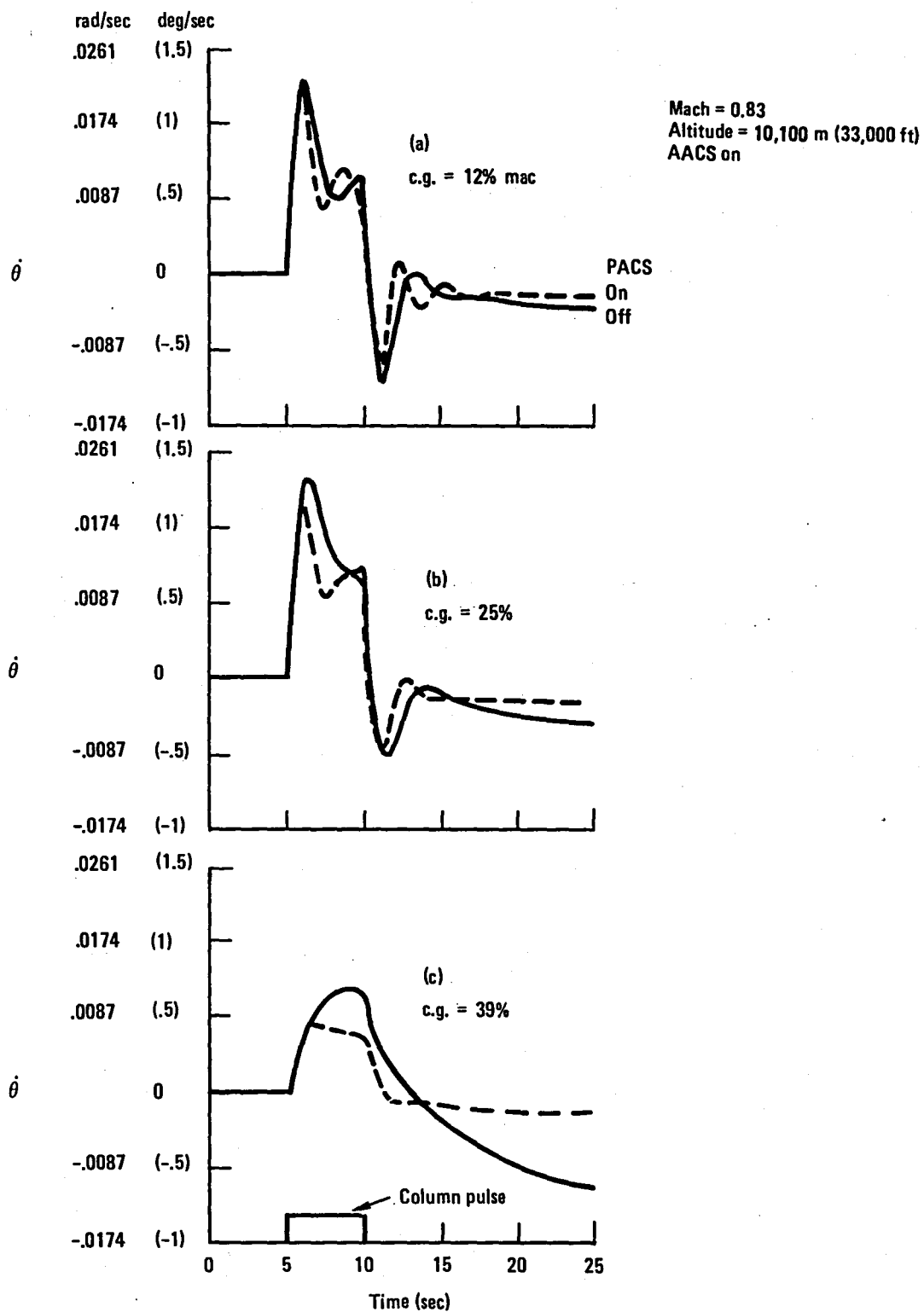


Figure 32. - Pitch rate response for $\alpha < .087$ rad (5 deg) with PACS on and off.

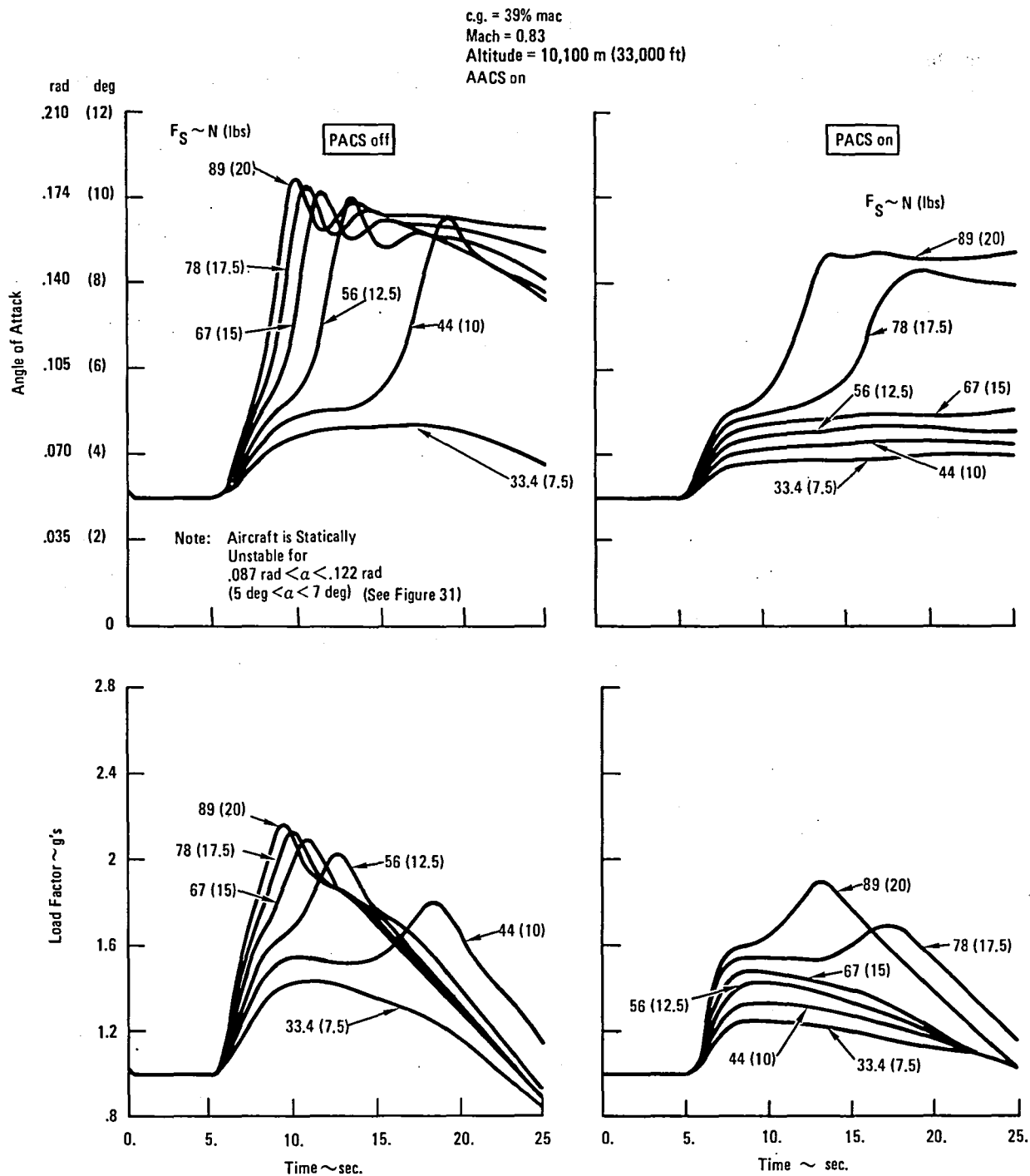


Figure 33. - Angle of attack (α) and load factor response for pilot step force commands with PACS on and off.

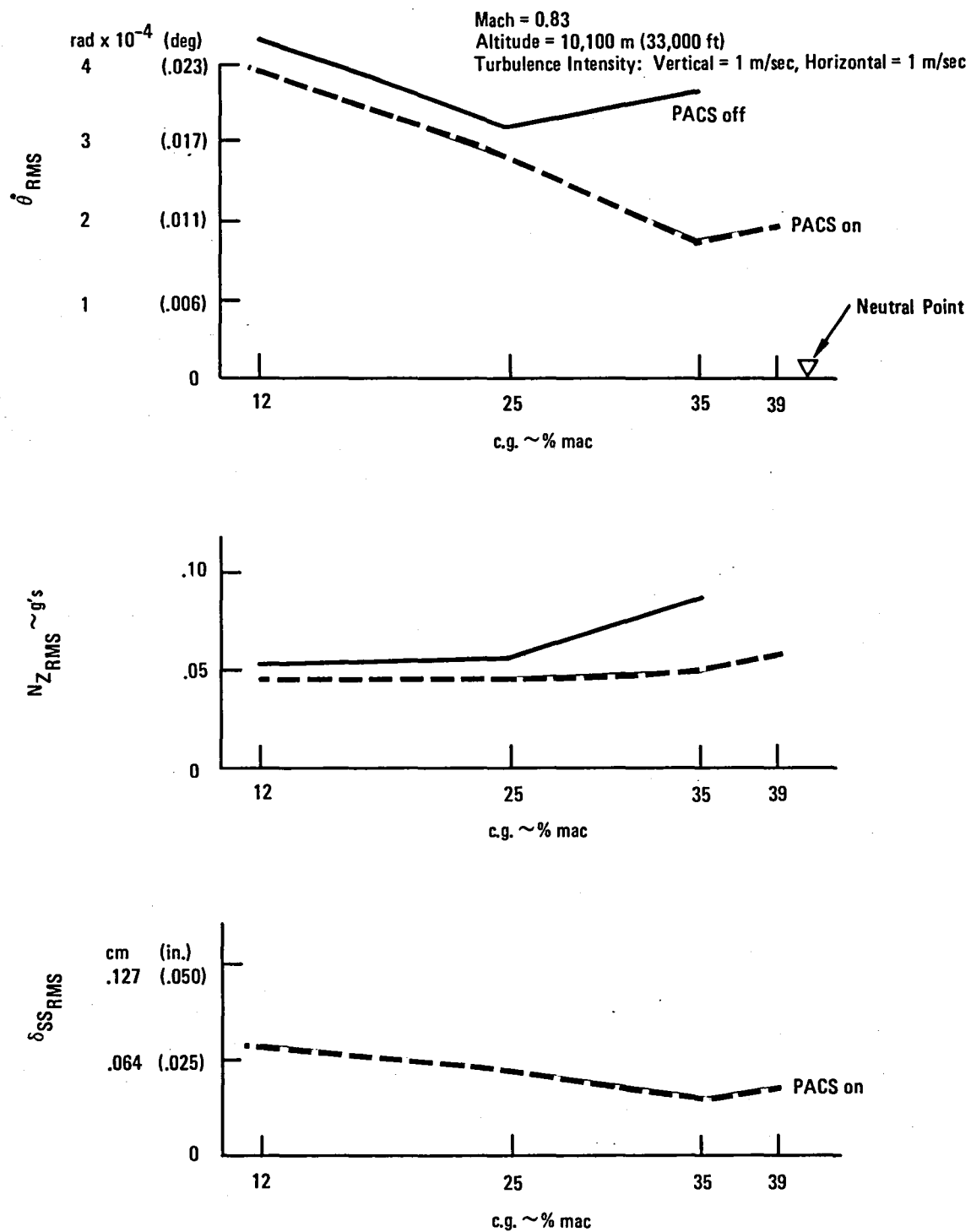


Figure 34. - RMS turbulence response, cruise.

turbulence intensity of 1 m/sec in both the vertical and horizontal directions. The following observations are made from Figure 34.

1. With PACS on, the RMS pitch rate decreases nearly linearly as the c.g. moves toward the neutral point while the RMS vertical acceleration remain nearly constant. These trends are expected since the vertical gust coupling into the pitching moment equation is through $C_{m\alpha}$ which is proportional to static margin. The vertical gust coupling into the lift equation is through $C_{L\alpha}$ which is independent of static margin. At the aft c.g.'s the aircraft responds mostly in a plunge mode rather than a pitch mode.
2. The above trends are reflected in the response RMS values until the dynamic stability of the airplane is reduced sufficiently to reverse the trend. With the PACS off, this reversal begins at 25% c.g. and increases as the c.g. moves aft. At 39% c.g. the phugoid is unstable and the RMS values diverge. With PACS on this reversal occurs aft of the 35% c.g.
3. The figure also indicates that servo saturation is most likely to occur at the forward c.g. limit where the pitch rate response is highest. However, the effect of saturation at this c.g. is small since the unaugmented airplane is inherently very stable. Relative to the unaugmented airplane, there is a 15% reduction in the RMS pitch rate and vertical acceleration responses with the PACS on. Extrapolation of the RMS servo response (δ_{ss}) from 1 m/sec to 7 m/sec turbulence intensity (Thunderstorm level), increased the RMS servo response to 30% of the available authority. Therefore, at this flight condition the pitch rate gain is high enough to satisfy dynamic stability requirements at the aft c.g. and low enough to avoid saturation effects at the forward c.g.

The lower pitch rate exhibited at aft c.g.'s is one argument favoring the use of pitch rate as an active feedback rather than vertical acceleration which tends to increase slightly as the c.g. moves aft.

3.4 Stress

Stress activities included analysis of primary structure components, analysis of the modified system components, and development of proof and operation test requirements for the PACS flight test aircraft.

3.4.1 Primary Structure Analysis.—External loads analysis was concentrated on the outer wing box and horizontal stabilizer areas. The outer wing box structure was of concern because the flight test aircraft has a prototype installation for the extended-span wing which did not increase structural

strength of the outer wing box wet bay area. Flight restrictions were already imposed on the aircraft because of this installation. The stabilizer structure was of concern because of the downrigged elevator configuration. Bending/torsion and shear/torsion limit strength envelopes were developed to assist in determining structural operating restrictions.

Preliminary limit strength envelopes were developed at two locations on the outer wing box and one location on the horizontal stabilizer. The envelopes were developed by using known loads within the existing design limit load envelopes and the margin of safety (M.S.) data of the structure prior to PACS modification. Each point on the strength envelopes was obtained by multiplying the known load at a point by the corresponding factor $(1 + \text{M.S.})$. The method is reliable for low M.S. values (i.e. the load envelope is close to the strength envelope) but considerable engineering judgment is required for high M.S. values.

These preliminary limit strength envelopes aided in selecting critical conditions on the PACS aircraft. A set of distributed net panel point loads for each selected critical condition was provided for further evaluation and to aid in updating the limit strength envelopes.

The distributed loads were applied to the finite element models of the wing and horizontal stabilizer. Internal loads generated on these models by the computer program were subsequently input to three separate margin-of-safety computer programs: surface panel analysis, surface panel spanwise splice analysis and spar analysis.

As shown in Figure 35, many of the critical load conditions on the horizontal stabilizer were significantly outside the original design limit load envelopes and in some cases outside the limit strength envelopes. A similar situation also existed on the wing envelopes. Using the minimum margins-of-safety for these conditions, it was possible to better define and update the limit strength envelopes for the PACS aircraft. These updated envelopes were provided so that operating restrictions on the PACS aircraft could be determined.

3.4.2 System Component Analysis.

3.4.2.1 Ballast system installation: The water ballast tanks and the fixed ballast installations are required to be arranged such that the allowable floor strength, both in terms of load per unit area and load per unit length along the fuselage, was not exceeded when design flight and landing load factors are applied. Studies were performed on various ballast arrangements on the cargo and passenger floor areas to insure that the strength limitations were not exceeded.

At Horizontal Stabilizer Station 107

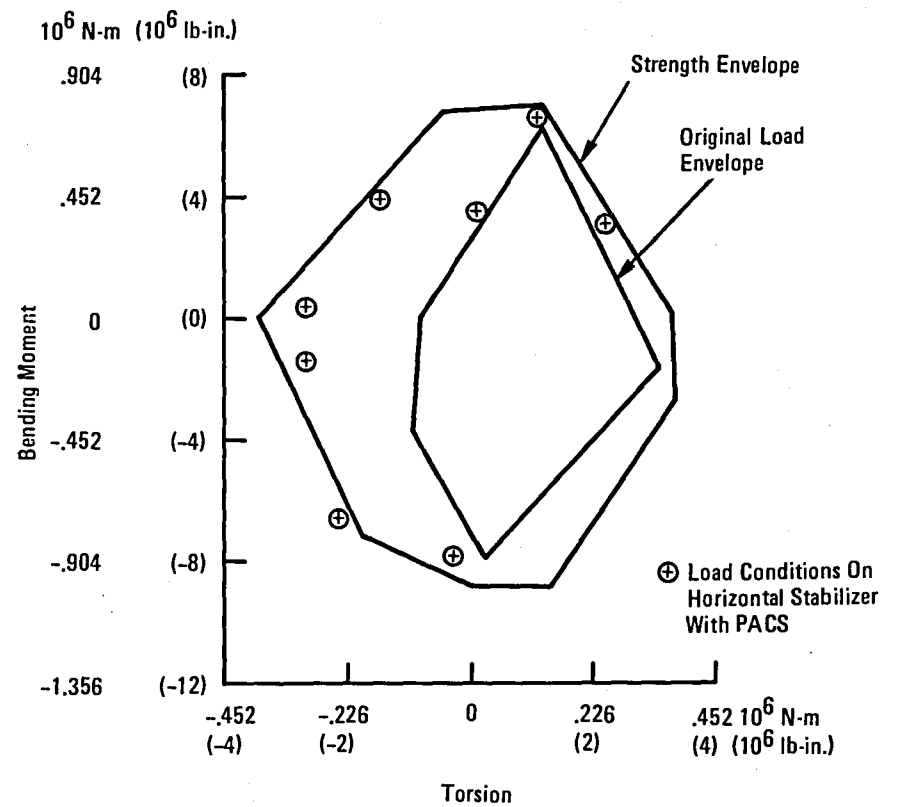
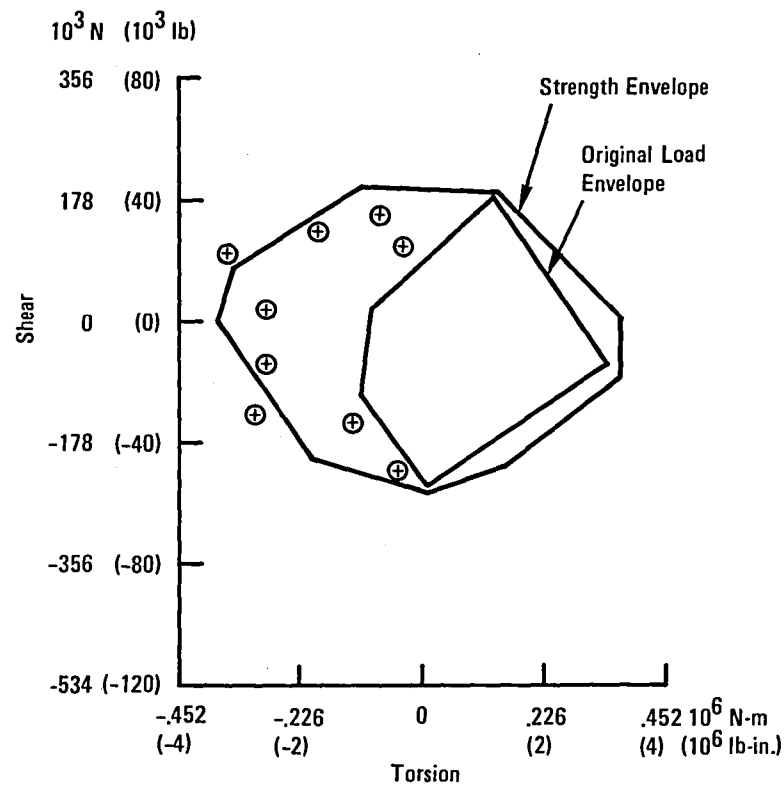


Figure 35. - Horizontal stabilizer load and strength envelope.

The water ballast tanks and fixed ballast installation in the aft passenger cabin are required to withstand emergency landing load factors in addition to the flight and landing load factors. Analyses were performed as required to insure that the complete ballast support system in this area will distribute the emergency landing loads to the fuselage sidewall.

3.4.2.2 Elevator system modifications: The modifications to the elevator drive push rod and the counterbalance support arms (see Appendix B) were analyzed as required to insure the modifications met both static and fatigue strength requirements.

The critical loads on parts of the unmodified control system were increased because of the downrigged elevator. As shown on Figure 36 the negative elevator hinge moment (trailing edge up) exceeded the original design hinge moment of the unmodified aircraft. This load increase resulted in a required minor modification to the cable support structure. The return cable strength is also critical for this load increase. Lockheed strength criteria requires a safety factor of 2.0 for cable strength to account for factors such as environment, fatigue, et cetera over the lifetime of an aircraft. Normal strength criteria for loads on most aircraft components requires a safety factor of 1.5. Consequently, an assessment was made to determine the risk involved in reducing the safety factor of this cable below the 2.0 value. Because of the limited duration of the flight test program the reduction of safety factor to between 1.5 and 2.0 was acceptable.

3.4.3 Proof and Operation Test Requirements.— Proof and operation test requirements on the PACS aircraft were based on the Lockheed requirement for preflight testing. These tests were included in the overall ground test program (Section 4.5).

On the PACS aircraft testing was required on the parts of the pitch control system which were new and on existing control system parts that were subjected to higher loads than the parts had been previously qualified. The PACS aircraft parts affected by this criteria were the elevator drive system, parts of the pitch trim system, and the series servo.

A series of five tests (three proof and two operation tests) was defined due to the increase in negative elevator hinge moment (trailing edge up), shown in Figure 36 to demonstrate the structural integrity of the existing elevator control system. Two tests were defined to demonstrate the capability of the new parts in the pitch trim system to sustain loads due to limit pilot effort at the trim wheel. A test of the series servo output linkage for loads due to the limit output force (2.14×10^7 Pa, 3100 psi) of the series servo was also defined.

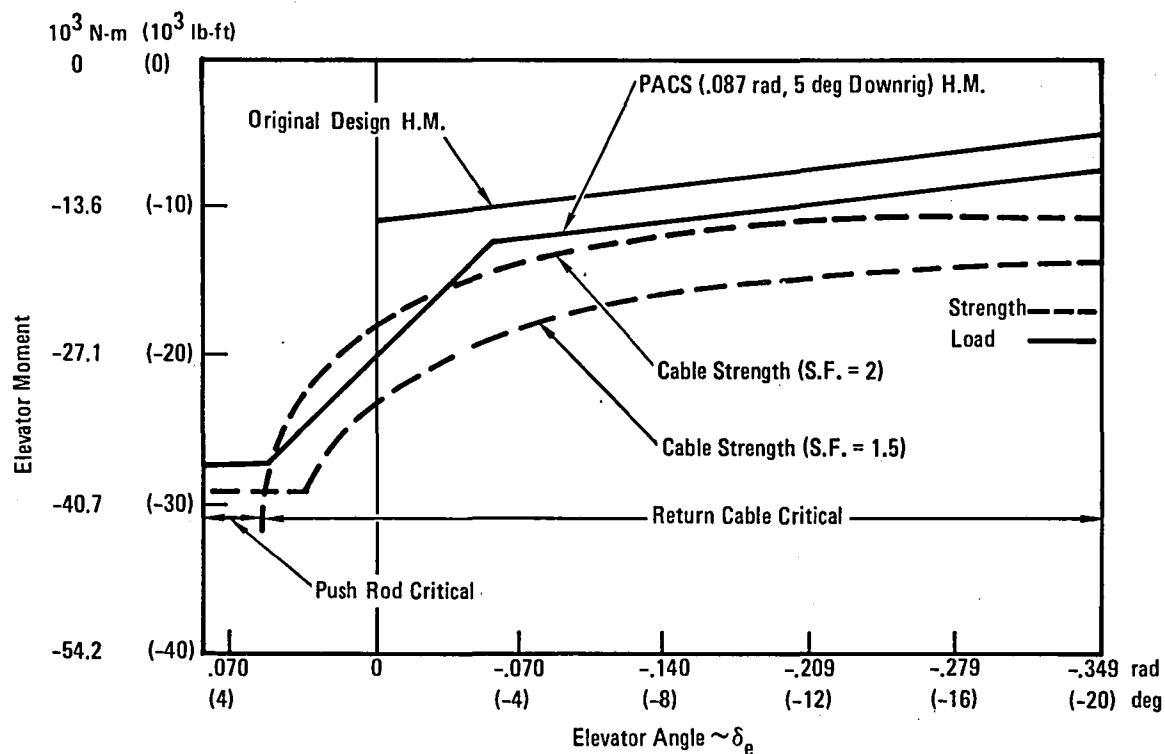


Figure 36. - Elevator control system limit strength and hinge moment envelopes.

3.5 Weight and Ballast

Weight and balance tasks included maintaining weight and balance status of the flight test aircraft, determining c.g. management system ballast distribution, and providing inertia data for structural loads and flutter analyses.

3.5.1 Weight and Ballast Status.— The operational empty weight of the flight test aircraft was periodically updated during the PACS analysis and design phase. This weight included all PACS components, test instrumentation and equipment, and crew allowance. Also, the aircraft balance and weight was maintained throughout the flight test program.

3.5.2 C.G. Management System.— Design criteria for the aircraft ballast included available space restrictions, structural limitations, c.g. range and maximum weight, capability to transfer ballast distribution in flight, and dump provision.

Space considerations determined that the ballast be located in the lower cargo deck of the aircraft (forward, center, aft cargo compartments) and the aft passenger floor. Structural limitation loads for these areas are given in Table 5. The c.g. range requirement was from 25 to 39% mac. Capability to transfer the ballast and dump provisions were a design consideration discussed in Appendix C.

3.5.2.1 Ballast system configuration: The ballast location requirements necessary to comply with the weight requirements and provide the required c.g. range is given in Figure 37. The physical layout of the ballast on the passenger floor and cargo deck that complies with the structural loading limitations is shown in Figure 38. The crosshatched areas represent fixed ballast such as lead. Water ballast on the passenger floor is not transferable but it can be dumped. Water ballast on the cargo floor can be transferred from the tanks in the forward cargo area to the tanks in the center cargo area. Also, water in this system can be dumped. The table at the top of Figure 38 shows the ballast weight required at each of the fuselage stations shown in the figure.

3.5.2.2 C.G. management: Center-of-gravity envelopes give the range within which the aircraft must be loaded. Both the flight and taxi restrictions are indicated. Figure 39 represents the flight test aircraft envelope with loading vectors included. The plot starts with the operational empty weight (OEW), adds fixed ballast, fixed water, and forward transferable water to obtain zero fuel weight (ZFW). The fuel vector is shown in two positions:

TABLE 5. - LOADING LIMITS

| LOCATION | LOADING LIMITS | | |
|---|-------------------|--|-------------------|
| | kg/cm (lbs/ft) | kg/cm ² (lbs/ft ²) | kg Total (lbs) |
| Passenger floor | 11.16 (750) | .022 (2) (45) | — |
| Fwd cargo | 19.35 (1300) | .073 (150) | 8164.6 (18000) |
| Center cargo | 19.35 (1300) | .073 (150) | 8164.6 (18000) |
| Aft cargo | (1) | .073 (150) | 4422.5 (9750) |
| (1) Tapers from 13.39 kg/cm (900 lb/ft) at FS 1625 to 8.04 kg/cm (540 lb/ft) at FS 1792. | | | |
| (2) Aft of FS 1792 the loading limit is .0146 kg/cm ² (30 lb/ft ²) | | | |

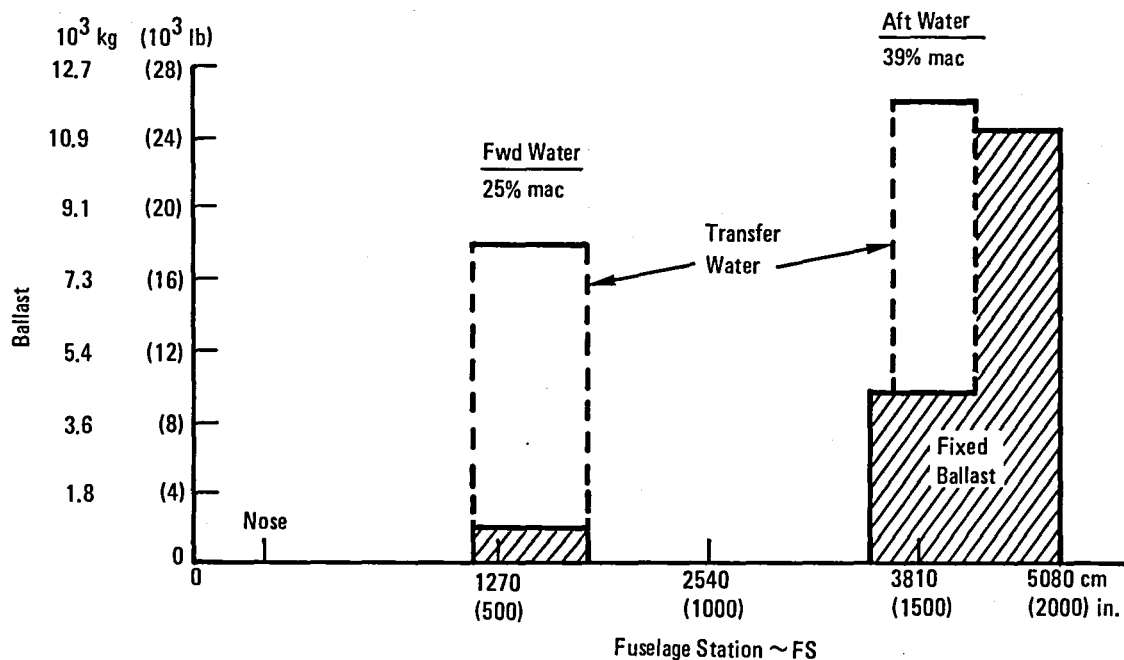


Figure 37. - Ballast location requirements.

forward for takeoff and landing, and aft for testing at a c.g. of 39% mac. Fuel usage is shown sequenced such that the fuel vector coincides with the aft limit.

3.5.3 Inertia Data.— Aircraft weight and c.g. points for the inertia cases are summarized in Figure 40. The Weight Distribution Program requires input data by panel point. The aircraft is divided into panels, and each weight (empty, payload and fuel) and c.g.'s are input. The program can compute the integrated unit inertia shears and moments, and mass moments of inertia for each case specified. An example of integrated data is shown in Figure 41 where the aft body shears and moments are plotted. Similar data were computed for the forward body, wing and tail.

In addition to the total aircraft inertia, selected component inertia data was calculated. Figure 42 illustrates the data prepared for the modified elevator balance weights and supports. Data of the type given in the table was used to compute the static moment and the moment of inertia about the hinge line.

| Location | Ballast | |
|-------------------------|------------------------|-----------------------------|
| | c.g. FS cm (in.) | Weight kg Total (lbs) |
| Passenger Floor – Fixed | 3838 (1511) | 4309 (9500) |
| Passenger Floor – Water | 4227 (1664) | 5715 (12600) |
| Fwd Cargo – Fixed | 1552 (611) | 907 (2000) |
| Fwd Cargo – Water | 1552 (611) | 7257 (16000)* |
| Center Cargo – Fixed | 3884 (1529) | 907 (2000) |
| Center Cargo – Water | 3884 (1529) | 7257 (16000)* |
| Aft Cargo – Fixed | 4343 (1710) | 4422 (9750) |

*Water is Either in Forward
or Center Compartment
Tanks

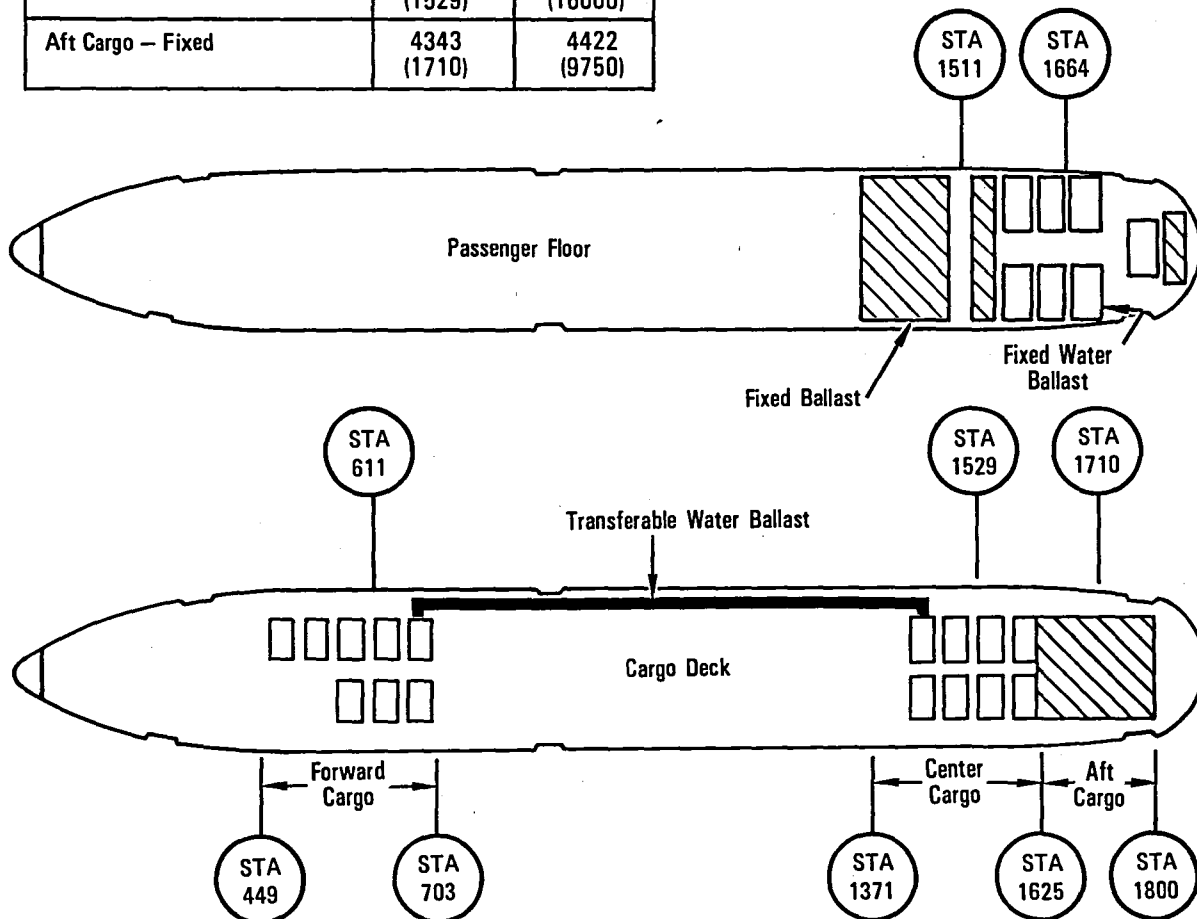


Figure 38. - Ballast configuration that complies with space and floor loading requirements.

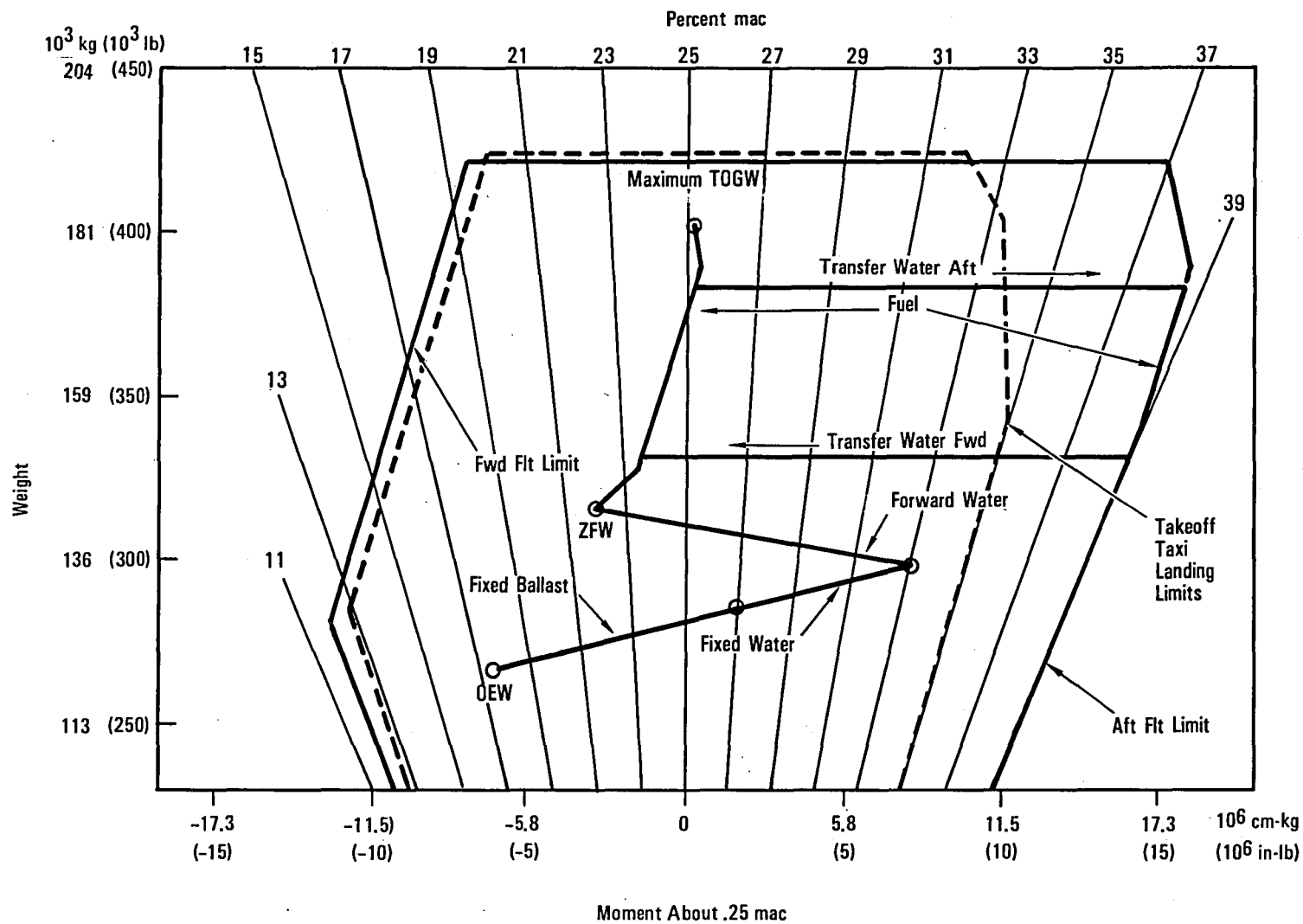


Figure 39. - C.G. envelope and travel.

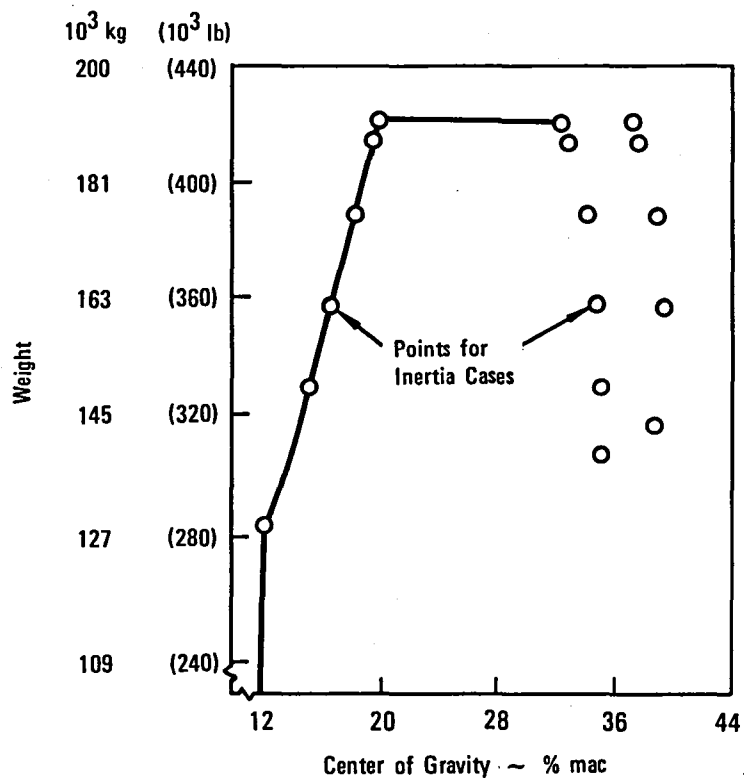


Figure 40. - Aircraft inertia cases.

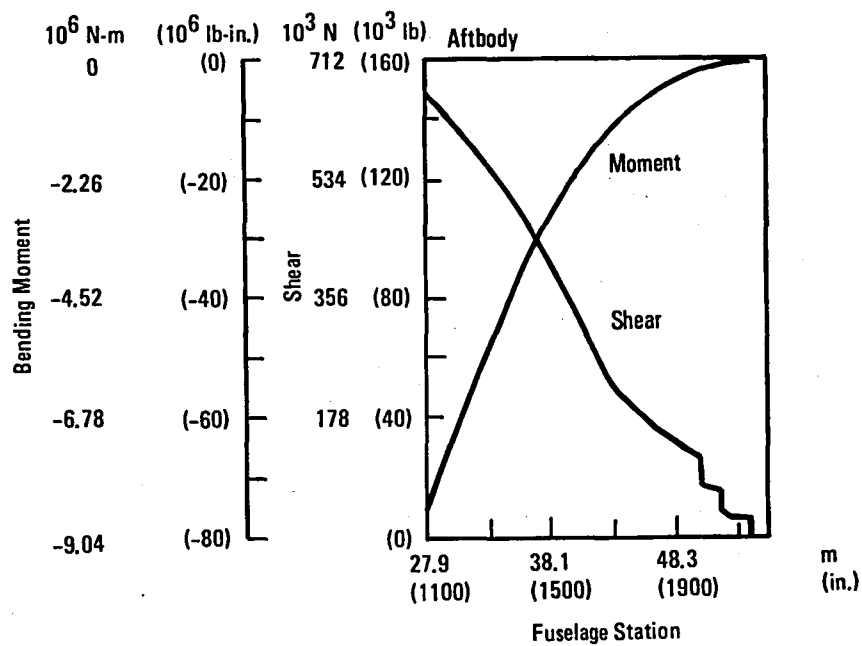
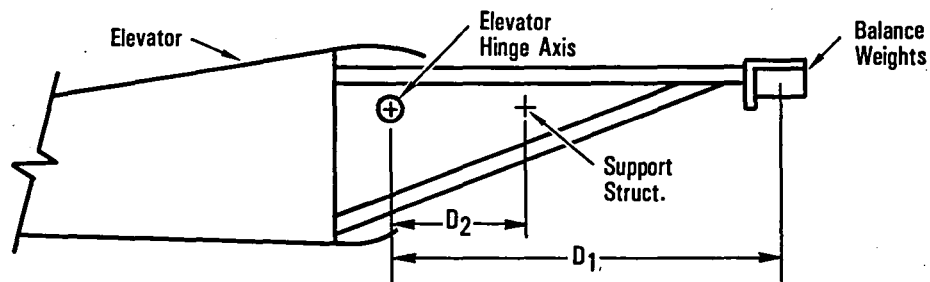


Figure 41. - Aircraft inertia data.



| Bay | Balance Weights | D_1 | Support struct. Weights | D_2 |
|--------|-----------------|-------|-------------------------|-------|
| A | 12.7 | -10.5 | 2.0 | -5.2 |
| B | 9.0 | -11.8 | 1.9 | -5.9 |
| C | 8.0 | -12.8 | 2.7 | -6.9 |
| | | | | |
| L | 30.5 | -25.8 | 6.6 | -12.9 |
| M | 23.1 | -28.1 | 7.2 | -14.0 |
| TOTALS | 190.2 | -20.3 | 60.2 | -11.6 |

Figure 42. - Component inertia data.

3.6 Structural Loads Analysis

The overall objective of structural loads analysis is to assure that structural capability of the flight test aircraft is not exceeded during PACS flight testing.

3.6.1 Analysis Methods.

3.6.1.1 Overview of methods: The structural loads analysis objective of assuring that flight test aircraft structural capability is not exceeded was met through issuance of a set of structural operating restrictions and requirements as a part of the flight safety procedure. Normally, established design limit load levels are used as a basis for establishing prototype flight testing structural operating restrictions. However, since the flight test aircraft has significant restrictions due to installation of the extended-span wing and additional restrictions were expected from the more

aft center-of-gravity location, downrigged elevator, and PACS-equipped horizontal tail, it was necessary to utilize inherent structural limit strength capability beyond design limit load levels to provide sufficiently wide operating limits for PACS flight testing.

The major loads analysis effort was directed toward determining distributed net loads (panel loads) for the complete airframe. In addition, increased elevator trailing-edge-up hinge moments resulting from the .087 rad (5 deg) downrig were determined. In general, static and dynamic loads were obtained using well established methods developed during the design of the basic L-1011 aircraft and its derivatives.

The analysis criteria and methods used to develop limit loads and define structural operating restrictions based on these loads relative to structural capability are described below.

3.6.1.2 Loads analysis criteria: Structural loads analysis criteria based on normal transport category FAR 25 (Reference 2) structural design requirements were developed early in the loads analysis process. These included basic structural design loads criteria, fatigue and fail-safe requirements, analysis model grid systems, relevant aerodynamic data for structural design, and a procedure for incorporating the resulting loads.

Dynamic gust loads were determined in accordance with the design envelope criterion for continuous turbulence. The design envelope criterion as opposed to the mission profile criterion is considered better suited to the PACS program since only limited test flying is involved at specific flight envelope points and the loads are not dependent on anticipated fleet operational usage. Both the design envelope and mission profile criteria comply with the continuous turbulence requirements of Reference 2.

Pilot recovery 2.0 seconds after a PACS undetected hardover failure was adopted as a reasonable criterion for the PACS flight test program in lieu of the more conservative FAR 25 criterion of FAR AC No. 25.1329-1A. Further, based on actual pilot response to abrupt pitch attitude changes observed during earlier flight testing of L-1011 aircraft at aft c.g. low stability regions, the recovery response established for analysis is a rapid movement of 0.14 radians/second (8.0 deg/sec) of tail position to 0.026 radian (1.5 degree) beyond trim and then a 0.017 radians/second (1.0 deg/sec) return to trim.

3.6.1.3 Static loads methods: Static loads analysis consists of:

- Generating transient maneuver and PACS failure condition time histories

- Determining maneuver and PACS failure condition distributed loads
- Selection of critical distributed loads

Transient maneuver and PACS failure condition time histories were generated with a three-degree-of-freedom Continuous System Modeling Program (CSMP). Output quantities of load factor, pitch rate, and pitch acceleration, which are usually selected at the time of occurrence of maximum tail load, were used as input to a static aeroelastic loads program for determining distributed airframe loads. Sixty transient maneuver conditions were simulated. From these, sixteen were selected for distributed loads analysis.

Approximately two hundred PACS failure condition time histories were simulated using CSMP. Both detected and undetected hardover failures were investigated over a wide range of variables (series servo authority limit, weight/center of gravity, speed/altitude, aircraft configuration, pilot recovery response time) to determine the most critical conditions in terms of peak load factor and tail load. Failure characteristics, supplied by the Avionics Group, were used to provide the horizontal stabilizer movement with time (independent variable) for these simulations. Once anticipated satisfactory authority limits and critical flight parameters were established through time history analysis, distributed loads were computed for the eight most critical cases. The relationship of these loads to limit strength capability along with failure probabilities were used to define structurally allowable series servo authority limits.

The static aeroelastic loads program was used to generate maneuver and PACS failure condition vertical and axial distributed net loads for a balanced flexible airplane utilizing a network grid of 261 load points. The airload distributions associated with this program were derived from extensive wind-tunnel model surface pressure measurements obtained during the initial L-1011 design phase. Distributed net loads were developed for seventy-seven maneuver/flight-condition combinations. A critical set of loads from twenty-eight of these was selected for transmittal to the Stress Group for use in assessing the structural capability of the flight test aircraft.

Critical distributed loads were selected using a loads ranking procedure referred to as stacking/scanning. This is a computerized technique for identifying critical loads from an array of loads which have been combined (stacked) for assessment (scanning). The scanned quantities are integrated net loads at selected airframe locations. Both two-dimensional scans (e.g., vertical shear versus torsion) and three-dimensional scans (vertical shear versus torsion versus bending moment) were made to determine which load values define outer boundary points of the load envelopes. These boundary load values are identified as critical. Through this stacking/scanning procedure a minimum set of critical loads was selected for evaluation by using a large finite element model program. The load-envelope plots formed by this procedure are the fundamental visual tool for assessing loads.

3.6.1.4 Dynamic loads methods: The PACS dynamic loads analysis consists of the following items:

- Determining the statistically defined integrated loads (shear, bending moment, and torsion) due to vertical gust
- Developing distributed panel load conditions which represent the statistically defined vertical gust loads, including proper load phasing
- Determining oscillatory failure net loads

Incremental dynamic vertical gust RMS loads (shear, bending moment, and torsion) were obtained using the vertical gust analysis (VGA) power spectral density loads program. The program utilizes twenty structural modes, unsteady aerodynamics representation, and provides for active controls modeling in the determination of statistical load properties for a unit gust input. In accordance with the design envelope criterion, a selection of flight conditions were analyzed encompassing a wide range of weight/center-of-gravity and speed/altitude combinations. Twenty-eight analysis cases were obtained from which the five most critical were selected for evaluation of active control systems effects.

A selected number of distributed net panel loads conditions were then developed which when integrated match properly phased shear, bending moment and torsions as established by the VGA analysis. Phasing is accomplished utilizing statistical correlation coefficients computed from the results of the VGA analysis. The panel load conditions are produced using the linear optimization program for matching conditions which applies linear optimization programming techniques to the matching condition procedure. The matching condition procedure and the use of correlation coefficients are discussed in detail in Reference 5 (FAA-ADS-53) and its companion report, Reference 6 (FAA-ADS-54).

The oscillatory failure analysis was performed using a variation of the VGA program in which the gust input is replaced by a .017 rad (1.0 deg) of amplitude stabilizer aerodynamic input. The resulting airplane response is in terms of modulus and phase angle for each load quantity. The oscillatory failure loads are then adjusted to account for system mechanical and rate limiting effects on the amplitude of oscillation.

3.6.1.5 Loads evaluation: Operating restrictions include the limits of maneuver load factor within the desired flight test operating envelope for which predicted loads do not exceed aircraft limit strength capability. Strength capability for various segments of the aircraft structure was developed through an iterative process. Limit strength capability data was developed to aid in selecting potentially critical maneuver, gust, and PACS failure load conditions. A set of distributed net loads representing

the most critical conditions was then determined. After analysis of these loads using the finite element model, updated limit strength capability data were generated.

Through this iterative process and through comparison of loads to strength capability, using the load envelopes described in Section 3.6.1.3, the maneuver load factor and gust load limitations were determined.

3.6.2 Analysis Results.

3.6.2.1 Static aeroelastic loads: The result of static aeroelastic loads analysis is a set of predicted airframe loads representing the most critical combinations of aircraft maneuver type and flight parameters (gross weight, center of gravity, speed/altitude, controls configuration) within the design criteria envelope boundaries. These boundaries extend beyond the desired handling qualities flight test condition requirements in order to provide flight flutter clearance speed/altitude margins and, in general, to obtain as large a flight operating envelope as feasible within the structural strength capability of the flight test aircraft.

Typical load envelope plots at one wing station and one horizontal tail station are shown in Figures 43 and 44, respectively. These figures show the limit structural capability boundary and some of the loads from the set used to define this capability boundary. Loads shown outside the capability boundary were subsequently reduced by imposition of load factor restrictions. The most severe wing loads of Figure 43 (large positive shear and bending) represent full FAR 25 load factor positive steady maneuvers. Figure 44 illustrates the relatively large negative torsion tail loads caused by the .087 rad (5 deg) elevator downrig. The effects of this downrig were the most influential on structural operating restrictions.

3.6.2.2 Dynamic gust loads: Net dynamic vertical gust integrated loads (shear, bending moment, and torsion) for the PACS configuration were compared to limit structural capability or limit design load envelopes. The effect of the PACS configuration was most significant on the horizontal tail component, primarily due to the shift in 1 g flight loads associated with the downrigged elevator. As a result of this comparison, a set of thirty horizontal tail panel load conditions were provided for stress analysis.

Gust loads, including those for the horizontal tail were within the structural capability of the flight test aircraft. Figure 45 shows typical horizontal tail dynamic gust load results (circled points) relative to the limit structural capability boundary. It can be seen from this figure that the criticality of the horizontal tail gust loads is heavily influenced by the large negative torsion associated with the elevator downrig.

NOTE: Loads (⊗ symbols) in excess of structural limit strength capability (solid boundary) were subsequently reduced by imposition of maneuver load factor restrictions.

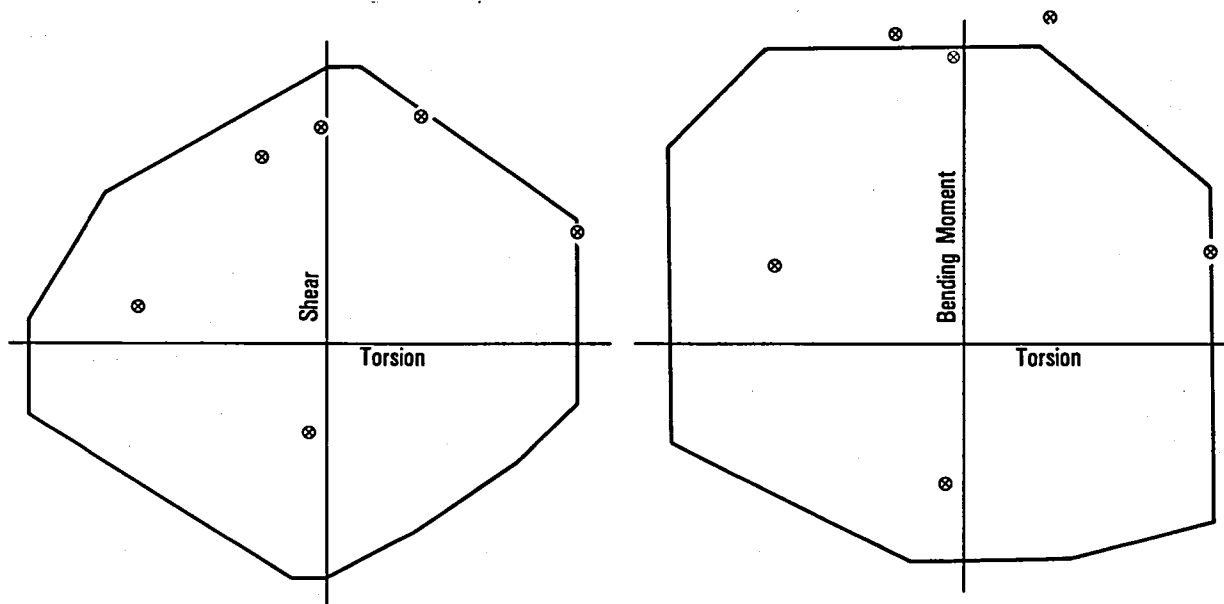


Figure 43. - Wing limit static loads, 75% semispan.

NOTE: Loads (⊗ symbols) in excess of structural limit strength capability (solid boundary) were subsequently reduced by imposition of maneuver load factor restrictions.

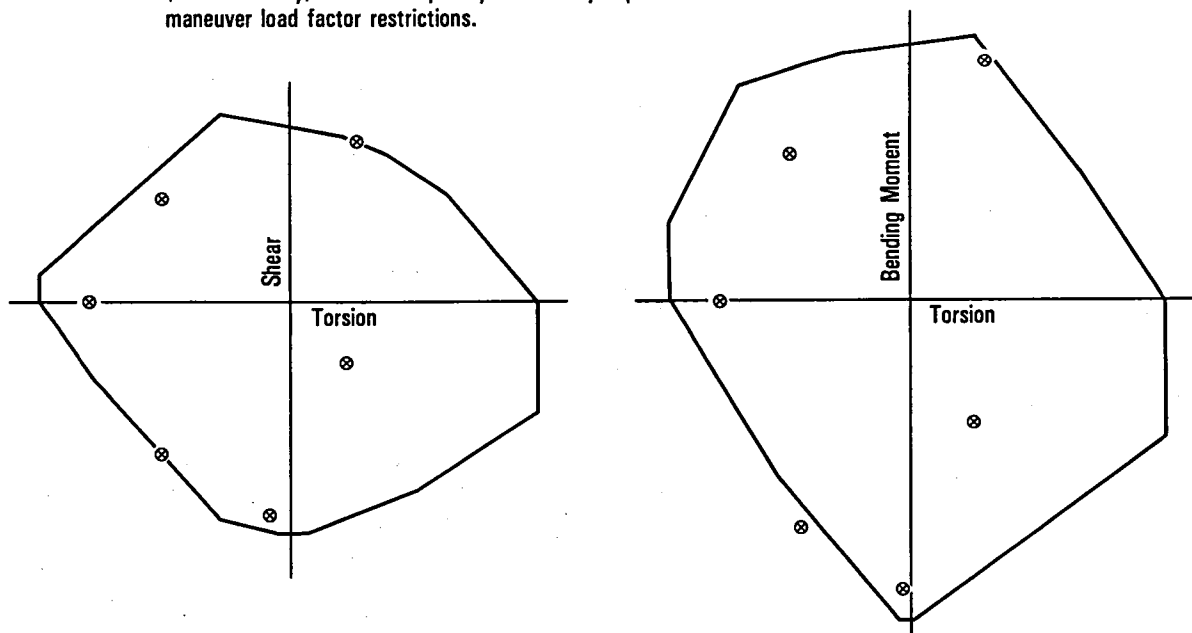


Figure 44. - Horizontal tail limit static loads, 32% semispan.

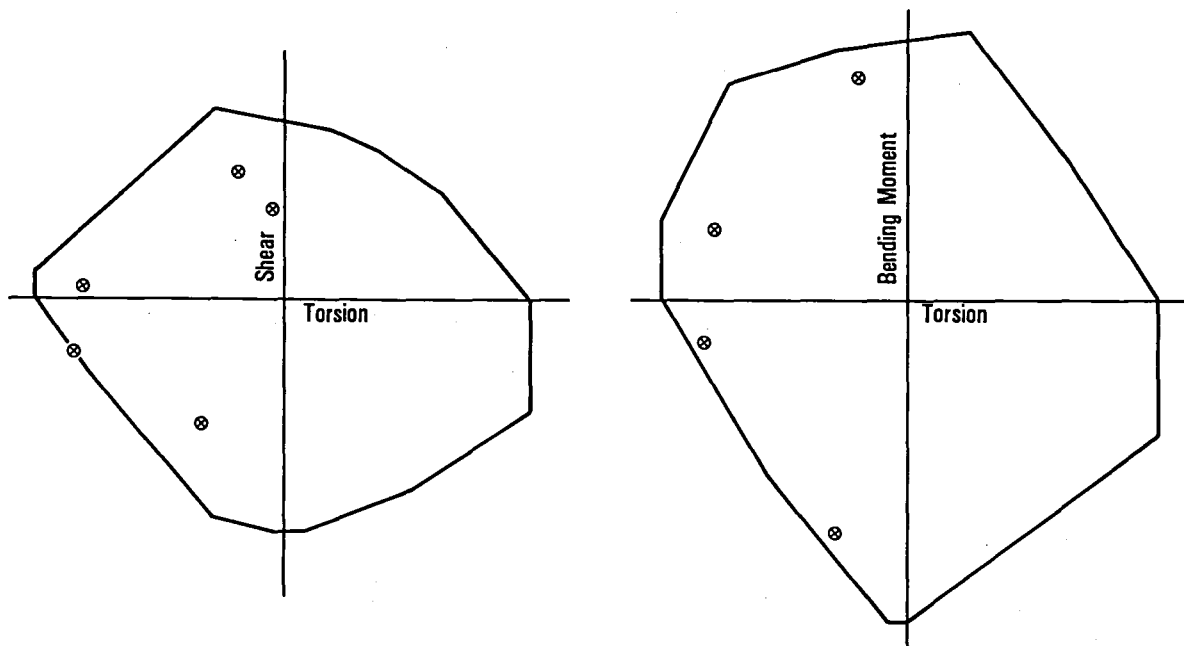


Figure 45. - Horizontal tail limit dynamic gust loads, 32% semispan.

3.6.2.3 PACS failure conditions analysis: Three basic types of PACS failure conditions were evaluated: hardover, slowover, and oscillatory.

The undetected hardover is the most severe type of non-oscillatory failure. The loads resulting from this type of failure along with its probability of occurrence determined the structurally allowable series servo authority limits: .012 rad (.7 deg) aircraft nose up and .016 rad (.9 deg) aircraft nose down at a $-.017$ rad (-1.0 deg) trim setting. The sequence of this failure is a rapid movement of stabilizer from trim by an amount equal to the authority limit, then holding this position until a simulated pilot recovery is initiated. Figure 46 shows a typical time history of load factor for an aircraft nose up undetected hardover with a simulated pilot recovery at 1.0, 2.0, 3.0 and 4.0 seconds after occurrence of failure. Maximum load factor of 3.8 occurs approximately 3 seconds after start of failure for this case. Pilot recovery after this time does not reduce peak load factor. The 2.0 seconds recovery criterion discussed in Section 3.6.1.2 results in a peak load factor of 3.1.

Oscillatory failure condition net loads were determined using a variation of the vertical gust analysis program. The results of this analysis are illustrated in Figure 47 in which the largest horizontal tail loads due to oscillatory failure, obtained at 5.6 Hz and rate-limited to $\pm .0063$ radians (± 0.36 deg) amplitude by the power servo response characteristics, are shown

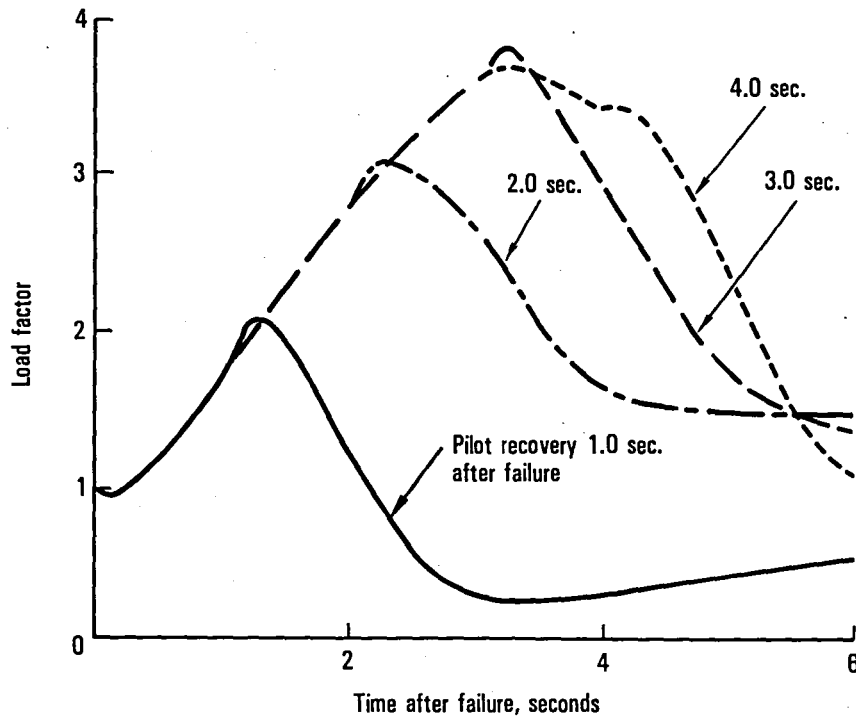


Figure 46. - Effect of pilot recovery time on peak load factor during PACS undetected hardover failure.

superimposed on the limit strength envelope. These loads, conservatively neglecting load component phasing and plotted as an envelope of maxima, are seen to be within structural capability.

3.6.3 Structural Operating Restrictions.- The structural operating restrictions and requirements are the end product of the structural loads analysis task and reflect the structurally safe operating environment limits of the PACS flight test aircraft based on predicted loads relative to structural capability. Restrictions include aircraft load factor, speed/altitude, aircraft weight and center-of-gravity limits (including ballast distribution), fuel loading and ground restrictions, and allowable turbulence and buffet limits. Requirements include telemetry and/or onboard loads monitoring. This material was specified through a revision to the existing L-1011 operating restrictions report and issuance of two Aircraft Structural Operating Limitations Memos.

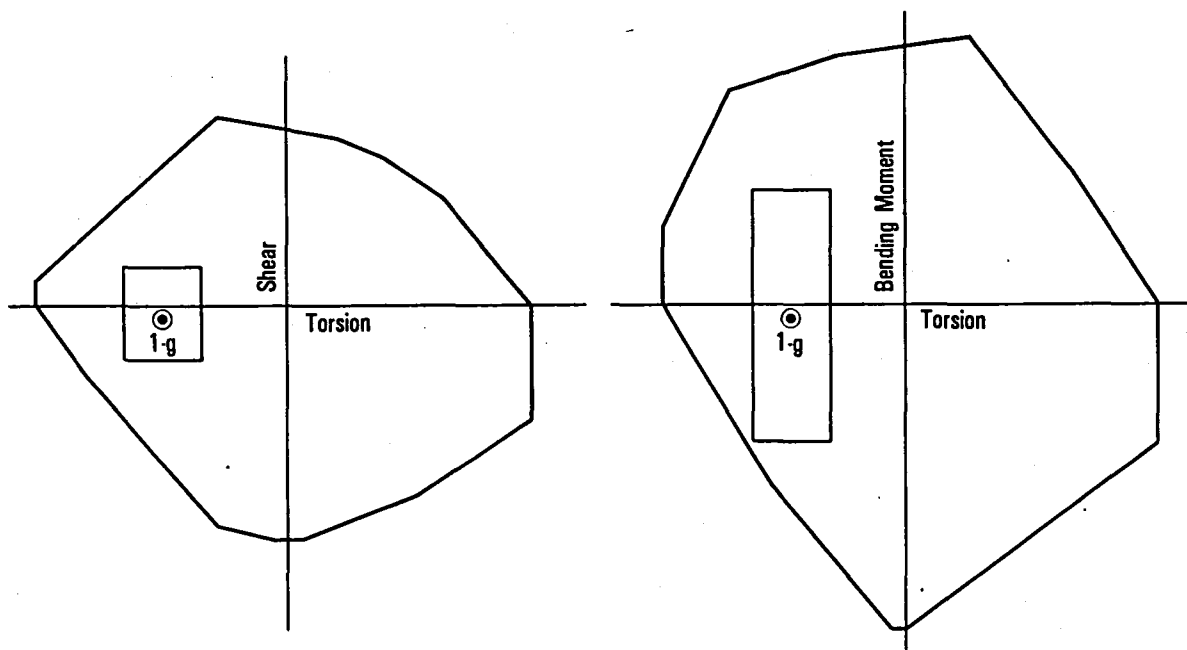


Figure 47. - Horizontal tail PACS oscillatory failure limit loads, 32% semispan.

Figure 48 shows a composite summary of the more significant restrictions. Maneuver load factor restrictions applicable to the flight test aircraft prior to PACS configuration testing were maintained without additional restriction within the complete design cruising speed envelope and expanded 39% mac aft center-of-gravity envelope through the utilization of inherent structural limit strength capability beyond design limit load levels.

3.7 Flutter

3.7.1 Introduction. - The objective for performing flutter analysis is to assure that flutter margins of the flight test aircraft equipped with a PACS meet the flutter criteria for flight safety.

3.7.2 Analysis Methods. - Two different procedures were used to investigate flutter stability of the aircraft. One procedure was the classical method known as the velocity versus frequency and velocity versus damping solution. The other procedure was the phase versus gain method which

WEIGHT AND BALANCE RESTRICTIONS

The following maximum gross weights in conjunction with the center-of-gravity envelope and the ballast system limits are not to be exceeded during flight test operations of the subject configuration.

| | | |
|--------------------------|------------|-------------|
| Maximum Ramp Weight | 192,326 kg | 424,000 lb. |
| Maximum Takeoff Weight | 191,419 kg | 422,000 lb. |
| Maximum Landing Weight | 162,389 kg | 358,000 lb. |
| Maximum Zero Fuel Weight | 141,732 kg | 312,460 lb. |

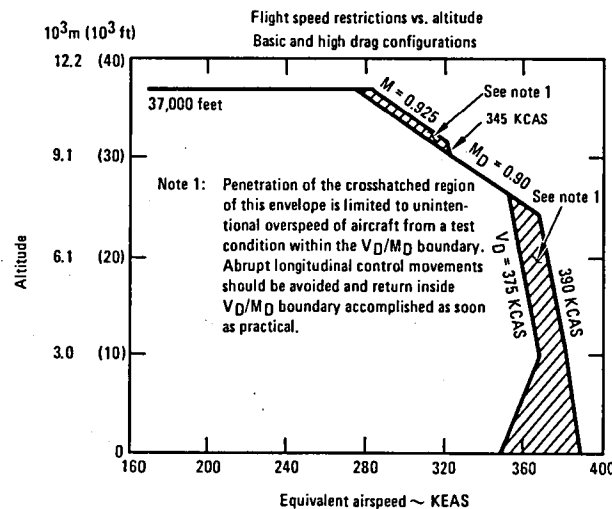
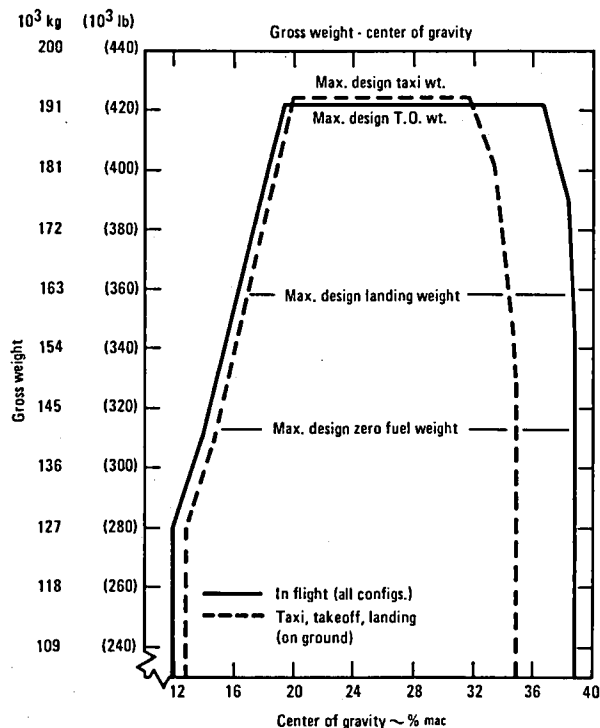
MANEUVER LOAD FACTOR RESTRICTIONS

The following maneuver load factor restrictions apply in combination with weight and balance restrictions unless further restricted by an ASTOL. These load factors are applicable when the gust boom is not installed.

| Configuration | Load Factor | |
|-----------------------|-------------|------------|
| | AACS Off | AACS On |
| • Symmetric Maneuvers | | |
| Basic and High Drag | 0.0 to 2.0 | 0.0 to 2.2 |
| Flaps Extended | 0.0 to 1.8 | 0.0 to 1.9 |

NON-STANDARD CONFIGURATION ITEMS

1. Extended wing tips and outboard aileron installed.
2. Outboard aileron rigged such that, in flight, it is 0.035 rad (2 deg) trailing edge up from faired position (AACS off)
3. Pylon nacelles downtilted 0.035 rad (2 deg)
4. Wing active control system (AACS) installed.
5. Near term pitch active control system (PACS) installed.
6. Elevator downrigged 0.087 rad (5 deg)



ADDITIONAL LIMITATIONS

Flight in turbulence restrictions, including CG load factor monitoring shall be observed.

Maneuvering load factor shall be limited to 0.75 to 1.25 (1.0 ± 0.25) while intentionally flying in light turbulence such that total load factor from maneuver plus turbulence would normally be within 0.50 to 1.50, and every precaution is taken to not exceed 0.25 to 1.75 (1.0 ± 0.75).

Loads at wing BL 702, tail BL 126, and in elevator link shall be monitored onboard. These loads shall also be monitored at telemetry ground station during the first maneuvering flight, and thereafter will not be a requirement for flight safety unless specifically requested.

Buffet penetration beyond onset will require additional loads monitoring onboard and/or at telemetry ground station: tail BL 126, left hand vs. right hand bending moment; middle and outboard elevator counterweight accelerations. Limits on load levels and exposure time will be established based on monitored data.

Figure 48. - Composite summary of structural operating restrictions.

assesses the phase and gain margins of the system/structure at specific flight conditions.

The classical method utilizes modalized flutter equations. A vibration analysis is performed first. Before the first flight, the analytical vibration modes are verified by a ground vibration test (Section 4.5). Eigenvectors obtained from this analysis are used to modalize the flutter equation. The flutter analyses were performed at $M = 0.88$ using Kernel Function aerodynamic theory (Reference 7). Open (without PACS) and closed (with PACS feedback) loop flutter analyses were performed. The control laws used in the analysis were subsequently verified by transfer function tests on the aircraft prior to the first flight (Section 4.5). Forty-two (2 rigid body and 40 elastic) modes were used for each flutter analysis.

Application of the phase versus gain method provides a plot for a specific flight condition of phase (rad, deg) as a function of Feedback Amplitude Ratio Margin (FARM) in dB for the frequency range of interest (frequencies in Hz shown adjacent to the curve). FARM is defined as the negative of the open-loop logarithmic ratio of the output signal (δ_{out}) to the input signal (δ_{in}) as shown in Figure 49. A typical phase versus FARM plot is shown in Figure 50. The gain and phase margins are determined in the same manner as for the classical Bode plot. The value of FARM at zero phase angle defines the gain margin and the absolute value of feedback phase angle at zero FARM defines the phase margin. The curves in Figure 50 are for frequency values from 0.11 Hz to 5.11 Hz. However, analyses were performed for frequencies to 25 Hz. The higher frequency modes had values of phase and gain which provided large flutter margins. The flutter margin is satisfied when the nominal gain curve is outside of the cross hatched region shown in Figure 50. This region provides suitable gain and phase margins to allow for unannounced/undetected failures of the PACS which result in significant gain and phase changes. The criteria used to define the region boundaries is based on the L-1011 AACS flutter certification criteria. The FARM solution shown on Figure 50 was performed at two times nominal gain.

3.7.3 Conditions Analyzed.— Analyses encompassed the range of flight conditions for each aircraft configuration to be evaluated during the flight tests.

The classical method was used to investigate the intact aircraft (no failures) and the case of one free elevator. Aircraft parameters evaluated were wing fuel (minimum to heavy), center of gravity (24 to 39% mac), horizontal stabilizer incidence angles (elevator gearing ratio and stabilizer gain values), and PACS gains (0.5, 1.0, and 2.0 times nominal). All flutter analyses solved for the stability over the speed range of 20 to 600 KEAS for a constant Mach number of 0.88.

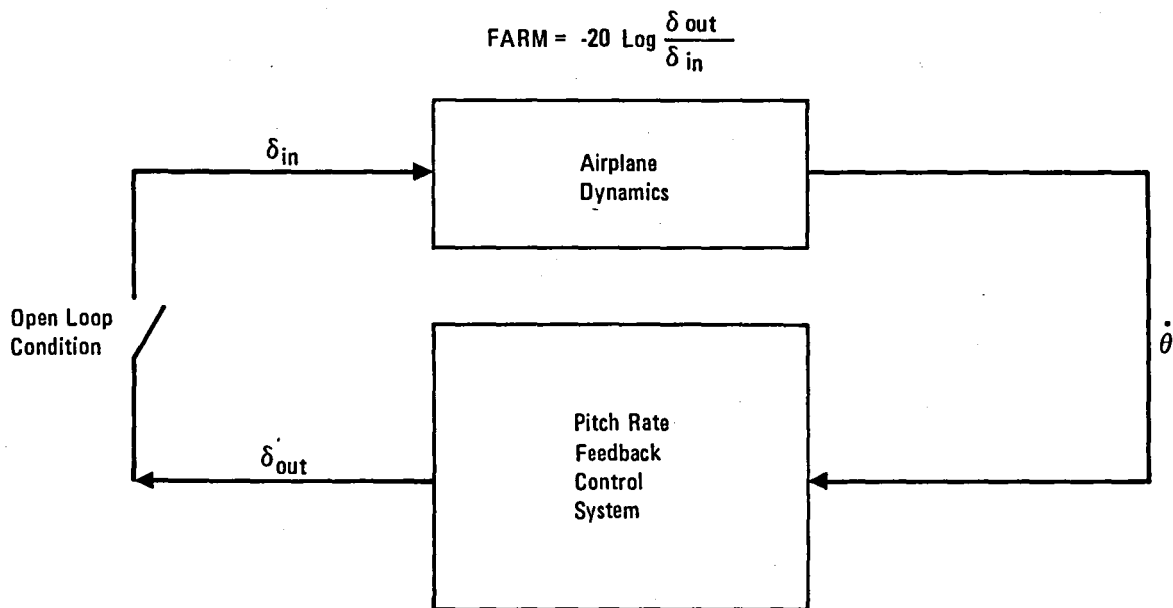


Figure 49. - Definition of feedback amplitude ratio margin (FARM).

The FARM technique was used to examine the 0.1 to 25 Hz frequency range which covers all significant rigid body modes and flexible aircraft modes through the horizontal stabilizer first torsion mode. Aircraft conditions evaluated were minimum fuel (at 24 and 39% mac) and heavy fuel (at 24 and 39% mac). Specific flight conditions were evaluated from 258 to 390 KEAS and altitudes of 3658 m (12,000 ft) to 11,278 m (37,000 ft).

3.7.4 Analysis Results.- The classical flutter analysis method showed the flight test aircraft to be free from flutter to $1.2 V_D/M_D$. Table 6 shows a comparison of modal frequency and damping characteristics for open loop and closed loop (2 times nominal gain) analyses. At this typical condition (402 KEAS at Mach 0.88) the frequency and damping are nearly identical. The same result was true for all of the conditions analyzed. Thus, two times nominal PACS gain with the loop closed produces a negligible difference relative to modal stability of the flight test aircraft with the PACS open loop.

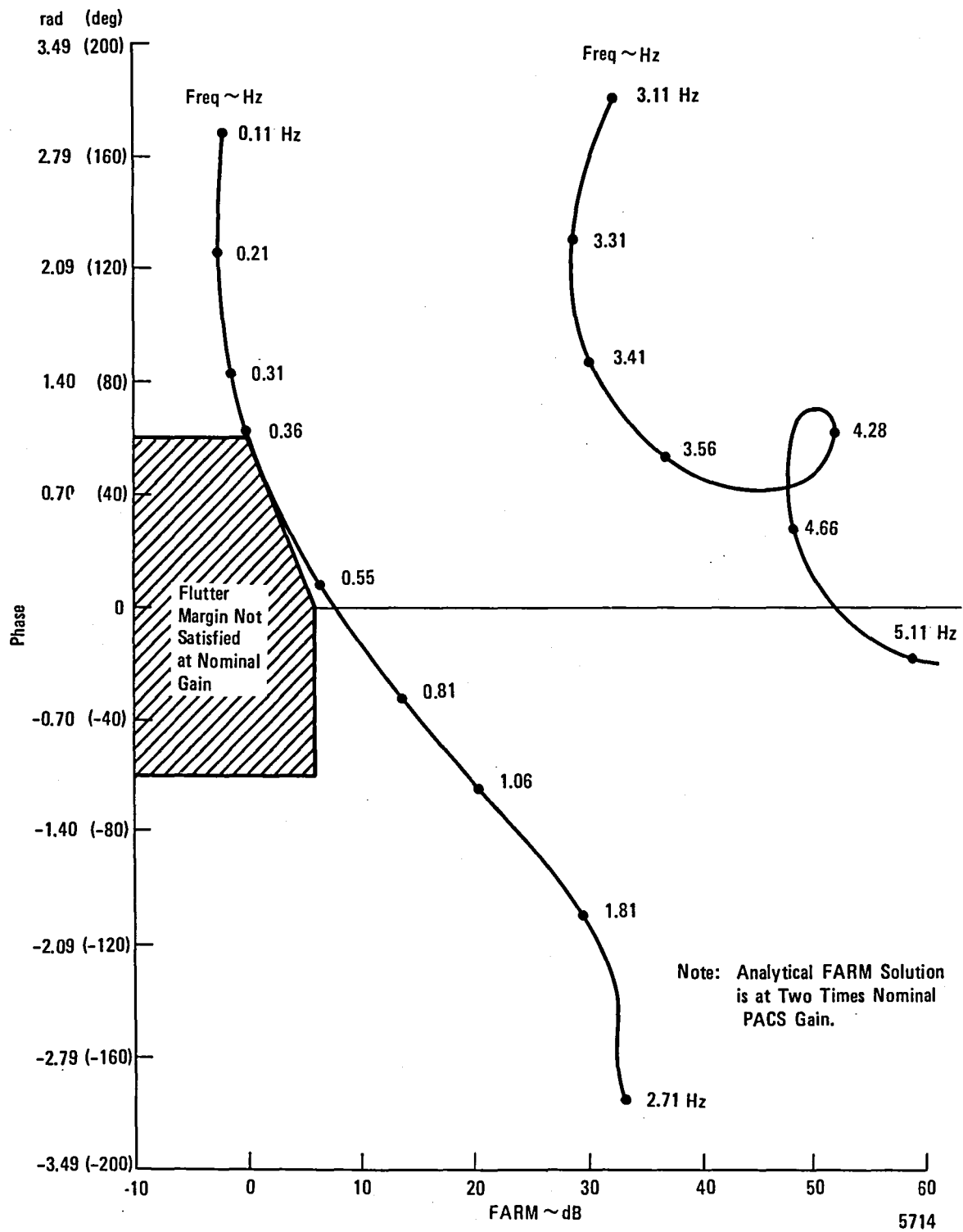


Figure 50. - Typical phase vs FARM plot.

TABLE 6. - COMPARISON OF FREQUENCY AND DAMPING FOR OPEN AND CLOSED LOOP (2 TIMES NOMINAL GAIN) ANALYSES

| Mode No. | FREQUENCY - Hz | | DAMPING | |
|----------|----------------|-------------|-----------|-------------|
| | Open Loop | Closed Loop | Open Loop | Closed Loop |
| 1 | 2.091 | 2.091 | -0.0987 | -0.0984 |
| 2 | 2.579 | 2.579 | -0.2729 | -0.2727 |
| 3 | 2.661 | 2.661 | -0.0369 | -0.0367 |
| 4 | 3.675 | 3.670 | -0.0825 | -0.0826 |
| 5 | 5.050 | 5.050 | -0.1221 | -0.1223 |
| 6 | 5.319 | 5.319 | -0.1993 | -0.1992 |
| 7 | 6.166 | 6.166 | -0.0426 | -0.0426 |
| 8 | 7.409 | 7.409 | -0.0787 | -0.0787 |
| 9 | 8.721 | 8.721 | -0.0285 | -0.0285 |
| 10 | 9.492 | 9.492 | -0.1550 | -0.1550 |

Flight Test Aircraft Condition: 1/6 wing fuel

Flight Condition: 402 KEAS at Mach 0.88

The phase versus gain (FARM) method showed that the flutter margins were satisfied. Figure 51 shows a comparison of analysis and flight test data for an aircraft condition of heavy wing fuel and for a flight condition of 389 KEAS. Since the curves are outside of the cross hatched region even for the two times nominal gain case discussed in Section 3.7.2, the flutter margin criteria are more than satisfied. Results of analysis and flight test data are almost identical over the 0.11 to 2.71 Hz frequency range. For the 3.11 to 3.81 frequency range the analysis showed greater flutter margins than the flight test. However, the flight test flutter margin is still considerably in excess of the required criteria. Nominal modal frequencies of interest are the wing first bending mode (1.8 Hz), the engine mode (2.7 Hz), and the fuselage first bending mode (3.5 Hz).

3.7.5 Conclusions.- The flight test aircraft was shown to be flutter free by analyses and was approved for flight testing.

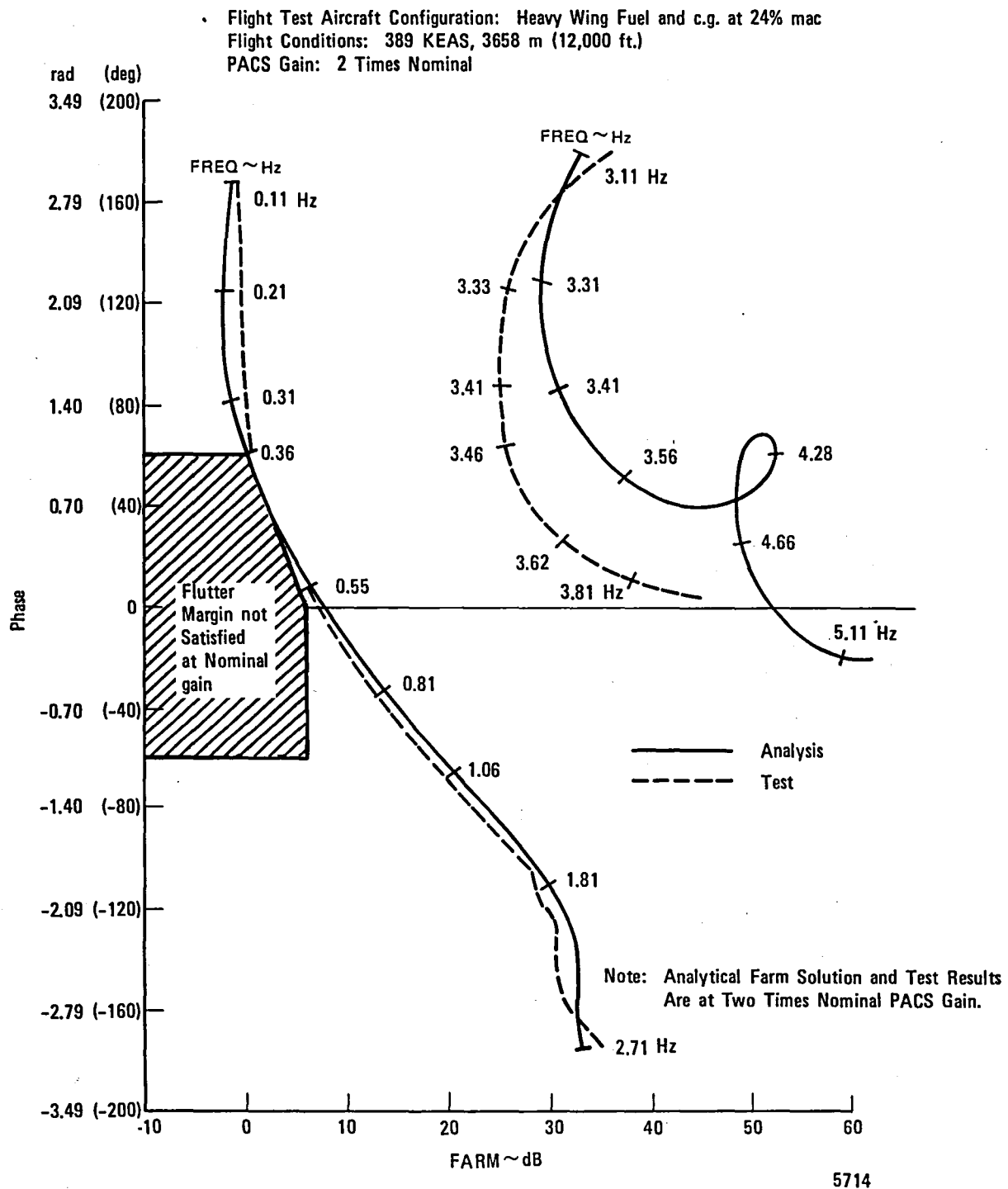


Figure 51. - Phase vs FARM comparison of analysis and flight test data.

3.8 Safety Analysis

Policies exist at Lockheed which require safety reviews to be conducted before and during the flight test program of a modified flight test aircraft. Thus, the safety reviews prior to first flight of L-1011 S/N1001 equipped with PACS included:

- Flight Test Safety Board Review
- Operational Safety Board Review
- First Flight Safety Review.

Also, at the completion of one month flying a safety review was conducted by the Safety Review Board. All of the reviews determined that the aircraft was safe for flight within the constraints and that the probability of a hazard was acceptably remote.

Preparation for the safety review meetings required that analysis be performed on the near-term PACS and associated aircraft systems to identify potential hazards caused by malfunctions of the PACS and to assess the probability of their occurrence during the flight test program. All significant single and multiple failures in the system hardware were considered. The following PACS components and associated aircraft systems were analyzed to assess hazards due to hardware failures:

- Sensors
- Digital computers and test pallet
- FCES panel
- Dual series servo
- Series servo summing linkages
- Aircraft electrical power system
- Aircraft hydraulic system.

Validation of the software was accomplished by software design reviews (walkthroughs) and VSS testing.

3.8.1 Analysis Approach.— Single failures are bound to occur and it is impossible to predict exactly when they will happen. Therefore, for flight

control systems, the design aim is to incorporate safety provisions to protect the system against critical effects of any single failure. Also, the flight crew needs to be warned of any failure, critical or not, so that the exposure time for the build up of possibly hazardous multiple failures is limited. The design aim is accomplished when there are no critical single failures and the probability of potentially hazardous multiple failures is acceptably remote. The objective of the safety analysis is to determine whether or not the design aim has been achieved.

The general approach is as follows:

- Identify the significant critical effects
- Determine how each critical effect can occur due to single or multiple failures in the PACS or the related airplane systems.
- Compute the probability of occurrence for each critical effect
- Assess the risk due to each effect by taking into account the ability of the crew to recognize the effect and to avoid a catastrophic outcome.

The basic methods used for performing the safety analyses are presented in the next two sections.

3.8.1.1 Bottom-up method (Failure Modes and Effects Analysis method): The bottom-up method is used for assessing single failures to determine whether the safety provisions provide adequate protection. The failure modes of each part are analyzed or simulated, one failure at a time, to determine the effect at the system output.

After the flight critical effects (potential hazards) have been identified, they are assessed by examining the equipment safety provisions. Separate analyses are performed on each piece of equipment in the PACS, electrical supply, and hydraulic supply to determine the effect of single failures. The failure effects fall into the four categories listed below.

1. Failures detected by safety provisions which switch out the faulty channel without significant transients.
2. Failures detected by safety provisions which cause significant transients.
3. Failures not detected (dormant failures) by safety provisions which are insignificant by themselves.
4. Failures not detected by safety provisions which cause a critical effect.

The first type of failure does not provide a critical effect and only needs to be considered in the analyses of multiple faults.

The second type of failure may be critical. It indicates a design deficiency.

The third type of failure does not cause a significant effect itself. However, this undetected failure can remain in the system and then when concurrent with another failure may result in a critical effect. For example, if the hardover detection monitor fails and then a hardover failure occurs the effect could be critical.

Identification of the fourth type of failures provide the basis for the major safety analyses effort.

3.8.1.2 Top-down method: The top-down method is used to assess multiple failure effects. Multiple failures are two or more independent single failures. The failures must exist concurrently but they need not occur simultaneously. The critical effect at the system output is first defined. Then, the analysis proceeds backward through the system components to identify all failures which can cause the critical effect. The analysis is repeated for each critical effect identified. By assigning proper failure rates and exposure times, the probability of each critical effect can be calculated. The exposure time is dependent on how and when the failure is detected.

The probability of independent failures occurring simultaneously, or even nearly simultaneously, is generally negligible because of the short exposure time. This is usually true when the first failure is detected and switched out of the system. Then, the exposure time for multiple failures is typically only a second or two. However, longer exposure times do occur in some cases. For example, when complete loss of the system is a significant hazard even without accompanying transients. Another example relevant to the PACS is the case where one system is disengaged because of a detected failure. For this case a servo hardover in the engaged system can cause a transient in excess of 1g before disengaging. Consequently when the exposure time is relatively long, the risk due to multiple failures may not be negligible and may require imposition of operating restrictions after the first detected failure.

Since undetected failures may remain in the system for long periods of time it is important that the failure rate of these dormant failures be small to limit the probability of their occurrence. The safety provisions should detect all significant single failures. One purpose of analysis and VSS testing is to identify all dormant faults and to assess their contribution to potentially hazardous situations.

3.8.2 PACS Safety Provisions.- Safety provisions are incorporated into the PACS to protect it against the critical effects of failure conditions.

The PACS employs redundant monitored components to provide system safety and failure survival capability (see Section 2.3.1 and Appendix D). The redundant design of the PACS is based on that of the AACS which is currently in airline service.

The automatic monitoring system monitors sensor signals, digital data bus signals, servo command signals, series servo position, and currents in the series servo EHV's. The status of the monitoring system is displayed on the display panel.

The PACS computer has self-test capabilities. Test switches and corresponding display lights are on the front of the computer panel.

The series servo authority is limited by mechanical stops so that a servo hardover is not an immediate structural hazard. However, subsequent build up of external loads on the aircraft structure depends on how long the hardover remains in the system.

3.8.3 Analysis Results.- A number of possibly hazardous failure effects were identified for the PACS and some of them could not be shown to be extremely improbable as defined in Figure 52. These hazards are due to the experimental nature of the system and would be corrected for a production design. Since the PACS will be engaged in flight only when the system is being tested, the flight crew can be expected to be alert and cope with the failure effects. This may not be the case in airline service. Each of the potential hazards identified are discussed in the following sections.

3.8.3.1 Complete loss of pitch control: The only failure effect identified that will result in complete loss of pitch control is a break in the series servo output-shaft/tie-in-mechanism load path. This path provides the reaction forces (ground point) required for manual and automatic pitch control. Pitch control is flight critical and a break in the output-shaft/tie-in-mechanism load path would probably result in loss of the aircraft. Therefore, both the tie-in mechanism and output shaft have dual mechanical linkages. Thus, complete loss of the pitch control is considered extremely improbable.

3.8.3.2 Partial loss of pitch control: The only failure effect identified that will result in partial loss of pitch control is failure of the PACS series servo lock when neither the servo active or standby channels are operating. A jam of the lock can only occur while the PACS is engaged and probability of the lock jam was determined to be 2×10^{-8} /hour. Ground tests with PACS off will ensure that the servo lock is functioning prior to take-off. In case of lock failure the degree of control loss depends on the

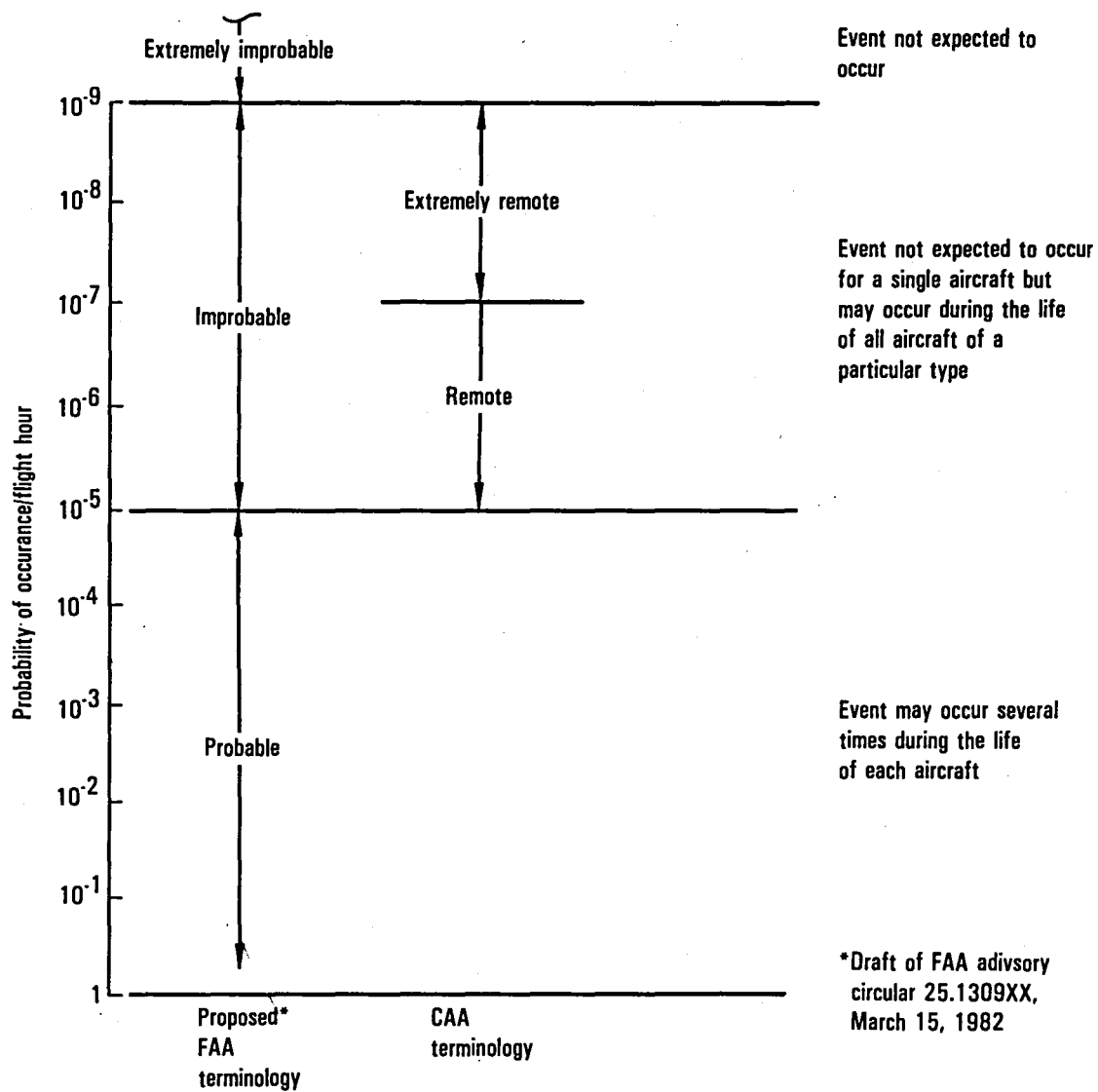


Figure 52. - Probability versus consequence of occurrence.

friction force provided by the series servo mod pistons. Laboratory tests showed the friction force to be sufficient to provide the pitch control. However, if there is insufficient servo friction partial loss of pitch control may be critical. Because of tests performed prior to takeoff, a lock failure probability of 2×10^{-8} /hr which applies only when the PACS is engaged, and capability for engagement of the series servo active or standby channel to regain control, the risk is acceptable.

3.8.3.3 Undetected hardover: At the time of the system engagement, hardover signals in two sensors of a sensor group or both channels of the computer that drives the engaged series servo channel can result in a stabilizer hardover. PACS tests performed prior to takeoff will detect these failures. The probability of these failures occurring during flight prior to engagement of the PACS has been very conservatively determined to be 10^{-6} /hr.

After system engagement, monitor failures in the computer or failure effects in the pallet that houses the computer can lead to stabilizer hardover. These effects are discussed separately in the following paragraphs.

If both monitors of a monitor set in a computer fail, a subsequent hardover failure normally detected by these monitors may occur. Although these monitor failures are dormant, three failures are required to cause a hardover and this makes these failure sequences extremely improbable.

Since the pallet houses the PACS computers and the four separate core memories which control them, the pallet contains all of the system interconnect wiring. There are virtually no segregation precautions regarding interconnections of the various components. Thus, interchannel shorts are possible. The probability of this occurrence resulting in a stabilizer hardover is estimated to be 10^{-7} /hr.

Power transients can scramble both core memories associated with one computer which may cause a hardover.

Since the master processor (minicomputer on the test pallet) has access to all four computational channels via four test adapters, failures or inadvertent operation could cause hardovers. Four switches are provided to lock out each adapter during flight test. Safety is dependent on precautions taken by the flight crew. With proper precautions the probability of a hardover is acceptably remote.

Two switches on the pallet which connect power to two relays provide for test signal injection into the four computer channels. One switch injects kicker inputs which are adequately protected against hardovers in the software. Thus, a hardover is extremely improbable. The other switch is not used in flight and is guarded against inadvertent operation. A hot short in the pair of relays associated with this switch or human error could inject test signals and cause a hardover. Safety is dependent on precautions taken by

the flight test personnel. With proper precautions the probability of a hardover should be acceptably remote.

An undetected hardover at critical high-speed flight conditions will result in aircraft external loads approximately 120% of limit in about 2 seconds unless the pilot intervenes. The pilot will probably save the aircraft in flight test but there could be injuries to the occupants. Thus, this failure condition is considered to be flight critical.

3.8.3.4 Detected hardover: A detected hardover is detected by servo system monitors but significant transients occur before the servo is returned to the null position. With both systems engaged the transient duration is approximately one-half second and does not cause a significant hazard. However, when one system is off, the transient may produce stabilizer motion that results in approximately 90% of aircraft limit loads. Operating procedures require that both PACS be engaged and operating correctly for the flight tests. Therefore, two failures are required before a significant transient occurs. The first failure may be dormant as was demonstrated by VSS test, which showed that loss of hydraulics in one servo channel only is not detected by the system monitors. This hydraulics loss is detected during the preflight checkout tests. Consequently, a very conservative probability of a significant transient is no greater than 10^{-5} /hr. This probability is considered acceptable since the limit load is not exceeded.

A detected hardover is not considered to be flight critical since loss of the airplane is not likely to occur. However, it is considered a significant potential hazard.

3.8.3.5 Unwarned total disconnect: This is a total disconnect of the PACS without adequate warnings. There may be no warnings at all or there may be only one warning which implies that one system is still engaged. The probability of an unwarned total disconnect is considered no greater than 10^{-8} /hr.

An unwarned total disconnect is not considered flight critical for flight tests. However, it is considered a significant potential hazard.

3.8.3.6 Warned total disconnect: This is a disconnect of the PACS with proper warning. The probability is approximately 10^{-5} /hour. There is little risk since the aircraft will be operated at all times at flight conditions which can be safely flown by the pilot without the PACS being engaged.

A jammed servo linkage causes a warned total disconnect and can also cause loss of the pitch trim. However, the jam leaves the pilot adequate pitch control to safely fly the aircraft. A jammed linkage is not a probable failure so the risk is negligible.

4. LABORATORY AND GROUND TESTS

This section discusses the wind-tunnel tests performed to verify that the .087 rad (5 deg) downrigged elevator provided sufficient nose down authority, PACS component tests, vehicle flight simulator tests, vehicle system simulator tests, and the aircraft ground tests.

4.1 Wind-Tunnel Tests

In order to flight test the L-1011 at relaxed static stability conditions, analysis shows that the elevator must be downrigged five degrees to compensate for the loss in nose-down control which results from moving the c.g. aft. Consequently, it was necessary to wind-tunnel test the L-1011 model to:

- Verify results of the analysis.
- Determine the effect of the elevator downrig on stabilizer/elevator aerodynamic loads and hinge moments.

Both low-speed and high-speed tests were performed. However, for the low-speed test it was necessary to determine only the control effectiveness of the stabilizer with downrigged elevator, since structural loading conditions are not critical at low speed conditions.

4.1.1 Low Speed.— Low speed testing was performed in the Lockheed 8-ft by 12-ft Wind Tunnel. A 1/20th scale model of the L-1011-1 configuration was used for the test. The objective of the test was to determine the effect of elevator downrig on static trim characteristics and on overall capability for the takeoff, landing, and clean configurations.

Complete configuration force and moment data were obtained for a series of stabilizer/elevator gearing settings selected to show the effect of elevator downrig on trim and control characteristics at flap settings of 0, .454 rad (26 deg), and .785 rad (45 deg). These settings encompass the range of L-1011 flap settings. The test was primarily concerned with longitudinal stability and control characteristics; therefore, no lateral-directional conditions were examined.

The low-speed wind-tunnel test results, which illustrate the nose-down control effectiveness of the downrigged elevator configuration, are shown in Figure 53. These data are presented along with some estimates of elevator nose-down control capability that were made prior to the test. The low-speed force test results are in good agreement with the basic controls undeflected aerodynamic predictions, but show a more effective elevator control increment for positive deflections than was estimated based on negative deflection data.

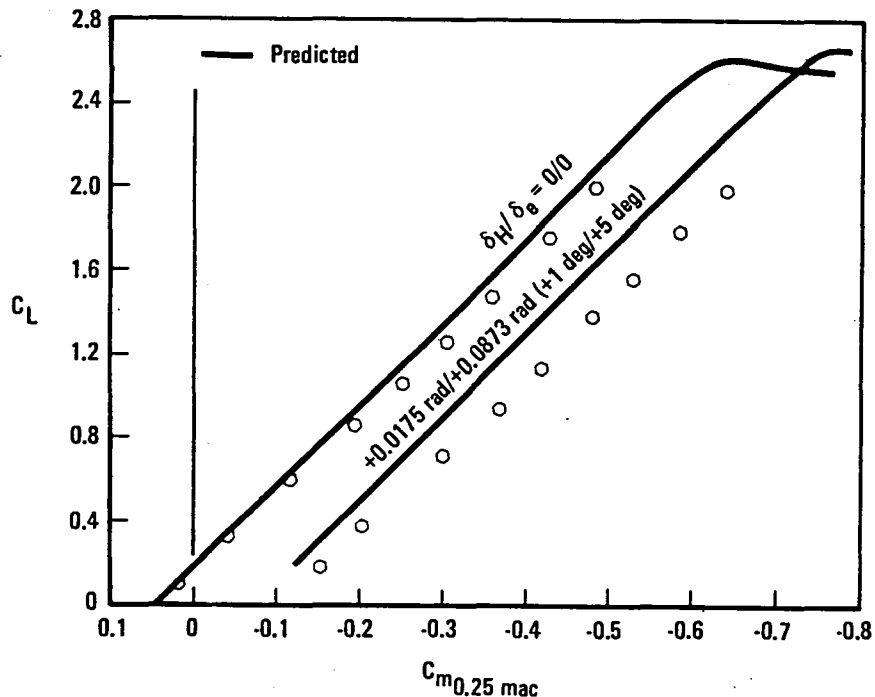


Figure 53. - Low-speed longitudinal stability and nose-down controllability for the landing configuration $\delta_F = .785$ rad (45 deg)

4.1.2 High Speed. - The high-speed test was performed in the Calspan 8-ft Transonic Wind-Tunnel Facility. A 1/30th scale model of the L-1011 with downrigged elevator was used for the test. Complete configuration six-component forces and moments and stabilizer/elevator hinge moments were obtained in the Mach number range of 0.7 to 0.95 and at angles of attack extending to the limit determined by model dynamics. The stabilizer pivot loads were measured by means of a three-component simple-beam balance at the left-hand stabilizer pivot, and the elevator hinge moments were measured by means of a strain gauge at the right-hand elevator hinge line. Force and moment data were also obtained with the horizontal tail removed. Since the wind-tunnel test was primarily concerned with longitudinal stability and control characteristics, boundary layer transition grit was not used for the test.

Figure 54 presents high-speed elevator control effectiveness data for various elevator downrig deflections at one of the critical Mach numbers for nose-down control: $M = 0.86$. These data illustrate the linearity of control effectiveness data for downrig elevator deflections up to $+0.104$ rad ($+6$ deg).

Stabilizer and elevator hinge moment data are shown in Figures 55 and 56. These data are for a Mach number of 0.9, one of the critical conditions for structural loads analysis. The consistency and alignment of the stabilizer hinge moment data (Figure 55) illustrate the excellent measurement quality obtained with the three-component internal tail plane load balance. The elevator hinge moment data (Figure 56) were obtained by means of strain gage measurements. These data are also of excellent quality and illustrate the linearity of hinge moment for elevator downrig deflections up to $+0.104$ rad ($+6$ deg).

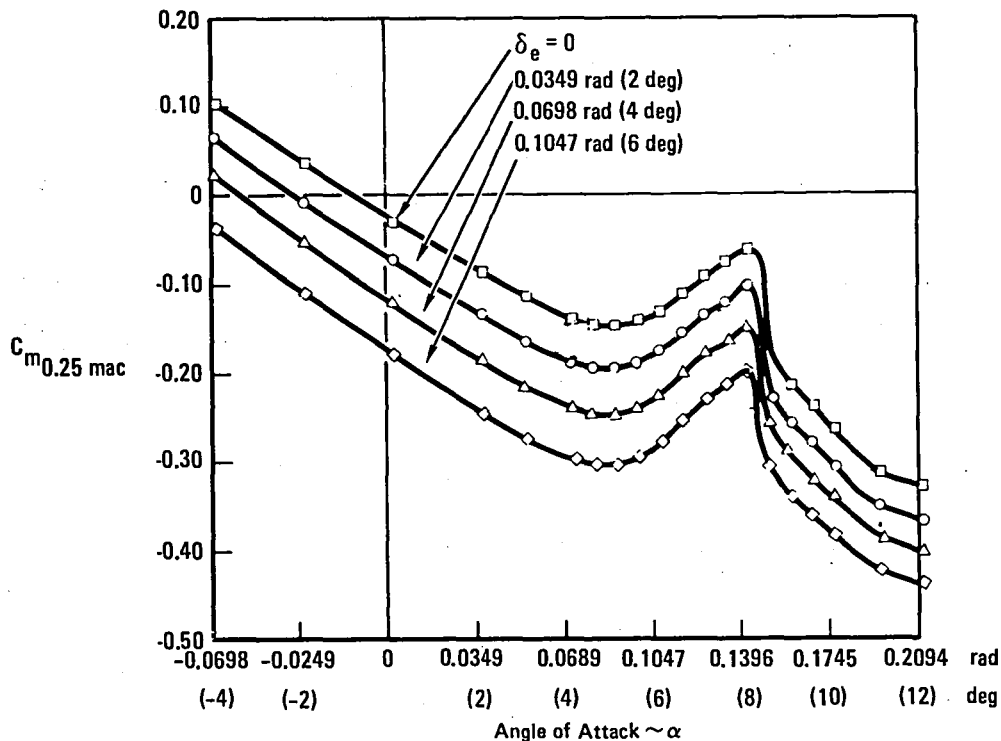


Figure 54. - Elevator nose-down control effectiveness
 $M = 0.86$, $\delta_H = +0.017$ rad (1 deg)

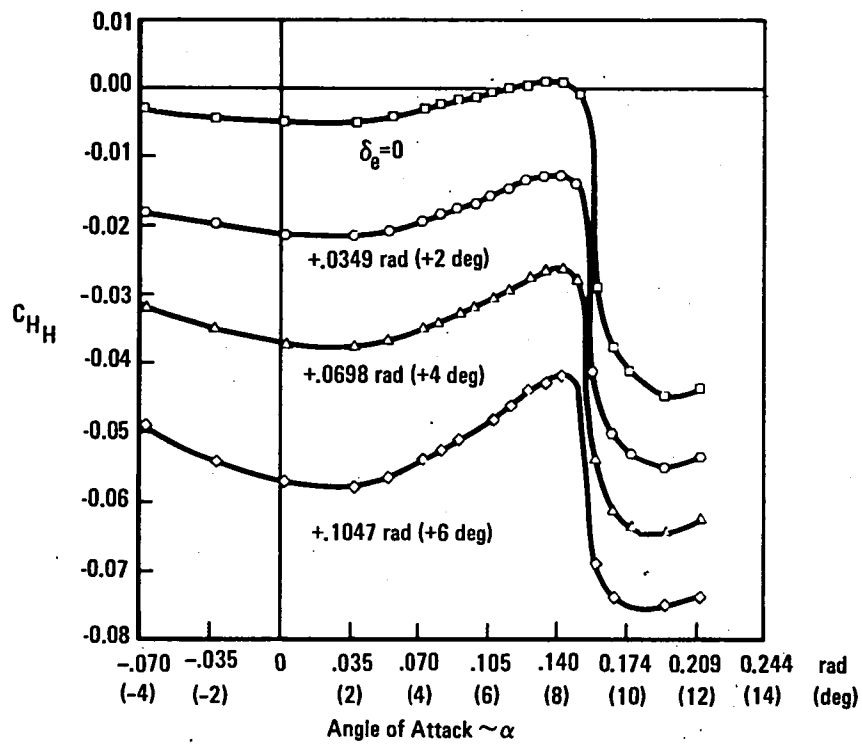


Figure 55. - Effect of elevator downrig on stabilizer hinge moment. $M = 0.9$ $\delta_H = +0.17 \text{ rad (1 deg)}$

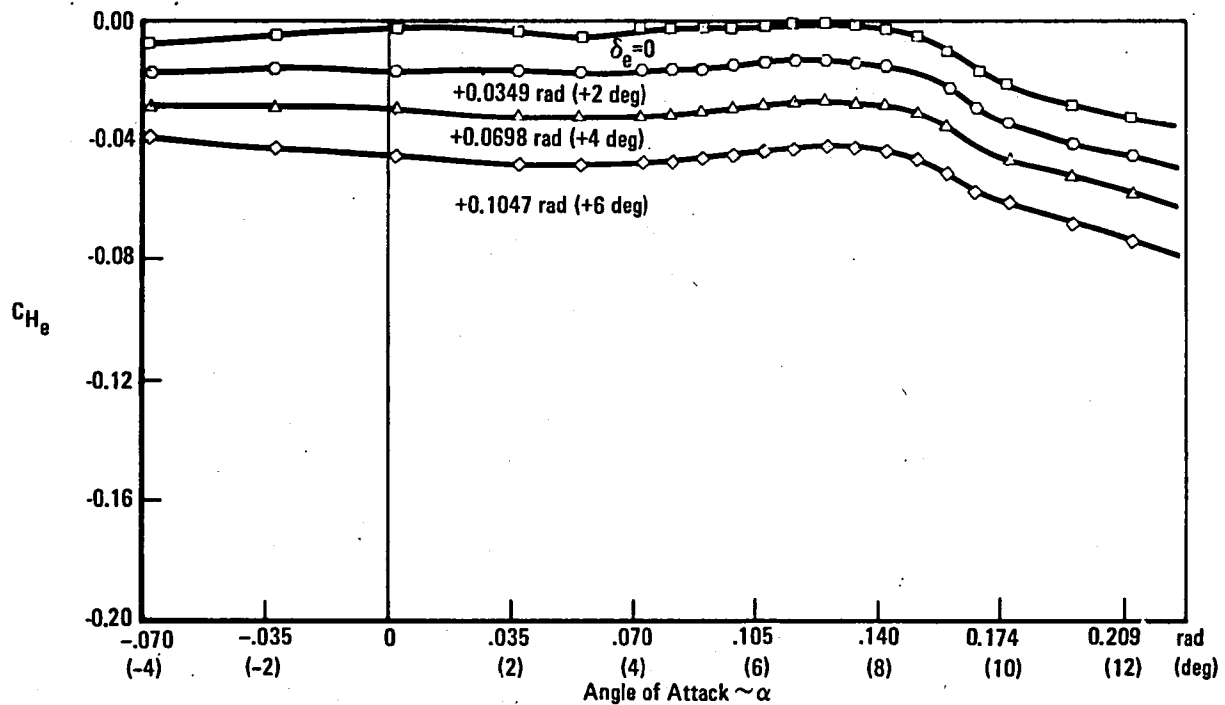


Figure 56. - Effect of downrig on elevator hinge moment. $M = 0.9$, $\delta_H = +0.17 \text{ rad (1 deg)}$

4.2 PACS Component Tests

To assure a high degree of success during the complete system testing on the Vehicle Systems Simulator (VSS), and during flight tests each component of the PACS system was tested individually to its respective specification. Two components used in the PACS system had been previously tested during the earlier evaluation of the L-1011 AACS. These components are the column minus trim (C-T) transducer and the dynamic pressure transducer (Q_c).

4.2.1 Components Tested.- The three major components tested during this phase of the program were:

- PACS digital computers
- Series servo
- Rate gyros.

Actually, the testing of the computers entailed more than just verification of the computer. As the computers were installed in a semi-portable rack (the Pallet) that contained all interface wiring, core memory, computer control panels (The Test Adapters), and miscellaneous breakout panels, the complete pallet assembly was tested as a unit.

The series servo was tested on the bench as a servo and again as installed on the VSS as part of the pitch axis control system.

The rate gyros were tested as individual sensors.

4.2.2 Pallet Tests.- The two computers and support equipment as installed in the pallet had been used previously as part of the L-1011 aileron active controls system. Thus, a major part of internal wiring, core memory, and support panels had been tested. The required computer modifications were verified through open-loop static and dynamic tests. Each input and output signal path was verified by injecting appropriate signals and monitoring the input to output relationship.

All data were recorded by the Rye Canyon Laboratory Data Central System, a digital data recording system that allows not only the recording of data but long-term storage of data as well as various methods of data reduction.

Following the verification of the computer input and output circuits the application software was loaded and verified. Again this was through

open loop static and dynamic testing. All logic and comparator thresholds and time constants were verified in a similar manner.

4.2.3 Series Servo Tests.- The series servo was subjected to two individual tests. The unit as received was installed in a bench test fixture and tested as a servo per the manufacturers specifications.

After successful completion of the bench tests the servo, along with the required control system linkages, et cetera, was installed on the VSS. Both static and dynamic tests were performed. These tests were designed to verify that when the series servo was not engaged the pitch axis control system was unaffected and when the servo was engaged its operation was as required.

4.2.4 Rate Gyro Tests.- The rate gyros used in the PACS system as a source of pitch rate information had been previously used in the L-1011 yaw stability augmentation system as yaw rate gyros. These gyros were installed on a rate table such that the signal would be proportional to the pitching rates. They were tested per the manufacturers specifications and met the requirements for use in the PACS system.

Though these laboratory tests showed conformance to the specification, once installed in the aircraft the gyros appeared to be susceptible to acceleration inputs. Further laboratory testing determined that the gyros did not meet the manufacturers specifications with regard to acceleration inputs. However, this susceptibility was shown to have no detrimental effects on the flight tests.

4.2.5 Vibration Qualification Tests.- The PACS components were required to meet the vibration requirements of the L-1011 by test, analysis, or similarity. Analysis was performed, in lieu of testing, on the modified elevator push rod. The modifications were found to be insignificant from a structural dynamics standpoint. The pitch rate gyros and computers were qualified by similarity.

The series servo successfully passed a nine hour vibration qualification test. Flight test vibration measurements were subsequently taken in three mutually perpendicular axes which confirmed that the vibration test levels used in the lab were adequate.

4.3 Visual Flight Simulation

Piloted visual flight simulation of the near-term PACS was conducted with sixty hours of actual pilot-in-the-loop test time being required to complete the simulation. Three Lockheed Engineering Flight Test pilots participated in the test, which was performed at the Lockheed Rye Canyon Flight Simulator Facility. The piloted simulator evaluation was required to:

- Identify acceptable and unacceptable configurations so that subsequent tests to be conducted on the VSS and on the flight test airplane could be limited to the best configurations.
- Familiarize the pilots with the PACS and identify any pilot/system interface problems.
- Evaluate the basic airplane handling qualities at the most aft c.g. without the PACS operating.
- Determine any PACS configuration changes required due to the aileron active control system (AACS) on and off.
- Investigate the effect of PACS failures and establish recovery procedures should the failure occur on the test airplane.
- Incorporate the results of this simulation into the flight test plan.

The simulation effort was subdivided into two parts:

- PACS optimization
- Failure simulation

4.3.1 PACS Optimization. - Evaluation of the various PACS configurations was based primarily on each pilot's opinion of acceptability determined by using his own techniques for performing certain specified tasks and flight maneuvers. Each pilot evaluated the various test configurations based on his ability to perform the following tasks:

- Control the airplane in pitch during windup turns, pushovers, and pullups - evaluated in terms of workload imposed by column forces and pitch attitude excursions.
- Perform small and large pitch attitude changes and stabilize on a target pitch attitude.
- Roll into a banked turn, stop at a desired bank angle, and roll out on a new heading while maintaining speed and altitude.
- Hold altitude and pitch attitude in turbulence.
- Ease of trimming and maintaining trim (speed stability) at a particular flight condition.

The pilots also evaluated the localizer and glideslope tracking capability for landing configurations, and the speed and pitch attitude control capabilities for takeoff configurations.

Pilot ratings were determined according to the Cooper-Harper handling qualities chart shown in Figure 57. Pilot comments were also recorded to further describe the handling qualities characteristics of a particular PACS configuration at a flight condition.

Flight conditions investigated during the simulation are defined in Table 2. The test covered a range of c.g. conditions from 25% mac (mid-c.g.) to 39% mac where the airplane is close to being neutrally stable at high altitude cruise conditions.

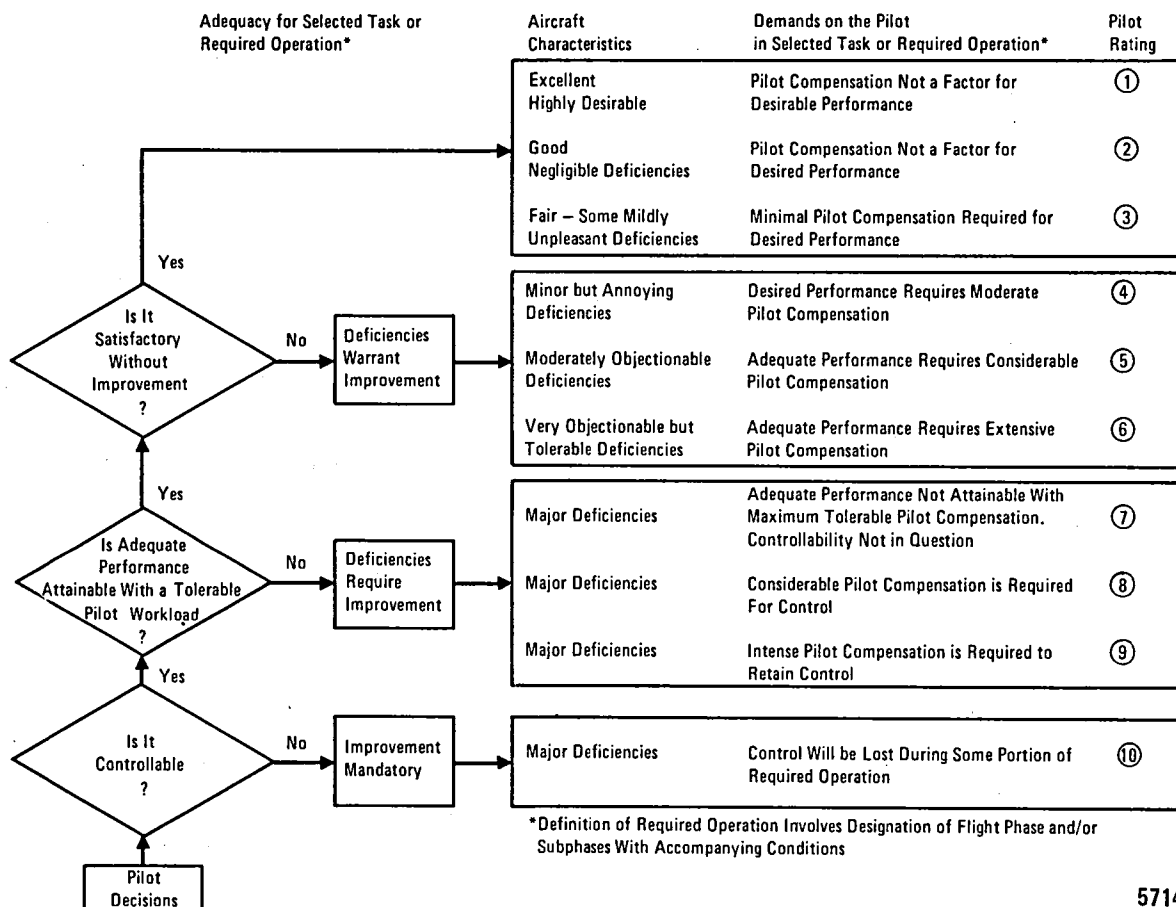
The PACS is defined by the block diagram in Figure 24 of Section 3.3.1. The following components of this system were selected as variables for flight simulation:

- Pitch damper gain and lag time constant
- Pilot feed-forward loop gain
- Pilot feed-forward loop washout.

The test airplane is configured with an AACS that automatically repositions outboard ailerons to reduce wing loads under maneuvering flight conditions. Longitudinal stability is reduced by the AACS operation. Consequently, the pitch damper gain was analytically optimized for both AACS on and off operation. The pilots could distinguish only a small difference between AACS on and off and found the high pitch gain schedule suitable for both. Therefore, the test was conducted using only the high pitch gain schedule. Table 7 summarizes the PACS configurations tested. The simulation concentrated primarily on the three high-speed flight conditions (two cruise conditions and one overspeed condition) which place the heaviest demands on the PACS. The various PACS configurations were evaluated with and without moderate turbulence. All three high-speed flight conditions were evaluated by two pilots and the high-altitude cruise condition was evaluated by three pilots. Takeoff, holding, and landing conditions were evaluated primarily by one pilot.

The following conclusions were drawn from the piloted flight simulation test of the PACS:

- All three PACS configurations were found to provide an improvement to the unaugmented airplane. The increments of improvement increased as the c.g. moved aft. The most optimum PACS configuration sometimes varied from pilot to pilot or from one flight condition to another, however, the pilots agreed that all three systems configurations should be available for evaluation on the flight test airplane.
- The effect of the AACS on PACS optimization was small. The same PACS can be used for AACS on or off.



5714

Figure 57. - Handling qualities rating scale.

TABLE 7. - PACS CONFIGURATIONS TESTED

| PACS CONFIGURATION | AACS | DAMPER | FEED FWD | FEED FWD WASHOUT |
|--------------------|-----------|------------------------|------------|------------------|
| 0 | On Off | Off Off | — — | — — |
| 1 | On Off | High gain High gain | No No | — — |
| 2 | On Off | High gain High gain | Yes Yes | No No |
| 3 | On Off | High gain High gain | Yes Yes | Yes Yes |

- The PACS made the 39% c.g. airplane fly as well as the unaugmented airplane at 25% c.g.

- PACS configuration 3 (feed-forward with washout) with AACS on was favored by two of the pilots while the remaining pilot showed a slight preference for configuration 2 (feed-forward without washout).

An example of the pilot ratings obtained from the flight simulation is shown in Figure 58. These data are for Flight Condition 10 (Table 2) and configuration 3 (Table 7). The results show that the PACS eliminates the tendency for handling qualities to degrade with aft c.g. movement in the range of 25 to 39% mac.

4.3.2 Simulated Failures.— Potential PACS failures which could occur during the flight test program were identified and evaluated in the flight simulation. Table 8 gives a brief description of the failures that could occur.

Failure simulation concentrated on the high-speed conditions where structural loading effects are critical. The augmented airplane was exposed to light turbulence to provide the pilot with a representative workload and to realistically simulate the actual conditions likely to be encountered in the flight test program. The failure simulation was performed using configuration 3: the best to emerge from the flying qualities portion of the evaluation. Failures were initiated at random during straight and level flight and wind-up turn maneuvers.

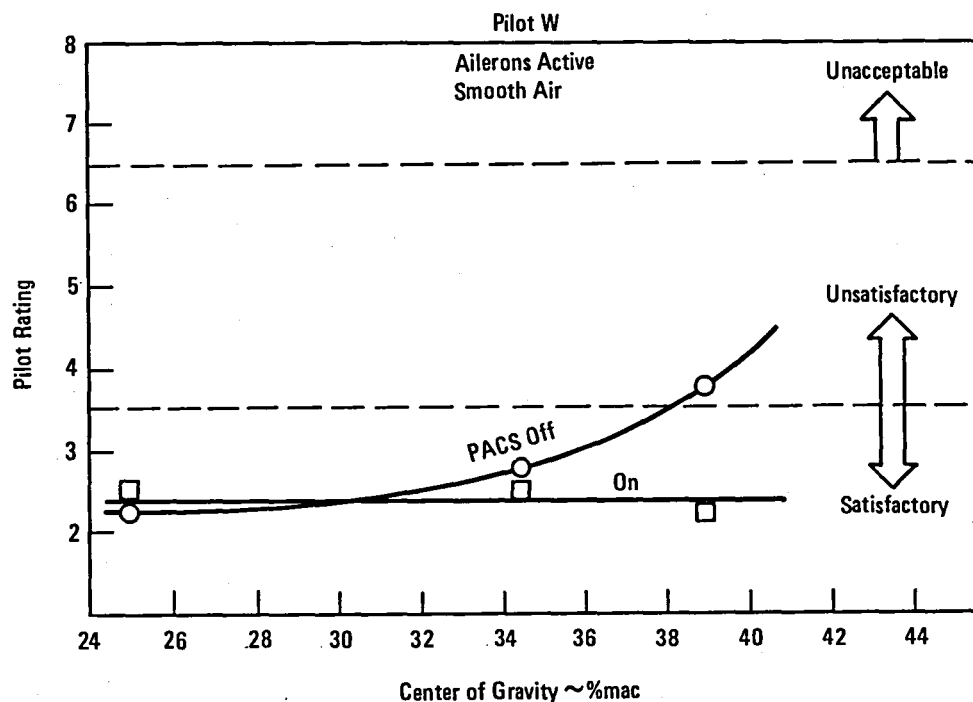


Figure 58. - Flight simulation results in cruise - condition 10, configuration 3.

5714

TABLE 8. - SIMULATED FAILURES

| FAILURES | DESCRIPTION |
|----------|---|
| 1 | HARDOVER-DUAL CHANNEL - DETECTED |
| | Both series servos are operating in an active/standby configuration. Active servo fails and goes hardover. Failure is detected, active is automatically shutdown and standby takes over. |
| 2 | HARDOVER-SINGLE CHANNEL - DETECTED |
| | Only one series servo channel is operating. It fails and goes hardover. Failure is detected and servo is automatically shut down. |
| 3 | HARDOVER-KICKER LIMIT - UNDETECTED |
| | The series servo is driven electrically to evaluate coupling modes between the horizontal tail and PACS. The electrical signal fails and the series servo goes into a limited hardover, since the signal is limited. The failure can be removed by deactivating the PACS. |
| 4 | HARDOVER-FULL PACS AUTHORITY - UNDETECTED |
| | Same as (3) but signal going into the series servo is not limited. The series servo goes into a full authority hardover. The failure can be removed by deactivating the PACS. |
| 5 | PITCH RATE FAILURE |
| | Assumes that the pitch rate signal is lost and only the column feed forward loop is operating. |
| 6 | GAIN SCHEDULE FAILURE |
| | Assumes the Q_c signal fails. All gains and lags may be set for the wrong flight regime. |
| 7 | FEED FORWARD HARDOVER |
| | The column-minus-trim signal fails. The column feed-forward loop of the PACS goes hardover. The pitch feedback loop continues to operate. |
| 8 | DISCONNECT |
| | The PACS quits operating. There is no signal going into the series servo and the servo returns to the null position. |

The severity of the various simulated failures was evaluated based on:

- Pilot comments on the aircraft response and recovery procedures following a failure.
- Strip chart recordings of the dynamic response (load factor in particular) resulting from a failure and from the subsequent corrective action taken by the pilot to recover from the failure.

Two pilots participated in the evaluation.

Results of the failure simulation can be summarized as follows:

- The unaugmented airplane was determined to be safely flyable at all flight conditions at 39% c.g.; however, the workload at high altitudes and high speeds was considered excessive. Therefore, in the event of a PACS failure with the c.g. aft of 35% it was recommended that the airplane decelerate to Mach = 0.80 and descend until the pilot considered flying qualities to be satisfactory.
- Satisfactory recoveries from detected and undetected PACS hardovers were demonstrated at all flight conditions using the primary longitudinal control system. The full servo authority nose-up hardover of the PACS reached 2.2 g at flight condition 16 with 39% mac c.g. when recovery was initiated at 1.6 g. This is within the limit maneuvering envelope of the airplane. It was recommended that flight at high-speed/Mach number conditions ($V > 300$ Kts/Mach $> .82$) be avoided if possible because of the rapid rise in load factor from the hardover. When tests are to be conducted at these conditions the pilot should always fly with hands on the control column.

4.4 Vehicle System Simulator Tests

The purpose of the Vehicle System Simulator (VSS) testing was to test the complete PACS hardware in a closed loop configuration and to show that the system performance matched flying qualities of the visual flight simulator.

In addition to the performance tests, all performed under fault-free conditions, an in-depth evaluation of selected failures was made. These failure tests confirmed the capability of the system to detect failures, warn the pilots and reconfigure the system.

4.4.1 VSS Description.-- The VSS is essentially a full-size, rigid body simulation of the L-1011. All primary and secondary control systems are fully operative. Actual aircraft parts (servos, surfaces, cables, hydraulic systems, etc.) are installed as they would be in the actual aircraft. A complete cockpit, including instruments, control wheel, et cetera, are installed for use when a pilot is in the loop.

In addition to the VSS, a digital simulation of the L-1011 aircraft dynamics was used during the closed loop testing and the pilot evaluation testing.

The system tested is shown in Figure 59. The open loop tests were performed without the simulated aircraft dynamics. Closed loop testing was accomplished at flight conditions 10, 15, 16 and 18 given in Table 2. These selected flight conditions represent the more important regions of the flight envelope.

4.4.2 Data Acquisition.— During the testing of the system, the following conditions applied.

- All hydraulic power systems active (2,200 RPM, 3,000 psi).
- No simulated aerodynamic loads on control surface.
- Mach trim operative.
- Maneuver direct lift control (MDLC) spoilers inoperative.
- Direct Lift Control (DLC) computer operative.

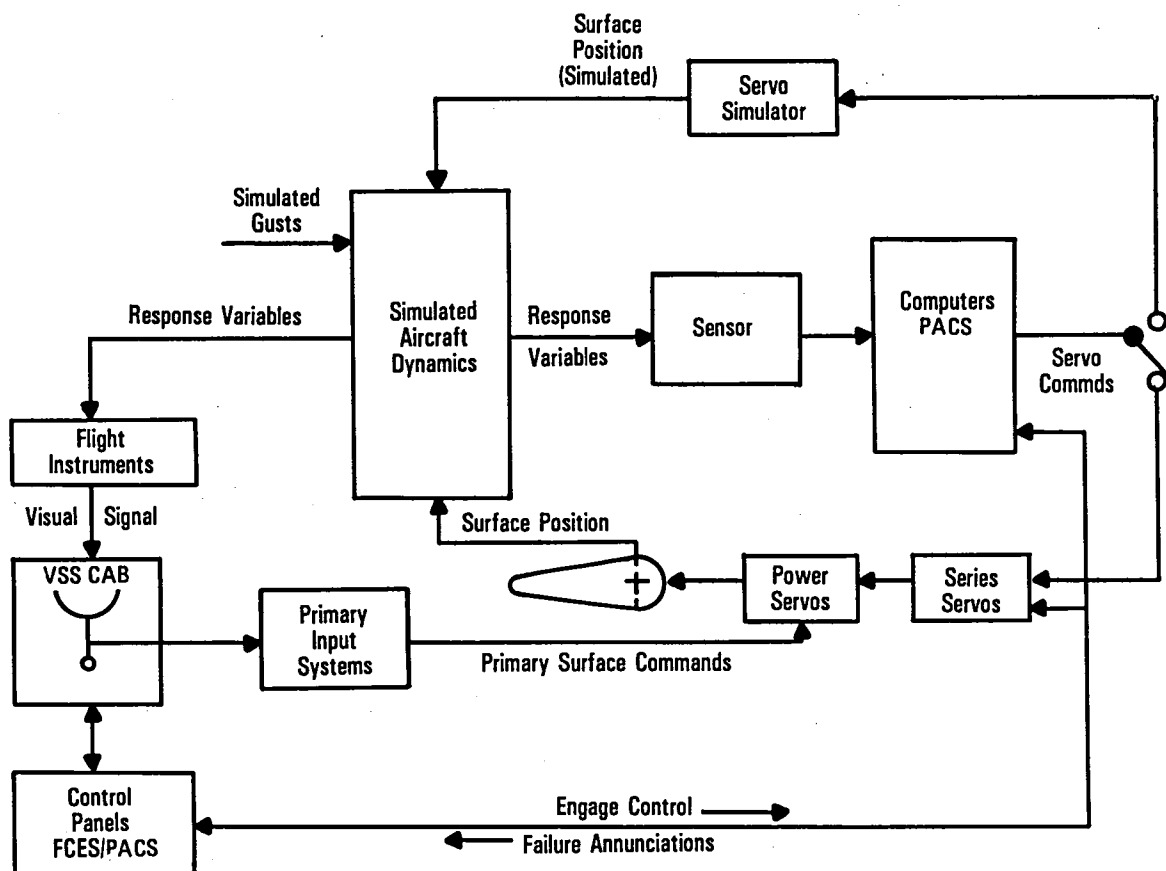


Figure 59. - PACS vehicle system simulator test configuration.

- Simulated horizontal stabilizer surfaces installed.
- Autopilot disengaged.
- Horizontal stabilizer properly rigged.
- Pitch series servo installed.
- PACS computers and VSS properly interfaced.
- AACS operative.

The system parameters were monitored during the tests. Signals associated with control system functions were obtained from VSS hardware. The PACS sensor signals were monitored at both the simulated or actual sensor analog outputs and at the associated PACS addresses for the processed digital signals. Digital-to-analog converters located in PACS test adapters processed the digital signals into analog time histories.

The test results were recorded in the Rye Canyon Laboratory Data Central System and each test performed has been assigned a Data Central test and run number.

Standard procedures governed each test as follows:

- In addition to relevant x-y plots, time histories of all signals were recorded on a hard copy.
- The nominal conditions applied except where differences were specified.
- The system was in a steady-state condition (constant, steady, or stationary) at the beginning of any recorded run.
- For each frequency response test, the amplitude of the sinusoidal input signal was set at the frequency of 0.01 Hz and was maintained constant over the entire frequency range.

Functional tests were performed on the following configurations:

- One PACS computer hardware and software.
- Two PACS computers hardware and software.

4.4.3 Test Results and Conclusions.- VSS closed loop testing and the pilot evaluation of the system verified results of the visual flight simulator tests. Addition of the PACS improved handling qualities of the relaxed

static stability airplane significantly. The tests also verified that the PACS monitoring did detect and isolate failures with proper cockpit annunciation and system reconfiguration with minimal effects on the controllability of the airplane.

4.5 Aircraft Ground Test

This section presents a description of the ground tests performed on the test aircraft with the near-term PACS installed. The primary purpose of these tests was to establish that the new and modified systems associated with the near-term PACS functioned to the design intent. The tests performed consisted of functional verification of the modified water ballast system, a controls proof operations test, functional and voter reconfiguration tests of the PACS avionics, and a ground vibration test series.

4.5.1. Water Ballast System.- The modified water ballast system was subjected to a thorough functional checkout prior to first flight with the PACS installed. These tests included verification of the proper functioning of the control panel, transfer valves, individual tank shut-off valves, transfer pump operation and each tank full and tank empty light switches. Water transfer rates were also checked and found to be satisfactory - about 2 minutes per tank. The water dump rate was also established to be satisfactory, about 1-1/2 minutes for an individual tank.

4.5.2 Controls Proof and Operations.- A series of proof and operations tests were conducted on the elevator drive and pitch control system parts which were new or subjected to higher loads than previously used to qualify these systems. Specifically, the elevator drive system was tested for increased negative hinge movements resulting from the downrig of the elevator. The new pitch control system hardware associated with the pitch series servo was subjected to limit pilot effort trim wheel load and also to limit series servo output load. These tests demonstrated that the pitch control system could sustain the limit loads defined for these tests and function properly.

4.5.3 PACS Verification.- A series of functional and operational tests were conducted to verify the performance of the PACS in the test aircraft environment. Prior to conducting all-up system tests, end-to-end continuity and signal path power checks were completed. A few minor discrepancies were

revealed by this procedure and corrected. Specific PACS tests involved system static gain checks, system monitor and voter reconfiguration tests and checkout of the flight test peculiar functions of the PACS pallet. The system power supply was monitored throughout the tests. The A Phase voltage was between 25.92 and 25.99 VAC, the B Phase varied from 26.3 to 26.4 VAC. No corrections have been made to the results for these minor variations from the nominal 26 VAC.

4.5.3.1 Kicker fader operation: Operating the loop OPEN/CLOSE switch SW₅ (Figure 13) with a large input command existing verified that when switching from closed to open loop the system response was immediate. When switching from open to closed loop the system response was delayed by the 4-second linear fader. Operation of this switch did not trip any system monitors.

4.5.3.2 Pitch rate static gain: Pitch rate static gain ($K_Q = \text{servo-stroke}/\dot{\theta}$) was measured by applying simulated pitch rate voltages to the PACS computers and measuring the corresponding series servo output stroke. The following discussion is based on Figure 13. Simulated pitch rate gyro input signals ($\dot{\theta}$) were equivalent to .0436 radian/second (2.5 deg/sec) aircraft rotation at the low dynamic pressure conditions (Q_c equivalent to KCAS ≤ 160 ; high K_Q range) and .0524 radian/second (3.0 deg/sec) at the high dynamic pressure conditions (Q_c equivalent to KCAS ≥ 320 ; low K_Q range). Series servo displacements were measured for both nose up (+ voltage) and nose down (- voltage) gyro input signal polarities with system gain settings (K_3) of 0.5, 1, and 2. The resulting pitch rate gains are compared to design values in Table 9.

TABLE 9. - PITCH RATE STATIC GAIN

| Q_c | AIRCRAFT INPUT POLARITY | K_3 SYSTEM GAIN SETTING | K_Q cm/rad/sec (in/deg/sec) | |
|-------|-------------------------------|---------------------------------|----------------------------------|-------------|
| | | | Design | Measured |
| Low | Nose Dn | 1 | 35.0 (.24) | 39.3 (.270) |
| Low | Nose Up | 1 | 35.0 (.24) | 35.1 (.241) |
| High | Nose Dn | 1 | 26.2 (.18) | 29.1 (.200) |
| High | Nose Up | 1 | 26.2 (.18) | 26.5 (.182) |
| High | Nose Dn | 0.5 | 13.1 (.09) | 14.7 (.101) |
| High | Nose Up | 0.5 | 13.1 (.09) | 13.1 (.090) |
| High | Nose Dn | 2 | 52.4 (.36) | 55.7 (.383) |
| High | Nose Up | 2 | 52.4 (.36) | 52.8 (.363) |

Opening each gyro input PR signal individually (see Figure 12) had negligible effect on the static gains, but did give a transient servo deflection when the pitch rate input was nose-down at the time it was opened. There were no transients when the pitch rate input was nose-up. Opening the No. 1 or No. 2 gyro inputs with either input signal voltage polarity, or the No. 3 gyro input with a positive voltage applied, always gave a First Fail indication. However, if the No. 3 gyro inputs to both systems were opened simultaneously with a negative voltage input applied, a First Fail warning was not generated. The warning was generated when the input removals were not simultaneous. Note that simultaneous faults are a realistic condition since both inputs are from a single gyro source.

4.5.3.3. Column-minus-trim static gain: These tests were performed with the input signal washout (Figure 13) inoperative and the overall system gain (K₃) set to 1. A 4.44 VDC, equivalent to 1.041 cm (.41 in) cable signal, was applied to all four C-T inputs (Figure 12). A comparison of the design and measured column minus trim gain (KFFD) values is presented in Table 10. There were no gain changes and no transients when each of the four inputs was opened individually. Opening the 1A or 2A input set a First Fail in both systems. Opening the 1B input set a First Fail in the No. 1 system only. Opening the 2B input set a First Fail in the No. 2 system only.

4.5.3.4 Servo monitor checks: Opening one of the PACS servo feedback signals (Figure 12) resulted in a FAIL annunciation on the appropriate switchlight. Opening a No. 1 servo feedback caused operation to transfer to the No. 2 system as per design. The No. 1 system continued to operate normally when a No. 2 servo feedback was opened.

4.5.3.5 Stabilizer maximum deflection checks: The purpose of these tests was to establish the maximum stabilizer deflection should a system

TABLE 10. - COLUMN MINUS TRIM STATIC GAIN (SYSTEM GAIN SETTING = 1)

| Q _c | AIRCRAFT INPUT POLARITY | KFFD (cm servo/cm cable) | |
|----------------|-------------------------------|-----------------------------|----------|
| | | Design | Measured |
| Low | Nose Up | 1.36 | 1.22 |
| Low | Nose Dn | 1.36 | 1.28 |
| High | Nose Up | 0.68 | 0.613 |

hardover be experienced. These tests were performed with a 10 volt input to the kicker and the PACS open-loop. The results, presented in Table 11 show that the maximum deflection is no greater than that used in the failure analyses.

4.5.4 Ground Vibration Test.— The purpose of the ground vibration test (GVT) was to verify the stability of the control system and the effect on structural modes from the pitch active control system and the downrigged elevator. The free play of the elevators was also measured. The tests are summarized in Tables 12 and 13.

4.5.4.1 Procedures: Stability tests were made using an Unholtz-Dickie shaker system and a Spectral-Dynamics sweep oscillator with a logarithmic frequency sweep function. Shakes were conducted with shakers at the nose and stabilizer positions. Smaller Calidyne shakers were used on the elevators. Modal tests were conducted using one of two methods, either by sine dwelling at a resonant frequency and surveying the mode or using a Hewlett Packard HP5451C Fourier Analyzer. The sine dwelling technique utilized the Unholtz-Dickie system by dwelling on the elevator

TABLE 11. - STABILIZER DEFLECTION

| STABILIZER TRIM UNITS | AIRCRAFT INPUT POLARITY | PACS SERVO DISPLACEMENT | | STABILIZER DISPLACEMENT |
|-----------------------------|-------------------------------|----------------------------|---------|----------------------------|
| | | cm | (in) | Rad (Deg) |
| 0 | Nose Dn | .650 | (.256) | .003 (+.18) |
| 0 | Nose Up | .638 | (.251) | -.003 (-.17) |
| 0 | Nose Dn | .650 | (.256) | .003 (+.18) |
| 0 | Nose Up | .640 | (.252) | -.003 (-.17) |
| 2 | Nose Dn | .650 | (.256) | .005 (+.26) |
| 2 | Nose Up | .638 | (.251) | -.005 (-.28) |
| 4 | Nose Dn | .653 | (.257) | .006 (+.32) |
| 4 | Nose Up | .635 | (.250) | -.006 (-.33) |
| 1 | Nose Dn | .650 | (.256) | .004 (+.24) |
| 1 | Nose Up | .643 | (.253) | -.004 (-.21) |
| 1 | Nose Dn | 2.075 | (.817) | .012 (+.68) |
| 1 | Nose Up | 1.775* | (.699)* | -.012 (-.67) |

* 8.8 volt input — the system disconnected with a 10 volt input (at this condition only).

TABLE 12. - PACS FUNCTIONAL AND MODAL GROUND VIBRATION TEST SERIES

| TEST NO. | SHAKERS | | | INPUT TYPE | PACS | | STABILIZER POSITION | | DATA COLLECTED |
|----------|-------------------|--------------------------|----------------------|------------------------|--------|--------|---------------------|-------|-----------------------------------|
| | Location | Level/each | | | Loop | Gain | rad | (deg) | |
| | | N | (lb) | | | | | | |
| IA-C | BAVCO osc. | { .017 ra/sec } | | Sine dwell 0.1 Hz | Closed | X.5-X2 | 0 | (0) | Stab. position/input signal |
| IIAC | BAVCO osc. | { (1.0 deg/sec) } | | Sine dwell 0.3 Hz | Closed | X.5-X2 | 0 | (0) | Stab. position/input signal |
| IA1a | Nose | 2224 | (500) | Sine sweep 0.5 - 40 | Closed | X1 | 0 | (0) | L&RH stab. LE tip & elev. root |
| IB1a | Nose | 2224 | (500) | Sine sweep 0.5 - 26 | Closed | X1 | -.122 | (-7) | L&RH stab. LE tip & elev. root |
| IC1a | Nose | 2224 | (500) | Sine sweep 0.5 - 26 | Closed | .5 | -.244 | (-14) | L&RH stab. LE tip & elev. root |
| IC1b | Nose | 2224 | (500) | Sine sweep 0.5 - 26 | Closed | X1 | -.244 | (-14) | L&RH stab. LE tip & elev. root |
| IC1c | Nose | 2224 | (500) | Sine sweep 0.5 - 40 | Closed | X2 | -.244 | (-14) | L&RH stab. LE tip & elev. root |
| IE1 | Nose | 2224 | (500) | Sine sweep 0.5 - 40 | Closed | X2 | -.017 | (-1) | LH elev. stab. nose & sting |
| IE2 | Nose | 2224 | (500) | Sine sweep 0.5 - 40 | Closed | X2 | -.244 | (-14) | LH elev. stab. nose & sting |
| IIA1B | Stab. inbd. LE | 890 | (200) | Sine sweep 0.5 - 30 | Closed | X1 | 0 | (0) | LH & RH elev. & stab. tip |
| IIA2B1 | Elev. root | 133 | (30) | Sine sweep 0.5 - 30 | Closed | X1 | -.052 | (-3) | LH & RH elev. & stab. tip |
| IIA2B2 | Elev. root | 133 | (30) | Dwell @ 8.2 Hz | Closed | X1 | -.052 | (-3) | Stabilizer mode survey |
| IIA2b3 | Elev. root | 222 | (50) | Dwell | Closed | X1 | -.052 | (-3) | Modal frequency |
| IIA2C1 | Elev. root | 222 | (50) | Pink noise | Closed | X1 | -.052 | (-3) | Modal survey |
| IIA4b2 | Elev. root | 178 | (40) | Sweep 30 - 80 | Closed | X1 | -.052 | (-3) | Mid-span balance wt. |
| IIA4b3 | Elev. root | 178 | (40) | Sweep 30 - 80 | Closed | X1 | -.052 | (-3) | Inbd. balance wt. |
| IIA4b4 | Elev. root | 178 | (40) | Sweep 30 - 80 | Closed | X1 | -.052 | (-3) | Outbd. balance wt. |
| IIA.7a | Stab. LE mid span | 178 | (40) | Sweep 0.5 - 40 Hz | Open | | -.017 | (-1) | LH & RH stab. & elev. tip |
| IIA.7b | Stab. LE mid span | 178 | (40) | Sweep 0.5 - 40 Hz | Closed | X2 | -.017 | (-1) | LH & RH stab. & elev. tip |
| IIA.7a.1 | Stab. LE mid span | 667 | (150) | Pink noise | Open | | -.017 | (-1) | Modal survey |
| IIA.7b.1 | Stab. LE mid span | 667 | (150) | Pink noise | Closed | X2 | -.017 | (-1) | Modal survey |
| IIA.7c | Stab. LE mid span | 334 | (75) | Pink noise | Closed | X2 | -.017 | (-1) | Modal survey |
| IIA.8 | N/A | N/A | | N/A | - | - | - | - | LH & RH elev. freeplay |
| IIIC.2a | Elev. root | 111 222 267 | (25) (50) (60) | Tuned modes | Open | | -.244 | (-14) | Frequency of elevator |
| IIID.2a | Elev. root | 111 222 267 | (25) (50) (60) | Tuned modes | Open | | -.122 | (-7) | Frequency of elevator |
| IIIE.2a | Elev. root | { 111 (25) 178 (40) } | | Dwells | Open | | 0 | (0) | Frequency of elevator |
| IIIE.2b | Elev. root | { 222 (50) 267 (60) } | | Dwells | Closed | X2 | 0 | (0) | Frequency of elevator |

TABLE 13. - PACS TRANSFER FUNCTION TEST SERIES

| TEST NO. | EXCITATION | | PACS | | STAB. POSITION | DATA COLLECTED | COMMENTS |
|--|---|---|--------|---|---------------------|--|--|
| | Type | Level | Loop | Gain | | | |
| IIIA. | Sweep $\dot{\theta}$ 5-10 Hz 600 sec/dec. | rad/sec | Closed | Nominal | 0 rad (deg) | $Y/\dot{\theta} \quad X/\dot{\theta} \quad \delta_H/\dot{\theta}$ (Pilot $\ddot{Z})/\dot{\theta}$ (c.g. $\ddot{Z})/\dot{\theta}$ | Grounded wire in pitch rate gyro |
| IIIA3 | | deg/sec | | | | | |
| IIIA3.1 | | | | | | | |
| III.B | Chirp 0.5 - 10 Hz | .017 -.052 | (1-3) | Closed | Nominal | 0 rad (deg) | Same as above |
| III.C.1.a III.C.1.b | Sweep 0.5-40 Hz Kicker | Volts $\pm 4V$ peak to peak | Open | — | 0 rad (deg) | $Y/\dot{\theta} \quad X/\dot{\theta} \quad \delta_H/\dot{\theta}$ (c.g. $\ddot{Z})/\dot{\theta}$ (Col-Trim)/ $\dot{\theta}$ | Column minus trim |
| III.C.2.a | Chirp 0.5-40 Hz Kicker | ± 2 peak to peak | Open | — | 0 rad (deg) | $Y/\dot{\theta} \quad X/\dot{\theta} \quad \delta_H/\dot{\theta}$ | |
| III.D.1.a.1 III.D.1.a.2 III.D.a.2 III.D.b.1 III.D.b.1a III.D.b.2 III.D.b.3 | Sweep 0.5-40 Hz Kicker | ± 2 ± 2 ± 4 ± 2 ± 2 ± 4 ± 2 | Closed | Nominal Nominal Nominal 2 2 2 2 | 0 rad (deg) | $Y/\dot{\theta} \quad X/\dot{\theta} \quad \delta_H/\dot{\theta}$ (pilot $\ddot{Z})/\dot{\theta}$ (c.g. $\ddot{Z})/\dot{\theta}$ (Col-Trim)/ $\dot{\theta}$ | Column trim in Column trim out Column trim in Column trim in Column trim out Column trim out Column trim out |
| III.E. | Control column pulse | Pilot induced | Closed | 2 | -.244 rad (-14 deg) | Observe response only of Y, δ_H & structure | |

- x — Series Servo Position Signal
 y — Command Signal to Series Servo
 z — Aircraft Normal Acceleration

rotation frequency and measuring the magnitude and phase between a roving accelerometer and a reference accelerometer. The HP5451C Fourier Analyzer technique measures a force input and aircraft response time histories to obtain a Laplace description of the frequency response function. The response functions are used to obtain mode shapes, frequencies, and damping values. Transfer function tests of the PACS at 0.5, 1, and 2 times nominal gain were conducted using a Boonshaft and Fuchs Company (BAFCO) analyzer oscillator to provide the forcing functional signal. Response functions were plotted as bode diagrams and phase lag plots using an analog plotter to provide an on-site examination of results.

4.5.4.2 Elevator free play: The free play deflections of the elevator relative to an arm rigidly mounted on the stabilizer were 2.269×10^{-3} rad (.13 deg) and 2.44×10^{-3} rad (.14 deg) degree for the left and right hand elevators respectively. These values are within the acceptance limits for L-1011 aircraft.

4.5.4.3 Static gain data: Table 14 presents a summary of the pretest static gain and phase at 0.1 and 0.3 Hz for system overall gain factors of 0.5, 1.0 and 2.0 times nominal. The theoretical values at nominal gain are also shown for comparison.

4.5.4.4 Frequency sweep data: Table 15 is a summary of resonances found from the response plots made by the slow sine wave sweeps. The summary table shows that all the fundamental modes and some secondary modes were excited in the frequency range of interest.

TABLE 14. - STATIC GAIN PACS CLOSED LOOP

| CONDITION | PITCH RATE | FREQ. HZ | GAIN FACTOR | SERVO A CHANNEL LVDT | | | | SERVO B CHANNEL LVDT | | THEORETICAL | | |
|-----------|--------------------------------|----------|-------------|----------------------|-------|--------|---------|----------------------|-------|---------------------------|--------|---------|
| | | | | dB ratio | | Phase | | dB ratio | | rad/rad/sec (deg/deg/sec) | Phase | |
| | | | | V/V | * | rad | (deg) | V/V | * | | rad | (deg) |
| 1.B.1 | .017 rad/sec (1 degree/second) | 0.1 | 0.5 | 6.0 | -21.7 | -.799 | (-45.8) | 4.3 | -23.4 | -16.27 | -.513 | (-29.4) |
| | | | 1.0 | 11.5 | -16.2 | -.681 | (-39.0) | 10.9 | -16.8 | | | |
| | | | 2.0 | 16.3 | -11.4 | -.585 | (-33.5) | 16.2 | -11.5 | | | |
| | | 0.3 | 0.5 | -1.0 | -28.7 | -1.660 | (-95.1) | -0.1 | -27.8 | -19.76 | -1.311 | (-75.1) |
| | | | 1.0 | 7.7 | -20.0 | -1.440 | (-82.5) | 6.5 | -21.2 | | | |
| | | | 2.9 | 14.0 | -13.7 | -1.307 | (-74.9) | 13.9 | -13.8 | | | |

*Ratio rad/rad/sec (deg/deg/sec) = dB volt/volt - 27.69

TABLE 15. - SUMMARY OF AIRCRAFT GROUND VIBRATION TEST
MODAL FREQUENCIES ~ Hz

| MODE IDENTIFICATION | IA1a | IB1a | IC1b | IC1b | IC1c - | IE1 | IE2 | IIA1b | IIa2b1 | IIA4b | IIA7a | IIA7b |
|---------------------|------|------|------|------|---------|------|-------|----------|--------|-------|-------|-------|
| Rigid body pitch | 0.98 | 0.98 | 0.98 | 0.98 | 0.98 | 0.98 | 0.98 | 0.99 | | | | |
| Rigid body plunge | 1.65 | 1.60 | 1.60 | 1.65 | 1.63 | 1.63 | 1.61 | 1.65 | | | | |
| 1st wing bending | | | | | | 1.8 | | | | | | |
| Eng. lateral | | 2.0 | 2.2 | 2.2 | 2.35 | 2.82 | 2.8 | | | | | |
| Eng. vertical | 2.8 | 2.8 | 2.9 | 2.85 | 2.7/3.1 | | | 3.1 | | | | |
| Fus. bending | 3.95 | 4.0 | 4.05 | 4.0 | 4.1 | 4.0 | 4.0 | 4.05 | 3.90 | | 4.0 | 4.0 |
| Horiz. 1st bending | 5.0 | 4.8 | 5.0 | 4.8 | 4.85 | | | 4.9 | | | 4.8 | 4.8 |
| 2nd wing bending | 5.2 | 5.2 | 5.2 | 5.2 | 5.2 | 5.2 | 5.2 | 5.2 | 5.1 | | 5.2 | 5.2 |
| Eng. pitch-roll | 7.6 | 7.6 | 7.6 | 7.6 | 7.6 | 7.6 | 7.7 | 7.5 | 6.8 | | | |
| Elev. rotation | | 10.2 | 10.4 | 10.3 | 10.5 | | | 9.8/10.7 | 8.45 | | | |
| | 12.0 | 12.1 | 12.1 | 12.1 | 12.4 | | | 11.6 | 11.0 | | | |
| | 14.0 | 13.7 | 13.6 | 13.6 | 13.9 | 14.0 | 13.8 | 14.2 | 14.5 | | | |
| 2nd stab. bending | 15.1 | 15.1 | 15.4 | 15.5 | 15.5 | 15.6 | 15.35 | 15.3 | 15.1 | | 15.0 | 15.0 |
| | 17.4 | 17.5 | 17.5 | 17.6 | 17.6 | | | | | | 17.6 | |
| | | | 18.6 | 18.9 | 19.0 | 19.1 | 19.2 | 18.4 | 18.6 | | 19.2 | 18.9 |
| Elev. bending | 20.0 | 20.7 | 20.4 | 20.6 | 20.8 | | | 22.6 | 20.4 | | | 19.4 |
| Eng. pitch | 24.7 | 24.8 | 24.8 | | | | | 24.8 | 27.0 | | 26.2 | 25.1 |
| | 28.8 | | | | | | | | 28.0 | | 28.2 | 28.0 |
| | 30.6 | | | | 30.0 | 29.0 | | | 29.2 | 31.6 | | |
| Elev. 2nd bending | 32.5 | | | | 32.5 | | | | | 33.8 | 34.5 | 34.6 |
| | 36.2 | | | | 36.3 | | | | | | 36.8 | 37.0 |
| Inbd. balance wt. | | | | | | | | | | 46.12 | | |
| Middle balance wt. | | | | | | | | | | 53.6 | | |
| Outbd. balance wt. | | | | | | | | | | 64.8 | | |

4.5.4.5 Modal analysis: Modal results from the HP5451C analyzer are summarized in Table 16 for symmetric modes only. The dwell and survey method concentrated more force at the elevator rotation frequency and had a 0.6 Hz higher resonance than did the Hewlett Packard HP5451C with the pink noise input procedure.

4.5.4.6 Transfer function data: Stabilizer position data were examined at inputs of .017 rad/sec (1 deg/sec), .035 rad/sec (2 deg/sec), and .052 rad/sec (3 deg/sec) pitch rate to note any nonlinearities due to amplitude. Some nonlinear effects were found above 1 Hz. However, the command signal output and series servo position show little nonlinearity effect at the tested input levels. This indicates the stabilizer actuating system contributes the nonlinear effect seen in the stabilizer position. Good correlation was found for the complete system between analytical predictions and test data for feedback amplitude ratios.

4.5.4.7 Conclusions: The ground vibration test successfully measured key structural modes by two techniques with the PACS system on and off and found no significant effect on the structural modes of the aircraft. Transfer function tests demonstrated that the PACS was stable and performed operationally per design.

TABLE 16. - MODAL RESULTS

| MODE IDENTIFICATION | PACS CLOSED LOOP | | | | | | PACS CLOSED LOOP | | PACS CLOSED $\delta_H = 0$ rad (deg) analytical Freq. (Hz) |
|--|---|--------------|---|--------------|--|--------------|--|--------------|--|
| | Elev. root $\delta_H = -.052$ rad (-3 deg) | | $\delta_H = -.017$ rad (-1 deg) Mid-span LE HS 334N(75 lb) | | $\delta_H = -.017$ rad (-1 deg) Mid-span LE HS 689N(155 lb) | | $\delta_H = -.017$ rad (-1 deg) Mid-span LE HS 689N(155 lb) | | |
| | Freq. (Hz) | Damp. (c) | Freq. (Hz) | Damp. (c) | Freq. (Hz) | Damp. (c) | Freq. (Hz) | Damp. (c) | |
| Fuselage bending horiz. 1st bending | — | — | 4.76 | 0.016 | 4.70 | 0.025 | 4.58 | 0.025 | 4.572 |
| 2nd wing bending | — | — | 5.25 | 0.064 | 5.15 | 0.040 | 5.27 | 0.041 | 5.137 |
| Elevator rotation | 7.52 | 0.078 | — | — | — | — | — | — | 10.623 |
| 2nd stab. bending | 14.76 | 0.018 | 14.76 | 0.021 | 14.78 | 0.021 | 14.75 | 0.021 | 13.86 |
| Stabilizer torsion | — | — | 18.95 | 0.051 | 18.90 | 0.052 | 18.90 | 0.055 | 17.944 |
| Elev. 1st bending | 21.21 | 0.020 | — | — | — | — | — | — | — |
| 3rd stab. bending | 28.40 | 0.031 | — | — | — | — | — | — | — |
| Elev. 2nd bending | 34.07 | 0.027 | — | — | — | — | — | — | — |

5. FLIGHT TEST

5.1 Flight Flutter Test

A flight flutter test was conducted to verify the stability and flutter integrity of the aircraft equipped with a PACS.

5.1.1 Data Acquisition.— Table 17 lists the sensors that were monitored and/or recorded during the program to observe aircraft and component PACS response during the flights. The parameters were recorded on flight tapes as well as telemetered to a ground station for display on strip chart pen recorders, Lissajous patterns on oscilloscopes, and x-y plots of the feedback gain and phase. Flight tape data were later reduced to obtain transfer functions of aircraft structural response points and PACS system signals.

5.1.2 Test Procedure.— Flutter clearance for the modified flight test aircraft required tests to be performed with the PACS on and off. The flutter tests were performed in the center of gravity range from 21 to 25% mac to ensure that structural loads were not exceeded in the event of PACS undetected hardover failures at speeds in excess of 193 m/sec (375 KCAS).

Flight test techniques usually started with pilot induced stick raps to obtain a quick look at aircraft response. The raps indicated if adequate stability of structural and system modes existed. The Lissajous patterns were used to indicate any possible unfavorable trends for wing and stabilizer loads.

For some test points damping characteristics were checked by driving the pitch series servo with a function generator at a resonance frequency to excite a specific structural mode. A quick stop of the function generator input provided a response decay of the aircraft structure which indicates the modal damping. Strip charts were monitored for wing, horizontal stabilizer, and engine responses to observe the modal damping.

Table 18 is a summary of test conditions and data collected for the flight flutter program, which reflect the requirements outlined in the Test Plan. Most data points were taken during level flight. Some data at higher speeds were taken in shallow dives.

TABLE 17. - TRANSDUCERS MONITORED FOR FLUTTER TESTS

| MEASURE- MENT NUMBER | SENSOR IDENTIFICATION | MEASURE- MENT NUMBER | SENSOR IDENTIFICATION |
|----------------------------|--|----------------------------|--|
| 2 | Normal accel. c.g. | 18001 | Static pressure-PSR (PCM) |
| 4 | Normal accel. pilot's seat | 10007 | Total pressure-PTT (PCM) |
| 7 | Lateral accel. Eng-1 | 18656 | Airspeed (PTT-PSR2) (CKPT) |
| 16 | Normal accel. left wing tip | 18658 | Mach (PTT-PSR2) (CKPT) |
| 17 | Normal accel. right wing tip | 26001 | Ram air temperature-test-1 |
| 20 | Normal accel. left horiz. stab. tip | 30744 | PACS series servo-vertical accel. |
| 21 | Normal accel. right horiz. stab. tip | 30745 | PACS series servo-lateral accel. |
| 22 | Lateral accel. vert. fin tip | 30746 | PACS series servo-longitudinal accel. |
| 54 | Normal accel. lt. elevator Rear Beam Sta. 92 | 30747 | Lt. elevator inboard counterbalance N_z |
| 55 | Normal accel. rt. elevator Rear Beam Sta. 92 | 30748 | Lt. elevator mid-span counterbalance N_z |
| 69 | Normal accel. aft cabin floor BL 0 FS 1535 | 30749 | Lt. elevator outboard counterbalance N_z |
| 76 | Eng. No. 3 lateral acceleration | 36438 | BAFCO relative phase angle 2 |
| 85 | Engine No. 1 normal acceleration 12 o'clock | 36438 | BAFCO amplitude ratio 1 |
| 87 | Engine No. 3 normal acceleration 12 o'clock | 36439 | BAFCO amplitude ratio 2 |
| 192 | Longitudinal accel. left horiz. stab. tip | 36440 | AACS function generator output signal |
| 4019 | Elevator pos LH inbd. | 36441 | BAFCO reference log frequency |
| 4021 | Elevator pos. RH inbd. | 36455 | BAFCO relative phase angle 1 |
| 4225 | Stabilizer position 1A fine low range | 36469 | Pitch rate gyro 1 |
| 4227 | Stabilizer position 2A fine low range | 36470 | Pitch rate gyro 1 (fine) |
| 12023 | Lt. wing shear LWS 839 (BL 702) | 36472 | PACS series servo position 1A fine (PCM) |
| 13033 | Lt. wing bending moment LWS 839 (BL 702) | 36473 | PACS series servo position 2A (PCM) |
| 12041 | Lt. wing torsion moment LWS 839 (BL 702) | 36475 | PACS servo CMD 1A (PCM) |
| 12072 | Lt. horiz. stab. shear LWS 148 (BL 126) | 36260 | Function generator output (General) |
| 12073 | Rt. horiz. stab. shear LWS 148 (BL 126) | 36013 | Column minus trim (1A) |
| 12075 | Lt. horiz. stab. bending mom. LWS 148 (BL 126) | 36014 | Column minus trim (2A) |
| 12076 | Rt. horiz. stab. bending mom. LWS 148 (BL 126) | 8001 | Control wheel force |
| 12081 | Lt. stab. torsion mom. LWS 148 (BL 126) | 193 | Fwd. pitch rate beam normal accel. |
| 12082 | Rt. stab. torsion mom. LWS 148 (BL 126) | 194 | Aft pitch rate beam normal accel. |
| 12095 | Link load - left elevator actuator | 36079 | LH stab. position coarse |
| | | 36080 | RH stab. position coarse |

TABLE 18. - SUMMARY OF FLIGHT FLUTTER TEST (S.I. UNITS) (SHEET 1 of 4 SHEETS)

| TEST NO. | POINT NO. | FUEL CONFIGURATION | INPUT TYPES | | | | | | | | | | | | | QUICK STOP | SWEEPS | | COMMENTS |
|--------------|-----------|---|-------------|-----------|-------|--------|------------------------|----------|-------------|-----------|-----------|-----------|-------------|----------|-------------|------------|------------------------|------------------------------|----------|
| | | | ALT km | SPEED m/s | PACS | | O _C SEN m/s | ACS LOOP | STICK PULSE | DWELLS | | | | RANGE Hz | LEVEL VOLTS | | | | |
| | | | | | LOOP | GAIN | | | | FREQ 1 Hz | FREQ 2 Hz | FREQ 3 Hz | LEVEL VOLTS | | | | | | |
| 1704.11.A.1 | 0 | MINIMUM FUEL 156,500 kg GW 21.7% mac c.g. | 6.7 | 154 | Open | X2 | >164.6 | Off | 1 Fwd | | | | | | | | | | |
| | 2 | | 6.7 | 175 | Open | X2 | >164.6 | Off | 1 Fwd | | | | | | | | | | |
| | 1 | | 6.7 | 195 | Open | X2 | >164.6 | Off | 2 Fwd | | | | | | | | | | |
| 1704.11.A.2 | 1 | | 6.7 | 195 | Close | X2 | >164.6 | Off | 2 Fwd | | | | | | | | | | |
| 1704.11.A.3 | 4 | | 6.7 | 201 | Close | X2 | >164.6 | Off | 2 Fwd | | | | | | | | | | |
| 1704.11.A.4 | 1 | | 6.7 | 195 | Close | X2 | >164.6 | Off | | 2.65 | | | | 1.0 | YES | | | | |
| 1704.11.A.5 | 1 | 6.7 | 195 | Open | X2 | >164.6 | Off | | 2.65 | | | | 1.0 | YES | | | | | |
| 1704.11.C.1 | 5 | 6.7 | M.88 | Close | X2 | >164.6 | On | 2 Fwd | | | | | | | | | | | |
| 1704.11.C.2 | 5 | 6.7 | M.88 | Close | X2 | >164.6 | On | | 2.65 | | | | 1.5 | YES | | | | | |
| 1704.11.C.3 | 3 | 6.7 | 198 | Open | X2 | >164.6 | On | | 0.1 | 0.3 | 0.4 | | 1.5 | YES | 1.0/10. | 1.5 | 478 Sec/Dec Sweep Rate | | |
| 1704.11.D.1 | 6 | 146,100 kg GW 23% c.g. | 6.7 | 208 | Close | X2 | >164.6 | Off | Fwd | | | | | | | | | | |
| 1702.12.A.1 | 1 | HEAVY FUEL | 3.66 | 154 | Open | X1 | <82.3 | Off | Fwd-Aft | | | | | | | | | | |
| 1702.12.A.2 | 1 | HEAVY FUEL | 3.66 | 154 | Open | X1 | <82.3 | Off | | 2.65 | 3.82 | 4.30 | 2.0,2.0,3.0 | F1-F3* | | | | | |
| 1702.12.B.1 | 1 | 24.6% mac c.g. | 3.66 | 154 | Close | X1 | <82.3 | Off | Fwd-Aft | 2.65 | | | 2.0 | YES | | | | | |
| 1703.11.B.2 | 1 | | 3.66 | 154 | Close | X1 | <82.3 | Off | | 2.65 | | | 2.0 | YES | | | | | |
| 1702.12.B.3 | 1 | | 3.66 | 154 | Close | X2 | <82.3 | Off | Fwd-Aft | | | | | | | | | | |
| 1703.11.B.4 | 1 | | 3.66 | 154 | Close | X2 | <82.3 | Off | | 2.65 | | | 2 | YES | | | | | |
| 1703.11.BA.1 | 1 | | 3.66 | 154 | Open | X2 | <82.3 | Off | | 0.3 | | | 2 | NO | | | | | |
| 1702.12.C.1 | 2 | | 3.66 | 165 | Open | X2 | <82.3 | Off | Fwd-Aft | | | | | | | | | | |
| 1702.12.C.2 | 2 | | 3.66 | 165 | Open | X2 | <82.3 | Off | | 2.65 | 3.2 | 4.3 | 2.0,2.0,2.5 | F1-F3* | | | | | |
| 1702.12.C.3 | 2 | | 3.66 | 165 | Open | X2 | <82.3 | Off | | 0.1 | 0.3 | 0.4 | 2.0,2.5,2.0 | F1-F3* | 0.5/30 | 2.0 | | | |
| 1702.12.C.4 | 2 | | 3.66 | 165 | Open | X2 | <82.3 | Off | | | | | | | 0.5/30 | 2.0 | | 215 Sec/Dec - Sweep Too Fast | |
| 1703.11.D.1 | 2 | 175,600 kg | 3.66 | 165 | Close | X2 | <82.3 | Off | Fwd-Aft | | | | | | | | | | |
| 1703.11.D.2 | 2 | 24.1% mac c.g. | 3.66 | 165 | Close | X2 | <82.3 | Off | | 2.65 | | | 2.0 | YES | | | | | |
| 1703.11.D.3 | 2 | | 3.66 | 165 | Close | X2 | <82.3 | Off | | 0.1 | 0.3 | 0.5 | 2.0 | NO | 0.5/30 | 2.0 | | 478 Sec/Dec | |
| 1703.11.E.1 | 2 | | 3.66 | 165 | Close | X2 | <82.3 | On | | | | | | | | | | | |
| 1703.11.E.2 | 2 | | 3.66 | 165 | Close | X2 | <82.3 | On | | 2.65 | | | 2.0 | YES | | | | | |
| 1703.11.E.3 | 2 | | 3.66 | 165 | Close | X2 | <82.3 | On | | 0.1 | 0.3 | 0.5 | 2.0 | NO | 0.5/30 | 2.0 | | 478 Sec/Dec | |
| 1703.11.F.1 | 3 | | 3.66 | 185 | Open | X2 | >164.6 | Off | Fwd-Aft | | | | | | | | | | |
| 1703.11.F.2 | 3 | | 3.66 | 185 | Open | X2 | >164.6 | Off | | 2.65 | | | 2.0 | YES | | | | | |
| 1703.11.G.1 | 3 | | 3.66 | 185 | Close | X2 | >164.6 | Off | Fwd-Aft | | | | | | | | | | |
| 1703.11.G.2 | 3 | | 3.66 | 185 | Close | X2 | >164.6 | Off | | 2.60 | | | 2.0 | YES | | | | | |
| 1703.11.H.1 | 4 | 160,200 kg | 3.66 | 195 | Open | X2 | >164.6 | Off | Fwd-Aft | | | | | | | | | | |
| 1703.11.H.2 | 4 | 24.3% mac c.g. | 3.66 | 195 | Open | X2 | >164.6 | Off | | 2.65 | | | 2.0 | YES | | | | | |
| 1703.11.I.1 | 4 | | 3.66 | 195 | Close | X2 | >164.6 | Off | Fwd-Aft | | | | | | | | | | |
| 1703.11.I.2 | 4 | | 3.66 | 195 | Close | X2 | >164.6 | Off | | 2.65 | | | 2.0 | YES | | | | | |
| 1704.11.J.1 | 5 | | 3.66 | 206 | Open | X2 | >164.6 | Off | 2 Fwd | | | | | | | | | | |
| 1704.11.J.3 | 5 | | 3.66 | 206 | Open | X2 | >164.6 | Off | | 0.1 | | | 1.5 | NO | | | | | |

*Quick Stops on Freq 1 Through Freq 3

TABLE 18. - SUMMARY OF FLIGHT FLUTTER TEST (S.I. UNITS) (SHEET 2 OF 4 SHEETS)

| TEST NO. | POINT NO. | FUEL CONFIGURATION | INPUT TYPES | | | | | | | | | | | | | | | COMMENTS |
|-------------|-----------|---------------------------------|-------------|-----------|-------|--------|-----------|----------|-------------|-----------|-----------|-----------|---------------|------------|----------|----------------|----------------|----------|
| | | | ALT km | SPEED m/s | PACS | | QcSEN m/s | ACS LOOP | STICK PULSE | DWELLS | | | | QUICK STOP | SWEEPS | | | |
| | | | | | LOOP | GAIN | | | | FREQ 1 Hz | FREQ 2 Hz | FREQ 3 Hz | LEVEL VOLTS | | RANGE Hz | LEVEL VOLTS | | |
| 1704.11.K.3 | 5 | 182,100 kg GW 24.0% mac c.g. | 3.66 | 206 | Open | X2 | >164.6 | On | | 0.1 | 0.3 | 0.4 | 1.5 | NO | 1.0/10 | 1.5 | 478 Sec/Dec | |
| 1704.11.N.1 | 7 | | 6.7 | 154 | Open | X2 | < 82.3 | Off | Fwd-Aft | | | | | | | | | |
| 1704.11.N.2 | 7 | | 6.7 | 154 | Open | X2 | < 82.3 | Off | | 2.65 | | | 2.0 | YES | | | | |
| 1704.11.O.1 | 7 | | 6.7 | 154 | Close | X2 | < 82.3 | Off | Fwd-Aft | | | | | | | | | |
| 1704.11.O.2 | 7 | | 6.7 | 154 | Close | X2 | < 82.3 | Off | | 2.65 | | | 2.0 | YES | | | | |
| 1704.11.P.1 | 8 | | 6.7 | 161 | Open | X2 | < 82.3 | Off | Fwd-Aft | | | | | | | | | |
| 1704.11.P.2 | 8 | | 6.7 | 161 | Open | X2 | < 82.3 | Off | | 2.65 | | | 2.0 | YES | | | | |
| 1704.11.Q.1 | 8 | | 6.7 | 161 | Close | X2 | < 82.3 | Off | Fwd-Aft | | | | | | | | | |
| 1704.11.Q.2 | 8 | | 6.7 | 161 | Close | X2 | < 82.3 | Off | | 2.65 | | | 2.0 | YES | | | | |
| 1704.11.R.1 | 9 | | 6.7 | 177 | Open | X2 | >164.6 | Off | Fwd-Aft | | | | | | | | δH = .0436 Rad | |
| 1704.11.R.2 | 9 | | 6.7 | 177 | Open | X2 | >164.6 | Off | | 0.4 | 0.5 | 2.65 | 2.0 | F1&F3 | | | | |
| 1704.11.S.1 | 9 | | 6.7 | 177 | Close | X2 | >164.6 | Off | Fwd-Aft | | | | | | | | | |
| 1704.11.S.2 | 9 | | 6.7 | 177 | Close | X2 | >164.6 | Off | | 2.65 | | | 2.0 | YES | | | | |
| 1704.11.T.1 | 10 | | 6.7 | 185 | Open | X2 | >164.6 | Off | 2 Fwd | | | | | | | | δH = .0401 Rad | |
| 1704.11.T.2 | 10 | | 6.7 | 185 | Open | X2 | >164.6 | Off | | 2.65 | | | 2.0 | YES | | | | |
| 1704.11.U.1 | 10 | 6.7 | 185 | Close | X2 | >164.6 | Off | 2 Fwd | | | | | | | | | | |
| 1704.11.V.1 | 11 | 6.7 | 195 | Open | X2 | >164.6 | Off | 2 Fwd | | | | | | | | | | |
| 1704.11.V.3 | 11 | 6.7 | 195 | Open | X2 | >164.6 | Off | 0.2 | 0.4 | | | 2.0 | NO | | | | | |
| 1704.11.W.1 | 11 | 6.7 | 195 | Close | X2 | >164.6 | Off | 2 Fwd | | | | | | | | | | |
| 1704.11.X.1 | 12 | 6.7 | 193 | Open | X2 | >164.6 | Off | 2 Fwd | | | | | | | | | | |
| 1704.11.Y.1 | 12 | 174,200 kg GW | 6.7 | 193 | Close | X2 | >164.6 | On | 2 Fwd | | | | | | | δH = .0358 Rad | | |
| 1704.11.Y.3 | 12 | 24.1% mac c.g. | 6.7 | 193 | Open | X2 | >164.6 | On | | 0.1 | 0.3 | 0.5 | 2.0,1.5,1.5 | NO | 1.0/10. | 2.0 | 478 Sec/Dec | |
| 1705.11.A.1 | 13 | 187,300 kg GW | 6.7 | 193 | Open | X2 | >164.6 | Off | 2 Fwd | | | | | | | | | |
| 1705.11.B.1 | 13 | 24.1% mac c.g. | 6.7 | 193 | Close | X2 | >164.6 | On | 2 Fwd | | | | | | | | | |
| 1705.11.C.2 | 25 | 180,100 kg GW | 9.8 | M.90 | Close | X2 | >164.6 | Off | 2 Fwd | | | | | | | | | |
| 1705.11.C.3 | 26 | | 8.5 | M.90 | Close | X2 | >164.6 | Off | 2 Fwd | | | | | | | | | |
| 1705.11.C.4 | 32 | | 6.7 | M.90 | Close | X2 | >164.6 | Off | Fwd | | | | | | | | | |
| 1705.11.D.2 | 29 | 172,800 kg GW | 9.8 | M.95 | Close | X2 | >164.6 | Off | 2 Fwd | | | | | | | | | |
| 1705.11.D.3 | 30 | 24.1% mac c.g. | 8.9 | M.95 | Close | X2 | >164.6 | Off | — | | | | | | | | | |
| 1705.11.E.1 | 31 | | 7.3 | M.925 | Close | X2 | >164.6 | Off | 2 Fwd | | | | | | | | | |
| 1705.11.F.1 | 17 | | 11.3 | M.70 | Open | X2 | < 82.3 | Off | 2 Fwd | | | | | | | | | |
| 1705.11.G.1 | 17 | | 11.3 | M.70 | Close | X2 | < 82.3 | Off | 2 Fwd | | | | | | | | | |
| 1705.11.H.1 | 18 | | 11.3 | M.775 | Open | X2 | < 82.3 | Off | 2 Fwd | | | | | | | | | |
| 1705.11.I.1 | 18 | | 11.3 | M.775 | Close | X2 | < 82.3 | Off | 2 Fwd | | | | | | | | | |
| 1705.11.J.1 | 19 | 163,700 kg | 11.3 | M.85 | Open | X2 | < 82.3 | On | 2 Fwd | | | | | | | δH = .0532 Rad | | |
| 1705.11.J.2 | 19 | 24.2% mac c.g. | 11.3 | M.85 | Open | X2 | < 82.3 | On | | 0.1 | 0.3 | 0.4 | 1.0, .75, .75 | NO | 1.0/10. | 1.5 | 478 Sec/Dec | |
| 1705.11.K.1 | 19 | | 11.3 | M.85 | Close | X2 | < 82.3 | Off | 2 Fwd | | | | | | | | | |

*F1-F3 = Quick Stops On Freq 1 Through Freq 3

TABLE 18. - SUMMARY OF FLIGHT FLUTTER TEST (ENGLISH UNITS) (SHEET 3 OF 4 SHEETS)

| TEST NO. | POINT NO. | FUEL CONFIGURATION | ALT 1000 ft | SPEED KCAS | PACS | | Q _{SEN} KCAS | ACS LOOP | STICK PULSE | INPUT TYPES | | | | QUICK STOP | SWEEPS | | COMMENTS |
|--------------|-----------|---|-------------|------------|-------|------|-----------------------|----------|-------------|-------------|-----------|-----------|-------------|------------|----------|-------------|---|
| | | | | | LOOP | GAIN | | | | FREQ 1 Hz | FREQ 2 Hz | FREQ 3 Hz | LEVEL VOLTS | | RANGE Hz | LEVEL VOLTS | |
| 1704.11.A.1 | 0 | MINIMUM FUEL 345,000 lb GW 21.7% mac c.g. | 22 | 300 | Open | X2 | > 320 | Off | 1 Fwd | | | | | | | | |
| | 2 | | 22 | 340 | Open | X2 | > 320 | Off | 1 Fwd | | | | | | | | |
| | 1 | | 22 | 380 | Open | X2 | > 320 | Off | 2 Fwd | | | | | | | | |
| 1704.11.A.2 | 1 | | 22 | 380 | Close | X2 | > 320 | Off | 2 Fwd | | | | | | | | |
| 1704.11.A.3 | 4 | | 22 | 390 | Close | X2 | > 320 | Off | 2 Fwd | | | | | | | | |
| 1704.11.A.4 | 1 | | 22 | 380 | Close | X2 | > 320 | Off | | 2.65 | | | 1.0 | YES | | | |
| 1704.11.A.5 | 1 | 322,100 GW 23% c.g. | 22 | 380 | Open | X2 | > 320 | Off | | 2.65 | | | 1.0 | YES | | | |
| 1704.11.C.1 | 5 | | 22 | M.88 | Close | X2 | > 320 | On | 2 Fwd | | | | | | | | |
| 1704.11.C.2 | 5 | | 22 | M.88 | Close | X2 | > 320 | On | | 2.65 | | | 1.5 | YES | | | |
| 1704.11.C.3 | 3 | | 22 | 385 | Open | X2 | > 320 | On | | 0.1 | 0.3 | 0.4 | 1.5 | NO | 1.0/10. | 1.5 | 478 Sec/Dec Sweep Rate |
| 1704.11.D.1 | 6 | | 22 | 405 | Close | X2 | > 320 | Off | Fwd | | | | | | | | |
| 1702.12.A.1 | 1 | HEAVY FUEL 24.6% mac c.g. | 12 | 300 | Open | X1 | < 160 | Off | Fwd-Aft | | | | | | | | |
| 1702.12.A.2 | 1 | | 12 | 300 | Open | X1 | < 160 | Off | | 2.65 | 3.82 | 4.30 | 2.0,2.0,3.0 | F1-F3* | | | |
| 1702.12.B.1 | 1 | | 12 | 300 | Close | X1 | < 160 | Off | Fwd-Aft | 2.65 | | | 2.0 | YES | | | |
| 1703.11.B.2 | 1 | | 12 | 300 | Close | X1 | < 160 | Off | | 2.65 | | | 2.0 | YES | | | |
| 1702.12.B.3 | 1 | | 12 | 300 | Close | X2 | < 160 | Off | Fwd-Aft | | | | | | | | |
| 1703.11.B.4 | 1 | | 12 | 300 | Close | X2 | < 160 | Off | | 2.65 | | | 2 | YES | | | |
| 1703.11.BA.1 | 1 | 387,100 lb GW 24.1% mac c.g. | 12 | 300 | Open | X2 | < 160 | Off | | 0.3 | | | 2 | NO | | | |
| 1702.12.C.1 | 2 | | 12 | 320 | Open | X2 | < 160 | Off | Fwd-Aft | | | | | | | | |
| 1702.12.C.2 | 2 | | 12 | 320 | Open | X2 | < 160 | Off | | 2.65 | 3.2 | 4.3 | 2.0,2.0,2.5 | F1-F3* | | | |
| 1702.12.C.3 | 2 | | 12 | 320 | Open | X2 | < 160 | Off | | 0.1 | 0.3 | 0.4 | 2.0,2.5,2.0 | F1-F3* | 0.5/30 | 2.0 | 215 Sec/Dec - Sweep Too Fast Data Rejected |
| 1702.12.C.4 | 2 | | 12 | 320 | Open | X2 | < 160 | Off | | | | | | | 0.5/30 | 2.0 | |
| 1703.11.D.1 | 2 | | 12 | 320 | Close | X2 | < 160 | Off | Fwd-Aft | | | | | | | | |
| 1703.11.D.2 | 2 | 353,200 lb GW 24.3% mac c.g. | 12 | 320 | Close | X2 | < 160 | Off | | 2.65 | | | 2.0 | YES | | | |
| 1703.11.D.3 | 2 | | 12 | 320 | Close | X2 | < 160 | Off | | 0.1 | 0.3 | 0.5 | 2.0 | NO | 0.5/30 | 2.0 | 478 Sec/Dec |
| 1703.11.E.1 | 2 | | 12 | 320 | Close | X2 | < 160 | On | | | | | | | | | |
| 1703.11.E.2 | 2 | | 12 | 320 | Close | X2 | < 160 | On | | 2.65 | | | 2.0 | YES | | | |
| 1703.11.E.3 | 2 | | 12 | 320 | Close | X2 | < 160 | On | | 0.1 | 0.3 | 0.5 | 2.0 | NO | 0.5/30 | 2.0 | 478 Sec/Dec |
| 1703.11.F.1 | 3 | | 12 | 360 | Open | X2 | > 320 | Off | Fwd-Aft | | | | | | | | |
| 1703.11.F.2 | 3 | 401,400 lb GW 24.0% mac c.g. | 12 | 360 | Open | X2 | > 320 | Off | | 2.65 | | | 2.0 | YES | | | |
| 1703.11.G.1 | 3 | | 12 | 360 | Close | X2 | > 320 | Off | Fwd-Aft | | | | | | | | |
| 1703.11.G.2 | 3 | | 12 | 360 | Close | X2 | > 320 | Off | | 2.60 | | | 2.0 | YES | | | |
| 1703.11.H.1 | 4 | | 12 | 380 | Open | X2 | > 320 | Off | Fwd-Aft | | | | | | | | |
| 1703.11.H.2 | 4 | | 12 | 380 | Open | X2 | > 320 | Off | | 2.65 | | | 2.0 | YES | | | |
| 1703.11.I.1 | 4 | | 12 | 380 | Close | X2 | 320 | Off | Fwd-Aft | | | | | | | | |
| 1703.11.I.2 | 4 | 401,400 lb GW 24.0% mac c.g. | 12 | 380 | Close | X2 | 320 | Off | | 2.65 | | | 2.0 | YES | | | |
| 1704.11.J.1 | 5 | | 12 | 400 | Open | X2 | > 320 | Off | 2 Fwd | | | | | | | | |
| 1704.11.J.3 | 5 | | 12 | 400 | Open | X2 | > 320 | Off | | 0.1 | | | 1.5 | NO | | | |
| 1704.11.K.3 | 5 | | 12 | 400 | Open | X2 | > 320 | On | | 0.1 | 0.3 | 0.4 | 1.5 | NO | 1.0/10 | 1.5 | 478 Sec/Dec |
| 1704.11.N.1 | 7 | | 22 | 300 | Open | X2 | < 160 | Off | Fwd-Aft | | | | | | | | |
| 1704.11.N.2 | 7 | | 22 | 300 | Open | X2 | < 160 | Off | | 2.65 | | | 2.0 | YES | | | |
| 1704.11.O.1 | 7 | 401,400 lb GW 24.0% mac c.g. | 22 | 300 | Close | X2 | < 160 | Off | Fwd-Aft | | | | | | | | |
| 1704.11.O.2 | 7 | | 22 | 300 | Close | X2 | < 160 | Off | | 2.65 | | | 2.0 | YES | | | |
| 1704.11.P.1 | 8 | | 22 | 312 | Open | X2 | < 160 | Off | Fwd-Aft | | | | | | | | |
| 1704.11.P.2 | 8 | | 22 | 312 | Open | X2 | < 160 | Off | | 2.65 | | | 2.0 | YES | | | |

*Quick Stops on Freq 1 Through Freq 3

TABLE 18. - SUMMARY OF FLIGHT FLUTTER TEST (ENGLISH UNITS) (SHEET 4 OF 4 SHEETS)

| TEST NO. | POINT NO. | FUEL CONFIGURATION | ALT 1000 ft | SPEED KCAS | PACS | | Q _c SEN KCAS | ACS LOOP | STICK PULSE | INPUT TYPES | | | | QUICK STOP | SWEEPS | | COMMENTS |
|-------------|-----------|----------------------------------|-------------|------------|-------|------|-------------------------|----------|-------------|-------------|-----------|-----------|---------------|------------|----------|---------------------------|---------------------------|
| | | | | | LOOP | GAIN | | | | DWELLS | | | | | RANGE Hz | LEVEL VOLTS | |
| | | | | | | | | | | FREQ 1 Hz | FREQ 2 Hz | FREQ 3 Hz | LEVEL VOLTS | | | | |
| 1704.11.Q.1 | 8 | 384,100 lb GW 24% mac c.g. | 22 | 312 | Close | X2 | <160 | Off | Fwd-Aft | 2.65 | 0.5 | 2.65 | 2.0 | YES | F1&F3 | δH = 2.5° | |
| 1704.11.Q.2 | 8 | | 22 | 312 | Close | X2 | <160 | Off | | | | | | | | | |
| 1704.11.R.1 | 9 | | 22 | 345 | Open | X2 | >320 | Off | Fwd-Aft | 0.4 | 0.5 | 2.65 | 2.0 | YES | F1&F3 | | |
| 1704.11.R.2 | 9 | | 22 | 345 | Open | X2 | >320 | Off | | | | | | | | | |
| 1704.11.S.1 | 9 | | 22 | 345 | Close | X2 | >320 | Off | Fwd-Aft | 2.65 | 0.5 | 2.65 | 2.0 | YES | F1&F3 | | |
| 1704.11.S.2 | 9 | | 22 | 345 | Close | X2 | >320 | Off | | | | | | | | | |
| 1704.11.T.1 | 10 | | 22 | 360 | Open | X2 | >320 | Off | 2 Fwd | 2.65 | 0.5 | 2.65 | 2.0 | YES | F1&F3 | | |
| 1704.11.T.2 | 10 | | 22 | 360 | Open | X2 | >320 | Off | | | | | | | | | |
| 1704.11.U.1 | 10 | | 22 | 360 | Close | X2 | >320 | Off | 2 Fwd | 0.4 | 0.5 | 2.65 | 2.0 | YES | F1&F3 | | |
| 1704.11.V.1 | 11 | | 22 | 380 | Open | X2 | >320 | Off | 2 Fwd | | | | | | | | |
| 1704.11.V.3 | 11 | 22 | 380 | Open | X2 | >320 | Off | 0.2 | 0.4 | 0.5 | 2.65 | 2.0 | NO | F1&F3 | | | |
| 1704.11.W.1 | 11 | 22 | 380 | Close | X2 | >320 | Off | 2 Fwd | | | | | | | | | |
| 1704.11.X.1 | 12 | 413,000 lbs GW 24.1% mac c.g. | 22 | 375 | Open | X2 | >320 | Off | 2 Fwd | 0.1 | 0.3 | 0.5 | 2, 1.5, 1.5 | NO | 1.0/10. | δH = 2.05° 478 Sec/Dec | |
| 1704.11.Y.1 | 12 | | 22 | 375 | Close | X2 | >320 | On | 2 Fwd | | | | | | | | |
| 1704.11.Y.3 | 12 | | 22 | 375 | Open | X2 | >320 | On | | | | | | | | | |
| 1705.11.A.1 | 13 | | 22 | 375 | Open | X2 | >320 | Off | 2 Fwd | | | | | | | | |
| 1705.11.B.1 | 13 | 397,000 lb GW | 22 | 375 | Close | X2 | >320 | On | 2 Fwd | 0.1 | 0.3 | 0.5 | 2, 1.5, 1.5 | NO | 1.0/10. | δH = 2.05° 478 Sec/Dec | |
| 1705.11.C.2 | 25 | | 32 | M.90 | Close | X2 | >320 | Off | 2 Fwd | | | | | | | | |
| 1705.11.C.3 | 26 | | 28 | M.90 | Close | X2 | >320 | Off | 2 Fwd | | | | | | | | |
| 1705.11.C.4 | 32 | | 22 | M.90 | Close | X2 | >320 | Off | Fwd | | | | | | | | |
| 1705.11.D.2 | 29 | 381,000 lb GW 24.1% mac c.g. | 32 | M.95 | Close | X2 | >320 | Off | 2 Fwd | 0.1 | 0.3 | 0.5 | 1.0, .75, .75 | NO | 1.0/10. | δH = 3.05° 478 Sec/Dec | |
| 1705.11.D.3 | 30 | | 29.2 | M.95 | Close | X2 | >320 | Off | — | | | | | | | | |
| 1705.11.E.1 | 31 | | 24 | M.925 | Close | X2 | >320 | Off | 2 Fwd | | | | | | | | |
| 1705.11.F.1 | 17 | | 37 | M.70 | Open | X2 | <160 | Off | 2 Fwd | | | | | | | | |
| 1705.11.G.1 | 17 | 361,000 lb GW 24.2% mac c.g. | 37 | M.70 | Close | X2 | <160 | Off | 2 Fwd | 0.1 | 0.3 | 0.5 | 1.0, .75, .75 | NO | 1.0/10. | δH = 3.05° 478 Sec/Dec | |
| 1705.11.H.1 | 18 | | 37 | M.775 | Open | X2 | <160 | Off | 2 Fwd | | | | | | | | |
| 1705.11.I.1 | 18 | | 37 | M.775 | Close | X2 | <160 | Off | 2 Fwd | | | | | | | | |
| 1705.11.J.1 | 19 | | 37 | M.85 | Open | X2 | <160 | On | 2 Fwd | | | | | | | | |
| 1705.11.J.2 | 19 | 361,000 lb GW 24.2% mac c.g. | 37 | M.85 | Open | X2 | <160 | On | | 0.1 | 0.3 | 0.5 | 1.0, .75, .75 | NO | 1.0/10. | 1.5 | δH = 3.05° 478 Sec/Dec |
| 1705.11.K.1 | 19 | | 37 | M.85 | Close | X2 | <160 | Off | 2 Fwd | | | | | | | | |

*F1-F3 = Quick Stops On Freq 1 Through Freq 3

5.1.3 Flutter Clearance.— Early flight tests indicated that the stabilizer loads were going to approach limit loads at a dynamic pressure level lower than predicted. Consequently, the flutter clearance envelope was modified as shown in Figure 60.

Tests were conducted up to $M_D = .95$ for the heavy fuel configuration. Specific flight test points for the heavy and minimum fuel conditions are shown in Figures 61 and 62 respectively.

Flutter characteristics at high Mach operations of the aircraft were checked by dives starting at approximately 11278 meters (37,000 ft) altitude (Conditions 1705.11.C and 1705.11.D of Table 18). Forward pilot-induced stick raps were used to excite the aircraft structural modes. The 1705.11.C dive followed the $M = .90$ curve. The 1705.11.D dive hit the $M = .95$ curve at 9754 meters (32,000 ft) altitude but not for the 8900 meter (29,200 ft) altitude point. A later dive did. No flutter indications were observed during any of the dives. Thus, the flight envelope, shown on Figure 61, is considered flutter free with and without the PACS engaged.

A series of tests were made to determine the PACS effect on the damping characteristics of certain aircraft structural modes. Engine-wing bending, fuselage bending, and first horizontal stabilizer bending modal frequencies were monitored. However, early flight test points showed the fuselage bending and stabilizer bending modes were highly damped. Therefore, a decision was made to eliminate those two frequencies from further testing and to track the 2.6-2.7 Hz engine-wing bending mode. Tests at various flight points showed no significant change in stability with the PACS on or off.

5.1.4 PACS Feedback Transfer Functions.— The pitch series servo was driven by the signal generator operating in a logarithmic sweep mode at a 500 second per decade rate to obtain transfer functions. Various outputs in the PACS system were monitored to provide transfer functions over the frequency range of interest. The feedback function was monitored, on line, by telemetering the feedback amplitude ratio signal in dB and phase of the PACS series servo command signal relative to the series servo kicker input signal (see Figure 63). Frequency sweeps were performed for five different flight points designated by (\diamond) in Figures 61 and 62. Final transfer functions were obtained post-flight by reducing flight tape data over the frequency range of interest. The feedback function is presented as a Feedback Amplitude Ratio Margin (FARM) plot (see Section 3.7.2 for more details on FARM plots). The plots were all done for two times nominal gain (6 dB increase) over nominal conditions. Results are presented in Figure 63 for a heavy and minimum fuel aircraft. Acceptable flutter gain and phase margins for a nominal gain system are shown in each of the plots. This margin is based on a 6 dB gain margin or phase relationship which provides for unannounced failures of system components which may increase the gain or change the phase of the system. A comparison of Figures 63a through 63c (heavy fuel) for increasing altitude and Mach number shows a slightly decreasing flutter margin trend for the lower frequencies.

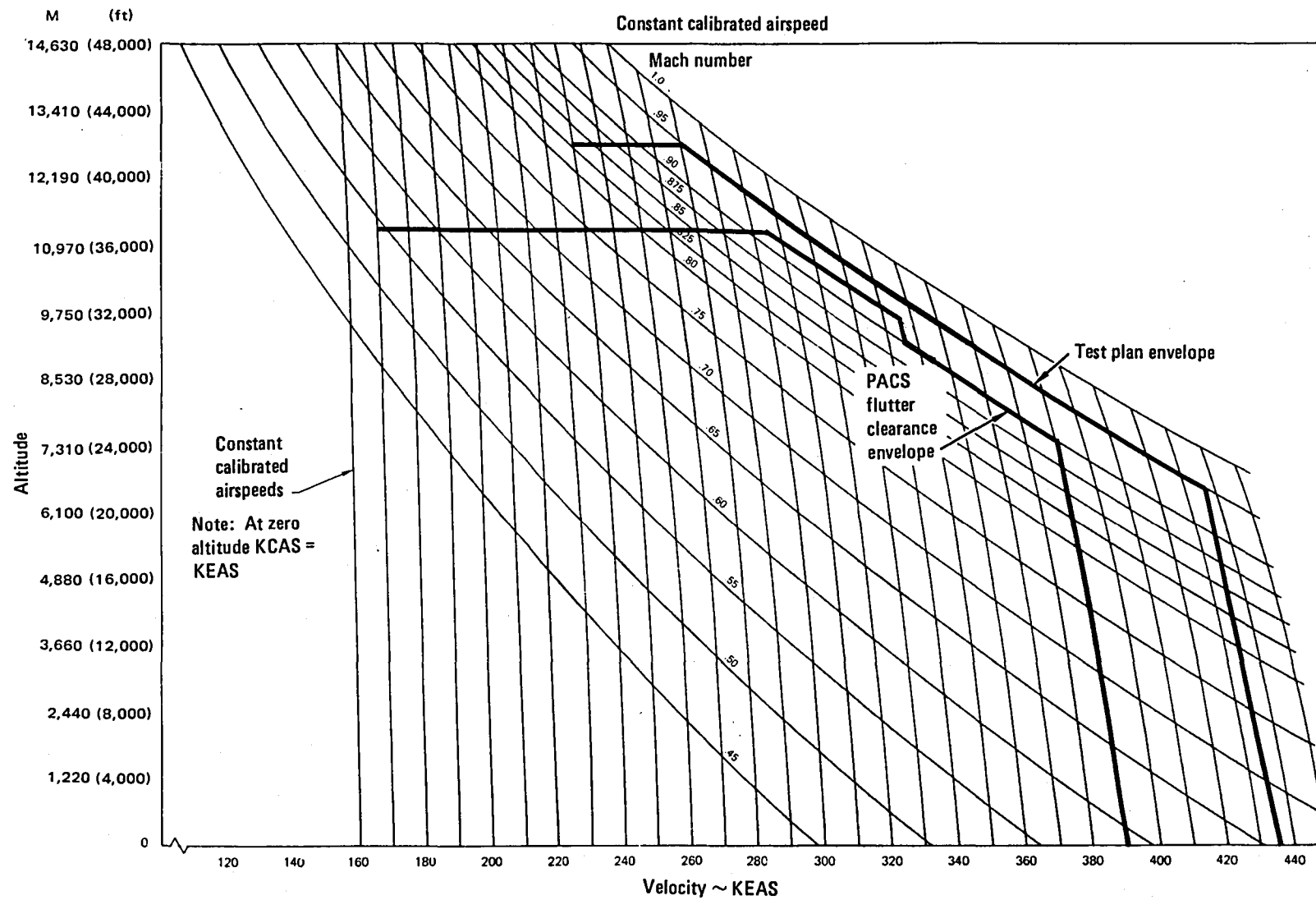
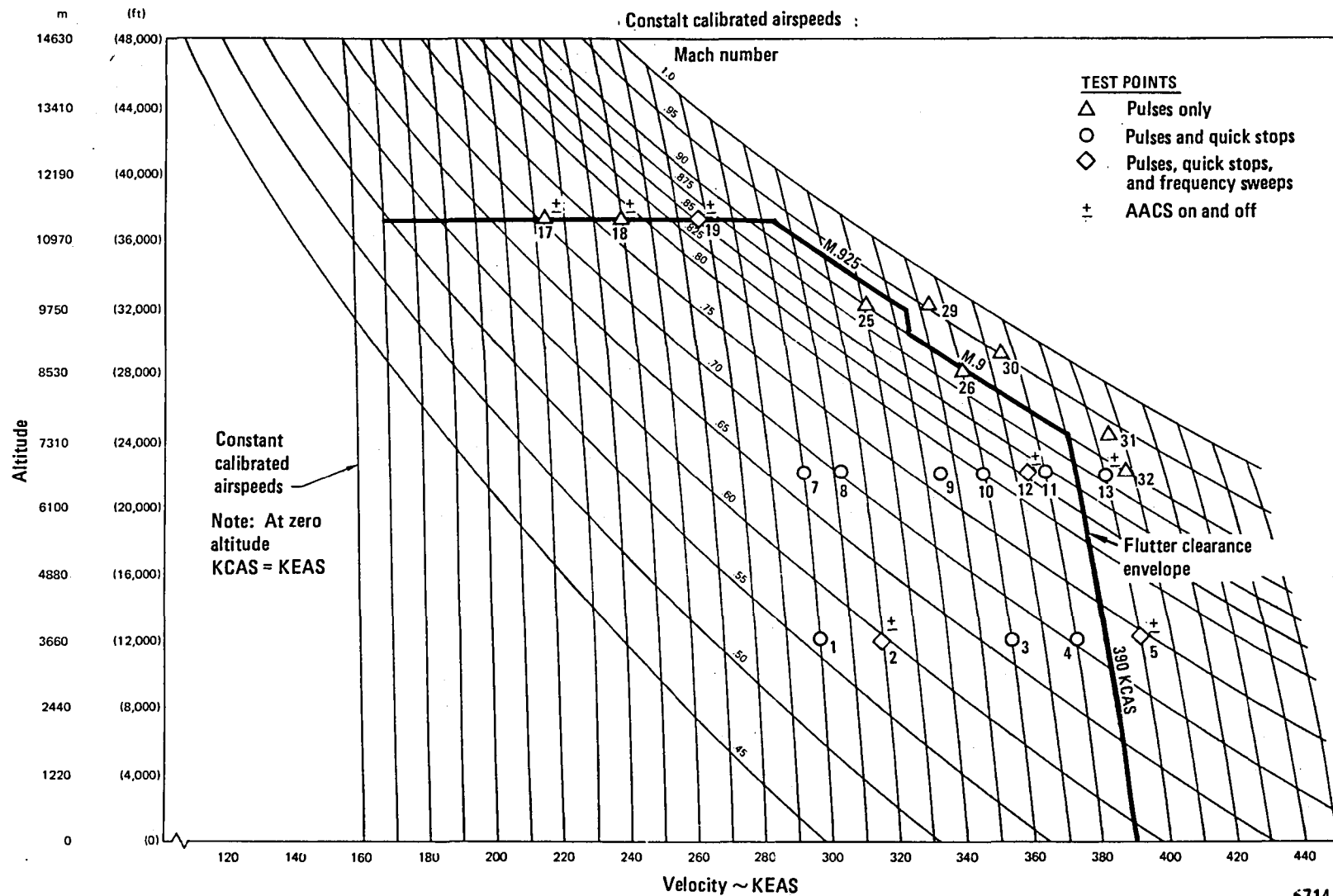
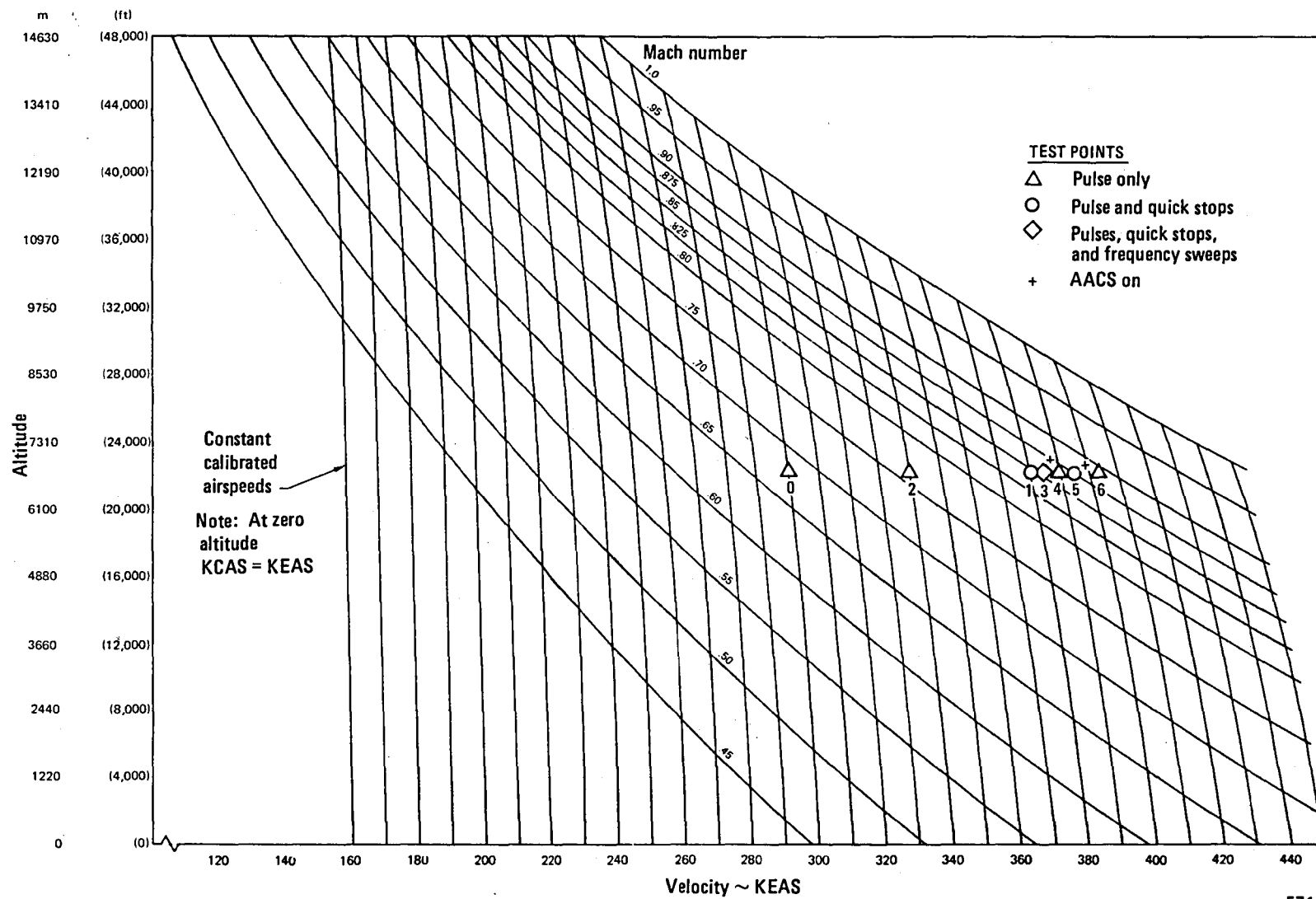


Figure 60. - PACS flight flutter clearance envelope.



5714

Figure 61. - PACS flight flutter test points for heavy fuel condition.



5714

Figure 62. - Flight flutter test points for minimum fuel condition.

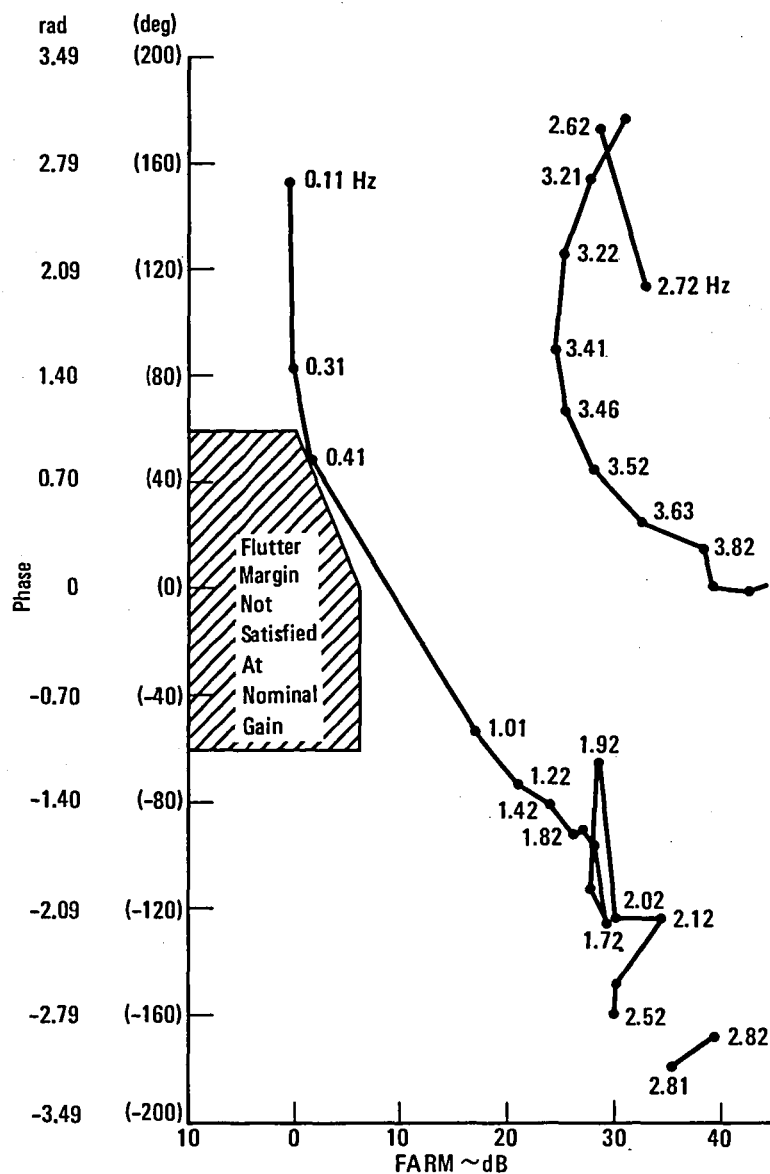


Figure 63a. - FARM plot for heavy fuel aircraft at 3658 meter (12,000 ft.) altitude at M = .74 (2x nominal gain).

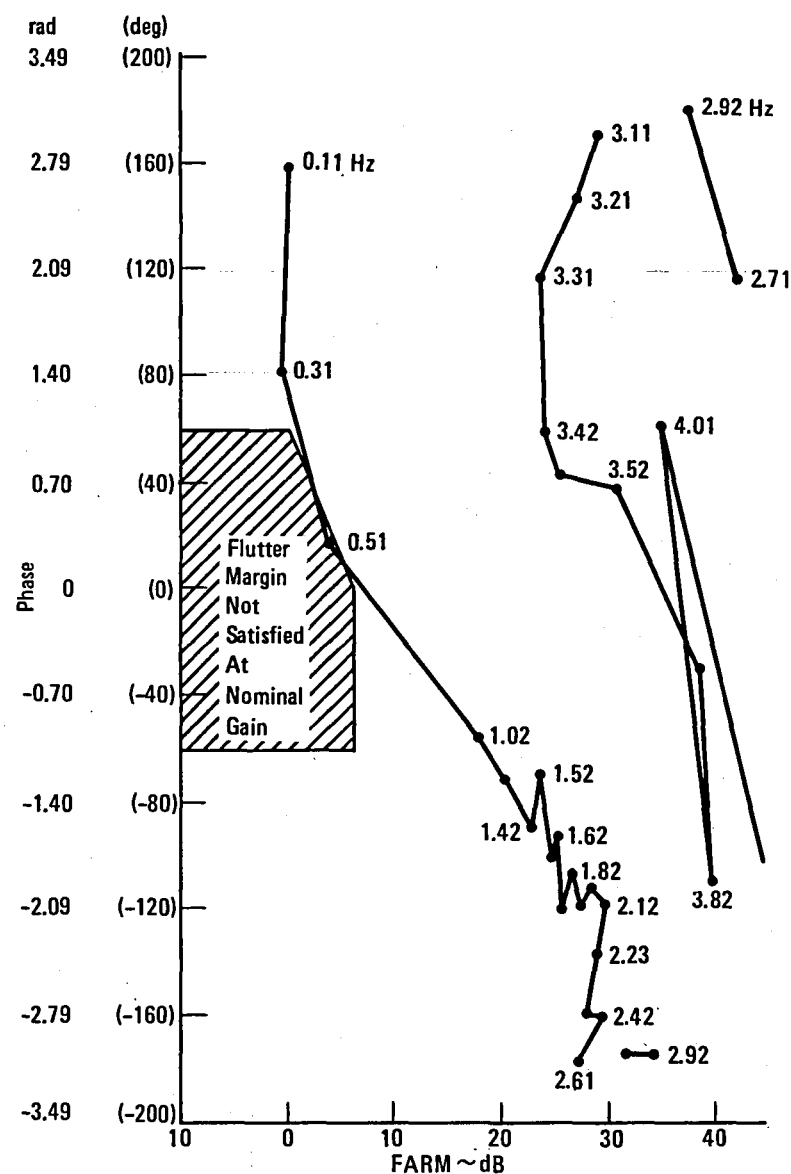


Figure 63b. - FARM plot for heavy fuel aircraft at 6706 meter (22,000 ft.) altitude at M = .83 (2x nominal gain).

5714

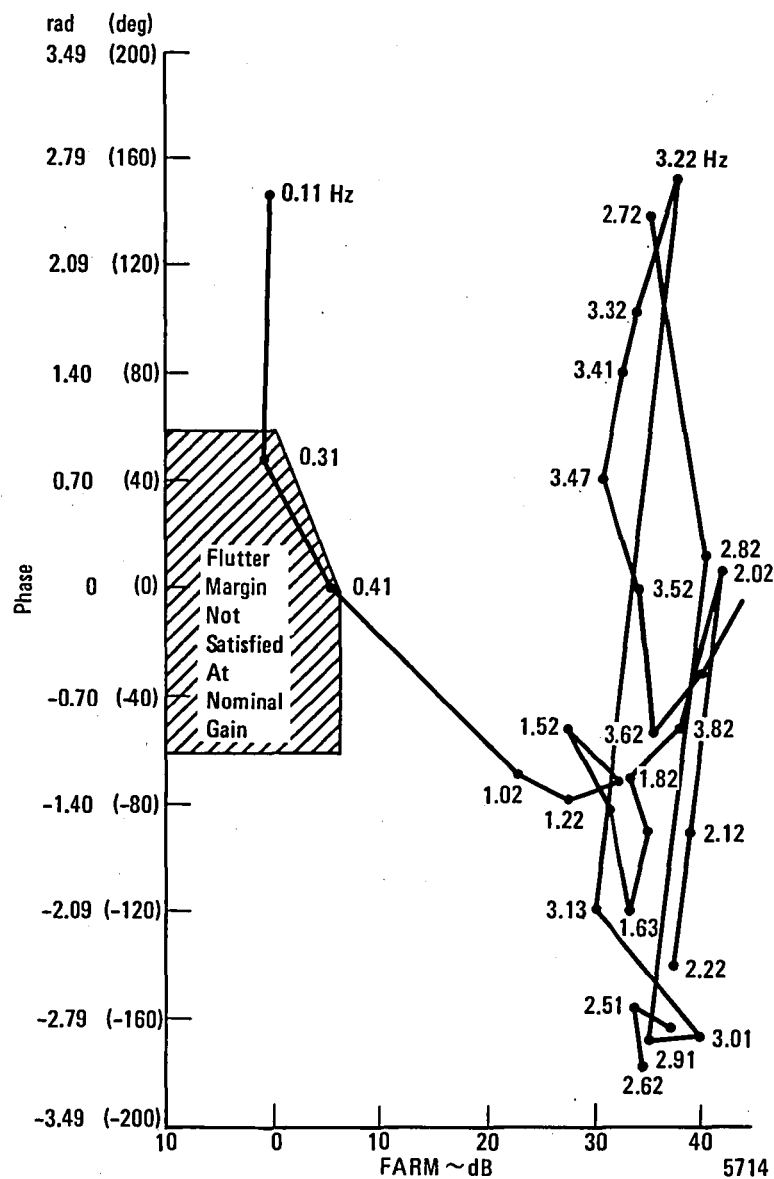


Figure 63c. - FARM plot for heavy fuel aircraft at 11278 meter (37,000 ft.) altitude at M = .85 (2x nominal gain).

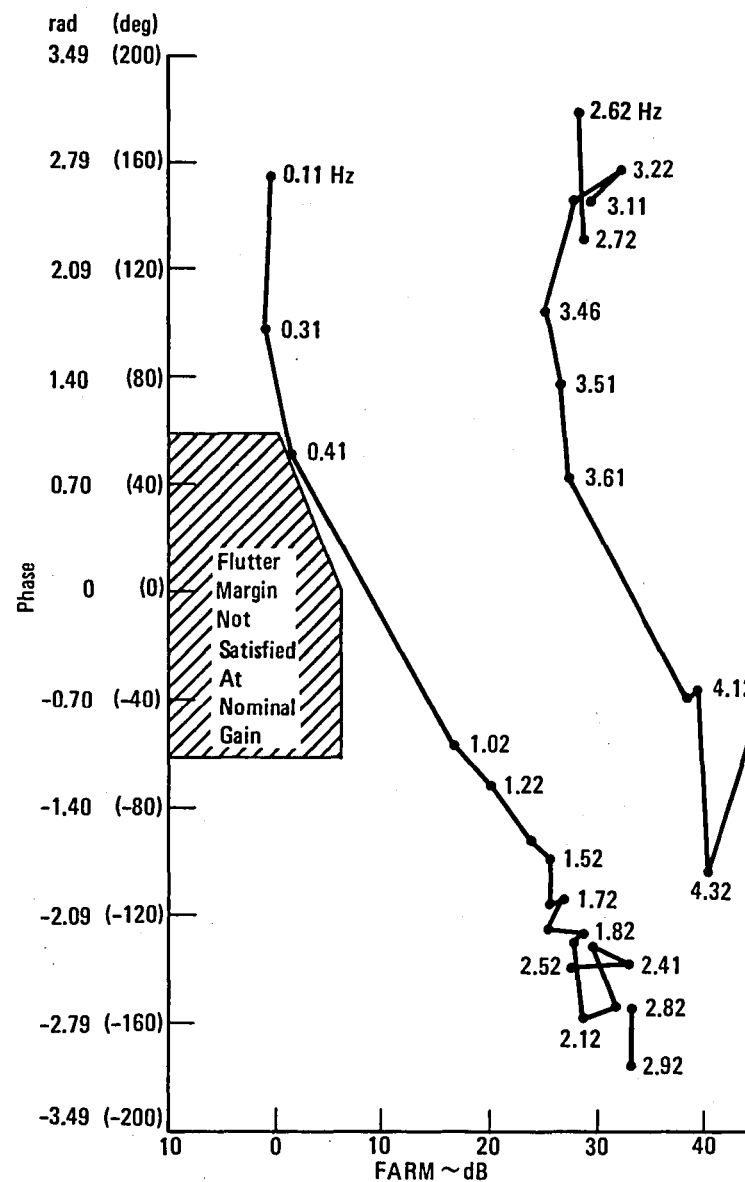


Figure 63d. - FARM plot for minimum fuel aircraft at 6706 meter (22,000 ft.) altitude at M = .87 (2x nominal gain).

The amplitude margin plot in Figure 63c is within the crosshatched flutter margin area. However, since the data are for two times nominal gain, the nominal gain flutter margin criteria were easily satisfied. Further, analytical results for the high altitude, high mach condition (11278 meters at Mach .925) show the aircraft to be flutter free. Figure 63d shows the flutter margin to be satisfied for the minimum fuel aircraft at the given flight condition. Partial loops in the FARM plots like the one shown in Figure 63a from 3 to 4 Hertz are feedback responses obtained for the flexible structural modes of the aircraft. The modal response levels always showed 24 dB or more of gain margin, indicating ample stability for the flexible structural modes in conjunction with the PACS system.

5.1.5 Conclusion.- Analytical flutter analysis reported in Section 3.7 showed the aircraft to be insensitive to c.g. location within the allowable structural limitation operating range. Therefore, with good correlation of analytical and experimental results and the successful demonstration of flutter margin for the mid range c.g. configuration, the aircraft has flutter clearance for its full gross weight/center of gravity envelope as shown in Figure 48.

5.2 Handling Qualities

The near-term PACS handling qualities demonstration flight testing was accomplished in approximately 30 flight hours.

The aircraft test configurations were:

- Basic aircraft (PACS Off)
- PACS with pitch rate damper only
- PACS with pitch rate damper and feed-forward command
- PACS with pitch rate damper and washed-out feed-forward command

These PACS configurations were considered to be the best of those evaluated in the Visual Flight Simulator (VFS) and the Vehicle Systems Simulator (VSS). The feed-forward command counteracts part of the increased maneuvering force generated by the pitch rate damper. The washed-out feed-forward command reduces the initial maneuvering force and retains higher forces during long term maneuvers.

5.2.1 Handling Qualities Tests.- Three Engineering Flight Test Pilots participated in the handling qualities evaluations.

5.2.1.1 Build-Up to aft c.g.: The near-term PACS design goal criteria required that the aircraft handling qualities with the c.g. at 39% mac be equivalent to those of the basic aircraft with the c.g. at 25% mac. Therefore, the flight testing was initiated with the c.g. at 25% mac to allow the pilots to evaluate handling qualities of each PACS configured with those of the baseline aircraft. The c.g. was then moved to 35% mac (the most aft c.g. for which the standard L-1011 aircraft is currently certified) and the PACS evaluation process was repeated. The 25% and 35% mac tests provided the pilots with sufficient confidence to perform PACS evaluation tests at 37% and 39% mac. Tests at each c.g. location were always initiated for the basic aircraft configuration with the AACS on so that the pilot could evaluate the most unstable configuration first.

5.2.1.2 Flight conditions: The flight conditions selected for flight testing are given in Table 19.

TABLE 19. - FLIGHT TEST CONDITIONS

| FLIGHT CONDITION | SPEED | ALTITUDE OR W/δ |
|---|----------|--|
| 10 Cruise | M.83 | $.64 \times 10^6$ kg (1.4×10^6 lb) W/δ |
| 15 Cruise | M.83 | $.73 \times 10^6$ kg (1.6×10^6 lb) W/δ |
| 16 V_{MO}/M_{MO} | 370 KCAS | 7620 m (25,000 ft) Alt. |
| 18 Landing ($\delta_F = .576$ rad, 33 deg) | 1.3 VS | Approach |
| 20 Cruise | M.83 | $.77 \times 10^6$ kg (1.7×10^6 lb) W/δ |

Tests 10, 15, and 20 in the table are Mach .83 cruise conditions, test 16 represents a high speed flight condition, and test 18 is the landing condition. The cruise conditions selected were those where the PACS provided the biggest payoff.

The cruise and high speed tests were primarily wind-up turns to buffet onset or 1.8g to evaluate maneuvering longitudinal stability (F_g/g), and control column displacements and releases to evaluate short period dynamic stability. The landing condition evaluation was an assessment of glide slope and localizer tracking with PACS on and off.

Aircraft trimmability was evaluated while setting up the F_g/g tests. General handling characteristics were evaluated during and between defined tasks. PACS operation in turbulence was evaluated during the few instances when turbulence was encountered.

5.2.2 Handling Qualities Test Results.- The test data were analyzed to assess the effect of PACS operations on maneuvering longitudinal stability, longitudinal short period response, trimmability, flight in turbulence, and landing approach. The overall pilot ratings were presented in terms of the Cooper-Harper rating scale for the aircraft with PACS on and off.

5.2.2.1 Maneuver longitudinal stability: Windup turns were performed for the Mach .83 cruise and high speed flight conditions to evaluate the PACS maneuver characteristics. Time histories of the windup turns were analyzed to determine the aircraft stability at specific load factors. A typical result of the analysis is given in Figure 64.

The plots shown are for a flight condition with the AACS on and c.g. at 39% mac. The top plot shows the stabilizer position as a function of load factor (c.g. normal acceleration, g's). The lower three plots show stick force as a function of load factor for the three PACS configurations tested. Test data is shown for three test runs as indicated by the symbols. Dashed lines represent predictions made by using the aerodynamic and control system models programmed in the VFS.

Some of the differences in predictions and test data are due to lack of the prediction model for a true representation of the control system and flight conditions. The predicted stick forces do not include control system friction or an 8.9 N (21 lb) detent spring force that centers the control column. The prediction for the PACS with pitch rate damper and washed-out feed-forward was made with the feed-forward not washed out. The wash-out force was neglected because the wash-out depends upon the rate (an unknown factor) in which the windup turn is entered.

Figure 64 shows that the elevator deflection and the stick force gradient for each PACS configuration increases linearly up to a load factor of 1.4g. Above 1.4g less stabilizer angle is required to maintain a specific load factor. Consequently, the stick force gradient is reversed until a load factor of about 1.7g is reached. The capability of each PACS configuration to compensate for the stick force reversal (non-linearity) was evaluated for load factors to buffet onset or 1.8g.

The stick force for the PACS off (basic aircraft) configuration is shown in Figure 64 to have a light force gradient which peaks at 58 N (13 lbs) at 1.4 g above which the gradient is reversed. Indications are that the stick force will be reversed (a push force) beyond buffet onset. The stick force for the PACS with pitch rate damping shows the force gradient to be about double that of the PACS off force gradient. Although the force gradient reverses when the 1.4g load factor is attained, the stick force remains a pull force. The stick force for the PACS configuration with pitch rate damping and washed-out feed-forward had a force gradient similar to the PACS with pitch rate damping only, but improved force characteristics were observed in the non-linear region.

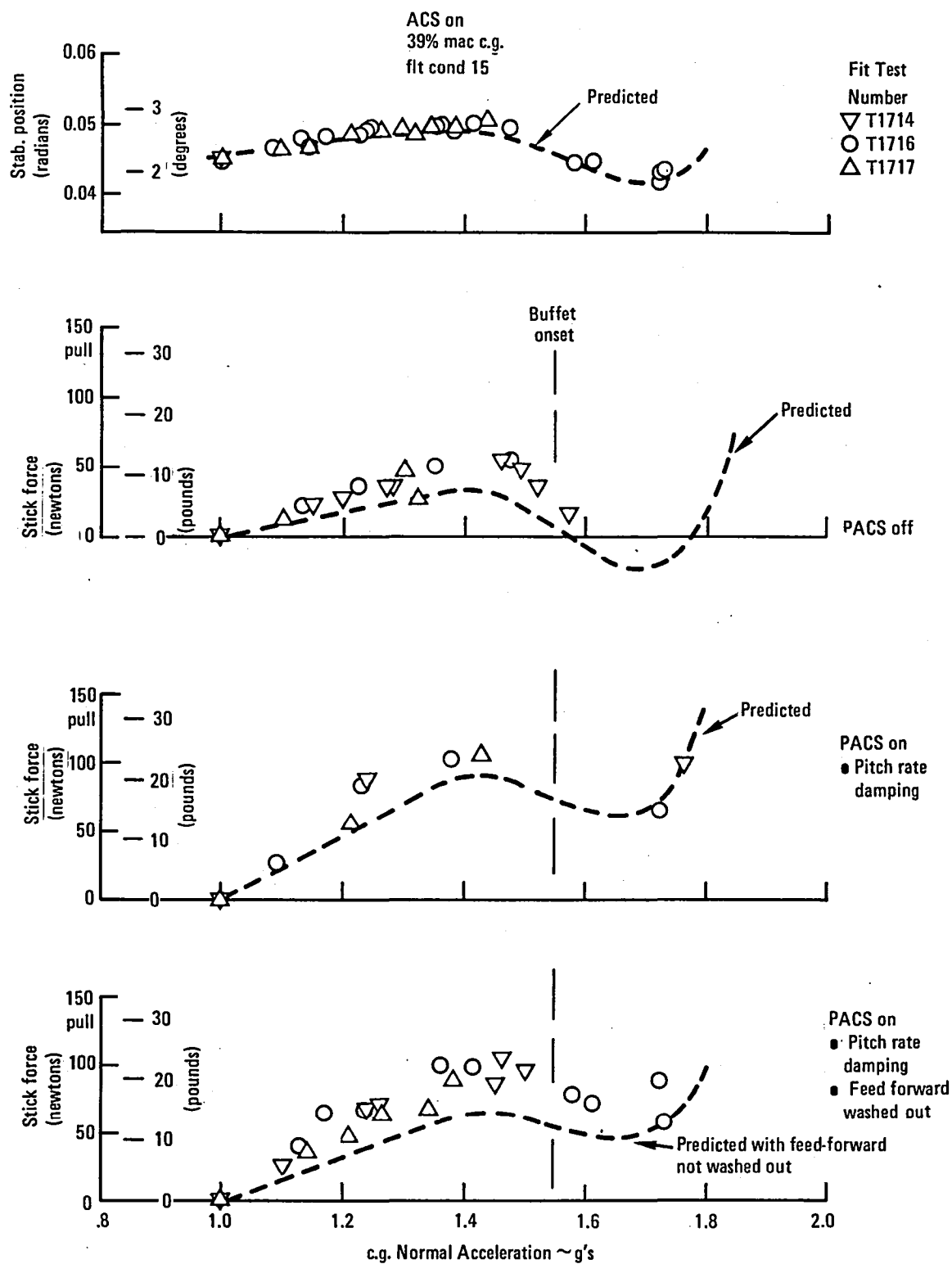


Figure 64. - Maneuvering characteristics, flight condition 15,
c.g. = 39% mac, AACS on

The pilots selected the PACS configuration with pitch rate damping and washed-out feed-forward to be the best. The configuration with pitch rate damping only was objectional because the stick forces were higher than desired. The PACS configuration with pitch damping and feed-forward (not shown in Figure 64) was rated second best.

5.2.2.2 Longitudinal short period response: The time histories selected for illustrating the damping response characteristics with PACS off and on are compared in Figure 65. The plots are for flight condition 15 with c.g. at 39% and the AACS active.

A stick pulse (F_s) was used to produce a pullup that resulted in an aircraft center-of-gravity acceleration ($N_{z_{c.g.}}$) of approximately 1.35g. Aircraft response was evaluated by observing the rate at which the aircraft returned to 1g and the characteristics of the pitch attitude (θ). Figure 65 shows that with the PACS off the aircraft exhibits a slow return to 1g and the pitch attitude is gradually increased. With the PACS on the return to 1g quickens and the pitch attitude is damped with one small overshoot.

While the test conditions for PACS off and on were similar, they were not exactly the same. This is shown on the right side of the figure. Slight differences in time histories of stabilizer angle (δ_H), aircraft pitch rate ($\dot{\theta}$), calibrated air speed (KCAS), and Mach number (M) are shown in Figure 65. These small differences are considered to be negligible for evaluation of the PACS characteristics.

5.2.2.3 Trimmability: Dedicated tests were not conducted to evaluate effect of the PACS on trimmability of the aircraft. However, this characteristic was judged by the length of time required to trim the aircraft for a specific flight condition prior to initiating a PACS evaluation test. Aft c.g. movement toward the neutral point, activation of the AACS, and turbulence contributed to noticeable degradation of the trimmability of the basic aircraft. All three pilots reported that engagement of the PACS improved the trimmability.

5.2.2.4 Flight in turbulence: Dedicated tests were not devoted to PACS evaluation for turbulent conditions. However, light turbulence was encountered several times during the flight test program. On those occasions the PACS was cycled on and off to evaluate its effect. The pilots reported that the handling qualities were improved when the PACS was active (see Table 20).

5.2.2.5 Landing approach: The PACS configuration with pitch damper and washed-out feed-forward was evaluated for manual control approaches down to 61m (200 ft) altitude above ground level. Most of the approaches were flown with the spoiler direct lift control (DCL) and AACS activated.

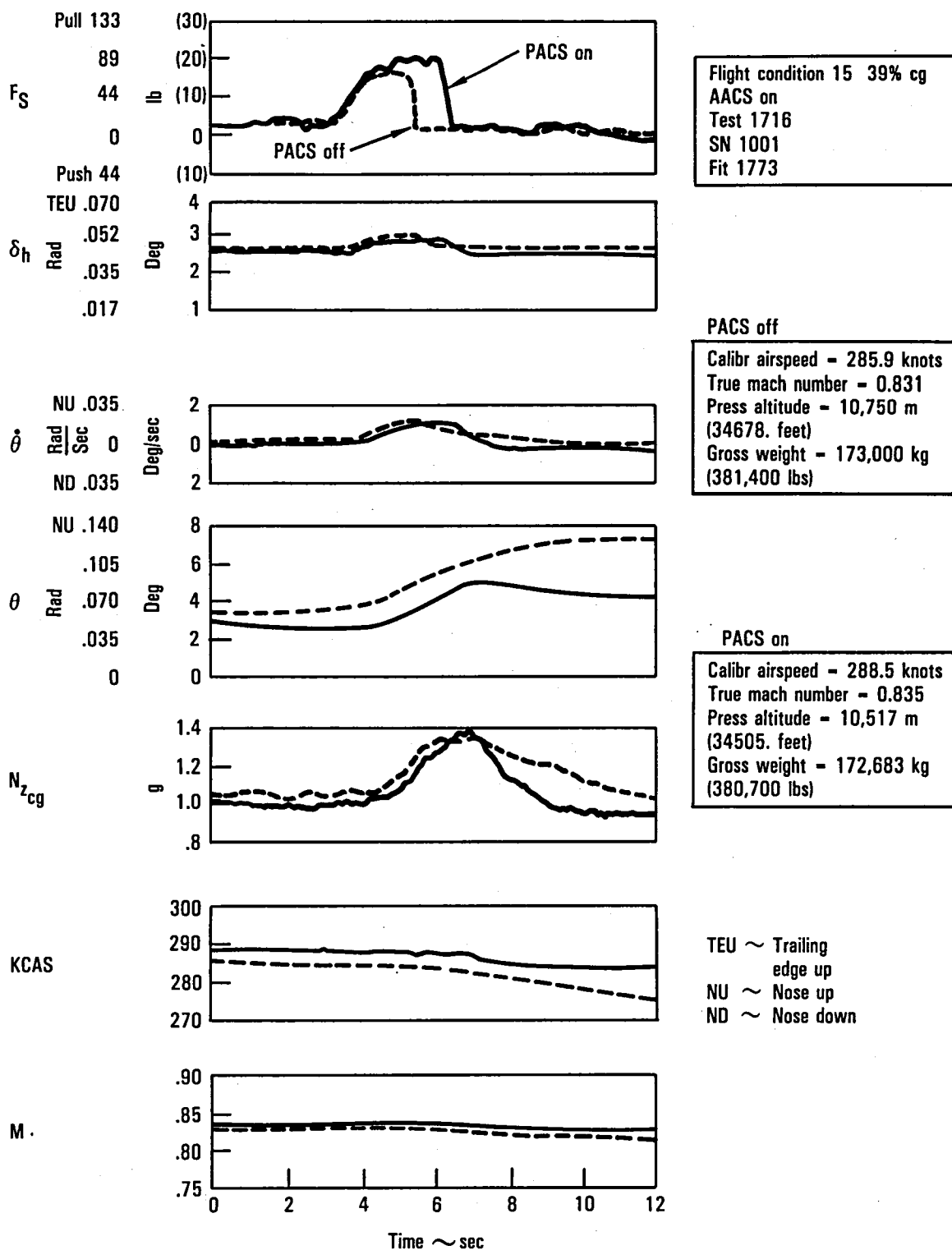


Figure 65. - Comparison of damping response characteristics, PACS off and on.

TABLE 20. - PILOT COMMENTS ON PACS OPERATION IN TURBULENCE

| FLIGHT CONDITION | c.g. % mac | PILOT COMMENTS |
|-----------------------------|------------|---|
| 250 KCAS/3962 m (13,000 ft) | 37% | The basic airplane doesn't feel good in turbulence. |
| Climb/9144 m (30,000 ft) | 35% | PACS really makes the airplane stiffer. |
| FC 15 | 39% | Does not require excessive pilot attention to fly in light turbulence with PACS on. |
| Cruise | 35% to 39% | Turbulence really aggravates trim with PACS off. |
| FC 10 | 37% | Basic airplane flyable in light turbulence but requires attention. |

Tests included tracking of the glideslope and localizer, and recapture of the glideslope beam. Approaches were flown with the PACS continuously engaged and with the PACS cycled on and off.

Benefits of the PACS during the landing approach were inconclusive. One pilot reported that the PACS significantly improved handling of the aircraft for each c.g. configuration. The other two pilots said that the PACS enhanced handling to a degree but the benefit diminished as the c.g. moved aft until there was no difference between the PACS on or off with the c.g. at 39% mac. The winds were calm during the evaluations with c.g. at 39% and PACS effects might have been more apparent in gusty conditions. However, the VFS tests showed only a small improvement in landing handling qualities with the PACS active.

5.2.2.6 Pilot ratings: The pilots provided Cooper-Harper ratings to express their opinion of the aircraft handling qualities with and without the PACS engaged. The PACS with pitch rate damper and washed-out feed-forward was selected as the best configuration. Pilot ratings for this preferred configuration are given for each of the pilots in Figure 66 for flight conditions 10, 15, and 16 with the AACS active. For each condition the rating with the c.g. at 39% and PACS on is shown to be equivalent to the rating with the c.g. at 25% and PACS off.

In order to assess the validity of the VFS for evaluation of a PACS, the average pilot ratings for the VFS tests and flight tests are plotted in Figure 67. The VFS ratings for the basic aircraft (PACS off) were better than the flight test ratings. For the PACS on configuration the VFS ratings were relatively flat over the c.g. range whereas the flight test ratings showed a slight increase as the c.g. was moved aft. In general the spread between VFS and flight test ratings did not exceed a value of 1.

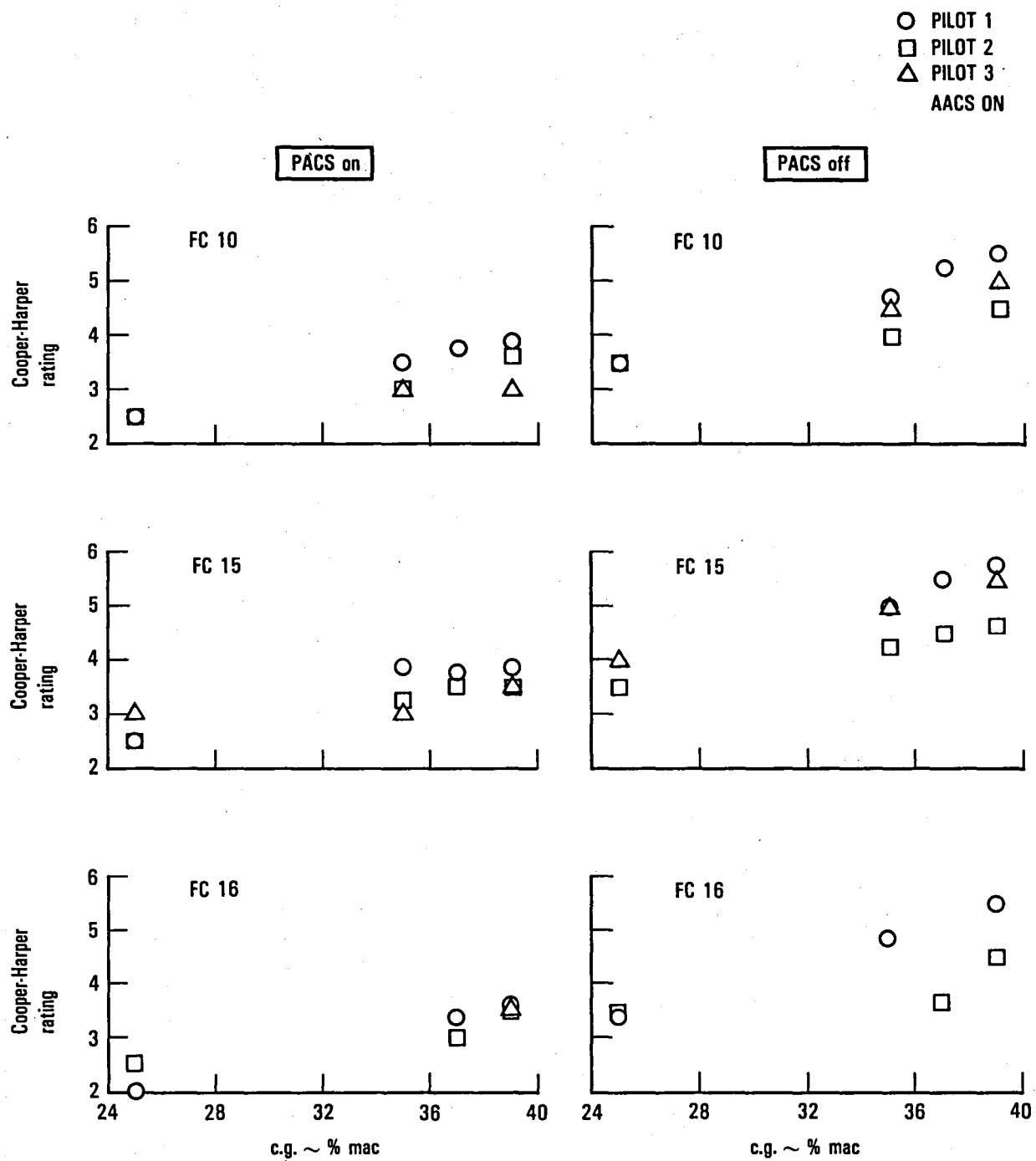


Figure 66. - Pilot Cooper-Harper ratings.

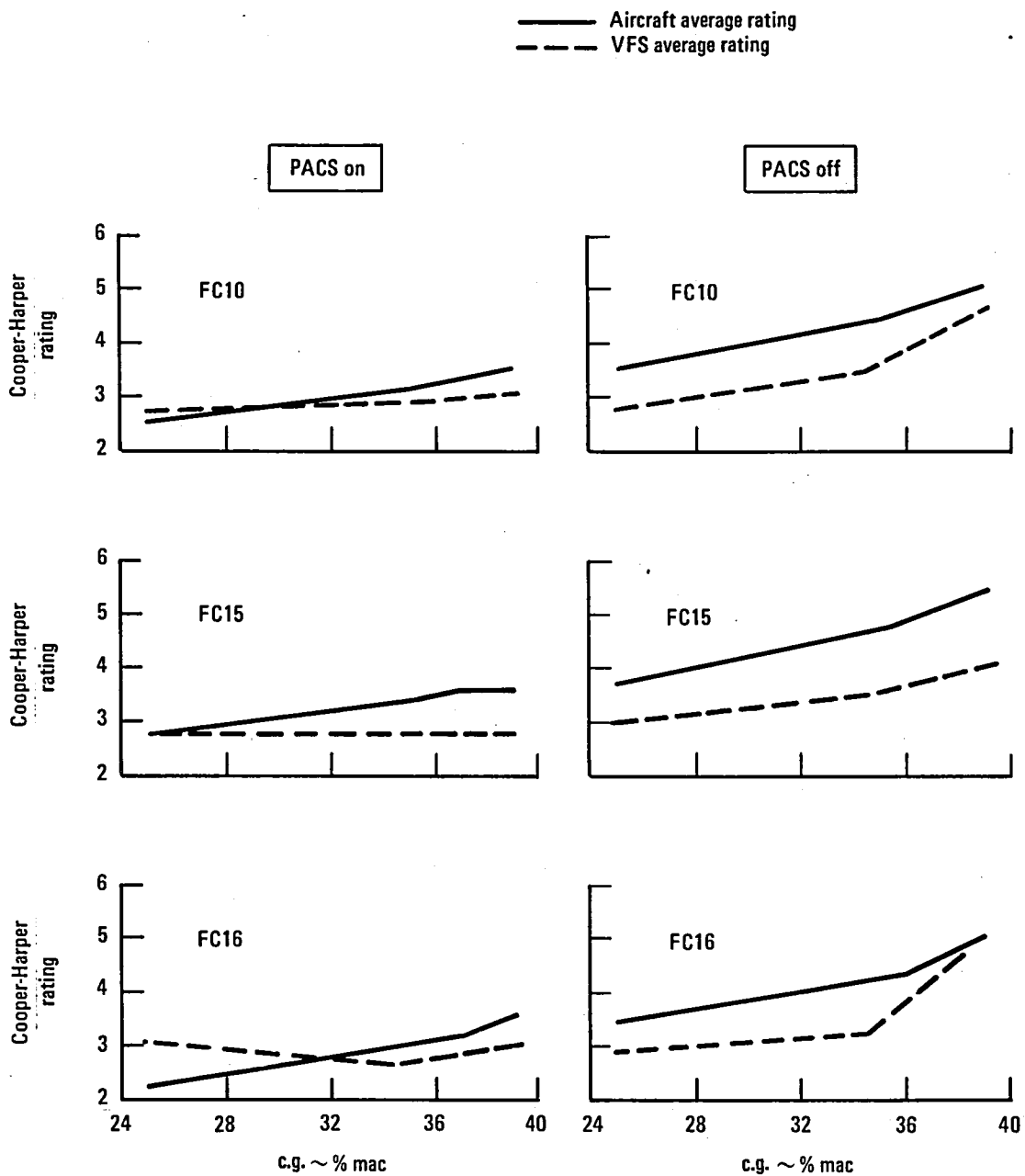


Figure 67. - VFS ratings compared to S/N1001, AACS on.

5.2.2.7 Conclusions: The flight tests demonstrated that the PACS significantly enhanced the aircraft flying qualities for Mach .83 cruise and high speed flight conditions over the c.g. range from 25% to 39% mac. For these conditions the handling qualities with the PACS on and the c.g. at 39% mac were shown to be equivalent to those of the basic aircraft with the c.g. at 25%. Thus, the PACS capabilities met the design objective. The preferred PACS configuration consisted of a pitch damper and washed-out feed-forward. PACS benefits for the landing approach were inconclusive. Additional testing is required to fully explore the effect of the PACS during the landing approach.

6. CONCLUSIONS AND RECOMMENDATIONS

Analysis and tests performed as part of previous programs indicate that c.g. management can be used to achieve 2% fuel savings for aircraft with current wing configurations and 4% fuel savings for aircraft with advanced technology wings. However, the c.g. must be moved aft which results in a reduction of static stability margins and a corresponding degradation of handling qualities.

This program has demonstrated that for linear stability flight conditions a pitch active control system (PACS) can be designed for a wide-body jet transport which maintains good handling qualities while the static stability margin is reduced from +15% to +1% mac. This technology could now be applied to current aircraft to achieve 2% fuel savings provided that other control systems provide the necessary control for nonlinear stability conditions.

Subsequent steps to be taken in development of a PACS are to provide control for nonlinear stability conditions, for flight at negative static stability margins (e.g. to -10% mac), and for gust load alleviation. The 10% mac negative static stability is required in order to achieve the 4% fuel savings for an aircraft equipped with advanced technology wing configurations. Operation at the negative relaxed static stability margins requires a high reliability PACS. Hardware failures must be extremely improbable for operation in adverse environments (e.g. lightning strikes) and for long periods of time under commercial airline operating conditions.

The path of technology development for a PACS that can be implemented on a future generation aircraft with advanced wing technology requires continued development and flight test of an advanced PACS along with a design and analysis study to provide the system architecture and component reliability necessary to make hazardous failures extremely improbable.

APPENDIX A FUEL SAVINGS

Reductions in fuel consumption by moving the aircraft center of gravity aft are highly dependent on the wing configuration. The potential benefits to be gained for a current technology (e.g. L-1011) and an advanced technology wing are 2 and 4% respectively as shown in Figure 68.

The 2% fuel savings for the current technology wing are based on analysis, wind tunnel tests, and flight test results for the L-1011. The circle on the current wing curve represents a reference normal cruise (25% mac) c.g. location for the L-1011-1 aircraft. The neutral point on an L-1011 is near 40% mac. Consequently, the static stability margin is normally 15%. By moving the c.g. aft to the point designated by the rectangle (35% mac), the stability margin is reduced to 5% mac and 2% fuel savings are achieved. Further aft movement of the c.g. results in increased fuel consumption. The current wing curve shown is a typical result and the shape of the curve is a function of lift coefficient.

The upper curve in Figure 68 shows that aft movement of the c.g. for the advanced wing can result in up to 4% fuel savings. This 4% is in addition to approximately 10% that is associated with the advanced wing relative to a current wing. However, the point on the advanced wing curve represented by

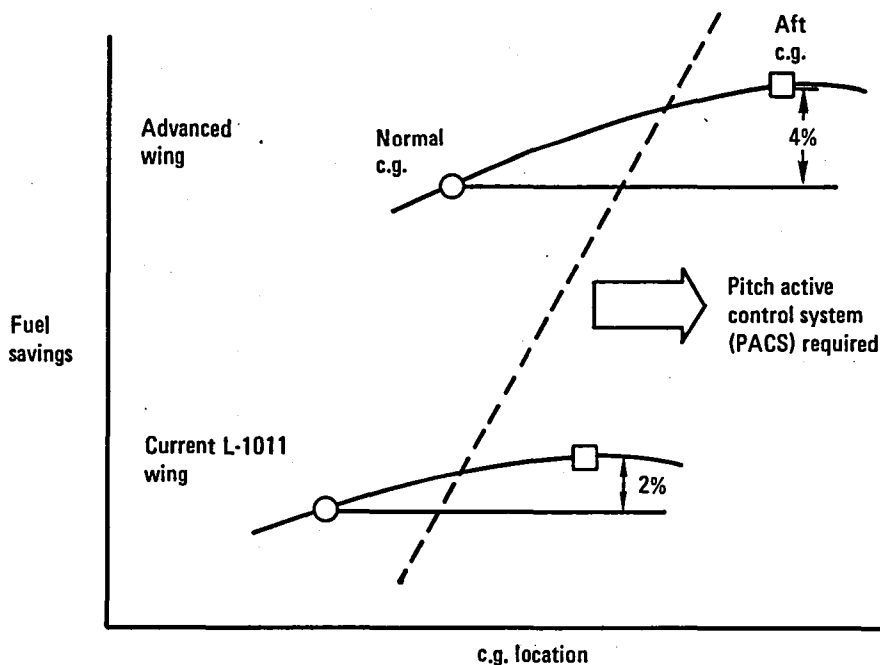


Figure 68. - Potential fuel savings for aft c.g. locations.

the rectangle corresponds to a negative stability margin of approximately 10% mac. The advanced wing curve is based on aerodynamic analysis and wind tunnel data cruise efficiency measurements. Additional advanced design studies are required for a specific aircraft configuration with a given flight profile to determine exact fuel savings as a function of c.g.

The dashed line in Figure 68 does not provide an exact c.g. location beyond which a pitch active control system is required. However, it does indicate that as the static stability is relaxed a PACS is required. This requirement is dependent on the wing design and controls provided on an aircraft for high W/δ flight conditions.

APPENDIX B DOWNRIGGED ELEVATOR MODIFICATIONS

The L-1011 elevator travel was designed to have normal travel of twenty-five degrees up and zero degrees down during flight. With the PACS installation, the elevator travel limits had to be modified to twenty degrees up and five degrees down (Figure 4).

B.1 Elevator Drive System

Changes made to allow the drive system to function properly were:

- The elevator push rod was shortened to lower the trailing edge of the elevator with respect to the stabilizer.
- The elevator fairings were modified to clear the elevator push rod and to clear any structural interference.
- Since the hinge moment reacted by the return cable of the drive system increased, the system was structurally analyzed for the increased loads.

B.2 Counterbalance Arms

The counterweights for static balance of the elevator are installed at the end of arms extending forward of the hinge line as shown in Figure 69. New travel limits for the counterweights and arms resulted in interference with the upper skin structure of the horizontal stabilizer. Therefore, a design study was made to define the optimum solution to the problem. The following approaches were investigated as to feasibility.

- Upper skin to be reworked by adding external blisters in the areas of interference.
- Angular rotation of counterbalance arms through the use of shims at spar attach points.
- Rework of the arms by cutting and splicing the outer end of the arm deflected down to provide the necessary clearances.

Cutting and splicing of the arms (Figure 70) proved to be most effective in cost and schedule. The blister configuration was deemed unacceptable because of the airflow distortion, and shimming of the arm attachment proved not feasible since elongated attach holes would result. Thirteen pairs of arms on each elevator had to be modified, and of these the outer four pairs were replaced by new machined parts. This was necessary because the width of the arms was too narrow to permit splicing without fabricating expensive

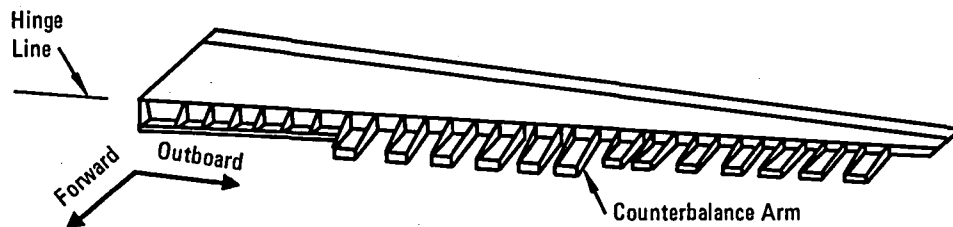
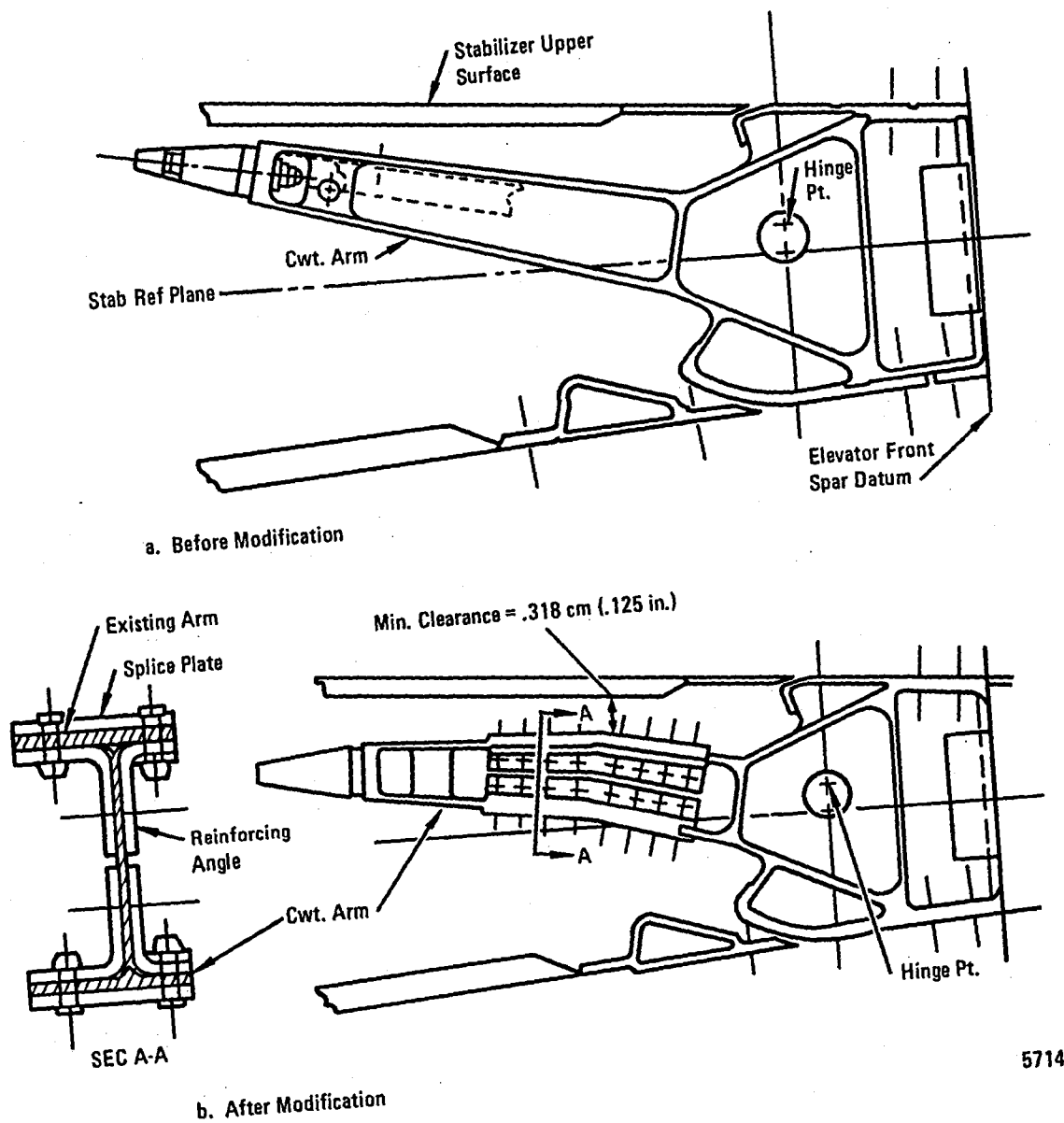


Figure 69. - Isometric view of elevator.

machined parts. Thus, the cost of developing the splice component exceeded the cost of machining new fittings. Figure 70 shows the counterbalance arms before and after modification.

B.3 Spare Elevator Refurbishment

Modification of the flight test aircraft elevators would have required grounding of the aircraft for a period of eleven weeks. This time span was considered excessive and solutions were reviewed for reducing it. Records indicated that there was a spare set of elevators available. The spare set was recovered from storage and found to be in need of repair to restore it to an airworthy condition. Restoring the elevator required the replacement of four parts: two leading edge fairings and the two piece trailing edge. All other operations required on the spare elevators were identical to those required on the flight test aircraft elevators. The total costs of parts was \$25,000.00 with less than 100 manhours required for installation. The aircraft down time was reduced to four days. This was considered sufficient justification to modify and refurbish the spare set for the PACS flight tests. Additionally, use of the spare counterbalance arms as patterns for machining of the outboard arms reduced the fabrication manhours.



5714

Figure 70. - Counter balance arms before and after modification.

APPENDIX C

C. G. MANAGEMENT SYSTEM

C.1 Design Criteria

The choice of a water-ballast c.g. management system was a natural one since 907 kg (2000 lb) capacity water tanks, water transfer pumps and motors used in the L-1011-1 flight test development program were available.

Design criteria for the c.g. management system included:

- Flight test c.g. location requirements
- Flight safety requirements
- Test aircraft structural strength limitations

The principal c.g. location requirements were a 39% mac aft c.g. for PACS testing, and sufficient ballast transfer capability to provide normal flight and on-the-ground/landing c.g. locations within the established weight c.g. envelope. Assurance that normal c.g. location could always be restored in flight was the major safety requirement. Inclusion of an emergency dump system for all water ballast provided this assurance. Other safety features were: water tank differential pressure vent tubes with negative-g stop valves, three system pressure relief valves, manual override on transfer and dump valves, double float switches to prevent over-filling tanks, and sight tube gages to visually monitor tank water levels. Capability of the entire c.g. management system and associated attachment structure to withstand adequate emergency landing load factors was an additional safety requirement. Ballast distribution was constrained by the existing structural strength limitations of the flight test aircraft. These limitations are expressed as allowable passenger and cargo compartment floor loadings in the L-1011-1 structural design loads criteria report.

C.2 System Description

The c.g. management system is shown in Figure 5. System ballast consisted of the following components:

- Fixed lead or steel ballast located in aft passenger cabin area, and aft cargo compartment.
- Fixed (non-transferable) water ballast in seven 1003 liter (265 gallon) tanks located in aft passenger cabin: each tank limited to 816 kg (1800 lb) of water due to floor loading limits.

- Transferable water ballast in eight 1003 liter (265 gallon) tanks in both forward and center cargo compartments: each tank limit was 907 kg (2000 lb).

A diagram of the water ballast system is shown in Figure 71. The fixed water ballast in the aft passenger cabin consists of seven tanks as shown in the upper left part of the figure. Water is put in these tanks through a 7.62 cm (3 in) fill valve. The valves marked DV-2A and DV-2B are used to dump water overboard at 907 kg/min (2000 lb/min) in case of an emergency.

The transferable water ballast system consists of sixteen water tanks, two water pumps, four control valves (CV-1A, 1B, 1A, 1B) and two dump valves (DV-1A, 1B) as shown in the lower part of the figure. A second 7.62 cm (3 in) fill valve is used for these tanks.

A sketch of a typical water tank is shown in the top center part of Figure 71. As indicated, features of the tanks include:

- 1.9 cm (.75 in) tygon sight tube to visually check water level
- Vent tube to prevent differential pressure buildup
- Negative-g valve to prevent water loss in negative-g flight conditions
- Full and empty float switches to signal tank level and actuate water control valves
- Inlet diffuser to prevent inlet water from activating float switches

C.3 System Operation

The water ballast system is electrically controlled from a single control panel at the Weight Engineer's Station located just aft of the flight station on the left side of the aircraft.

The control panel has switches to operate flow control valves, water pumps, and emergency dump valves. The panel is equipped with indicator lights to show:

- Power to relays
- Condition of the 23 water tanks (full or empty)
- Position of the dump valves (open or closed)

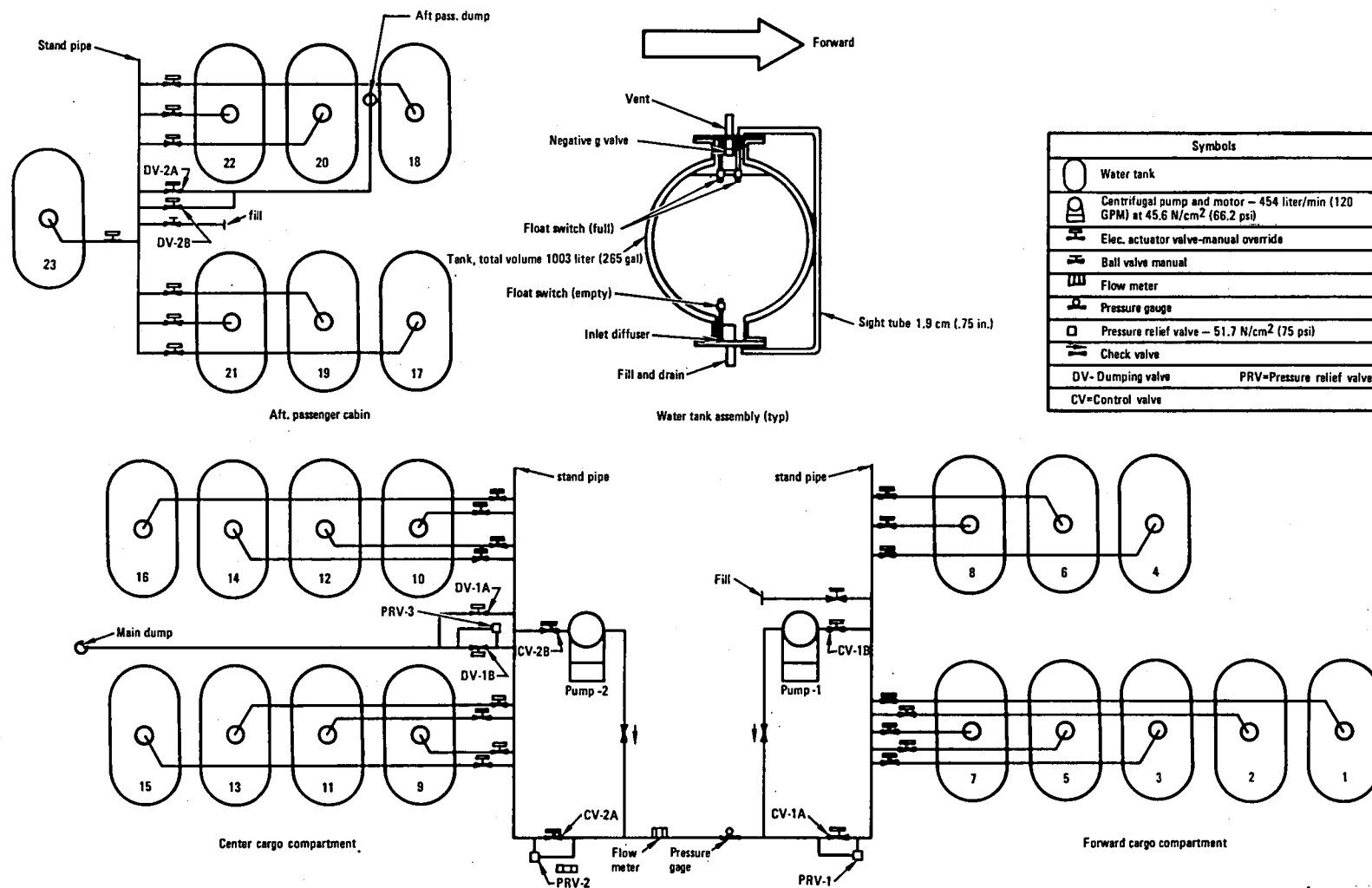


Figure 71. - Water ballast system.

A flow meter provides a visual display of water transfer between forward and center cargo compartment tanks.

Control relays are housed in three relay boxes. Two of these boxes provide control for the transferable water ballast system. One of these boxes, located in the forward cargo compartment, provides control of the following system components:

- Eight water tank valves located in the forward cargo compartment
- The P-1 (forward) water pump motor control
- Flow control valves CV-1A and CV-1B

The other relay box, located in the center cargo compartment, provides control of the following system components:

- Eight water tank valves located in the center cargo compartment
- The P-2 (aft) water pump motor control
- Flow control valves CV-2A and CV-2B
- Emergency dump valves DV-1A and DV-1B

The third relay control box, located in the aft passenger cabin, is used for control of the following fixed water ballast system components:

- Seven water tank valves located in the aft passenger cabin
- Emergency dump valves DV-2A and DV-2B

Switches that control the water tank valve relays are located in the water tanks. Each tank has two (a redundant set) flow switches for the full tank condition and one flow switch for the empty tank condition. These switches automatically operate the respective relays that provide power to open or close the electric tank valves. Control panel indicator lights show full or empty conditions of the water tanks.

The water pump motor control is also operated from the control panel. The pump motor control relay coils are wired in series with the pump motor thermal overload contacts to allow for automatic disconnect in case of over-heat conditions.

The electric circuits are protected by overload circuit breakers and the electric valves have manual override mechanisms.

Procedures for operating the water ballast system are shown in Table 21.

TABLE 21. - WATER BALLAST OPERATING PROCEDURES

| OPERATION | | PUMPS | | VALVES | | | | | | | | | | | | |
|--|-----------------------------------|-------------|---------|--------|-----|-----|-----|-----|-------|-------|-------|-------|-------|-------|-------|-------|
| | | Forward P-1 | Aft P-2 | FCV | ACV | PCV | FVF | FVP | DV-1A | DV-1B | DV-2A | DV-2B | CV-1A | CV-1B | CV-2A | CV-2B |
| Filling-tanks | Fixed water ballast tanks | OFF | OFF | - | - | 0 | - | 0 | - | - | X | X | - | - | - | - |
| | Transferable water ballast tanks. | OFF | OFF | - | 0 | - | 0 | - | - | - | - | - | X | X | - | - |
| Transfer water from forward to aft tanks | | ON | OFF | 0 | 0 | X | X | X | X | X | X | X | X | 0 | 0 | X |
| Transfer water from aft to forward | | OFF | ON | 0 | 0 | X | X | X | X | X | X | X | 0 | X | X | 0 |
| Emergency dump | Fixed water ballast tanks | OFF | OFF | - | - | 0 | - | - | - | - | 0 | 0 | - | - | - | - |
| | Transferable water ballast tanks | OFF | OFF | 0 | 0 | - | X | X | 0 | 0 | - | - | 0 | X | 0 | X |

X = Closed

0 = Opened

FCV = Actuator valve that controls each forward cargo tank
 ACV = Actuator valve that controls each center cargo tank
 PCV = Actuator valve that controls each aft-passenger deck tank
 FVF = Manual ball valve in forward cargo compartment
 FVP = Manual ball valve in aft passenger deck
 DV = Dumping valve (see Fig. 74)
 CV = Control valve (see Fig. 74)

APPENDIX D AVIONICS SYSTEM DESIGN

D.1 Avionics System Interface

A PACS system interface diagram is shown in Figure 72.

Sensor inputs are the same as shown in Figure 12. Additional elements shown in Figure 72 include:

- Stabilizer kicker
- Fault isolation panel
- Caution and warning panel (CAWP)
- Flight control electronic system (FCES) panel.

Also, interface between the computer and series servo is shown.

The stabilizer kicker provides a means in the pallet for inserting external signals into the PACS for use during ground checkouts and for flutter clearance tests.

The fault isolation panel provides a means for providing status of all the PACS monitors.

The CAWP contains the FIRST FAIL annunciator that illuminates in the event of a single failure in either of the four PACS computer channels.

The FCES panel provides a means for displaying the engagement and operational status of the two PACS channels. When a channel is engaged and operational, the corresponding PACS STAB switch light will be unlighted and flush with the FCES panel face. When a monitor detected failure has caused a channel disengagement, the corresponding switchlight FAIL annunciator will be lighted. Positive disengagement by the flight crew can be accomplished by pushing and releasing the switch light. The OFF annunciator will be lighted and the switch light will extend out from the face of the FCES panel.

D.2 Computer Description

The PACS computer function is to perform calculations that implement the control law (Figure 13). The computer converts the complete set of analog data every 1/595 second to digital data to provide current values for processing.

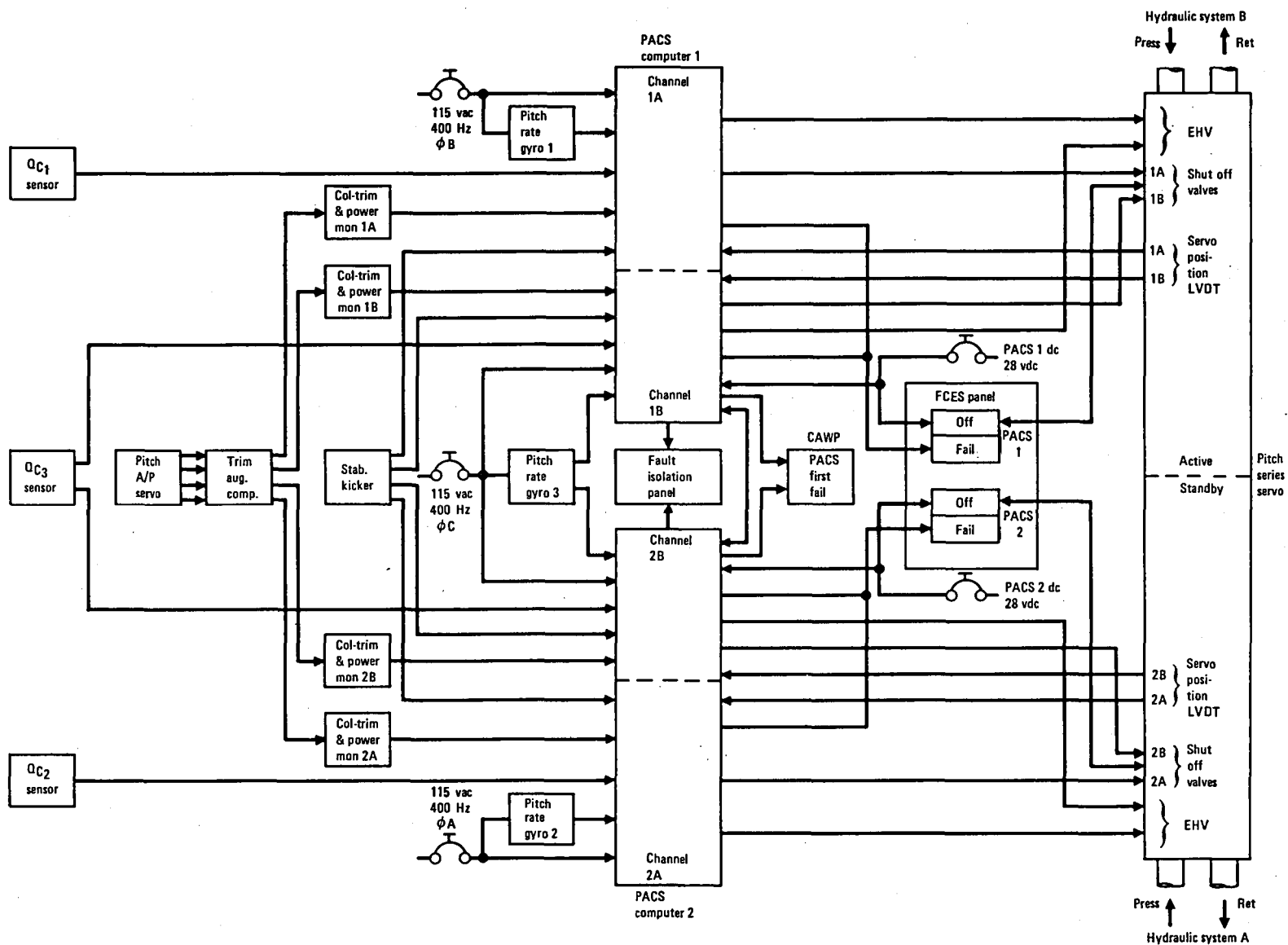


Figure 72. - Near-term PACS interface block diagram.

The front panel of the computer has a display and switches which allow maintenance functions to be performed.

The computer functions are shown in Figure 73 and listed below.

- Analog signal processing
- Digital data transfer
- Discrete signal processing
- Servo engage logic
- Servo control and monitoring
- Computer/pallet interface
- Data storage
- Digital signal processing
- Fault identification

Control of each channel is accomplished by the digital processor and the associated storage memories. Communication between functional elements of a channel is provided by the digital data transfer bus. Each section of the channel is scaled so that the intermediate or final results will not cause an arithmetic overflow.

Each computer is fed from a single source of a.c. electrical power which supplies both channels A and B of the associated computer.

D.2.1 Analog Signal Processing.— Analog signals from the C-T, PR, and Q_C sensors are filtered to eliminate digital frequency aliasing problems. These signals are routed to each computer channel. The C-T signals are arranged to provide stabilizer motion that is additive to the pilot inputs. The PR signals are arranged to provide stabilizer motion that is subtracted from the pilot inputs. Q_C signals are arranged to schedule the C-T and PR signals for control surface effectiveness and time constant change as a function of airspeed. Also, the series servo position (SP) signals are input to the analog signal receiver.

Analog signals from each sensor group (C-T, PR, or Q_C) are digitally processed to remove bias errors and to select the average signal levels. A significant difference between one signal and the others will cause each channel to reject the sensor which supplied the signal. A second signal disagreement from the same sensor group will result in complete system disconnect. The digital signals from the analog signal receiver are transmitted to the serial digital data bus.

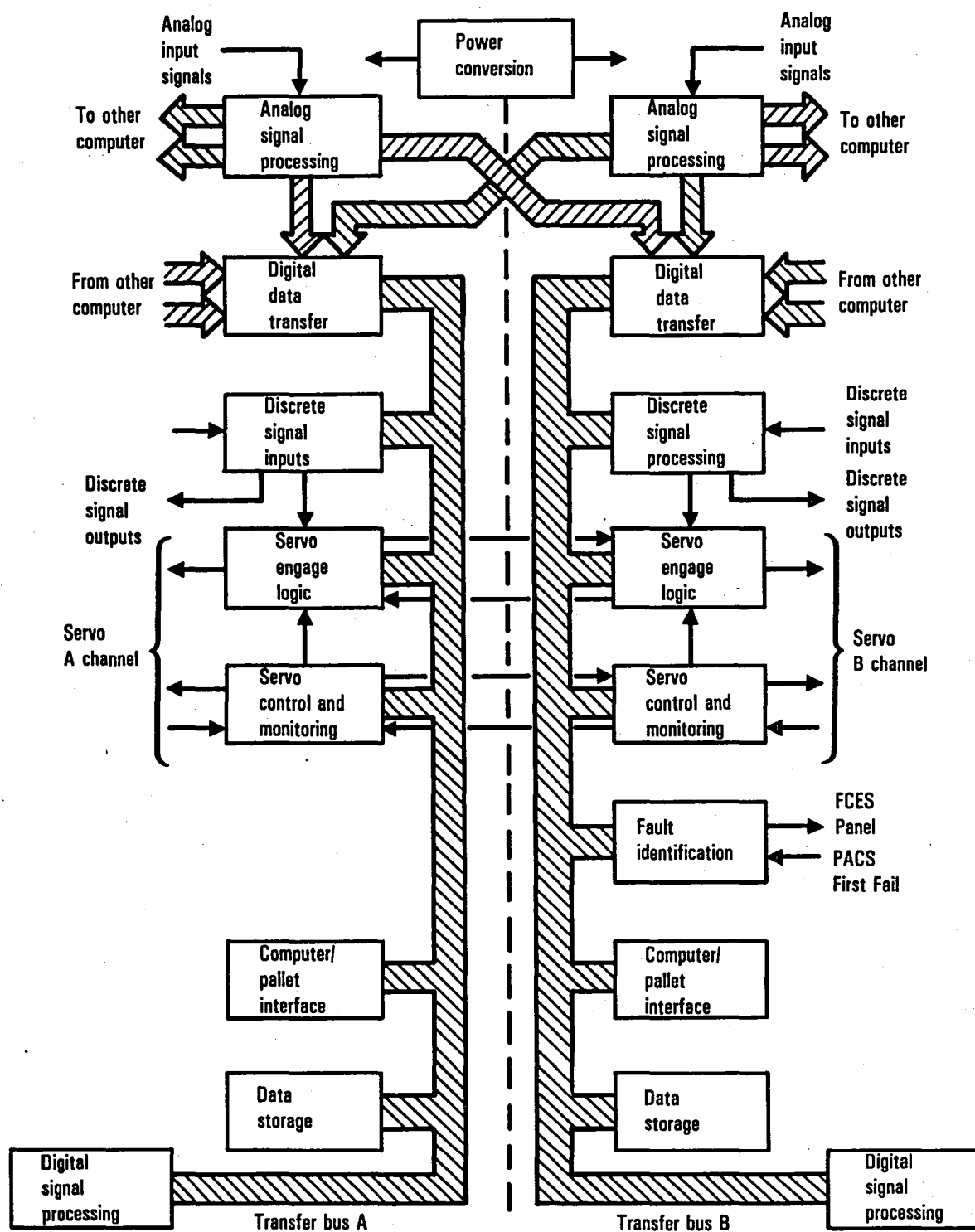


Figure 73. - Functional block diagram of modified ACC-201 computer.

D.2.2 Digital Data Transfer.-- The digital data from the sensors are serially transferred to the four processing channels and stored in addressable scratchpad registers. The four serial data bus lines are monitored to detect loss of signal activity. A tripped monitor will result in all signals carried on the bus being rejected by the processor.

D.2.3 Discrete Signal Processing.-- Discrete signal processing functions convert input discretes to equivalent digital signals. The digital signal discretes are servo engage enable (SEE), servo engage power (SEP), and power valid (PV).

D.2.4 Servo Engage Logic.-- The servo engage logic of each signal-processing channel of the computer controls the low side of one of the two solenoid operated hydraulic valves in the primary and secondary sections of the pitch series servo. The high sides of the solenoids are controlled by switches in the FCES panel. These switches provide for positive servo disengagement by the flight crew. Automatic engagement and disengagement is dependent upon discrete signals from associated equipment as well as logic signals provided by the servo monitors.

D.2.5 Servo Control and Monitoring.-- The servo control portion of each processing channel includes a digital to analog (D/A) signal converter, a servo amplifier for each of the two servos, and an AC to DC signal demodulator for each of the two LVDT position transducers used to close the servo loop.

The output of the 12 bit D/A converter is filtered with a low pass analog filter to reduce cross channel time skew differences seen by the dual servo monitors which compare the Channel A and B outputs for out of tolerance command discrepancies. In addition the response of each servo is compared against the response of a model for out of tolerance performance discrepancies.

D.2.6 Computer/Pallet Interface.-- Test equipment access to the transfer bus is provided when the Test Access/Terminator cards are removed from the flight computer and the test adapter cards are installed to provide for the interface with the pallet. The Test Access/Terminator card is at the high priority end of the bus and generates the bus grant logic such that, when the test adapter is installed, the test unit is the highest priority bus master.

D.2.7 Data Storage.-- A 1K words semiconductor random access memory (RAM) stores data resulting from computations and logic operations performed by the digital signal processor.

D.2.8 Digital Signal Processing.- The Collins adaptive processor system (CAPS-6) uses off the shelf MSI and bipolar bit slice LSI chip devices. Features of the CAPS-6 processor are:

- Speed: Addition 1.6 μ s
 Multiplication 7.1 μ s
 Division 8.9 μ s
- Instruction Set: 95 standard instructions, plus other user defined instructions via microprogramming
- Architecture: Microprogrammed bipolar bit-slice processor 2901
 16 bit word size
 Multiple stack organization
 8 prioritized stackable interrupts

The instruction set contains several special purpose instructions such as a signal selection algorithm (VOTER) and an interruptable memory instruction (CKSUM).

Fault identification and redundancy management are discussed in the following sections: sensor signal processing and servo monitoring.

D.2.8.1 Sensor signal processing: Input signals to the computer from each analog sensor group are equalized to avoid degraded system performance after a first sensor fault. Also, for the dynamic pressure sensors an abrupt change in system gain is avoided after a second sensor fault.

The procedure for dynamic pressure or pitch rate signal equalization is shown in Figure 74. For the column-minus-trim sensor group, sensor 3 is replaced by the C-T sensors 1B and 2B as shown in Figure 12. The equalizer outputs are averaged and integrated over a period of approximately 20 seconds and are applied to each equalizer to provide voter signal inputs equal to the true average of the sensor signals. For a dynamic pressure signal fault, the equalizer is switched into a slow follow-up mode and the equalizer averager drives the voter input signal to the same level as the other signals. For the column-minus-trim and pitch rate sensors, a signal fault results in the signal being sent to ground.

Figure 75 illustrates the computer software voting procedure. The voter first selects the three most positive of the four input signals. It then selects the most negative signals of the three most positive signals. As

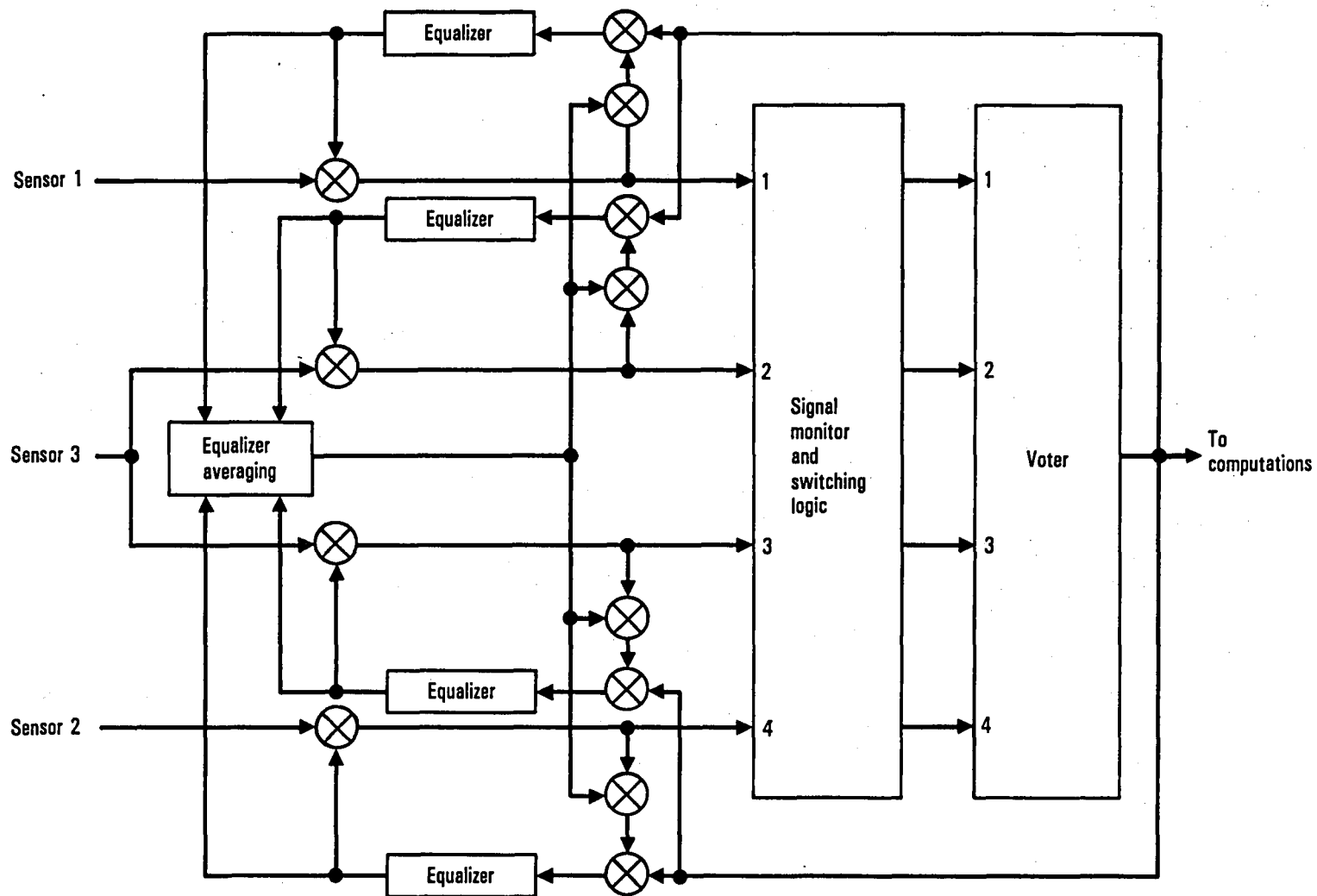
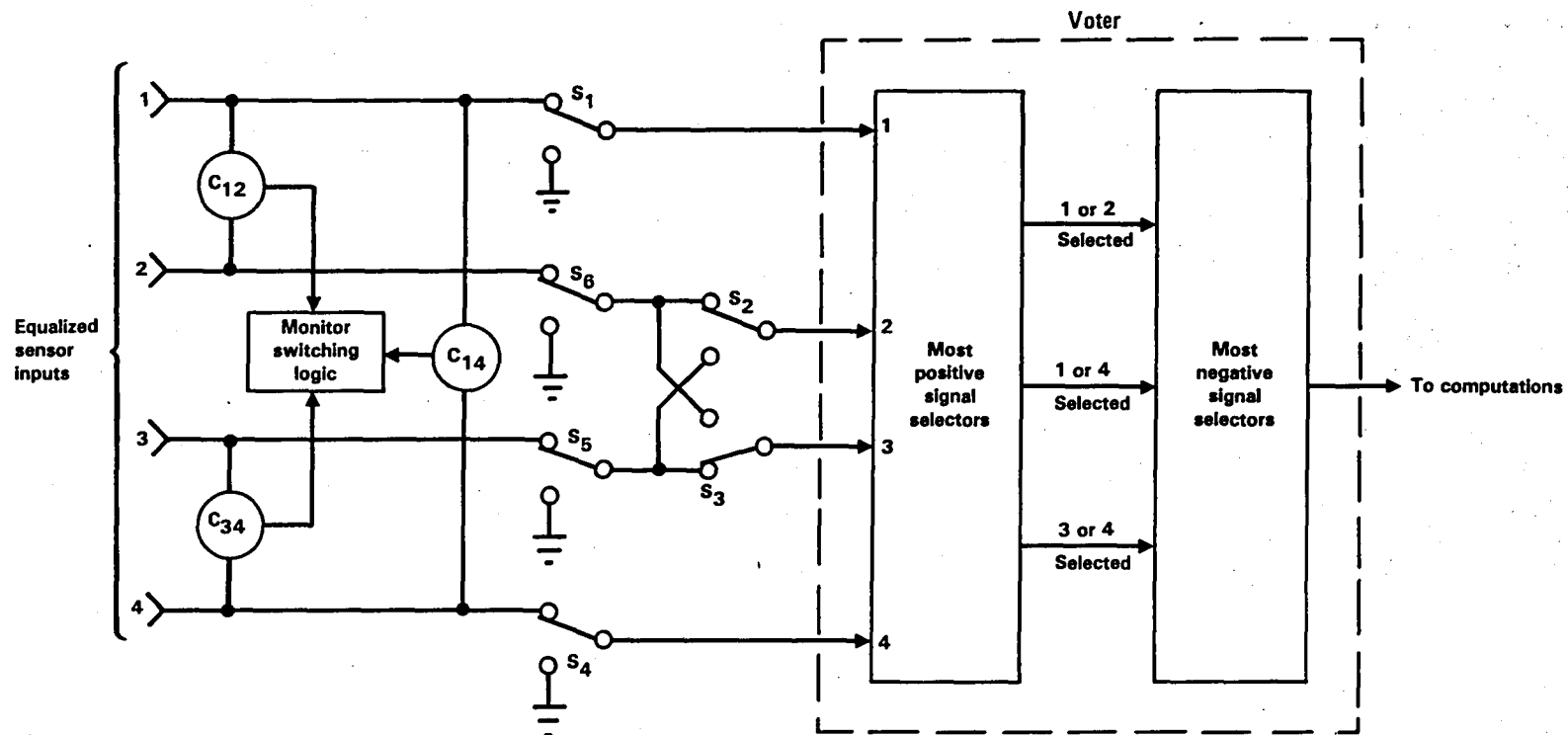


Figure 74. - PACS signal equalization.



| VOTER LOGIC TABLE | | | | | | | | | | | | | | | | | | | | | | | | |
|-------------------|---|---|---|---|---|---|---|---|---|---|---|---|---|---|---|---|---|---|---|---|---|---|---|---|
| Most positive | 1 | 1 | 1 | 1 | 1 | 2 | 2 | 2 | 2 | 2 | 2 | 3 | 3 | 3 | 3 | 3 | 4 | 4 | 4 | 4 | 4 | 4 | 4 | 4 |
| ↕ | 2 | 2 | 3 | 3 | 4 | 4 | 1 | 1 | 3 | 3 | 4 | 4 | 1 | 1 | 2 | 2 | 4 | 4 | 1 | 1 | 2 | 2 | 3 | 3 |
| ↕ | 3 | 4 | 2 | 4 | 2 | 3 | 3 | 4 | 1 | 4 | 1 | 3 | 2 | 4 | 1 | 4 | 1 | 2 | 2 | 3 | 1 | 3 | 1 | 2 |
| Most negative | 4 | 3 | 4 | 4 | 2 | 3 | 2 | 4 | 3 | 4 | 1 | 3 | 1 | 4 | 2 | 4 | 1 | 2 | 1 | 3 | 2 | 3 | 1 | 2 |

SWITCHING LOGIC TABLE

| FAULTED SIGNAL PATH | COMPARATOR SIGNAL INDICATING FAULTS | SWITCHES ACTUATED | SIGNAL INPUT SELECTED BY VOTER |
|---------------------|-------------------------------------|-------------------|--------------------------------|
| None | None | None | Per voter logic table |
| 1 | C ₁₂ and C ₁₄ | 1, 2, and 6 | Mid value of ground, 3 and 4 |
| 2 | C ₁₂ | 2 and 6 | Mid value of 1, 3, and 4 |
| 3 | C ₃₄ | 3 and 5 | Mid value of 1, 2, and 4 |
| 4 | C ₃₄ and C ₁₄ | 3, 4, and 5 | Mid value of ground, 1 and 2 |
| 2 and 3 | C ₁₂ and C ₃₄ | 2, 3, 5, and 6 | Mid value of ground, 1 and 4 |

Figure 75. - PACS computer software monitoring procedure.

indicated in the voter logic table, this process always results in selection of a middle signal level (shown as an enclosed number) and rejection of the most positive and most negative signals. As an example of the voter operation, assume that the input signal levels are as shown in column one of the table: signal 1 is most positive, signal 4 is most negative and signal 3 is selected. If, due to a fault, signal 3 becomes more negative than signal 4, the signal levels shift to the order shown in column two and signal 4 is selected.

Input signals from each group of three sensors are connected to the four voter inputs as follows:

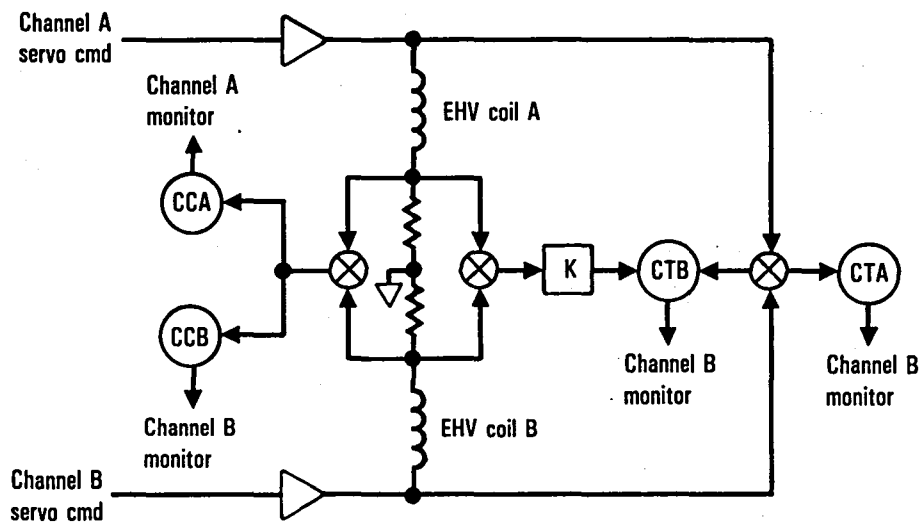
- Sensor 1 to input 1
- Sensor 2 to input 4
- Sensor 3 to inputs 2 and 3

Note that although sensor 3 is connected to voter inputs 2 and 3, the voter logic table shown in the figure still holds true, and the voter will reject faulted signals from sensor 3.

The signal comparators and monitor switching logic functions shown in the figure are provided to guard against a second signal failure which might result in voter selection of a faulty signal prior to automatic system disengagement. Each comparator transmits a non-valid signal to the switching logic as long as the difference between its two input signals exceeds a pre-set limit. If the non-valid signal or signals persist for approximately 200 milliseconds, which is indicative of a true fault condition, the monitor switching logic actuates appropriate switches as shown in the switching logic table. With the voter inputs reconfigured as indicated, second failure will result in voter selection of the remaining good signal or a zero-level (ground) signal.

To avoid nuisance fault indications due to temporary differences in signal levels, a pulse counter associated with each comparator is started each time a non-valid signal is transmitted. The counter accumulates pulses during the time the non-valid signal is present and will initiate the monitor switching logic when a pre-determined count is reached. If the non-valid signal is interrupted prior to this point, pulses are subtracted from the accumulated count, but at a rate equal to only one-half of the count-up rate. This rate difference acts to detect oscillatory fault conditions. Over a few cycles during which a comparator non-valid signal is repeatedly transmitted, a total count will be accumulated which is sufficient to initiate the monitor switching logic.

D.2.8.2 Series servo monitoring: Hardware and software signal comparators (Figures 76 and 77) monitor servo operation and isolate faults. Tripping of an executive comparator initiates the count-up/count-down procedure to



Note: CC comparators are executive
CT comparators are non-executive

Figure 76. - PACS servo monitor hardware comparators.

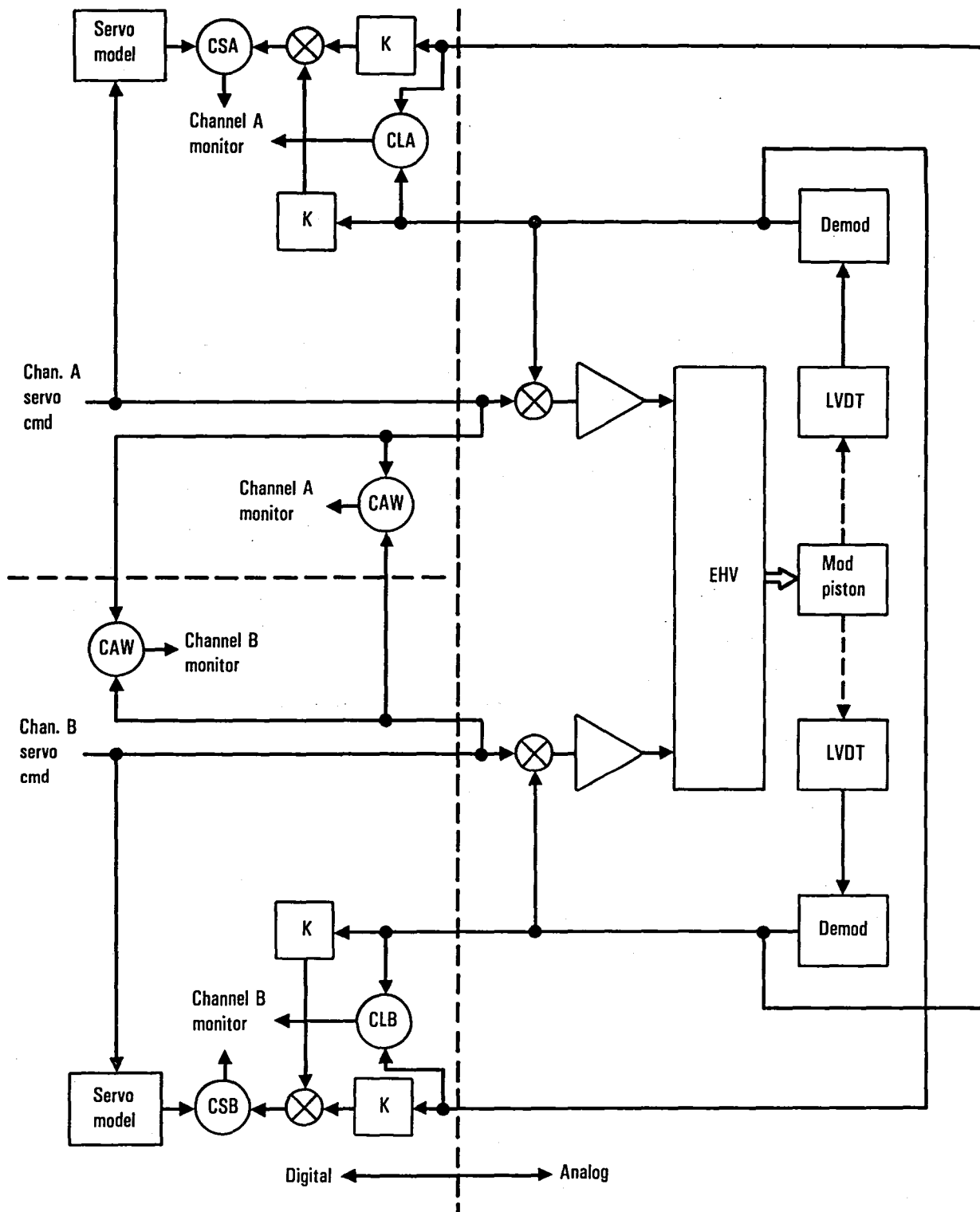


Figure 77. - PACS servo monitor software comparators.

detect oscillatory faults and disengage the associated servo channel. Tripping of non-executive comparators identify a fault but do not disengage the channel.

The CCA and CCB executive hardware signal comparators shown in Figure 76 detect differences between the channel A and B command signals transmitted to the servo, servo amplifier faults, and servo EHV coils open or short circuit conditions. Detection of the command signal differences is accomplished by a steady-state coil-current bias (not shown in the figure) which produces a voltage differential across the comparators when the channel A and B command signals are unbalanced. Also, the current bias permits detection of an EHV coil fault for zero-level command signals. The CTA and CTB non-executive hardware signal comparator outputs are transmitted to the digital computer B channel to identify which servo channel has failed.

All of the software comparators shown in Figure 77 are executive. The CSA and CSB comparators detect differences between the actual servo response and a model servo response. The CAW comparators detect differences between the signal-processing channel analog-signal outputs. The CLA and CLB comparators detect differences between two sections of the servo position LVDT and the associated demodulators.

D.2.9 Fault Identification.— Signal processing for fault identification is done in the B channel only. Monitor detected faults which illuminate the PACS FIRST FAIL annunciator on the caution and warning panel, or which illuminate the PACS STAB FAIL annunciator on the FCES panel are processed to isolate the fault to the line replacement unit (LRU). Identification of the LRU is accomplished by means of the code displays and the associated push lights on the face of each modified Collins ACC-201 computer.

D.3 Software Organization

To create a systematic and modular design, the software is written in a high-level algol-like language. The individual procedures are compiled creating a file of assembler statements. These statements are processed by an assembler to produce relocatable segments which can be linked into a computer program. The assembler listing gives references to variable labels and source line numbers so that there is visibility from the source code to the final program. This allows one to easily patch the program for testing purposes.

The program is divided into foreground and background and error routine programs as shown in Figure 78. A scheduler alternates the execution of the program between the foreground and the background. The foreground procedures are those procedures requiring high speed or real time execution such as control law calculations and certain testing and monitoring functions. The background program contains monitoring, self testing and fault isolation procedures. The error routine program contains bus timeout, stack overflow, accumulator overflow and illegal opcode.

The foreground program is executed at a rate of 80 times per second. Since the processors complete the foreground calculations in less than 1/80 second, the remainder of the time slice is used in the background calculations. There are four slow paths in the foreground which are sequentially executed once each foreground cycle yielding an iteration rate of 20 times per second. The slow paths contain procedures to monitor the sensors, schedule the gains, and control the servo engagement.

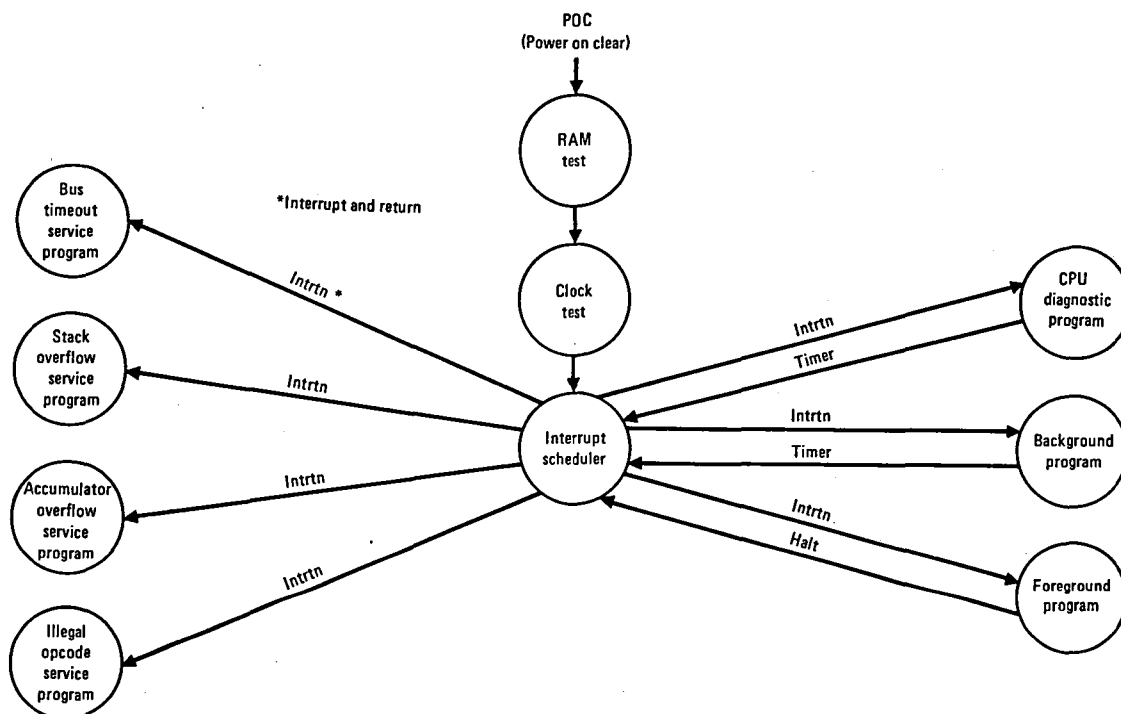


Figure 78. - Software organization.

REFERENCES

1. Urie, D.M., "Accelerated Development and Flight Evaluation of Active Controls Concepts for Subsonic Transport Aircraft - Volume II - Aft C.G. Simulation and Analysis," NASA CR 159098, September 1979.
2. Federal Aviation Agency, "Federal Aviation Regulations, Part 25, Airworthiness Standards: Transport Category Airplanes," February, 1965.
3. Anon., "Military Specification, Flying Qualities of Piloted Airplanes," MIL-F-8785C, 5 November 1980.
4. Anon., "Design Objectives for Flying Qualities of Civil Transport Aircraft," SAE-ARP 842B, 30 November 1970.
5. Hoblit, F.M., Paul, N., Shelton, J.D., Ashford, F.E., "Development of a Power-Spectral Gust Design Procedure for Civil Aircraft," FAA-ADS-53, January 1966.
6. Fuller, J.R., Richmond, L.D., Larkins, C.D., Russell, S.W., "Contributions to the Development of a Power-Spectral Gust Design Procedure for Civil Aircraft," FAA-ADS-54, January 1966.
7. Watkins, C.E., Woolston, D.S., Cunningham, H.J., "A Systematic Kernel Function Procedure for Determining Aerodynamic Forces on Oscillating or Steady Finite Wings at Subsonic Speeds," NASA TR R-48, 1959.

| | | | | | |
|---|--|--------------------------------------|--|--|--|
| 1. Report No. | | 2. Government Accession No. | | 3. Recipient's Catalog No. | |
| 4. Title and Subtitle Development and Flight Evaluation of an Augmented Stability Active Controls Concept with a Small Horizontal Tail - Phase I | | | | 5. Report Date Sept. 1, 1982 | |
| | | | | 6. Performing Organization Code | |
| 7. Author(s) Wiley A. Guinn* | | | | 8. Performing Organization Report No. LR 30208-2 | |
| 9. Performing Organization Name and Address Lockheed California Company | | | | 10. Work Unit No. | |
| | | | | 11. Contract or Grant No. NAS1-15326 | |
| | | | | 13. Type of Report and Period Covered Dec 1978-April 1982 | |
| 12. Sponsoring Agency Name and Address NASA Langley Research Center | | | | 14. Sponsoring Agency Code | |
| | | | | | |
| 15. Supplementary Notes *Authors: J.J. Rising, A.A. Kairys, C.A. Maass, C.D. Siegart, W.L. Rakness, R.D. Mijares, R.W. King, R.S. Peterson, S.R. Hurley, D. Wickson, D.M. Archibald, J.R. Cook, B.H. Wendler, C.S. Willey, and F.P. Streid | | | | | |
| 16. Abstract This report documents Task I for development and flight test of a limited authority pitch active control system (PACS) on a wide body jet transport (L-1011) with a flying horizontal stabilizer. Two dual channel digital computers and the associated software provide command signals to a dual channel series servo which controls the stabilizer power actuators. Input sensor signals to the computer are pitch rate, column-trim position, and dynamic pressure. Control laws are given for the PACS and the system architecture is defined. Discussions are given regarding piloted flight simulation and vehicle system simulation tests that are performed to verify control laws and system operation prior to installation on the aircraft. Modifications to the basic aircraft included installation of the PACS, addition of a c.g. management system to provide a c.g. range from 25 to 39% mac, and downrigging of the geared elevator to provide the required nose down control authority for aft c.g. flight test conditions. Three pilots used the Cooper-Harper Rating Scale to judge flying qualities of the aircraft with PACS on and off. The handling qualities for cruise and high speed flight conditions with the c.g. at 39% mac (+1% stability margin) and PACS operating were judged to be as good as the handling qualities with the c.g. at 25% mac (+15% stability margin) and PACS off. | | | | | |
| 17. Key Words (Suggested by Author(s)) Active Control System, Control System, Pitch Control, Longitudinal Control, Aircraft Fuel Savings | | | | 18. Distribution Statement | |
| 19. Security Classif. (of this report) Unclassified | | 20. Security Classif. (of this page) | | 21. No. of Pages 179 | |
| | | | | 22. Price* | |

End of Document